CHAIR OF METALLURGY
MONTANUNIVERSITAET LEOBEN

Thermochemical modelling of the FINEX® process to determine the material flow of alkalis, halides and zinc

Master Thesis

by

Thomas Leitner, BSc.

MONTAN UNIVERSITÄT

Preface

This thesis stands for finishing my studies at the Montanuniversity of Leoben. Therefore, I wish to thank all the people, who were supporting me during this time.

Since the work was done at the Chair of Ferrous Metallurgy, I wish to thank Univ.-Prof. Dipl.-Ing. Dr.techn. Johannes Schenk for making the work for this interesting and seminal topic possible and for all the theoretical input he got for me. In addition, Dipl.-Ing. Dr.mont. Anton Pichler and Dipl.-Ing. Daniel Spreitzer as well as the entire staff of the Chair of Ferrous Metallurgy were assisting me in case of demand.

Furthermore, thanks to POSCO as the corporate partner.

Finally, I wish to thank my whole family and friends for the financial and personal support during my whole studies in Leoben. I would not have reached this point without you.

Abstract

The knowledge about harmful elements, such as potassium, sodium, chlorine, fluorine and zinc in iron making processes is of high importance. These elements are volatile and build compounds which can harm the process, e.g. they can damage the refractory linings. Furthermore, the vaporization needs energy, which is then lost for melting the iron-bearing material. Of course, the blast furnace is the most important route for producing hot metal, but other technologies, such as the smelting reduction processes have huge benefits by means of usage of non-coking coal and iron ore fines. These aspects lead to environmentally beneficial processes.

This thesis describes the most important smelting reduction processes, i.e. the COREX®, FINEX®, OxyCup, Hismelt and Romelt process. Furthermore, the thermodynamic behaviour of volatile elements (potassium, sodium, chlorine, fluorine and zinc) is described in typical atmospheres for iron making processes.

As the FINEX® process is commercialized and processed by the steel producer Posco, a thermodynamic model was developed calculating the compounds in different stages of this smelting reduction process. Parameters, such as the hot gas cyclone temperature, the slag basicity and dust burner ratio were varied and the influences on the total output and enrichment of the elements are discussed.

Affirmation

I hereby declare that I have composed my Master's thesis independently using only those resources mentioned, and that I have as such identified all passages which I have taken from publications verbatim or in substance.

Date:

....
Thomas Leitner

Contents

General symbols

B   Basicity

f   Interaction parameter

K, k   Equilibrium constant / evaporation rate

p   Pressure

PtInp   Percentage of total input

R   Gas constant

T   Temperature

ΔG Gibbs free energy

ΔH Enthalpy

ΔS Entropy

λ Optical basicity

Acronyms

°C	degree Celsius (unit of temperature)
atm	atmosphere (unit of pressure)
BOF	blast oxygen furnace
$CaCl_2$	calcium chloride
CG	cooling gas
DBR	dust burner ratio
DRI	direct reduced iron
EAF	electric arc furnace
FB	fluidised bed reactor
g	gaseous
GG	generator gas
h	hour (unit of time)
HBI	hot briquetted iron
HCI	hot compacted iron
HGC	hot gas cyclone
ID	industrial data
J	Joule (unit of energy)

K   Kelvin (unit of temperature)

kg   kilo grams (1000 grams, unit of mass)

l, liq   liquid

ln   natural logarithm

log_{10} logarithm to the base 10 (common logarithm)

MG   melter gasifier

mol   mole (unit of amount of substance)

Nm^3 cubic meters in standard state (STP)

PTAT   Primetals Technologies Austria GmbH (former VAI)

PtInp   percentage of total input

s   solid

sec   seconds (unit of time)

SR   smelting reduction

Stm   standard model

STP   standard temperature and pressure (0 °C, 1 bar)

tHM   tons of hot metal

ULCOS   Ultra Low CO_2 Steelmaking

USSR   Union of Soviet Socialist Republics

VAI   Voest Alpine Industrieanlagenbau

vol-%   volume percent

WGSR   water-gas shift reaction

Chemical elements and compounds

Al_2O_3	alumina / aluminium oxide
C	carbon
CH_4	methan
Cl_2	chlorine
CO	carbon monoxide
CO_2	carbon dioxide
Fe_2O_3	iron oxide (hematite)
Fe_3O_4	iron oxide (magnetite)
$FeCl_2$	iron chloride
FeO	iron oxide (wuestite)
H, H_2	hydrogen
H_2O	water / steam
HCl	hydrogen chloride
HF	hydrogen fluoride
H_2S	hydrogen sulphide
K	potassium
K_2CO_3	potassium carbonate

K_2O_2	potassium peroxide
KCl	potassium chloride
KCN	potassium cyanide
KF	potassium fluoride
KH	potassium hydride
KNO_3	potassium nitrate
KO_2	potassium superoxide
KOH	potassium hydroxide
N, N_2	nitrogen
Na	sodium
Na_2CO_3	sodium carbonate
NaCl	sodium chloride
NaCN	sodium cyanide
NaF	sodium fluoride
NaH	sodium hydride
NaOH	sodium hydroxide
O, O_2	oxygen
SiO_2	silica / silicate
Zn	zinc
$ZnCl_2$	zinc chloride
ZnF_2	zinc fluoride
ZnO	zinc oxide
ZnS	zinc sulphide

List of figures

List of tables

1 Introduction

Iron and steel are one of the most important materials of human civilisation. The production of crude steel increased since the last decades (**Figure 1.1**). Although the blast furnace route is the main process for pig iron production, several other production routes for hot metal are being developed and are applied commercially. Especially, focussing on the environmental pollution the blast furnace route is not the gentlest one. Production of coke and sinter is necessary to provide a high stability of the burden material inside the furnace. Consequently, these production steps lead to an additional energy consumption and pollution by means of off-gases. Blast furnace operators minimalised the amount of coke, not least by injecting pulverised coal or other reducing agents at tuyères. However, coke can never be fully replaced in a blast furnace because of its burden supporting function.

Recent technologies, like smelting reduction technologies, deal with the production of hot metal by using coal instead of coke as the main reducing agent. Some of the technologies also replace pellets and sinter with iron ore fines.

Similar to the blast furnace process, volatile elements disturb the process in smelting reduction processes. These elements mostly are alkalis, such as potassium and sodium, and halides, e.g. chlorine and fluorine. Furthermore, zinc can also be mentioned as volatile element due to its chemical and physical behaviour at high temperatures. These elements appear in different compounds in the process. Depending on the temperature, the gas atmosphere and the pressure, these compounds could be in solid, liquid or gaseous state. Consequently, it is constructive, that they will vaporise in high temperature regions and deposit in liquid or solid state in areas with lower temperatures. The depositions mostly

damage the aggregate, e.g. the refractory linings. The frequent vaporising has also a negative influence on the energy effectivity of the process, as the heat is lost for melting.
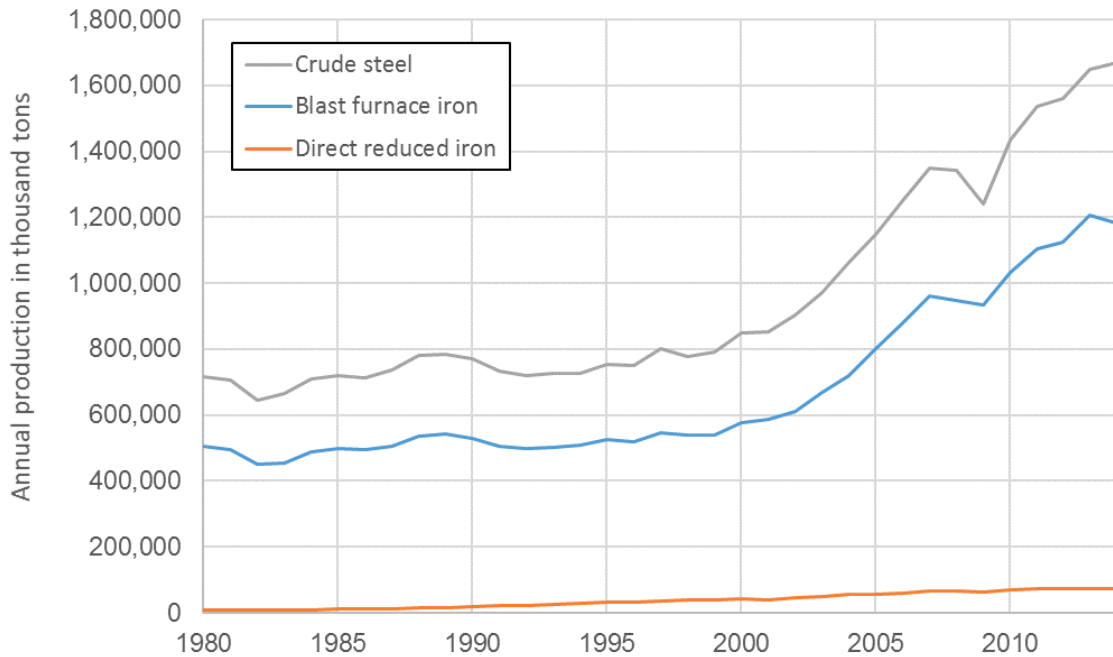
Figure 1.1: Annual world production from 1980 - 2014 [1]

The knowledge about the behaviour of the harmful compounds is necessary for a productive process. This thesis deals with the thermodynamic aspect of the different compounds of potassium, sodium, chlorine, fluorine and zinc in atmospheres which are typical for iron making processes.

Furthermore, an overview of the most important smelting reduction processes is given. As the FINEX® process is commercialised and processed by the steel producer Posco, a thermodynamic model was developed calculating the compounds of potassium, sodium, chlorine, fluorine and zinc in different stages of this smelting reduction process. The discharge of these compounds depends on valuable process parameters. Therefore, the influence of the temperature inside the hot gas cyclone, the slag basicity and the dust burner ratio is discussed.

2 Smelting reduction processes – an overview

Smelting reduction processes consists of two main units, prereduction of iron ore and smelting of the product in different stages. The reduction step first does not lead to a complete reduction of the iron oxide, only 30 to 70 % of oxygen is removed in the solid state. The final reduction takes place in the liquid state. That is why the second practical step is smelting, i.e. melting involving chemical reactions. The metallurgical advantages of high temperature operation in smelting reduction processes are faster reaction kinetics and prevention of sticking problems of solid state reactions at too high a temperature. Other advantages are the increased transport rates due to convection and a strong increase in the conversion rate because of an enlargement of specific phase contact areas in dispersed phases. [2]

In contrast to the blast furnace process, the smelting reduction aggregates use coal instead of coke as main reducing agent. For this reason, the expensive coke plant is not applicable and many environmental problems can be avoided. Of course, nearly all blast furnaces reduce their coke consumption significantly by means of reductant injection at tuyères, but coke can never be fully replaced, because of its burden supporting function in the blast furnace. [3]

An overview of the current steelmaking processes can be seen in **Figure 2.1**, including the blast furnace route, the direct reduction route and the smelting reduction route.

Generally, the smelting reduction employs two units. In the first, iron ore is heated and pre-reduced by a reduction gas. This gas is generated by the second unit, which is a smelter gasifier supplied with oxygen and coal. The partially reduced ore from the first unit is fed into the smelter gasifier and liquid hot metal or (in some cases) liquid steel is produced. The heat

is generated by gasifying the coal with oxygen. This produces a CO-rich hot gas which can further get oxidized to generate additional heat for smelting the iron. Smelting reduction technology enables a wide range of coals which can be used for ironmaking. [2–4]
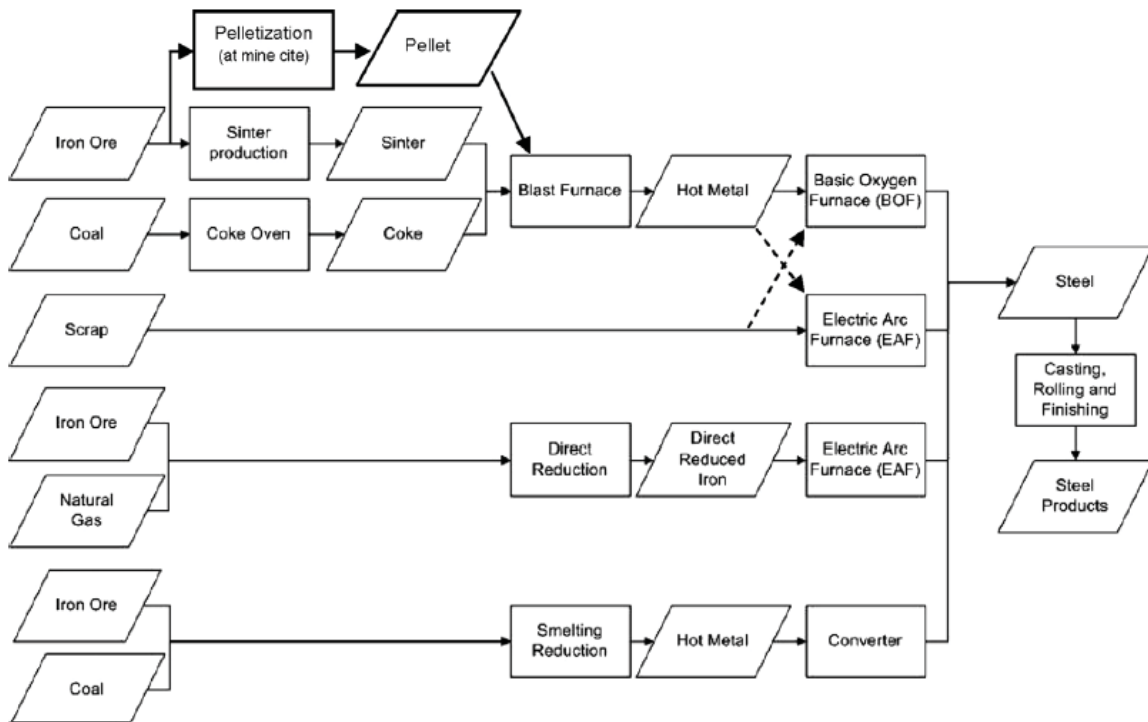
Figure 2.1: Overview of the current steelmaking routes [4]

In the following sub-sections, the most important smelting reduction processes are described. Because of the topic of this thesis, the description of the FINEX® process is more detailed. Several processes are under development, some of them are commercially proven (COREX®, FINEX®) and others are under demonstration (e.g. Hismelt) [4].

2.1 COREX®

The COREX® process was developed to industrial scale by Primetals Technologies Austria GmbH (former Siemens VAI). It uses a reduction shaft as pre-reduction aggregate, where the iron ore is partially reduced to DRI (**D**irect **R**educed **I**ron). Therefore, the sinter and coking plants are not required for the pre-treatment of iron ore and coal. The reduction gas is provided by the second aggregate, the melter gasifier. This fact enables the use of low cost raw materials, while both capital investment and production costs are lower. Additionally,

emissions like sulphur oxides, nitric oxides and dust can be decreased by about 90 % compared with a blast furnace [5].

The smelting is done by a melter gasifier. Reducing gas (CO and H_2) is supplied by the gasification of coal with oxygen inside the reactor. Also higher hydrocarbons from the coal are cracked into CO and H_2, so no by-products like tar, phenol, etc. are generated [3]. A fixed bed is formed in the melter gasifier. The heat from the partial combustion is used to melt the reduced iron. Hot metal and slag are discharged at the bottom by a conventional tapping procedure like that which is used by a typical blast furnace. The tapping temperature is between 1400 and 1500 °C [2]. The process is working at an elevated pressure, up to 5 bar [3]. A schematic diagram of the COREX® melter gasifier is shown in **Figure 2.2**. The coal charged into the melter gasifier at the top comes in contact with the hot reducing atmosphere and is dried and pyrolyzed.
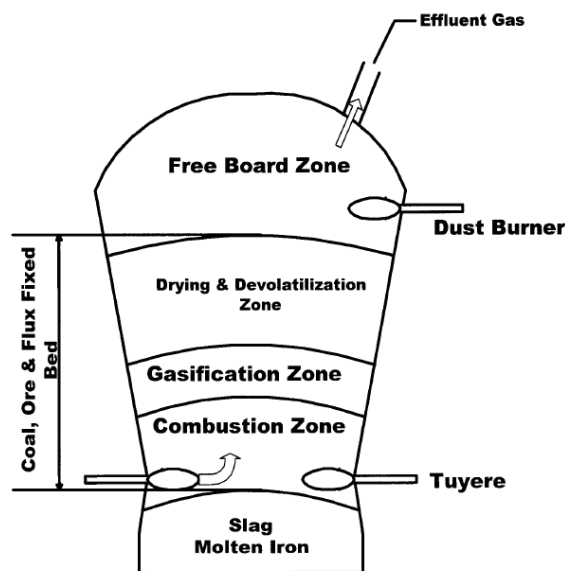
Figure 2.2: Schematic diagram of the COREX® melter gasifier [6]

The effluent gas (generator gas), which leaves the reactor at the top is cooled down to 800 to 900 °C by adding a stream of cooling gas. Then this gas gets separated from dust by using a hot gas cyclone. The dust is returned to the melter gasifier by using a dust burner, where additional oxygen is blown in [6]. The reduction gas is split into two streams. The vast bulk is conveyed to the COREX® shaft reducing the charged ore. The other part is cleaned in a series of wet-scrubbing steps and then used as cooling gas to decrease the temperature of the generator gas. The wet-scrubbing steps are also responsible for dissolving alkalis in water, and hence the charged alkalis are continuously removed [2].

The gas balance in the COREX® process is dependent on the type of coal which is used, especially its composition. The export gas generated during the production of hot metal is high grade, with a caloric value of approximately 7500 kJ/Nm³. It can be used for heating purposes in a steel plant (e.g. rolling mills) or in other industrial areas for power generation, to produce oxygen (in a COREX® plant), or as a synthesis gas in the chemical industry. The top gas has a temperature of approximately 450 °C [4]. **Figure 2.3** shows the basic flow sheet of the COREX® process. [2]
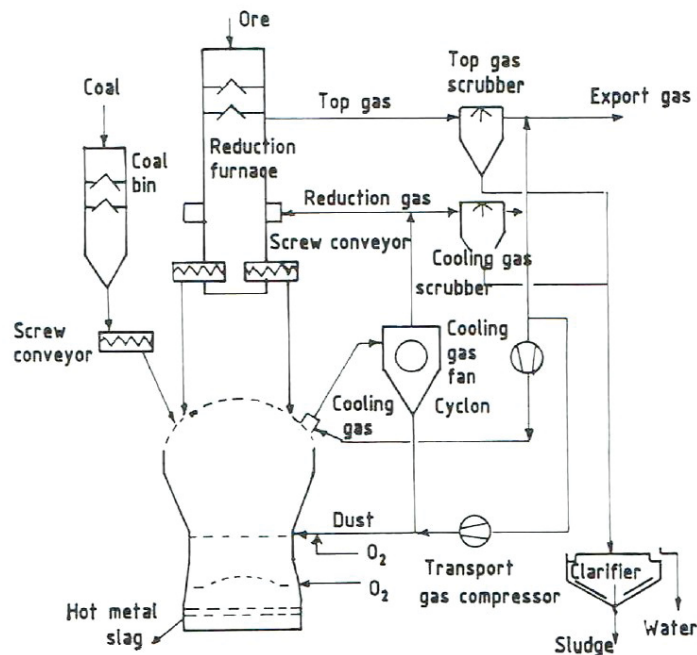
Figure 2.3: Basic flowsheet of the COREX® process [2]

As mentioned above, the COREX® process can use a large variety of coals with minimum effort for coal preparation. For the production of one ton hot metal about 900 kg coal is required [7]. The main characterisation is given by the volatile matter content, since this determines the gasification temperature for the combustion to CO and H_2. Other properties, such as the ash content of the coal and the softening behaviour, the swelling index and grindability have less or no influence. Coals with low volatile matter contents generate high temperatures during gasification with oxygen. For others, the volatile hydrocarbons must be cracked before gasification can occur, which results in lower temperatures. Such coals must be mixed with anthracite, low volatility bituminous coal, charcoal or coke breeze before use. The ash content is less critical, expect for acidic ashes of the coals, because a basic slag has to be formed. [2]

To adjust basic slags limestone and dolomite are used as additives. These fluxes are charged with coal to the melter gasifier or with the ore into the reduction shaft. The grain size of the fluxes fed into the shaft should be approximately in the same range as the ore. The size of those fed to the gasifier is about 4 to 10 mm. [2]

The choice of the optimum size of the iron oxide feed is crucial. Too big grains hamper the reducibility, whereas fine particles disturb the gas permeability inside the shaft furnace. For this reason, fines generated during handling and transportation must be screened before charging. Sticking of ores is not encountered in the COREX® process because the coal dust serves as a lubricant. [2]

Some of the limitations of the COREX® processes are [4]:

- Fine ores cannot be used directly.

- There are restrictions for non-coking coal (volatile matter of carbonaceous material to be maintained at around 25 %).

- Net export gas should be utilised very economically, otherwise the process becomes unviable.

Han et al. [8] investigated the influence of the burden distribution on the temperature distribution in a COREX® melter gasifier. Therefore, the researchers first varied the relative DRI to lump coal and coke volume ratio inside the length of the radius of the aggregate. Furthermore, they analysed the influence of the coke charging location (either in the centre or between centre and wall) and the coke size (3 or 5 mm). The study concluded that the temperature near the wall decreases if the volume ratio of DRI to lump coal and coke decreases, due to the increase of DRI in the wall region. The burden distribution is reasonable when the radial distribution is equal to 1:1. Moreover, with an increase of central coke charging amount, the temperature in the melter gasifier increases significantly. Whereas an increase of intermediate coke charging decreases the temperature near the wall region while the temperature in the intermediate region increases. It is supposed that the gas flow presents two streams ascending in the furnace. Last mentioned, the furnace temperature increases with the increase of coke size. The control of the particle diameters of lump coal and coke can optimise the gas flow in the COREX® melter gasifier.

2.2 FINEX®

The FINEX® smelting-reduction process was developed by Primetals Technologies Austria and the Korean steel manufacturer Posco. This process is also based on the direct use of non-coking coal. The major difference between the COREX® and FINEX® processes is that the FINEX® process can directly use iron ore fines (up to 12 mm) without any kind of agglomeration. [4]

The smelting step is provided by a melter gasifier like in the COREX® process. Instead of a shaft furnace for pre-reduction, the FINEX process uses a series of fluidised bed reactors in a counter-flow system. There the ore fines are reduced in three or four stages to DRI (Direct Reduced Iron). The upper reactor stage serves primarily as a preheating stage. In the succeeding stages, the iron ore is progressively reduced to fine-grained DRI. Skorianz et al. [9] investigated the reduction behaviour and structural evolution of iron ore fines under fluidized bed conditions. During their studies, they determined a standard test atmosphere in a three-stage fluidised bed pre-reduction step for the FINEX® process. The typical gas compositions and temperatures are listed in **Table 2-1** for the upper reactor stage (R3), the middle (R2) and the succeeding one (R1). **Figure 2.4** shows the operating points of the three-stage reduction in a Baur-Glaessner diagram. First, the iron ore is reduced by the process gas to magnetite (R3), then to wuestite (R2), and finally in the stability field of iron to a certain amount of metallic iron (R1).

Table 2-1: Typical gas atmosphere for a three-stage fluidised bed reactor for FINEX® [9]

	R1	R2	R3
Temperature [°C]	760	750	480
CO [%]	45.4	39.3	32.7
CO_2 [%]	20.4	29.2	26.7
H_2 [%]	17.2	16.9	14.3
H_2O [%]	5.4	7.3	7.8
N_2 [%]	11.6	6.6	18.4
CH_4 [%]	0.0	0.0	0.0

The typical iron oxide mix for FINEX® is hematite fine ore with a typical mean grain size of 1 to 2 mm (magnetite pellet feed ratio up to 30 %) [10]. After pre-reduction, the reduced iron gets compacted and directly charged in form of HCI (Hot Compacted Iron) into the melter gasifier through a lock-hopper system. [4]
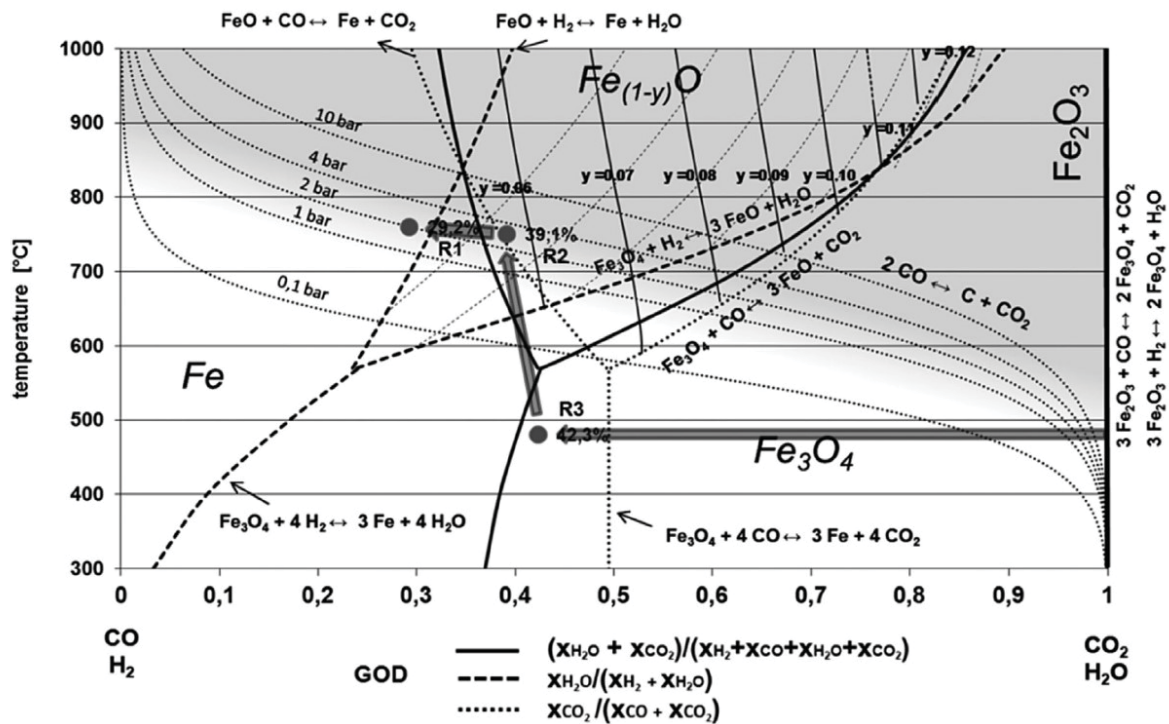
Figure 2.4: Baur-Glaessner diagram for reduction step of a three-stage fluidised bed reactor [9]

The smelting process in the melter gasifier, the return of dust using the hot gas cyclone and the gas management system are the same as described for the COREX® process in **chapter 2.1**. The FINEX® export gas is a highly valuable product and can be further used for DRI/HBI production, electric energy generation, or heating. **Figure 2.5** shows a simple illustration of the major differences between the blast furnace, the COREX® and the FINEX® processes. The main benefits of the FINEX® process are [4,10]:

- No need for pelletizing, sintering or agglomeration of iron-bearing materials.

- Direct use of fine concentrates.

- Capital costs claimed to be 20 % lower compared to a conventional blast furnace route, and production costs are 15 % lower.

- Lower emissions because of lower energy consumption and no need for coke making.

- Direct use of non-coking coals.

- High valuable export gas for a wide range of applications in metallurgical processes, energy production or natural gas substitution.

- Production of hot metal with quality similar to that produced in a blast furnace.

- CO_2 mitigation potential and no nitrogen-rich hot blast by using pure oxygen.

- Flexibility in raw materials selection and in the operation, e.g. utilisation of lower grade iron ores possible (e.g. iron ores with higher Al_2O_3 content).
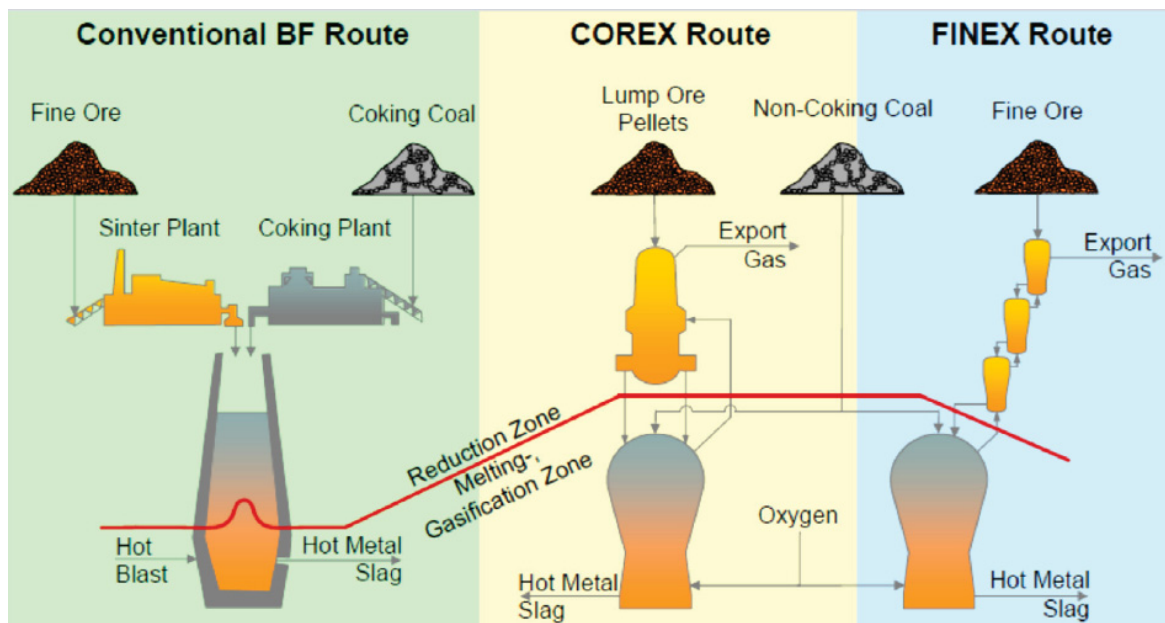
Figure 2.5: Comparison between blast furnace (BF), COREX® and FINEX® route [4]

Together with the HCI the coal is charged through the lock-hopper system into the melter gasifier. After the coal drops onto the char bed, pyrolysis takes place. The environmentally harmful hydrocarbons are dissociated immediately to CO and H_2 due to the high temperatures (about 1000 °C in the dome/freeboard, see **Figure 2.2**). The oxygen injected into the tuyères gasifies the coal generating heat for melting as well as a reduction gas consisting of mainly CO and H_2. [10]

Figure 2.6 shows a typical FINEX® process flow sheet including the gas management system and **Table 2-2** lists typical consumables depending on raw material qualities.

Identically to the COREX® process a large variety of coals can be used. A major criterion for an initial evaluation of coals or coal blends suitable for the FINEX® process is a fixed carbon content at a minimum of 55 %. Further contents for ash (up to 25 %), volatile content lower than 35 % and a sulphur content lower than 1 % are described [10]. A thermal stability is also required in order to allow a formation of a stable char bed in the melter gasifier.
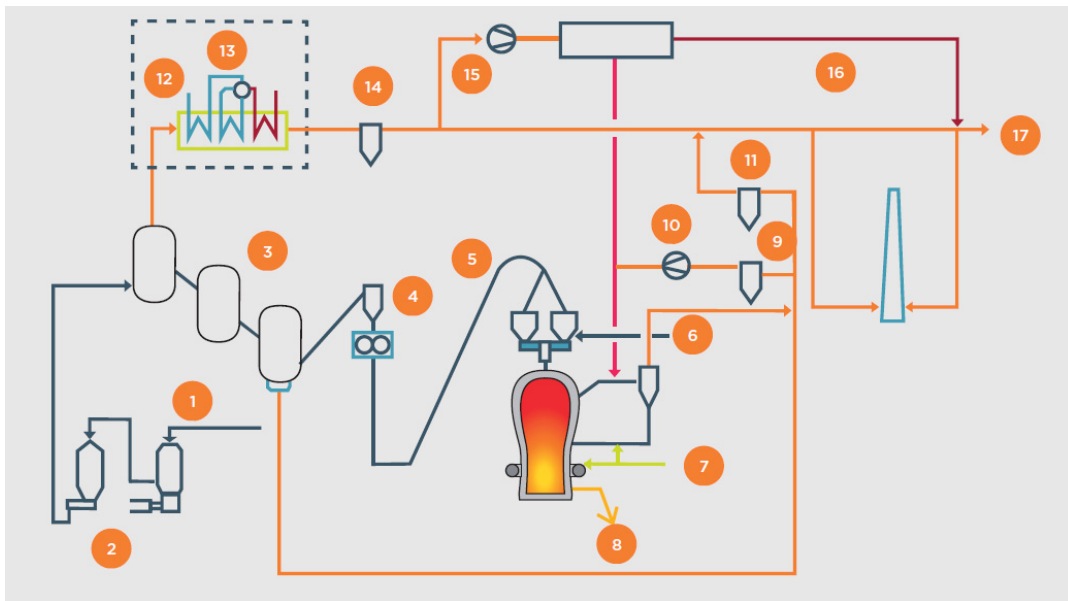
Figure 2.6: Typical FINEX® process flow sheet [10]

1 - ore, additive drier, 2 - pneumatic ore transport, 3 - fluidised bed, 4 - HCI plant, 5 - HCI hot conveyor, 6 - coal briquettes, 7 - oxygen/PCI, 8 - hot metal/slag, 9 - cooling gas scrubber, 10 - cooling gas compressor, 11 - excess gas scrubber, 12 - steam, 13 - waste heat recovery steam generation, 14 - top gas scrubber, 15 - recycle gas compressor, 16 - tail gas, 17 - export gas

Table 2-2: Typical consumables for the FINEX® process [10]

Fuel rate (dry)	720 - 800	kg/tHM
Ore	~ 1600	kg/tHM
Additives	~ 285	kg/tHM
Oxygen	~ 460	Nm³/tHM
Nitrogen	~ 270	Nm³/tHM
Industrial water	~ 1.5	m³/tHM
Electrical energy	~ 190	kWh/tHM
Refractories	~ 1.5	kg/tHM

Additionally to fine ore as feed material, 30 – 50 % pellets can be charged. A mixture of iron ores is possible considering chemical and physical properties such as total Fe content, composition structure, grain size etc. Generally, the Fe content of iron ore determines the productivity of the process as well as at the blast furnace process. Since higher alumina slag tapping is more tolerable in FINEX® than in blast furnace, higher alumina content of iron ore is also allowed. Hematite and goethite are preferred ores for the FINEX® process as seen in **Figure 2.7**. [10]
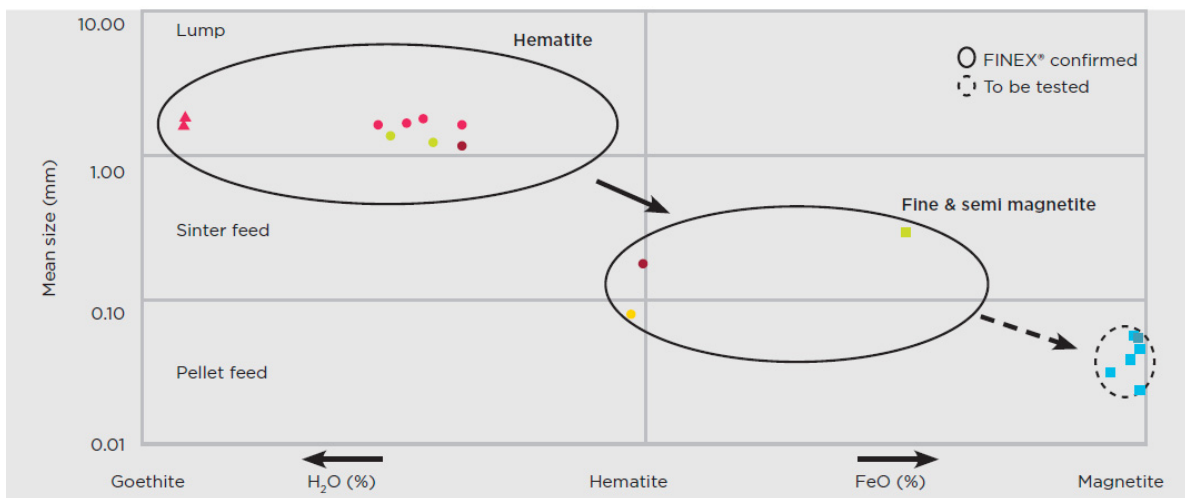
Figure 2.7: Flexibility of ores suitable for the FINEX® process [10]

The products of the FINEX® process are first hot metal, which is identical to that of the blast furnace [10]. On the other hand, the export gas can substitute natural gas, oil, coke and coal for numerous applications like the COREX® export gas, e.g. electrical power generation, heating purposes, steam generation, production of syntheses gas etc. The amount and the composition of the export gas can vary within defined limits depending on the composition of the coal. Typical values for the hot metal and the export gas are given in **Table 2-3**. Generation of high purity CO_2 is also possible ($CO_2 > 95$ %). It can be further used for sequestration, oil recovery enhancement or other economical use (e.g. chemical product, fuels or fertilizer). Due to the use of pure oxygen, the export gas contains less nitrogen. [10]

Table 2-3: Typical values for FINEX® hot metal and export gas [10]

Hot metal		Export gas		
Tapping temperature	1500 °C	CO	34	%
C	4.50 %	CO_2	43	%
Si	0.70 %	H_2	13	%
P	0.07 %	H_2O	3	%
S	0.04 %	CH_4	1	%
Mn	0.07 %	N_2 / Ar	6	%
		Dust	5	mg/Nm³
		Calorific value	5500 - 6250	kJ/Nm³
		Export gas credit	8	GJ/tHM

By comparing the two steelmaking routes, blast furnace and FINEX®, the main product, hot metal has the same quality. A huge difference is found in the environmental amenities and the economic benefits of the FINEX® process. The in-situ coking of the coal in the melter gasifier has many advantages, e.g. hydrocarbons are destroyed in the dome, a large portion of sulfur is captured in the slag which leads to a decrease of gaseous SO_2 or H_2S. Furthermore, pure oxygen is used instead of the hot air blast. Thus, lower nitrogen emissions in the form of NO_X appear, as shown in **Figure 2.8**. So, no additional investment or operational costs are incurred for a complex gas or disproportional waste water conditioning plant. [10]
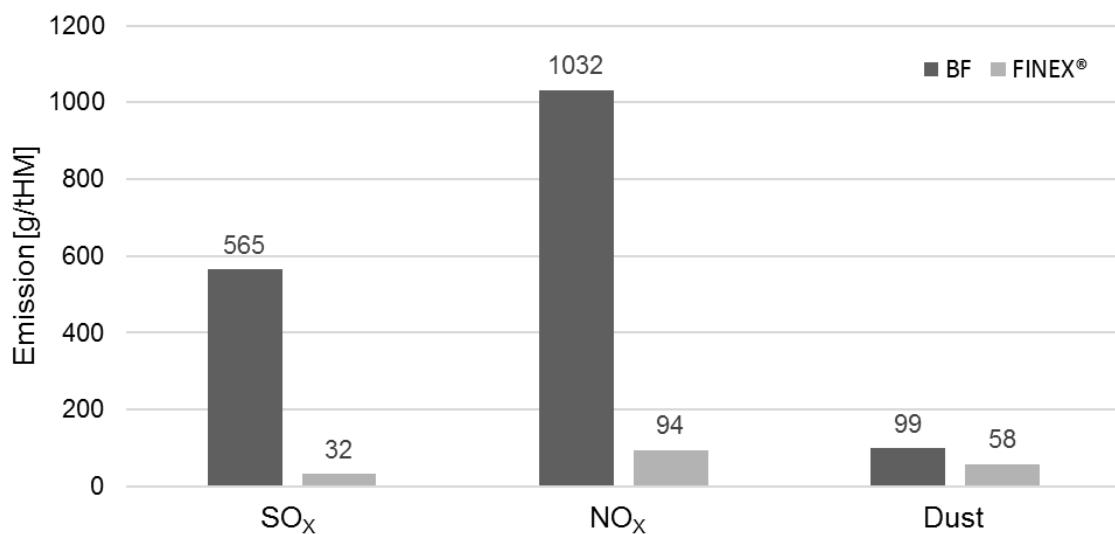
Figure 2.8: Comparison of emissions between blast furnace (BF) and FINEX® route [10]

Posco and Primetals Technologies Austria signed a cooperation agreement for the joint development of the FINEX process in December 1992. A pilot-plant was started up in 2003 in Pohang, Korea, with a nominal capacity of 2000 tons per day. Due to successful results a first commercial plant was built up in 2004. It commenced operation in April 2007 with an annual production capacity of 1.5 million tons). The biggest FINEX® plant has been put into operation in January 2014 with a nominal production capacity of 2 million tons per year. [10]

2.3 OxyCup

The OxyCup (or OxiCup) technology was developed by ThyssenKrupp Steel in Germany to recycle steel mill wastes into hot metal using a shaft furnace. It consists of two process stages. Self-reducing agglomerate bricks are produced from steel plant wastes by adding a binder. The wastes itself contains iron and carbon. Afterwards, the bricks are charged, reduced and smelted in a shaft furnace together with lumpy iron oxides, coke and other required additives. Charging of up to 70 % of HBI or approximately 20 % DRI from direct reduction plants is also possible. Tapping of hot metal and slag is carried out continuously at the bottom of the hearth. **Figure 2.9** shows a schematic diagram of the OxyCup furnace. The generated gas can be fed into the combined energy network of any steel plant. [11]
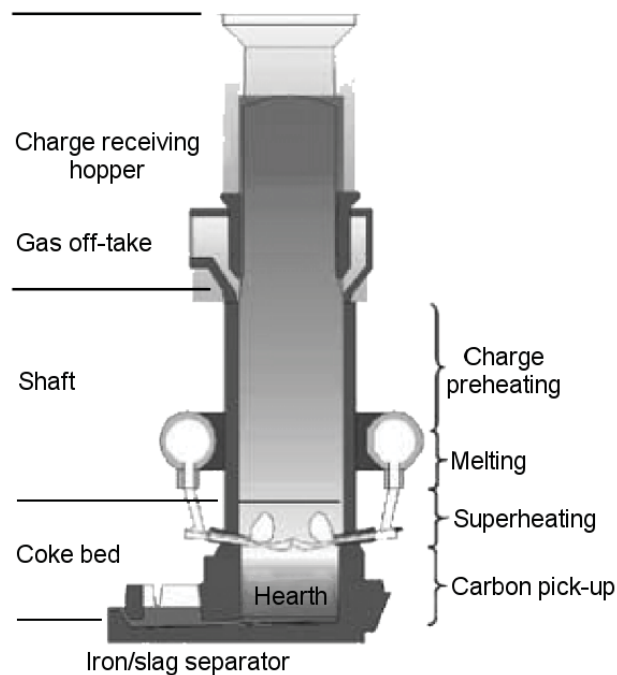
Figure 2.9: Section view of an OxyCup furnace [12]

The top of the furnace is smoke-free due to the arrangement of the charge-receiving hopper and the annular gas exhaust chamber at the upper part. The central part of the furnace is used for preheating and melting. The lowermost part contains the cupola hearth which always keeps filled with coke. [11]

As charging material all kinds of reverts such as BOF skulls, desulphurisation slags, dust from blast furnace or sintering plants, washing tower sludge, mill scale from hot rolling mills as well as sludge from cold rolling mills and coating lines can be used. If necessary, iron-

containing slag can also be processed. Generally, up to 100 % scrap can be charged. Furthermore, the furnace can be shut down within two minutes leading to high flexibility in production. The production costs are lower compared to a blast furnace. New products like zinc-rich sludge can be produced by using inexpensive zinc-coated scrap to produce hot metal for BOF steelmaking. The high-zinc containing dusts from steelmaking can be charged in form of self-reducing agglomerates. Subsequently, the zinc-rich sludge can be used for further zinc recovery by zinc producers. The slag generated in the OxyCup shaft furnace is completely inert and harder than granite. Hence, the slag is a suitable building material for dams, etc. [11]

Li et al. [12] evaluated the OxyCup process for steelmaking dust treatment based on calculation of mass and heat balance and determined the role of carbon inside the process. As seen in **Figure 2.10** most of carbon is burnt in front of the tuyères to provide energy for the reactions and heating charge material. Only 33.11 % of the carbon is used to reduce ferrous and non-ferrous oxides. Additionally, the heat release of complete combustion of coke is nearly three times that of incomplete combustion. Therefore, nearly 90 % of the heat source is from the combustion of coke in the OxyCup furnace.
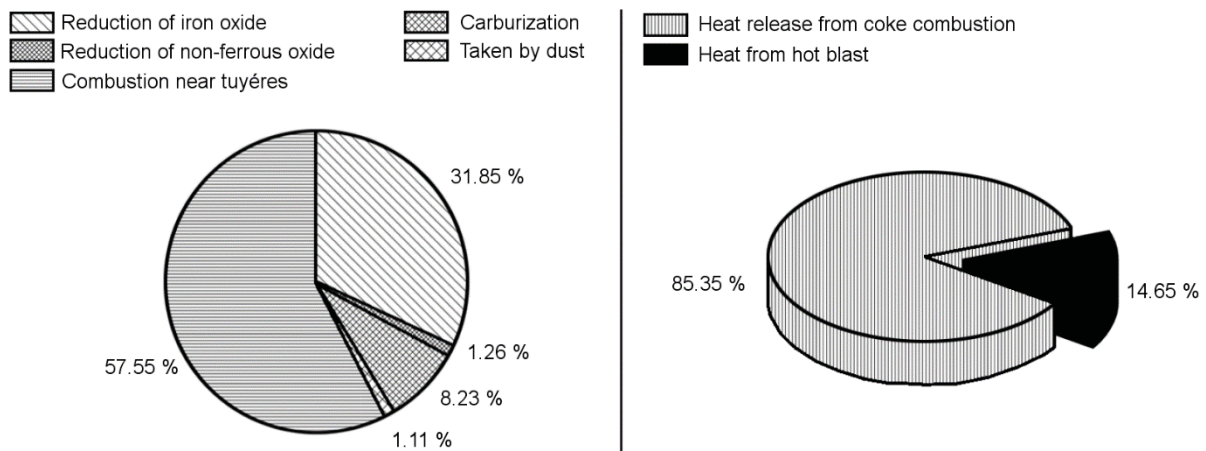
Figure 2.10: The role of carbon and heat source in the OxyCup process [12]

2.4 Hismelt

The Hismelt process is an Australian development in the field of smelting reduction. This process utilises fine iron oxide (including steel plant waste) and non-coking coal to produce molten hot metal. A small pilot plant was erected at the Maxhuette Steel Works in Southern Germany in 1984, which operated till 1990. The Hismelt process is illustrated schematically

in **Figure 2.11**. It consists of a vertical smelting reduction vessel, which is similar to a steelmaking converter. The vessel is refractory-lined in the hearth area and water-cooled in the top space above the metal bath. For pre-heating or pre-reduction of fine iron oxide, a set of circulating fluid bed reactors can be precede the smelting reduction vessel, if it is required. [11,13]
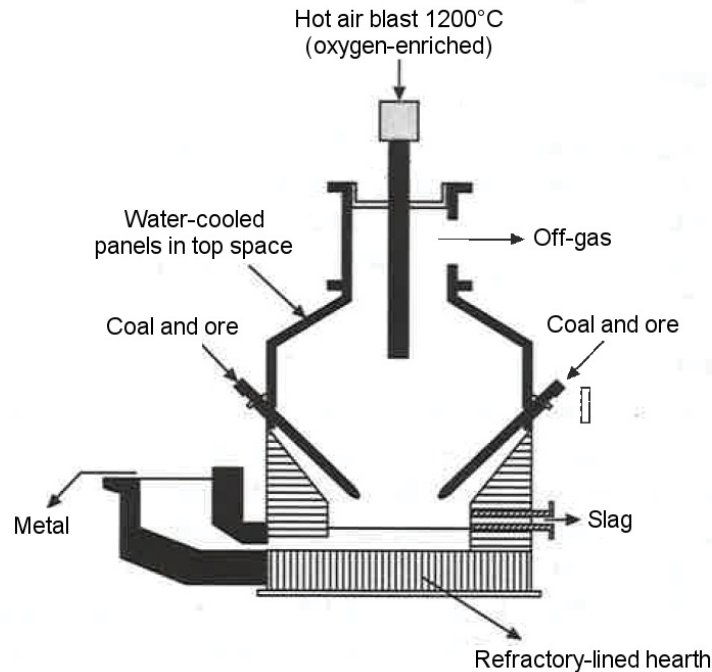
Figure 2.11: Schematic diagram of Hismelt process [11]

Charging is provided by water-cooled injection lances, which inject solid feed materials (iron ore and coal fines) as well as fluxes. Very high reaction rates during the reduction of iron oxide are obtained. The blast (pre-heated air at 1200 °C) is injected through a water-cooled lance above the bath to post-combust CO and hydrogen to CO_2 and H_2O. This liberates significant amounts of energy that becomes available for smelting the ore. A fountain of molten material, consisting largely of slag, erupts into the top space by the rapid expulsion of the carbon monoxide, hydrogen and nitrogen carrier gas form the molten bath. The blast can be enriched with oxygen, if it is required. The hot metal is continuously tapped through the forehearth, while slag is batch-tapped via a conventional blast furnace-like tap hole. The off-gas from the process is partially cooled in a membrane-tubed hood, before being used in the fluidised beds to pre-heat and pre-reduce the iron-bearing feed or for calcination of the fluxes. Then the off-gas is cleaned in a scrubber and used as fuel for the hot blast stoves or in a co-generation plant. [11,13]

An advantage of the Hismelt process in comparison to other SR processes is that the off-gas has not to assign any significant credit values to make the process economic. Furthermore, the process can consume steel plant wastes as well as its own waste products. Hence, it is extremely attractive from the environmental point of view. The overall emission of CO_2 is inherently less than that with the traditional blast furnace route due to the absence of pelletising, sinter and coke oven plants. Basically, it is a hot air-based process and does not need any oxygen plant. Further, Hismelt iron contains no silicon. Therefore, the slag volume in steelmaking can be considerably lowered. Additionally, high-phosphorus iron ores can be used, hence 90 – 95 % of the input phosphorus is discharged with the slag. [11]

In the Hismelt process, the metal bath is the primary reaction medium. In other SR processes this is done in the slag layer. Dissolved carbon in metal is a more readily available reductant than char in slag. Therefore, faster smelting rates are achieved in the Hismelt process by using carbon in a more active (i.e. dissolved) form. Additionally, the melt is well mixed, due to the direct injection of feed materials into the metal. A large volume of "deep gas" is generated. Under these conditions there is very little potential for establishing significant temperature gradients (greater than 20 – 30 °C) in the liquid phase and the system operates with an (essentially) isothermal melt. [13]

A further development was made by the ULCOS (Ultra Low CO_2 Steelmaking) project in cooperation with Hismelt, called the Hisarna process [14,15]. In this process the Hismelt bath smelting technology is combined with ore smelting and pre-reduction in a cyclone. In contrast to other pre-treatment steps, such as a reduction shaft or fluidised bed, the cyclone is directly connected to the smelter. It is the only pre-reduction technology that allows integration of both stages into a single reactor vessel. [15]

Since the cyclone is straight above the smelting reactor, the chemical and the thermal energy of the smelter gas is utilised directly. **Figure 2.12** shows the Hisarna process schematically. Quiet high pre-reduction rates are reached, although the gas has a high CO_2 content. This is due to the different equilibrium at the very high temperatures in the cyclone compared to a fluid bed or shaft furnace at more moderate temperatures. These reactors cannot operate at higher temperatures because of the risk of sticking and softening. Additional oxygen is injected to fully combust the gas and generate additional heat for the pre-reduction. The ore is molten inside the cyclone and drops down directly into the smelter. There is no need for intermediate product handling or transport. [15]
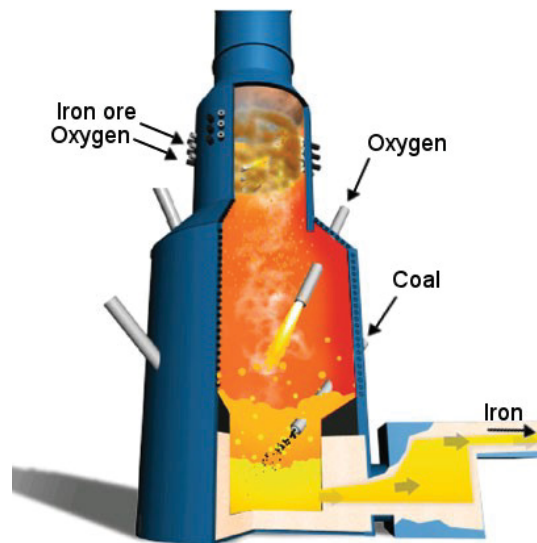
Figure 2.12: Hisarna process [15]

The final reduction and coal gasification stage is basically the same as at the Hismelt process with some modifications. In order to make the combination with the cyclone possible the process operates with pure oxygen instead of enriched hot blast. [15]

A pilot plant was set up in the works of Tata Steel Europe at IJmuiden, Netherlands. The first metal was tapped in May 2011. During the tests, 60 % of the injection capacity was achieved, although only for a short period. Two more trial campaigns for the pilot plant have been scheduled. The objective will be to achieve longer stable operating periods. Many improvements will be made to the installation and the operating procedures. [15]

2.5 Romelt

The Romelt process was developed at the Moscow Institute of Steel and Alloys (nowadays National University of Science and Technology "MISiS", Moscow, Russia) by Prof. V.A. **Ro**menets (hence the name) and his team. It further was known as the FLPR (**F**errous **L**iquid **P**hase **R**ecovery) process. Smelting and reduction is executed in a single rectangular-shaped reactor (like a small open-hearth steelmaking furnace). The reactor operates under a slight negative pressure induced by a suction fan at the gas treatment exit. There is no need for any complicated sealing of the reactor. [11]

In the Romelt process, iron-bearing materials and coal are charged through one or more openings at the top of a rectangle shaped furnace as shown in **Figure 2.13**. A part of the

charged coal gets oxidised, primarily to CO, by commercial purity (about 90 % purity) oxygen which is injected above the molten metal-slag bath through tuyères. The generated heat helps in melting the iron bearing materials. The rest of the coal is utilised for reduction. The result are three liquid zones of slag and metal on the hearth of the furnace – a lower zone of hot metal, a layer of relatively calm slag between the metal and the lower tuyéres and an upper slag layer that is intensely agitated by gas bubbles (reaction zone). About 70 tons of metal and 100 tons of slag are inside the furnace [16]. There is also the availability for additionally liquid, gaseous or solid pulverised fuel feeding into the bubble zone to speed up the combustion of coal and to improve the thermal conditions. Oxygen and air (in 50:50 portion) injected into the slag pool through a lower set of tuyères, agitates the slag and supplies heat to the slag by part-combustion of coal. The large surface area is conductive for efficient transfer of the post-combustion heat into the slag pool. Hot metal and slag are discharged through two separated tap holes over a siphon arrangement. [11]
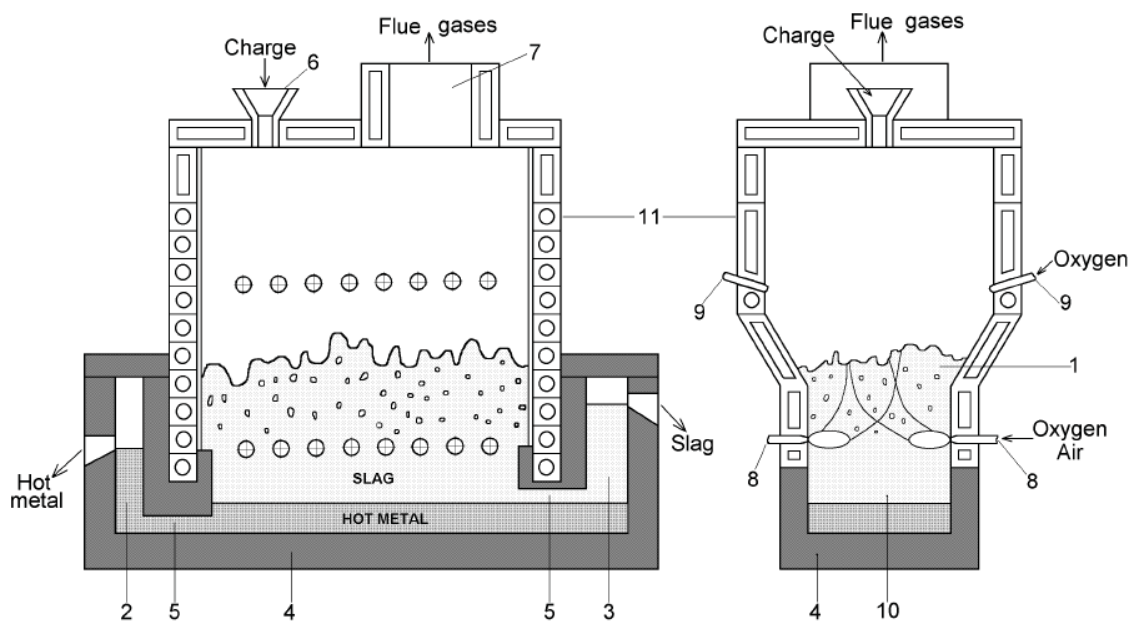
Figure 2.13: The Romelt furnace scheme [16]

1 – agitated slag, 2 – sump for slag, 3 – sump for hot metal, 4 – hearth with refractory lining,
5 – channels for slag and hot metal, 6 – feed tunnel, 7 – gas-escape branch pipe,
8 – lower tuyères, 9 – upper tuyères, 10 – calm slag, 11 – water-cooled panels

The bulk of the reduction takes place in the agitated slag zone where the iron bearing materials fall into it by top charging using weigh hoppers. The molten oxides get reduced in the bath and form liquid droplets, which descend into the calm zone by gravity. The gas evolved from the Romelt furnace at a temperature near that of the melt (above 1600 °C)

primarily consists of CO and H_2. This gas can be used as gaseous fuel or process-reducing gas. However, post-combustion is executed by tuyères above the bubble zone to improve the thermal efficiency. The efficiency of carbon utilisation is about 79 % (compared to typical values of 60 – 65 % in other processes like COREX®). [11,16]

A huge benefit of the Romelt process is, that the charge's iron content may be 48 – 52 % as well as much lower at around 30 %. Furthermore, the process can accept iron ore and non-coking coal size in a wide range from 0 – 20 mm. Unlike most other SR processes, the Romelt reactions take place in a single reactor and high degrees of post-combustion of the melter gas are achieved. Thus, a pre-reduction step is not needed. The oxygen, which is introduced in the upper tuyères, has quite low purity and mixed blast air (50 % air and 50 % oxygen) is injected in the lower tuyères. Hence, the process is less dependent on oxygen than other SR processes. Moreover, most of the sulphur and all the zinc and lead from the inputs reside in the gas phase. Phosphorus transfers to the mainly to the slag, hence high-phosphorus feedstock is acceptable. [11]

A pilot commercial plant with the hearth area of 20 m^2 was built at the Novolipetsky Steel Works in Lipetsk, Russia. During 1985 – 1998 more than 40,000 tons of hot metal were melted and used further in basic oxygen furnaces for steel making. [16]

3 Behaviour of selected elements in the FINEX® process

There are many elements such as alkalis, halides or low melting metals such as zinc which get into the melting reactor with the burden. These elements influence the whole process because it is difficult to discharge them, e.g. by the slag or the top gas. Consequently, they circulate in the melting reactor by vaporising in the high temperature zones and condensing in lower temperature zones. Furthermore, they also can react with the refractory lining which can end in destruction. It is also possible that they react with the burden and influence the gas flow.

The most research activities about the behaviour of such elements, i.e. potassium, sodium, chlorine, fluorine and zinc were done for the blast furnace. Due to the similar gas compositions and temperature ranges between the blast furnace and the FINEX® process, it is assumed that the thermochemical reactions are the same. In the following chapters, the reactions of these elements are described regarding their thermochemical stability. Additionally, stability diagrams are illustrated to determine the most stable phases.

These stability diagrams (or predominance diagrams) clearly show the principles of Gibbs energy minimisation and the Gibbs Phase Rule. To explain these diagrams an example is shown for the K-C-O system at 1000 K in **Figure 3.1**. The axes are the partial pressures of CO and CO_2, respectively. The diagram is divided into areas or domains of stability of the various liquid or solid compounds of K, C and O. For example, at $p(CO_2) = 10^{-6}$ and $p(CO) = 10^{-10}$ (point A) the stable phase is K_2CO_3. The lines and triple points show the conditions of the co-existence of two or three different phases.
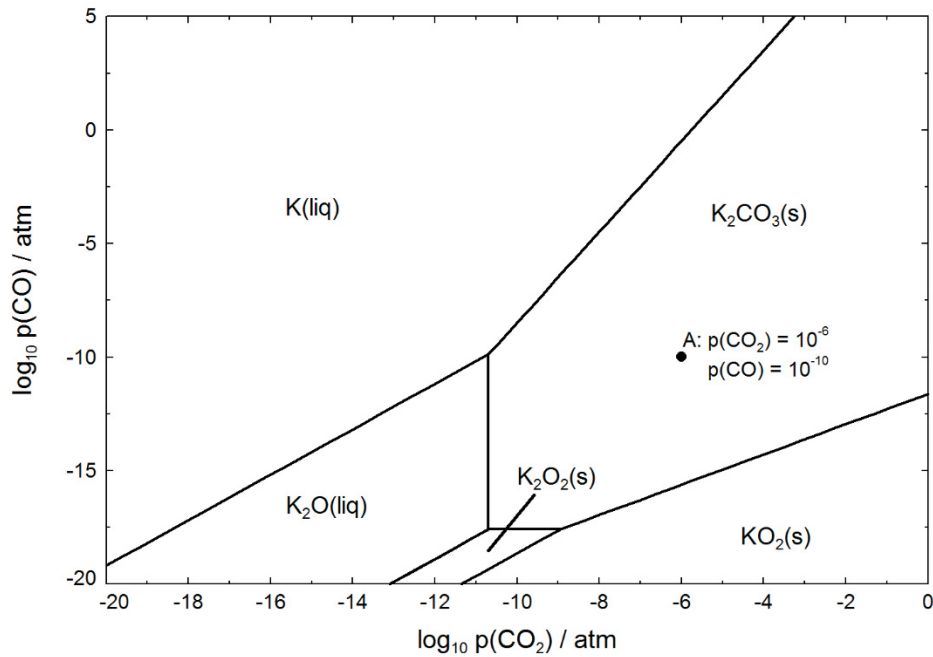
Figure 3.1: Stability diagram for the system K-C-O at 1000 K

For example, the phase boundary between K(liq) and K_2CO_3(s) follows the function of the equilibrium constant of the reaction seen in **equation (3-1)**.

$$K + CO_2(g) \rightarrow \frac{1}{2}K_2CO_3 + \frac{1}{2}CO(g) \tag{3-1}$$
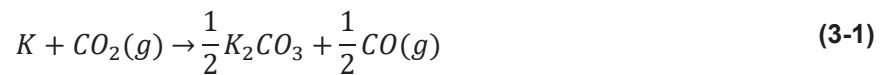
with the equilibrium constant K:

$$K = \frac{a_{K_2CO_3}^{1/2} \cdot p_{CO}^{1/2}}{a_K \cdot p_{CO_2}} = \frac{p_{CO}^{1/2}}{p_{CO_2}} = p_{CO}^{1/2} \cdot p_{CO_2}^{-1} \tag{3-2}$$

with a_i as the activity of species i (for solid and liquid compounds a = 1) and p_j as the partial pressure of gas j. After logarithmising and converting **equation (3-2)**, it can be seen, that the boundary line is thus a straight line with a slope of 2 in **Figure 3.1**:

$$\log p_{CO} = 2 \cdot \log p_{CO_2} + 2 \cdot \log K$$

In constructing stability diagrams, there is always a "base element" defined, which is present in all stable phases. For the example above, it is potassium. If there is a mutual solubility among the condensed phases, the phase boundary lines will not be straight. Normally such diagrams are drawn with the condition, that there is no mutual solubility [17]. Further, all different reactions for the formation of each phase can be formulated for one mole of the base element and involving the gaseous species whose pressures are used as the axes. For the example above **equations (3-3)** to **(3-6)** can be written:

$$K + 2\,CO_2 \rightarrow KO_2 + 2\,CO$$

$$\Delta G = \Delta G^{\emptyset} + R \cdot T \cdot \ln(p_{CO}^2 \cdot p_{CO_2}^{-2})$$

(3-3)

$$K + CO_2 \rightarrow \frac{1}{2}K_2O_2 + CO$$

$$\Delta G = \Delta G^{\emptyset} + R \cdot T \cdot \ln\left(p_{CO} \cdot p_{CO_2}^{-1}\right)$$

(3-4)

$$K + \frac{1}{2}CO_2 \rightarrow \frac{1}{2}K_2O + \frac{1}{2}CO$$

$$\Delta G = \Delta G^{\emptyset} + R \cdot T \cdot \ln\left(p_{CO}^{1/2} \cdot p_{CO_2}^{-1/2}\right)$$

(3-5)

$$K + CO_2 \rightarrow \frac{1}{2}K_2CO_3 + \frac{1}{2}CO$$

$$\Delta G = \Delta G^{\emptyset} + R \cdot T \cdot \ln(p_{CO}^{1/2} \cdot p_{CO_2}^{-1})$$

(3-6)

ΔG is the Gibbs energy for the reaction, $\Delta G^{\emptyset}$ is the standard Gibbs energy at standard pressure and temperature, R is the gas constant and T is the temperature. The values of $\Delta G^{\emptyset}$ are obtained from tables of thermodynamic properties. Each ΔG can be calculated for every value of partial pressures of CO and CO_2 at a given temperature. The most stable compound is simply the one with the most negative value for ΔG. If all the ΔG values are positive, then pure potassium is the stable compound. [17]

For the calculation it is not necessary which other compounds are in the gas phase above the liquid and solid compounds or if the partial pressure of one component may be higher than the total pressure. It must be emphasised that the gas phase is not considered in the phase equilibria. The partial pressure is simply a popular means of expressing the chemical potential of volatiles [18]. The total pressure influences the vapour pressure of the different compounds.

It is possible to increase the number of components. Therefore, a partial pressure for each additional component must be held constant. An example can be seen in **Figure 3.4** for the system K-C-O-H-N with constant partial pressures for H_2O and N_2. A detailed information for constructing predominance diagrams and the thermodynamic background was made by Pelton [17], Bale et al. [19] and Hillert [18].

The stability diagrams in this thesis were drawn with the Phase Diagram Module of FactSage™ 7.0 and its thermodynamical database FactPS.

3.1 Potassium and sodium

Alkali inputs (K, Na) in the blast furnace come from sinter, pellets, coke and injection coal, in the form of alkali silicates. A part of the alkali entering the furnace goes out with the slag, some as dust or gaseous compounds in the flue gas, another part is absorbed by refractory lining and the rest is circulating within the furnace. Excepting the alkalis which leaves the furnace with the slag, all other parts can create problems of varying difficulty. [20,21]

Especially when the top gas is needed as a product for power generation, the purity is very important and associated to high requirements. Potassium and Sodium can create corrosion occurrences at the blades of the combustion turbine because of sulphate and salt condensates. To moderate this problem, only the increase of the alkali output by the slag is useful. [22]

Other negative influences of the alkali load in the furnace are described in different literature sources [20–26]. The most interesting compounds of alkalis under the operation conditions are oxides, carbonates, cyanides and silicates [21]. If there are halides too, the creation of salts is possible, as shown in **chapter 3.2**. The potassium compounds cause more harm than the compounds of sodium because they are slightly less stable than those of sodium. The chemical behaviour of the two alkali metals is very similar according to salt formation. [21]

Kuwano et al. [27] investigated the distribution of absorbed alkalis in an experimental blast furnace. Therefore, the researchers used visual observation with an image fibre scope. **Figure 3.2** shows the relative spectral intensities of potassium and sodium absorbed to coke and pellets (samples) in the furnace, whereupon the intensity of vaporised K and Na at 1450 °C were measured. It can be seen, that the absorption to coke is slightly higher. The diagram also illustrates the circulation of alkalis in the furnace [27].
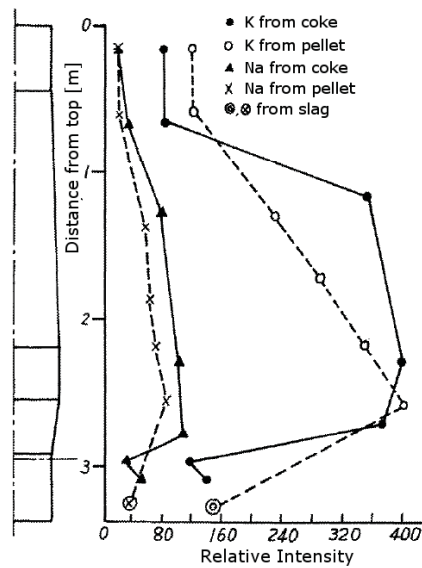
Figure 3.2: Relative spectral intensities of Na and K vaporised at 1450 °C from materials taken out of a dissected experimental furnace [27]

3.1.1 Different compounds and their reactions

The melting point of sodium silicate is at 1089 °C, potassium silicate melts at 997 °C. Carbon can reduce the alkali silicates to alkali metal vapour and silicon or silica only in the high-temperature zone and not in the low temperature regions, according to the **equations (3-7)** and **(3-8)**

$$2\,K_2SiO_3 + 2\,C \rightarrow 4\,K(g) + 2\,SiO_2 + 2\,CO(g) \qquad \text{(3-7)}$$

$$2\,K_2SiO_3 + 6\,C \rightarrow 4\,K(g) + 2\,Si + 6\,CO(g) \qquad \text{(3-8)}$$
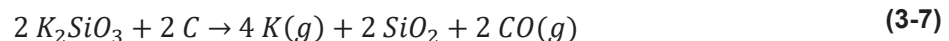
The reduction of potassium silicate with carbon can take place over 1550 °C, to give pure potassium vapour and CO gas at 1 atm. For the reduction of sodium silicate by carbon, the corresponding temperature is about 1700 °C. The reduction only happens, if the vapour pressure of alkalis is low enough, i.e. under 0.025 atm for potassium and 0.015 atm for sodium at 1500 °C. Thus, it is clear, that the reduction of alkali silicates to alkali metal vapour would occur in lower parts of the furnace, where the alkali load in the blast is very low. Since the gases are moving at high velocity, the equilibrium vapour pressure of the alkali metals will not be reached, and much lower values, 0.002 atm for potassium and 0.001 atm for sodium, are assumed. This explains why unreduced alkali metals are found in the slag during tapping. [21]

The reduction of potassium and sodium oxide and the partial pressure of the alkali metal-vapour depend on the ratio CO/CO_2, as seen in the **equations (3-9)** and **(3-10)** below.

Abraham et al. [21] describe that the equilibrium vapor pressure of potassium is 0.55 atm at 810 °C (just above the boiling point of potassium) with a CO/CO_2 ratio of 2.8. For the sodium vapour pressure at 1000 °C the calculation results in 0.06 atm. Consequently, Na_2O is more stable than K_2O.

$$K_2O + CO(g) \rightarrow 2\,K(g) + CO_2(g) \tag{3-9}$$

$$Na_2O + CO(g) \rightarrow 2\,Na(g) + CO_2(g) \tag{3-10}$$
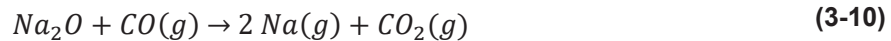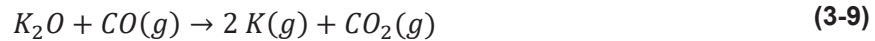
Pure alkali carbonates are not reduced in the blast furnace by carbon to alkali vapour and CO gas at 1 atm pressure till a temperature of about 1200 °C is reached. However, a reduction can occur below this temperature at a lower partial pressure of alkali vapour, according to the following **equation (3-11)**.

$$K_2CO_3 + CO(g) \rightarrow 2\,K(g) + 2\,CO_2(g) \tag{3-11}$$
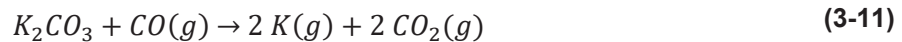
Abraham et al. [21] describe, that the formation of potassium and sodium carbonates could be happen from their vapours under conditions prevailing in the shaft of a blast furnace at temperatures below 900 °C. The carbonate formation follows **equation (3-12)** and **(3-13)**:

$$\frac{4}{3}K + \frac{2}{3}C + O_2 \rightarrow \frac{2}{3}K_2CO_3 \tag{3-12}$$

$$\frac{4}{3}Na + \frac{2}{3}C + O_2 \rightarrow \frac{2}{3}Na_2CO_3 \tag{3-13}$$

This solid carbonates are formed directly from the gas phase, so they will be divided and a huge portion passes out with the top gases. Some parts of the carbonate will deposit on the burden and get returned to the lower located zones of a furnace. There they dissociate to alkali vapour, which starts circulating again. [21]

A difference of the blast furnace and the melter gasifier is that the nitrogen potential inside the blast furnace is quite high because the hot blast consists of approximately 70 to 80 % gaseous nitrogen. The alkali cyanides are very stable at these conditions and can be formed by reactions according to **equation (3-14)** to **(3-17)**. If the activity of carbon and nitrogen is high enough, the cyanide can exist in gaseous and liquid state. [20,21]

$$2\,K(g) + 2\,C + N_2(g) \rightarrow 2\,KCN(g) \tag{3-14}$$

$$2\,K(g) + 2\,C + N_2(g) \rightarrow 2\,KCN(l) \tag{3-15}$$

$$2\,Na(g) + 2\,C + N_2(g) \rightarrow 2\,NaCN(g) \tag{3-16}$$

$$2\,Na(g) + 2\,C + N_2(g) \rightarrow 2\,NaCN(l) \tag{3-17}$$
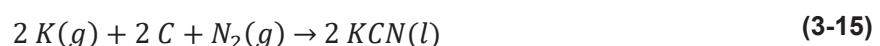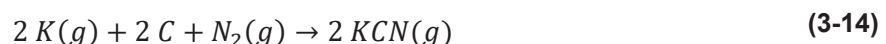
3.1.2 Stability diagrams

Figure 3.3 shows stability diagrams for the system K-CO-CO$_2$ for the various partial pressures of CO and CO$_2$ at different temperatures and a total pressure of 5 atm. This diagrams were drawn with the calculation software FactSage™ 7.0 (Database: FactPS) in combination with the descriptions of Gaskell [28] and other authors [17–19]. The diagrams show, that the area for elemental potassium increases with the temperature and so the gaseous potassium gets more stable.
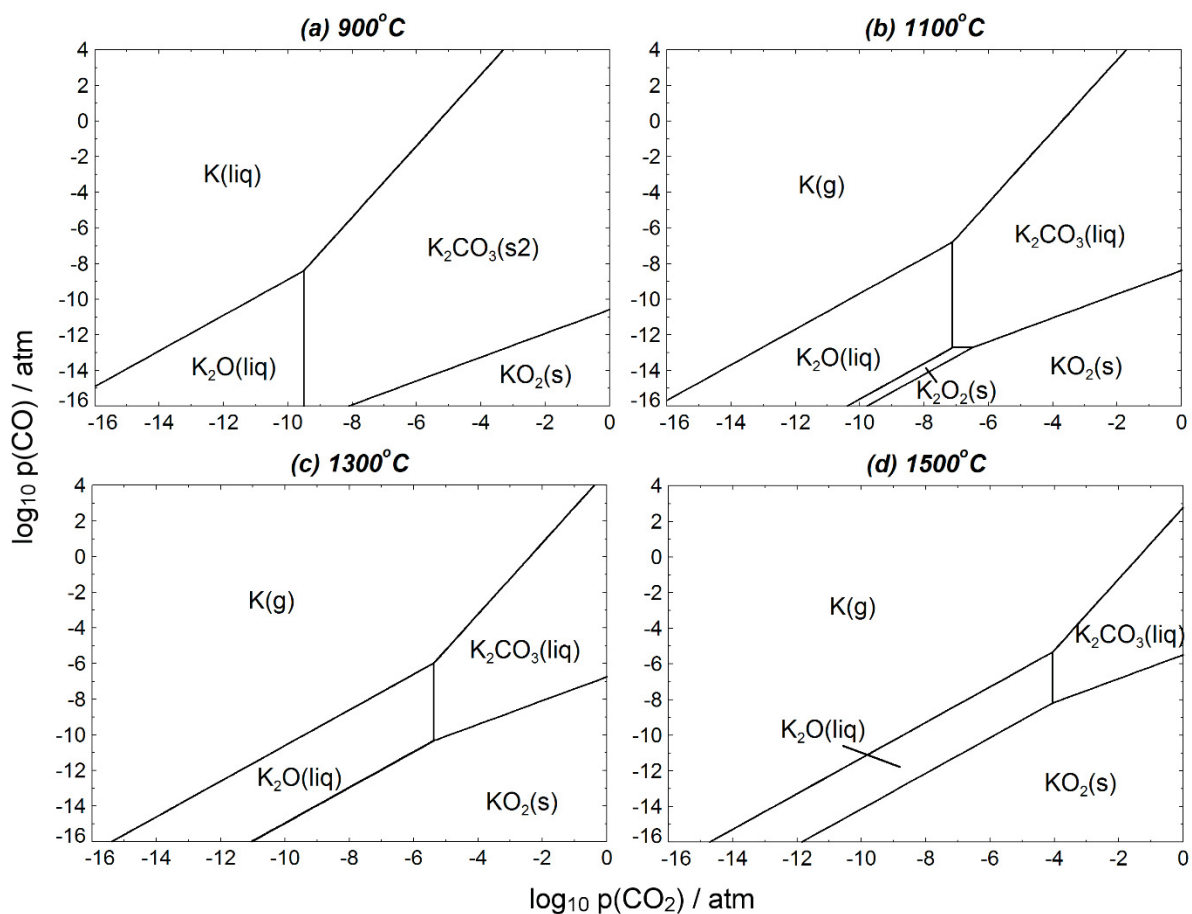
Figure 3.3: Stability diagrams for the system K-CO-CO$_2$ at different temperatures and 5 atm

In metallurgical processes, also gaseous nitrogen and water are present. **Figure 3.4** shows the stability diagrams for the same system as above at different temperatures and with constant partial pressures for nitrogen and water. A typical composition of a generator gas is specified in **Table 4-6**. The partial pressure for vapour water was set to 0.3 atm, because the ratio is 5.8 vol-% at a total pressure of 5 atm. A typical value of nitrogen content is 6.9 %, this leads to a partial pressure of 0.35 atm. With these conditions, no elemental

potassium is stable at high activity of CO. The gaseous phase, which exists in **Figure 3.4 (b-d)**, mainly consists of elemental potassium, and less potassium hydride (KH), potassium hydroxide (KOH) and potassium cyanide (KCN). Lin [20] describes that there is also gaseous KOH and NaOH formation possible in the reserve zone of a blast furnace, but in a lower amount compared to carbonate phases, which are stable in a condensed form and can precipitate at the surface of solids.
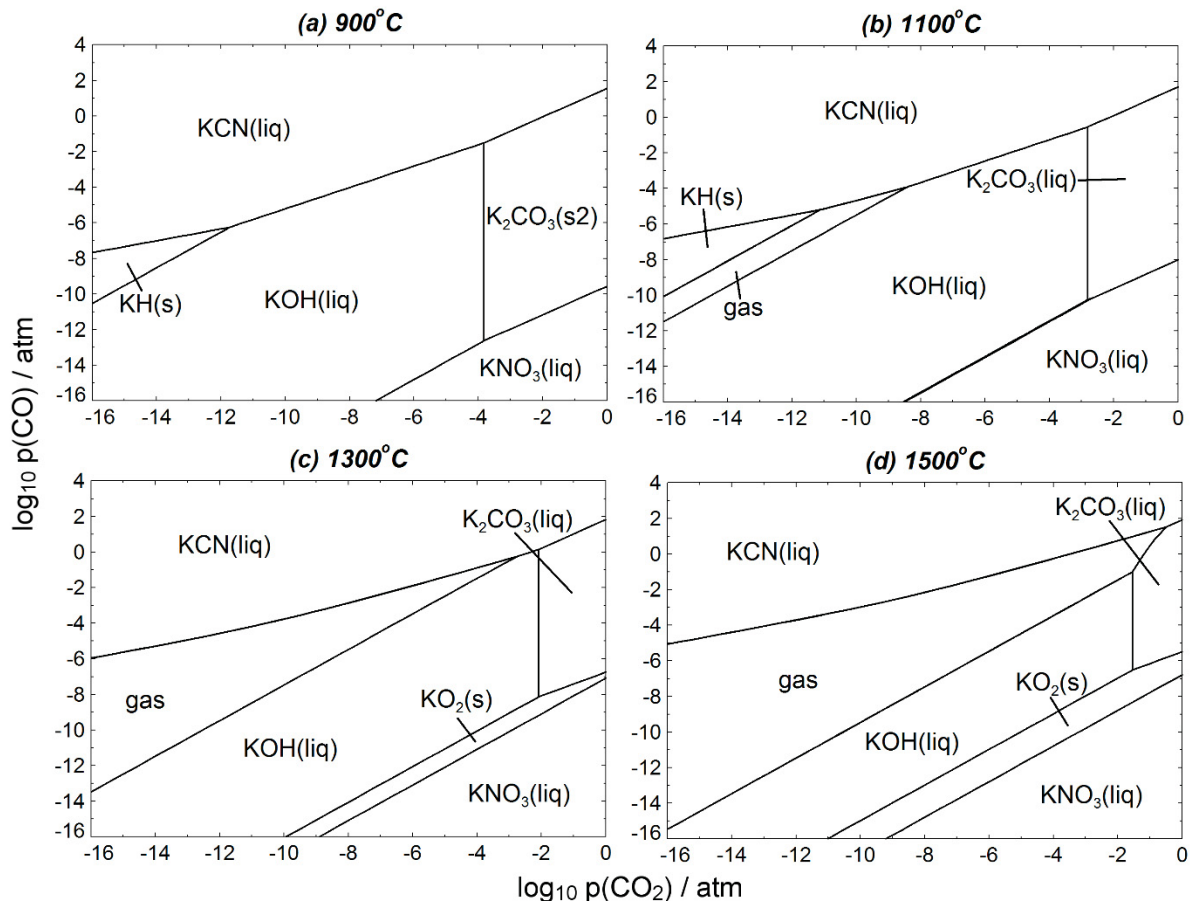
Figure 3.4: Stability diagrams for the system K-CO-CO_2 at different temperatures and 5 atm with $p(H_2O) = 0.3$ atm and $p(N_2) = 0.35$ atm

3.2 Chlorine and fluorine

Chlorine compounds are known to cause corrosion at different parts of the furnace. The effects can damage pipes of the gas distribution system, hot stoves and tuyères. Bartusch et al. [29] and other researchers investigated the main input and the behaviour of chlorine at the blast furnace process.

As main sources of chlorine coal, coke and also sinter can be identified. [20,29] There the chlorine is bound to coal in small particles with the alkalis potassium and sodium (KCl and NaCl). A minor fraction of the chlorine can also enter the furnace as part of residual coal moisture in a more complex form. The sum of all chlorine inputs into the furnace gives around 0.15 kg/t HM, where the coal is the main source with around 45 % of the whole input. The main output flow of chlorine is the top gas and dust. [20,29] **Figure 3.5** shows the input and output flows for chlorine at the blast furnace at Hüttenwerke Krupp Mannesmann (HKM).
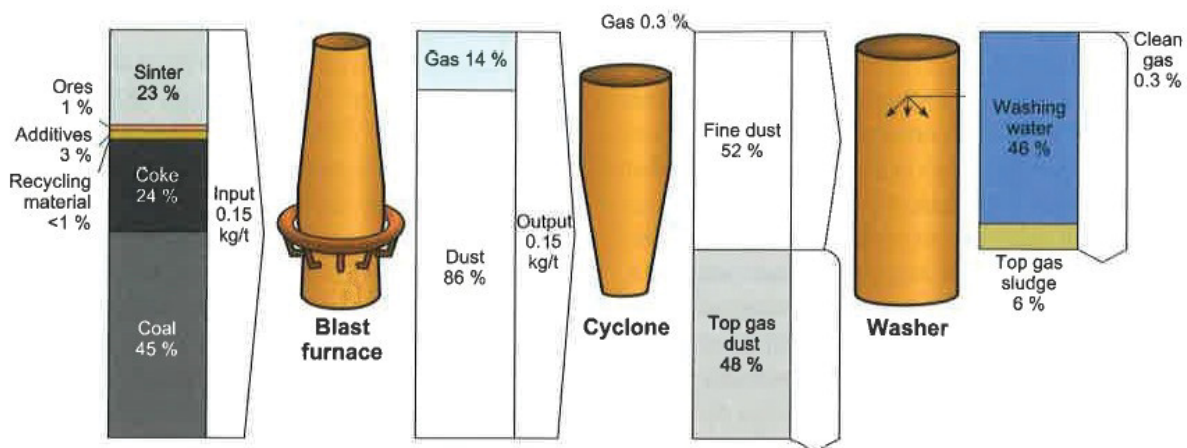
Figure 3.5: Chlorine balance: input and output flows of chlorine at HKM [29]

In metallurgical processes, the chlorine mainly forms alkali chlorides KCl and NaCl as shown from chemical equilibrium calculations. At high temperatures and chlorine concentrations or if the formation of alkali chlorides is inhibited also hydrochloric acid (HCl) and calcium chloride ($CaCl_2$) can be present. [20,29]

Bartusch et al. [29] also describe the equilibrium of chlorine compounds under blast furnace conditions. This was achieved by chemical equilibrium calculations using the FactSage software program and databases. The blast furnace was separated into different reaction zones over the height of the furnace. Each zone has different temperature and pressure conditions. The results are shown in **Figure 3.6**.
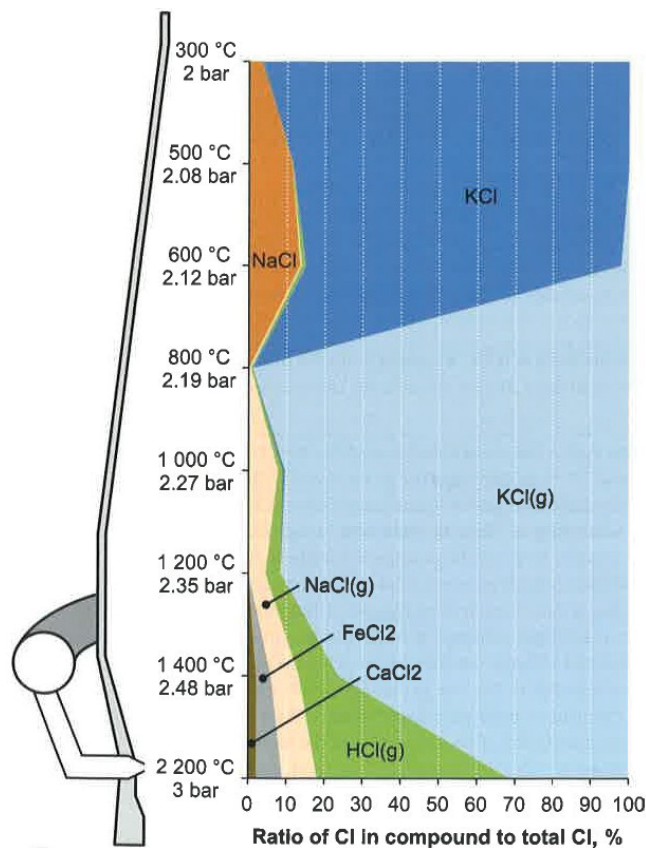
Figure 3.6: Equilibrium states of chlorine compounds at different blast furnace conditions [29]

From all possible chlorine compounds, only a few are relevant under these conditions. The alkali chlorides KCl and NaCl are present in the whole furnace, in both condensed and gaseous phase. Hydrogen chloride (HCl) and minor degrees of $FeCl_2$ and $CaCl_2$ appear at high temperatures. The cycle of chlorine is formed only by the mechanism of evaporation and condensation of alkali chlorides.

Figure 3.7 shows that the condensation occurs at around 750 °C in the throat zone of a blast furnace. In the race way about the half of the chlorine load from the coal reacts with hydrogen to form HCl. During the cooling the chemical equilibrium shifts towards the formation of alkali chlorides. A part of this alkali chlorides forms small dust particles, which are discharged with the top gas. A minor fraction of the chlorine leaves the blast furnace in the form of HCl and can be stable in the top gas even at low temperature, if it has no contact to alkalis. The effect of the Cl/K ratio on the distribution of the partial pressures has been studied by Lin [20]. As seen in **Figure 3.8** the amount of HCl in the gas phase becomes stronger, when the Cl/K ratio becomes larger than KCl stoichiometry. For Cl/K = 2, KCl and HCl amounts in the gas phase of a blast furnace are almost identical. HCl in the top gas is the main cause for corrosion in the top gas pipe system. [29]
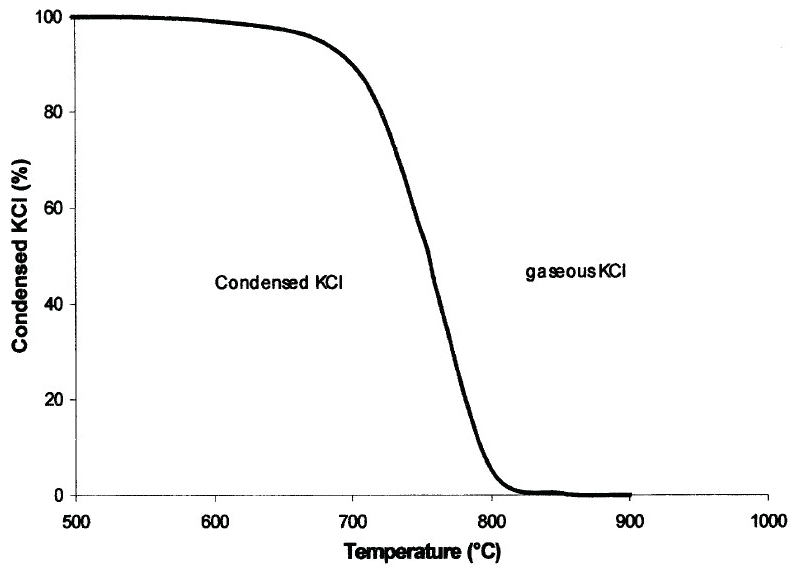
Figure 3.7: Condensation of KCl in the throat zone of a blast furnace [20]
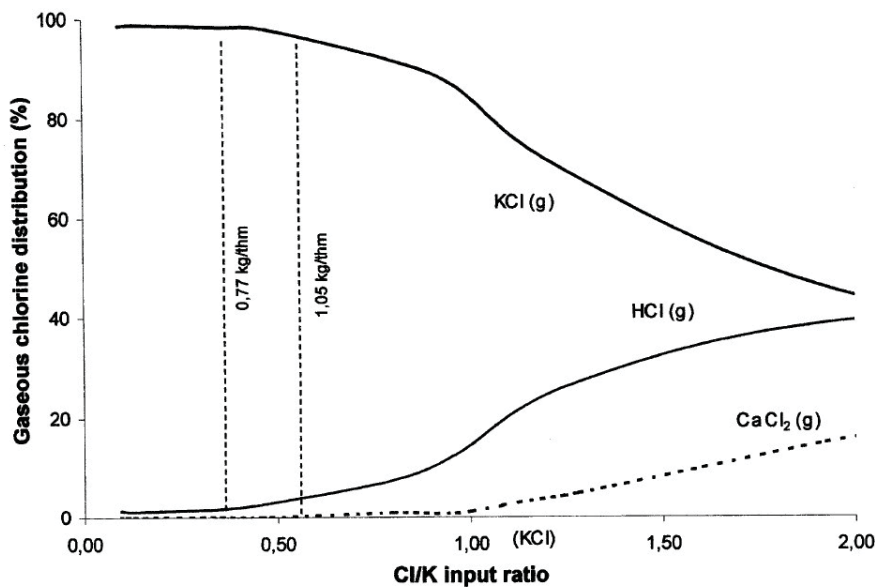
Figure 3.8: Dependence with Cl/K input ratio of the chlorine distribution in the gaseous phase in the bosh zone of a blast furnace [20]

3.2.1 Stability diagrams

The stability diagram shown in **Figure 3.9** for potassium compounds in a $CO_2/CO/Cl_2$ atmosphere was calculated with the FactSage^{TM} program and its thermochemical database FactPS. It can be seen, that the area of gaseous potassium increases with the temperature,

however, the partial pressure of Cl_2 must be under 10^{-15} atm that KCl would not be stable at 1450 °C anymore.
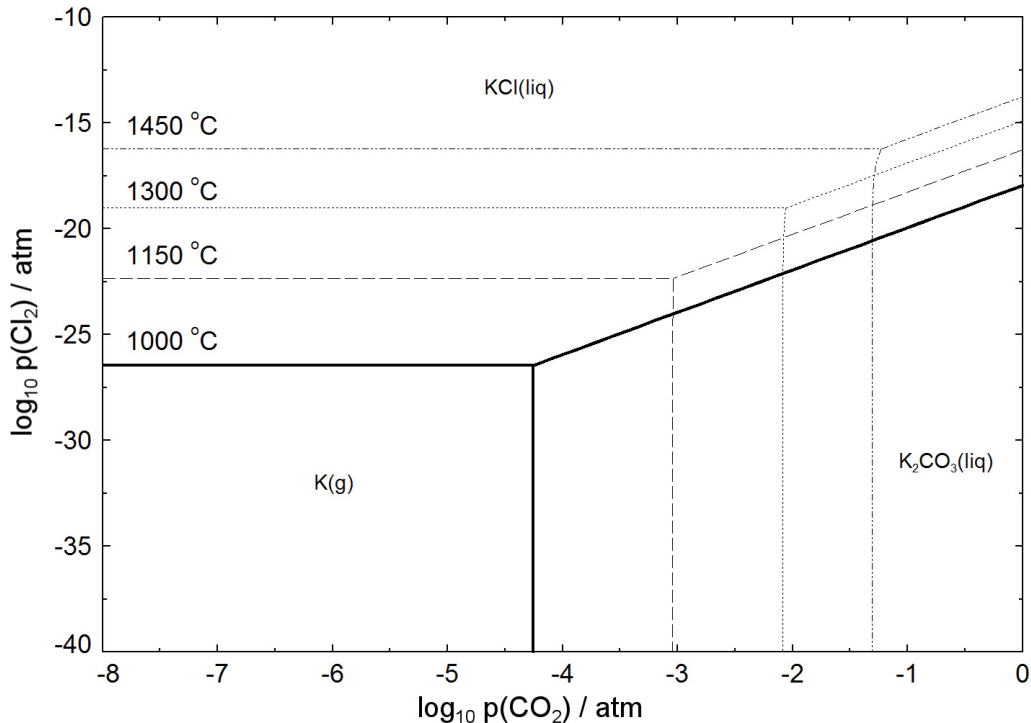
Figure 3.9: Stability diagram for the system K-CO$_2$-Cl$_2$ at 5 atm with a constant p(CO) = 4 atm

Figure 3.10 shows stability diagrams for potassium compounds at different temperatures for a total pressure of 5 atm. As seen in **Figure 3.6** the most stable chlorine compound in vapour state is hydrogen chloride (HCl), excluded alkali compounds. To illustrate the dependence of alkali compounds from chlorine, the logarithm of the partial pressure of hydrogen chloride and carbon dioxide (CO_2) were chosen as axes. The partial pressures of CO, H_2O and N_2 were kept constant, depending on their volume ratio in the generator gas. A typical composition of a generator gas is listed in **Table 4-6**. The gaseous phase in **Figure 3.10 (c)** and **(d)** mainly consists of elemental potassium, and less potassium chloride (KCl), potassium hydroxide (KOH), potassium cyanide (KCN) and potassium hydride (KH) with different concentrations depending on the partial pressure of HCl and CO_2.
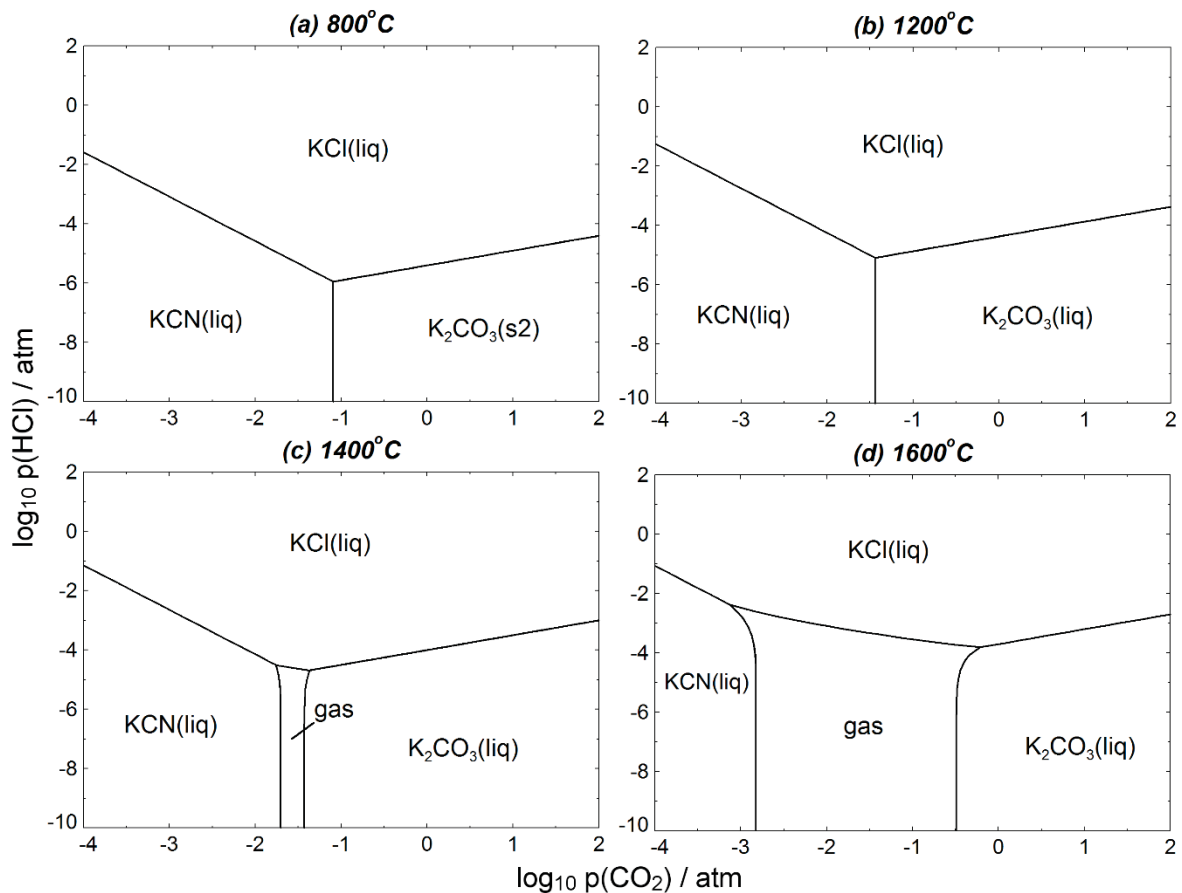
Figure 3.10: Stability diagrams for the system K-CO_2-HCl at different temperatures and 5 atm with p(CO) = 4 atm, p(H_2O) = 0.3 atm and p(N_2) = 0.35 atm

For the behaviour of fluorine at the same conditions no literature source could be found. There are no investigations by other researchers at the moment. Zabett et al. [30] describes that halides form compounds with alkalis generally. To identify stable compounds with fluoride, stability diagrams were drawn using FactSage™ and its thermodynamical databases. The results are shown in **Figure 3.11** for the system K-CO_2-HF as a function of the partial pressure of hydrogen fluoride (HF) and carbon dioxide (CO_2) at a total pressure of 5 atm with constant partial pressures for CO, H_2O and N_2, like the stability diagrams for chloride. It can be seen, that the most stable compounds under these conditions are potassium fluoride (KF), potassium cyanide (KCN) and potassium carbonate (K_2CO_3) at low temperatures. Potassium fluoride is even solid under its melting point of 857 °C. The gaseous phase, which occurs at about 1400 °C consists of elemental potassium (K) and less potassium hydroxide (KOH), potassium cyanide (KCN), potassium (K_2), potassium hydride (KH) and potassium fluoride (KF) depending on the partial pressure of HCl and CO_2.
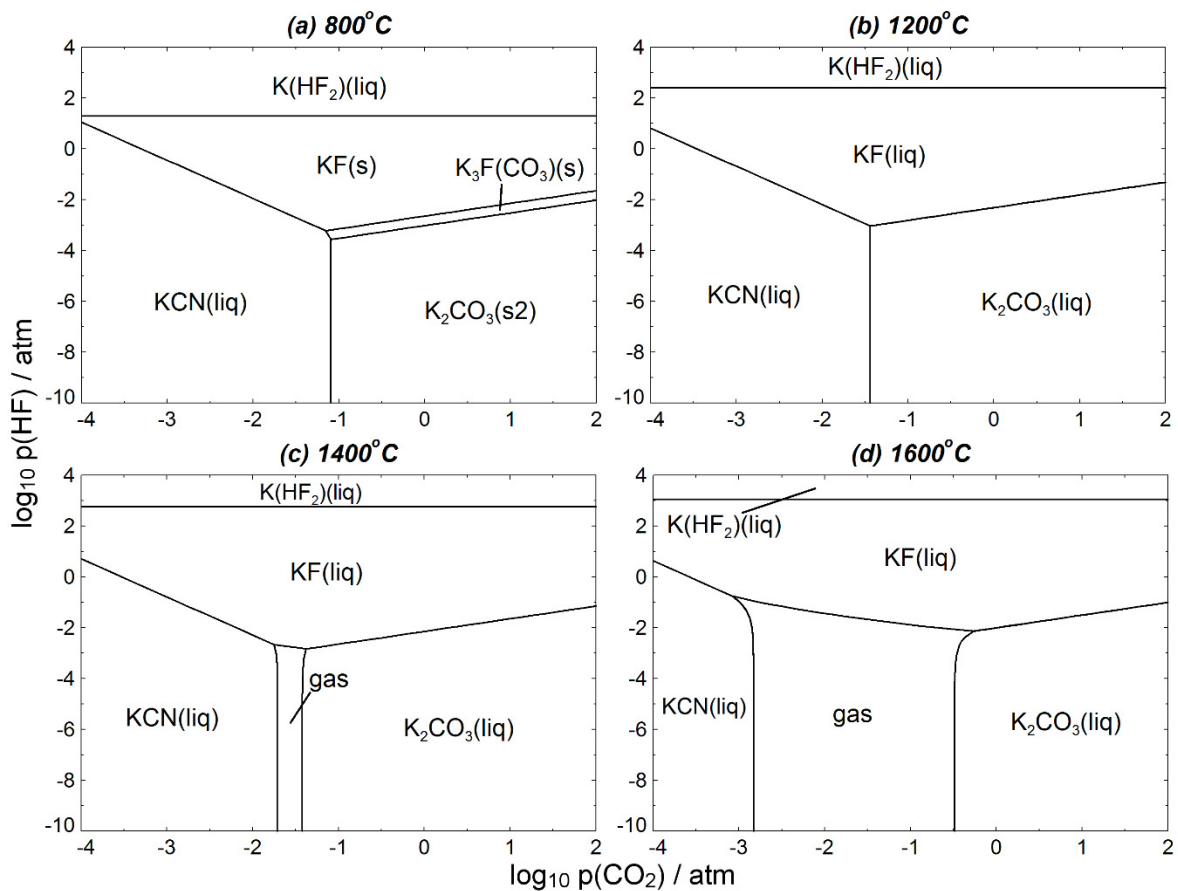
Figure 3.11: Stability diagrams for the system K-CO₂-HF at different temperatures and 5 atm with p(CO) = 4 atm, p(H₂O) = 0.3 atm and p(N₂) = 0.35 atm

To find stable chlorine and fluorine compounds it is advisable to search for the minimal Gibbs free energy of formation. Therefore, Richardson-Ellingham diagrams for selected chlorine and fluorine compounds were drawn. In such diagrams the Gibbs free energy of formation of different reactions of metals with 1 mol of gaseous chlorine (Cl_2) and fluorine (F_2), respectively, is plotted against the temperature with a total pressure of 5 atm. The thermodynamic data of FactSage™ 7.0 (Database: FactPS) were used. The results are shown in **Figure 3.12** and **Figure 3.13**, respectively.

The most stable compounds are located at lowest values for the Gibbs free energy of formation. It can be seen, that in case of chlorine, there are the two alkali compounds, potassium and sodium chloride, and calcium chloride. For the blast furnace process, Bartusch et al. [29] also calculated these compounds and additionally iron(II) chloride ($FeCl_2$) and hydrogen chloride (HCl) during the absence of alkalis (see **Figure 3.6**). The most stable compounds with fluoride are calcium fluoride (CaF_2), potassium fluoride (KF), sodium fluoride (NaF) and magnesium fluoride (MgF_2).
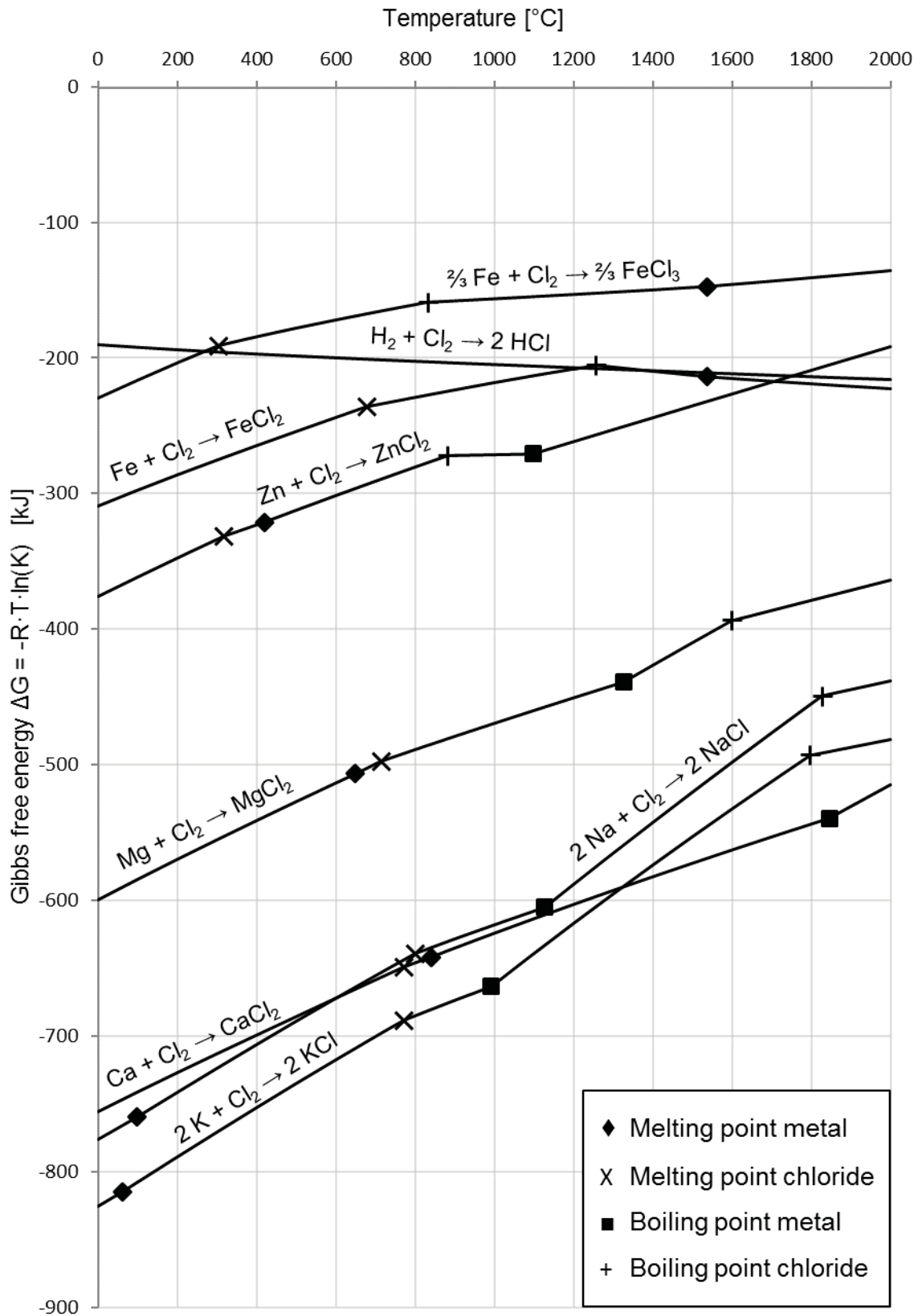
Figure 3.12: Richardson-Ellingham diagram for selected chlorides at 5 atm
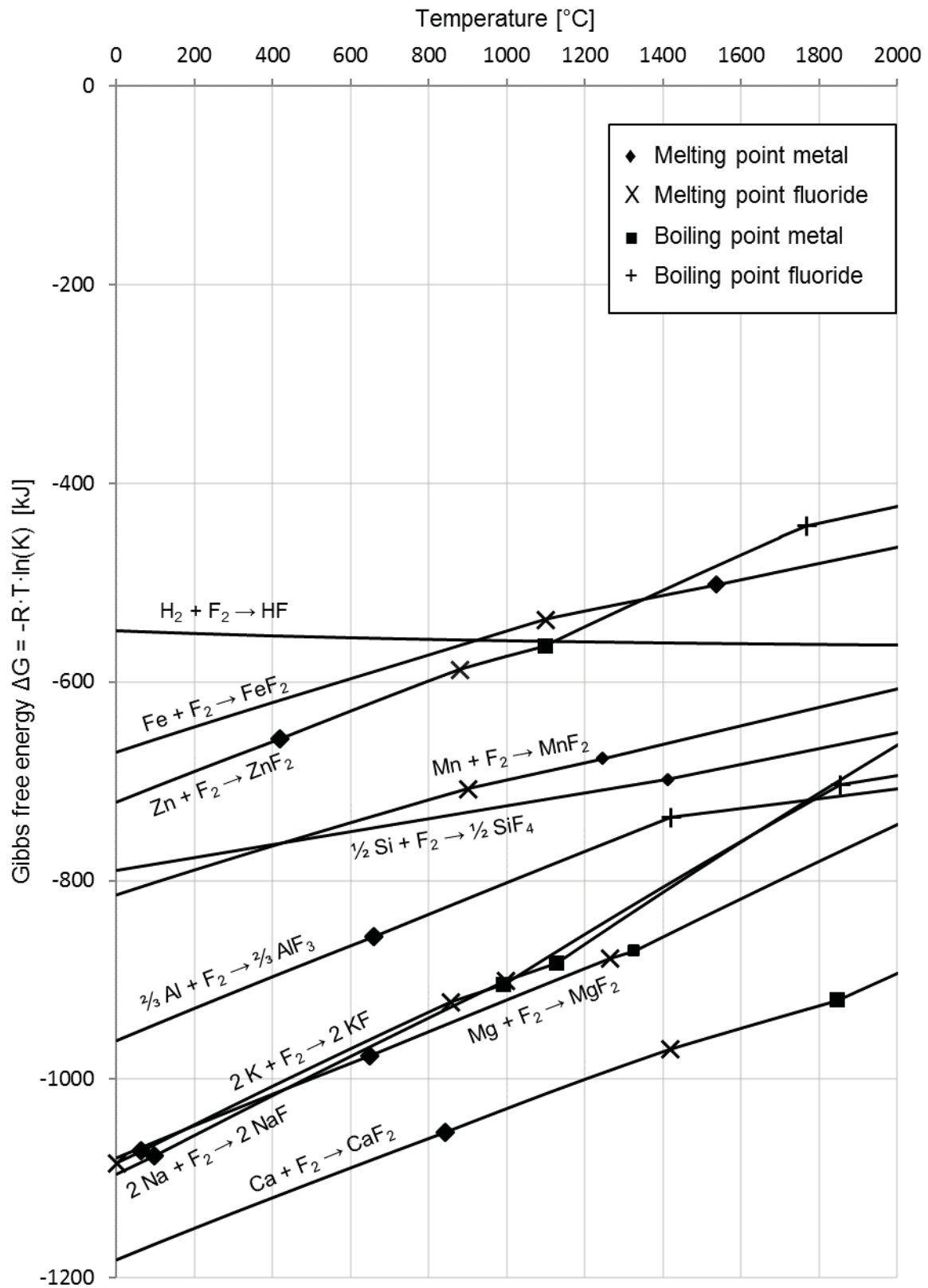
Figure 3.13: Richardson-Ellingham diagram for selected fluorides at 5 atm

3.3 Zinc

Zinc is charged into the furnace in form of oxides (ZnO), ferrites (ZnO·Fe$_2$O$_3$), silicates (2 ZnO·SiO$_2$) and sulphides (ZnS). The ore is the main source for zinc. Esezobor [31] and Pilz [25] refer contents from 0.09 kg per tHM up to 1 kg per tHM for a blast furnace. A high value for zinc input results from high amount of return materials.

Inside the furnace the zinc compounds could be reduced, vaporized, condensed and oxidized, which leads to a cycle of zinc within the furnace. The oxidised zinc (ZnO) penetrates regions with large surface areas such as pores, cracks and masonry. The linear expansion of zinc is higher than that of the refractory, consequently these areas cause severe damage. [31]

The zinc leaves the furnace mainly with the top gas as dust or gaseous compound (0.11 - 4.3 % of total top gas). Less amounts are contained in the hot metal (0.01 - 0.065 % of total hot metal) and the slag (0.002 - 0.006 % of total slag amount). A further part stays in the furnace in form of deposits at the brick lining or as circulating material. [25]

3.3.1 Different compounds and their reactions

Esezobor [31] investigated the zinc accumulation in the blast furnace and refers the reduction of zinc oxide, ferrite and silicate with the **equations (3-18)** to **(3-21)**. **Figure 3.15** shows the mechanism of zinc reduction, oxidation and circulation in a blast furnace. It can be seen, that the reduction starts at a temperature range between 900 and 1000 °C (1173 to 1273 K).

$$ZnO + CO(g) \rightarrow Zn(g) + CO_2(g) \tag{3-18}$$

$$ZnO \cdot Fe_2O_3 + 2\,CO(g) \rightarrow Zn(g) + 2\,CO_2(g) + 2\,FeO \tag{3-19}$$

$$ZnO \cdot SiO_2 + CO(g) \rightarrow Zn(g) + CO_2(g) + SiO_2 \tag{3-20}$$

$$ZnFe_2O_4\,(ZnSiO_3) + 3\,C \rightarrow Zn(g) + 3\,CO(g) + 2\,FeO\,(SiO_2) \tag{3-21}$$
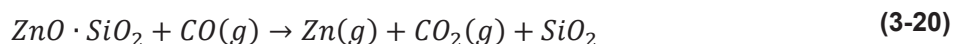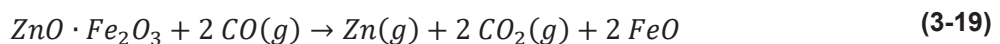
Zinc sulphide is not roasted in the furnace because there is no free oxygen in the atmosphere. Furthermore, it does not react with the calcium oxide (CaO) and carbon to form zinc oxide (ZnO) and calcium sulphite (CaS) and carbon monoxide (CO). The most probable reaction is with iron, due to a excellent mixture, according to **equation (3-22)** [25].

$$ZnS + Fe \rightarrow Zn + FeS \tag{3-22}$$

The Gibbs free energy as a function of temperature for the different reactions of 1 mol of zinc species is plotted in **Figure 3.14**. The total pressure is defined to 5 atm, and the partial pressures of CO, CO_2 and Zn were set to 4, 0.6 (80 % CO, 12 % CO_2) and 0.01 atm, respectively. The calculations were done with FactSage^{TM} 7.0 and its thermochemical data. It can be seen that the reduction of zinc ferrite is possible above 690 °C, for the oxide above 800 °C, for the silicate above 900 °C and the sulphide will be reduced above 1000 °C. The reduction temperatures increase rapidly if the partial pressure of zinc increases or the CO/CO_2 ratio decreases.
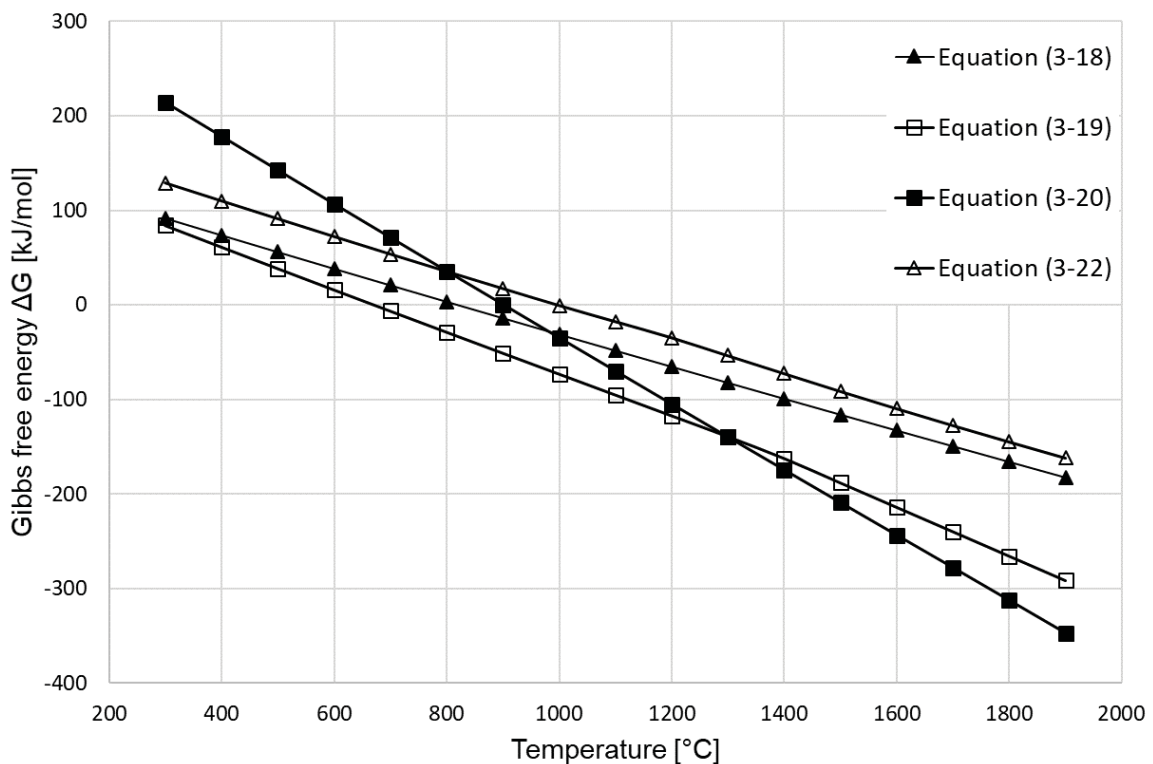
Figure 3.14: Gibbs free energy vs. temperature for different reactions of zinc compounds with a total pressure of 5 atm and p(CO) = 4 atm, p(CO₂) = 0.6 atm and p(Zn) = 0.01 atm

Bronson [32] describes in his thesis that the reoxidation of the vapour zinc mainly proceeds with carbon dioxide (CO_2) and water steam (H_2O) according to the **equations (3-23)** and **(3-24)**.

$$Zn(g) + CO_2(g) \rightarrow ZnO + CO(g) \qquad \textbf{(3-23)}$$

$$Zn(g) + H_2O(g) \rightarrow ZnO + H_2(g) \qquad \textbf{(3-24)}$$
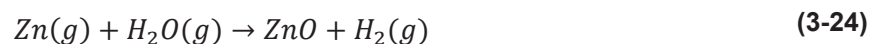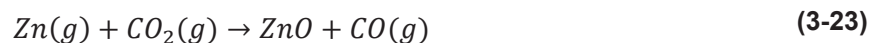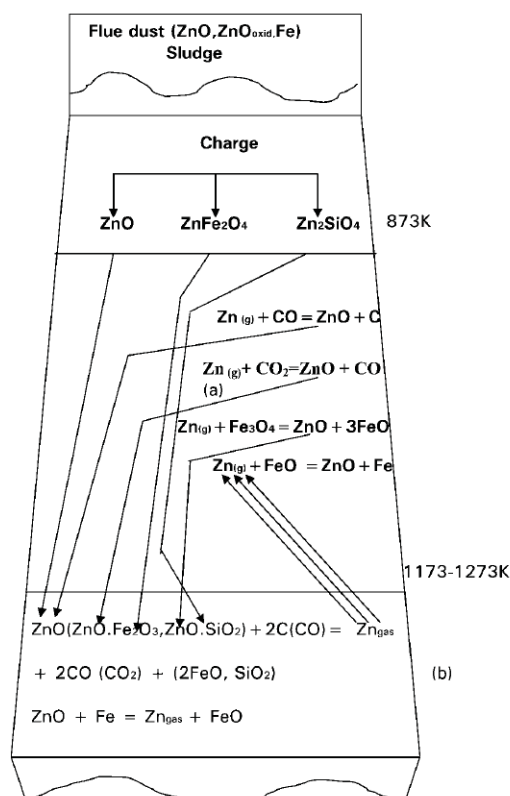
Figure 3.15: Mechanism of zinc reduction, oxidation and circulation in a blast furnace [31]

According to **equation (3-23)** the Gibbs free energy for the oxidation of zinc by carbon dioxide is shown in **Figure 3.16**. It can be seen that at a lower zinc partial pressure and under reducing conditions (p_{Zn} = 10^{-4}, CO_2/CO = 1/9) the formation of zinc oxide is only favourable at temperatures below 770 °C. At higher zinc partial pressures and oxidizing conditions (p_{Zn} = 10^{-2}, CO_2/CO = 40/7) the formation of zinc oxide can occur below 1300 °C. [32]
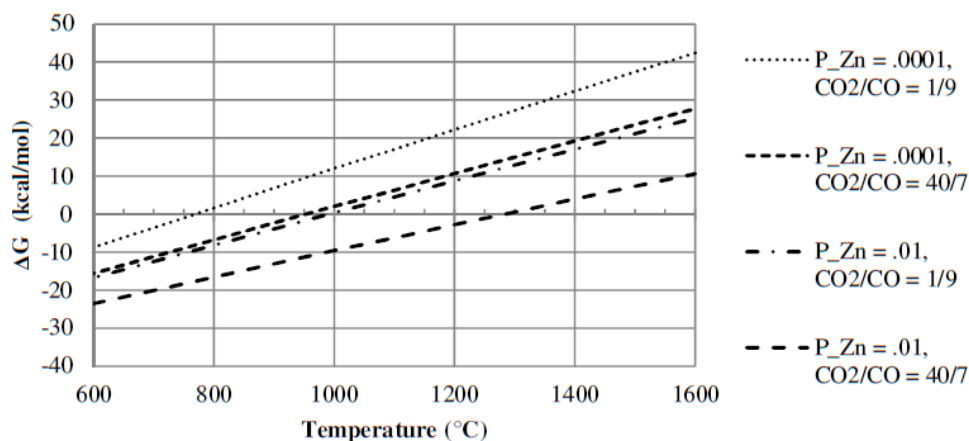
Figure 3.16: Gibbs free energy for zinc oxidation by CO_2 [32]

Figure 3.17 shows the change in Gibbs free energy for the oxidation of zinc by water vapour, according to **equation (3-24)**. Under a lower zinc partial pressure and reducing conditions (p_{Zn} = 10^{-4}, H_2O/H_2 = 15/2) the formation of zinc oxide is only favourable at temperatures below 980 °C. It can also be observed, that at a higher zinc partial pressure and oxidizing conditions (p_{Zn} = 10^{-2}, H_2O/H_2 = 50/1) the formation of zinc oxide if favourable at temperatures below 1430 °C. [32]

Bronson [32] also describes that the formation of zinc ferrite spinel ($ZnFe_2O_4$) is minimal according to equilibrium calculations. **Figure 3.18** shows the equilibrium composition for solid phases in a gas environment with 25 % H_2O, 1 % Zn(g) and CO_2/CO ratio of 1. It can be seen, that the equilibrium amount of the spinel phase is less than 1 % of the total moles of the solid phase. Therefore, it can be assumed that the formation of $ZnFe_2O_4$ is not favourable in the FINEX® process.
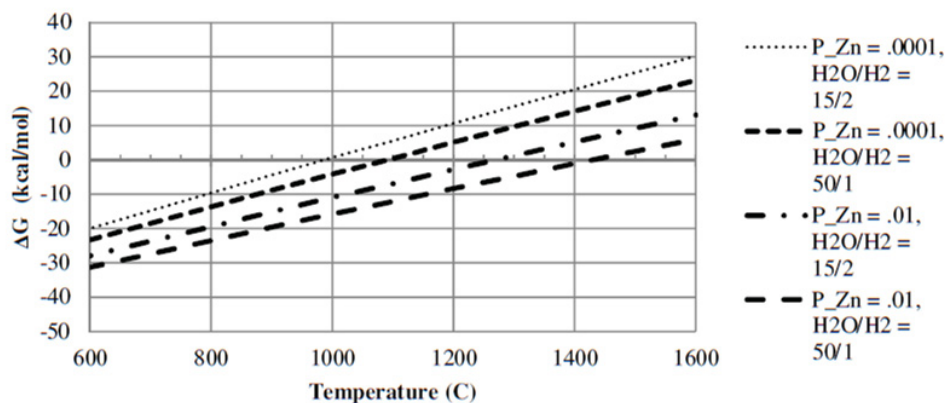
Figure 3.17: Gibbs free energy for zinc oxidation by H_2O [32]
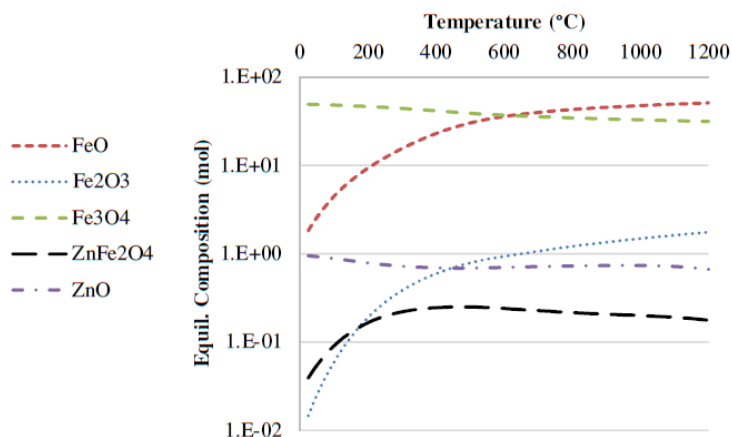
Figure 3.18: Equilibrium composition vs. temperature for a mixture for a 100 mol gas phase
(25 % H_2O, 1 % Zn, balance with CO_2/CO = 1) and
100 mol solid phase (50 % FeO, 50 % Fe_2O_3) [32]

Another important reaction in the system is the water-gas shift reaction (WGSR) described in **equation (3-25)**:

$$H_2O + CO \rightarrow H_2 + CO_2$$

<div align="right">**(3-25)**</div>

This reaction can occur whenever there is significant amount of water vapour and carbon monoxide in the system. An addition of 5 % H_2O to a system of CO, CO_2 and Zn does not effect the highest temperature fo ZnO deposition greatly, due to the WGSR. However, water steam can change the gas composition and therefore it effects the rate of deposition. [32,33]

Clark and Fray [34] investigated the morphology of depositions on a silica reactor during an experimental study. They found that the morphology is a function of temperature and partial pressure of zinc. At low temperatures (< 800 °C) and high zinc partial pressures (p_{Zn} = 0.04 to 0.08 atm), the deposits were coarse and large-grained. At higher temperatures (> 800 °C) and lower zinc partial pressures (p_{Zn} = 0 to 0.04 atm), the deposits were found to be fine-grained.

The reactions of zinc compounds with chlorine are also important. De Micco et al. [35] investigated the isothermal and non-isothermal chlorination of ZnO powder in a thermogravimetric analyser. The reactions of ZnO to form solid, liquid and gaseous $ZnCl_2$ are shown in **equation (3-26)**. They also mention the further reaction of $ZnCl_2$ with the oxygen, according to **equation (3-27)**. With a combination of **equation (3-26)** and **(3-27)** it is possible to obtain the formation of zinc oxychloride ZnOCl (**equation (3-28)**). However, the detection of ZnOCl was only reported for high pressures of O_2 (between 0.1 and 0.6 atm) and not for a pure Ar-Cl_2 atmosphere. Hence, ZnOCl is not formed inside the FINEX® process, due to the reducing atmosphere.

$$ZnO(s) + Cl_2(g) \rightarrow ZnCl_2(s,l,g) + \frac{1}{2}O_2(g)$$

<div align="right">**(3-26)**</div>

$$ZnCl_2(g) + \frac{1}{2}O_2(g) \rightarrow ZnOCl(g) + \frac{1}{2}Cl_2(g)$$

<div align="right">**(3-27)**</div>

$$ZnO(s) + \frac{1}{2}Cl_2(g) \rightarrow ZnOCl(g)$$

<div align="right">**(3-28)**</div>
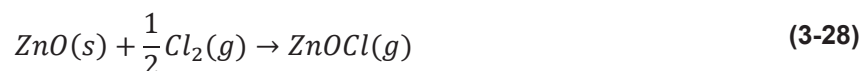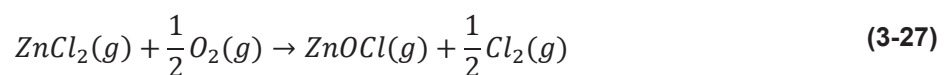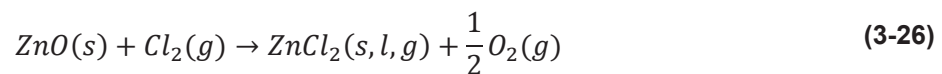
De Micco et al. [35] further determined that the zinc oxide powder starts slowly to lose mass at about 500 K and the mass loss increases significantly at approximately 720 K, denoting the formation of gaseous $ZnCl_2$. This is shown in **Figure 3.19**.
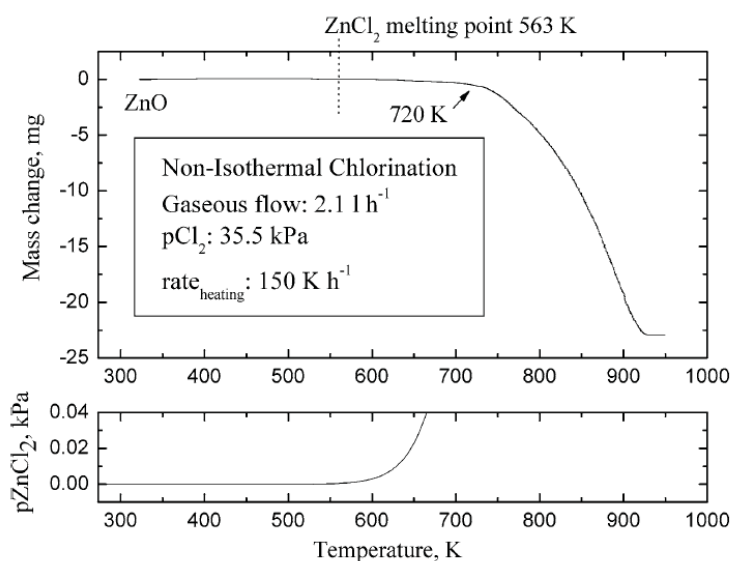
Figure 3.19: Thermogravimetric curve, mass loss of ZnO powder and partial pressure of ZnCl₂ [35]

Contrary to temperature, chlorine partial pressure has a slight influence on the reaction rate. De Micco et al. [35] varied the partial pressure of chlorine from 15 to 70 kPa during the chlorination of the same sample (40 mg ZnO powder). **Figure 3.20** shows the results for 873 K. It can be seen, that the mass loss increases with the partial pressure of chlorine (pCl_2). α indicates the reaction degree.
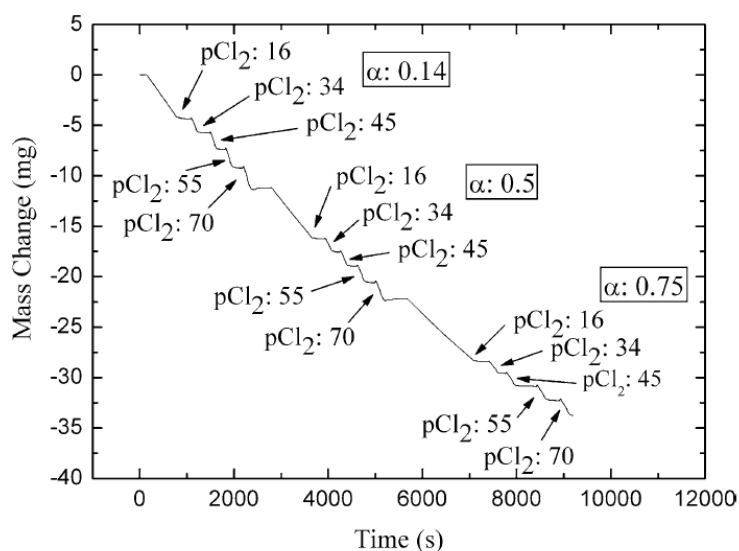
Figure 3.20: Thermogravimetric curve for the chlorination of 40 mg ZnO powder with partial pressures of chlorine between 0.16 and 0.7 bar [35]

Pickles [36] describes the thermodynamics of chlorination reactions for the pyrometall-urgical treatment of electric arc furnace dust. In this paper the carbochlorination of ZnO with gaseous chlorine and carbon is mentioned, according to **equation (3-29)**. The Gibbs free energy as a function of temperature for both the chlorination and the carbochlorination are shown in **Figure 3.21**. This diagram was drawn with FactSage™ 7.0. A comparison of the two reactions shows that the carbochlorination has a much lower free energy due to the formation of carbon monoxide, which is stable at high temperatures. [36]

$$ZnO + Cl_2(g) + C \rightarrow ZnCl_2(g) + CO(g) \tag{3-29}$$

Equation (3-30) and **(3-31)** show the chlorination and carbochlorination of zinc ferrite. **Figure 3.22** demonstrates the effect of temperature in the range of 298 K to 1998 K on the behaviours of the zinc species. It can be seen, that the major species at room temperature are zinc silicate, zinc ferrite and condensed zinc chloride. At about 900 K, gaseous zinc chloride begins to form in ever-increasing amounts and this consumes the other zinc-containing species. Consequently, their amounts continuously decrease. Additionally, a small amount of gaseous metallic zinc is formed at higher temperatures. [36]

$$ZnO \cdot Fe_2O_3 + Cl_2(g) \rightarrow ZnCl_2(g) + Fe_2O_3 + \frac{1}{2}O_2(g) \tag{3-30}$$

$$ZnO \cdot Fe_2O_3 + Cl_2(g) + C \rightarrow ZnCl_2(g) + Fe_2O_3 + CO(g) \tag{3-31}$$
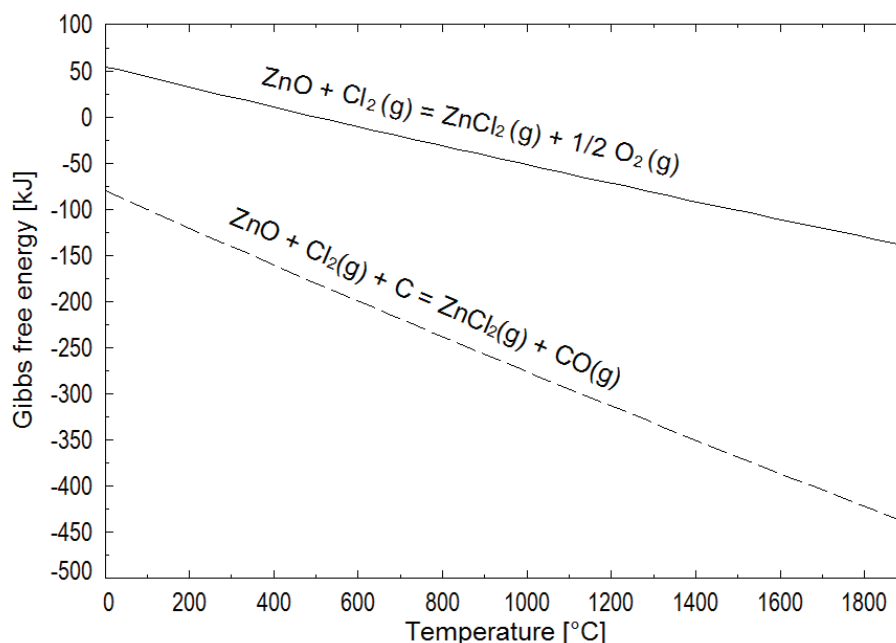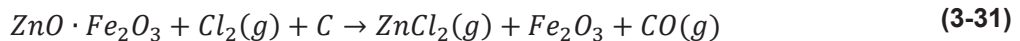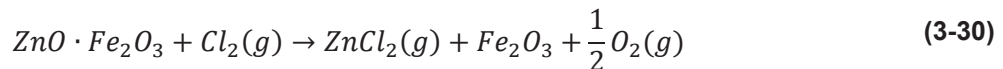
Figure 3.21: Gibbs free energy for chlorination and carbochlorination of ZnO for p = 1 atm
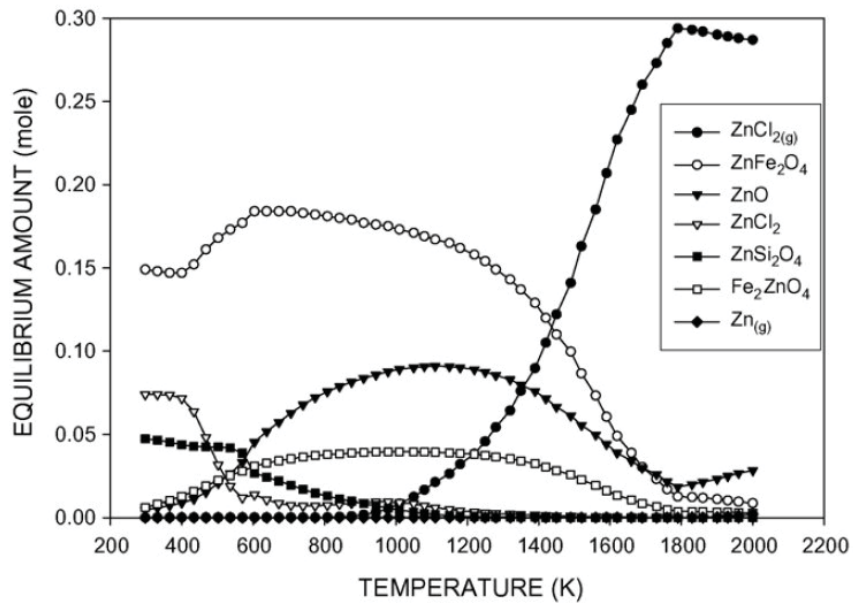
Figure 3.22: Equilibrium amounts of zinc-containing species as a function of temperature [36]

4 Investigations of circuit flows

In the following chapter, an evaluation of industrial data of a FINEX® process is shown. Sankey diagrams for potassium and sodium are devolved based on process data measurements and material samplings executed at different locations of a FINEX® plant.

4.1 Evaluation of industrial data

For the following Sankey diagrams in **chapter 4.1.1** the data of PTAT (Primetals Technologies Austria GmbH) [37] were used. They show the mass flow of alkalis at a Finex® plant. The fluidised bed reactor (FB), the melter gasifier (MG) and the hot gas cyclone (HGC) are used as various stages. The thickness of the arrows represents the mass ratio of the alkalis flowing in and out of the different stages. Between these stages, measurements were performed or a separation rate was assumed. Then the amount of potassium and sodium was calculated.

In the data tables for potassium and sodium (**Table 4-1** and **Table 4-2**, respectively) the values for PtInp mean the percentage of total input of potassium or sodium from ore, additives and coal calculated according to **equation (4-1)**:

$$PtInp = \frac{mass\ of\ alkali\ [\frac{kg}{tHM}]}{mass\ of\ total\ input\ of\ alkali\ [\frac{kg}{tHM}]} \cdot 100\ [\%] \qquad \textbf{(4-1)}$$

The total input of iron ore into the melter gasifier was set to 281.2 tons per hour and that for the additives to 23.95 tons per hour. The total production rate is 180 tons of hot metal per

hour. The slag amount is 326 kg per ton hot metal. The separation rate inside the fluidised bed reactor was set to 9:1, that means that only ten percent of the alkali oxides leave the fluidized bed reactor with the top gas.

4.1.1 Sankey-Diagrams

Figure 4.1 shows the Sankey diagram for the mass flow of potassium in different stages of the FINEX® plant. The input and output amounts are illustrated in **Table 4-1**. The total load of potassium in the iron ore is 0.008 %, that of the additives 0.058 %. This equates a total amount of 0.207 kg potassium per ton hot metal. The diagram clearly illustrates that a high amount of potassium circulates between the melter gasifier and the hot gas cyclone. The ratio of potassium oxide in the slag is 0.9 %, that equates to 2.4 kg K per ton hot metal for a total slag amount of 326 kg per ton hot metal. This means that only 6.44 % of the total alkali load in the melter gasifier leaves the furnace with the slag. The output of the fluidized bed reactor with the top gas is only 10 %, or 0.2 kg K per ton hot metal. Furthermore, the potassium load of the generator gas and HGC dust is more than 1000 %, i.e. for every ton hot metal the circulating mass is ten times higher than the total input mass.

Table 4-1: Data for Sankey diagram of potassium

Input FB	[kg/tHM]	[%]	Output FB	[kg/tHM]	[%]	PtInp [%]
Ore	0.13	5.57	DRI	2.097	90	65.55
Additives	0.077	3.32	Top Gas	0.233	10	7.28
Reducing Gas	2.123	91.12				
Sum	2.33	100	Sum	2.33	100	

Input MG	[kg/tHM]	[%]	Output MG	[kg/tHM]	[%]	PtInp [%]
Coal	2.992	7.91	Slag	2.436	6.44	76.15
HGC dust	32.731	86.54	Generator Gas	35.385	93.56	1106.13
DRI	2.097	5.54				
Sum	37.821	100	Sum	37.821	100	

Input HGC	[kg/tHM]	[%]	Output HGC	[kg/tHM]	[%]	PtInp [%]
Generator Gas	35.385	100	HGC dust	32.731	92.5	1023.16
Cooling Gas	0	0	Reducing Gas	2.123	6	66.36
			Cooling Gas	0.531	1.5	16.60
Sum	35.385	100	Sum	35.385	100	
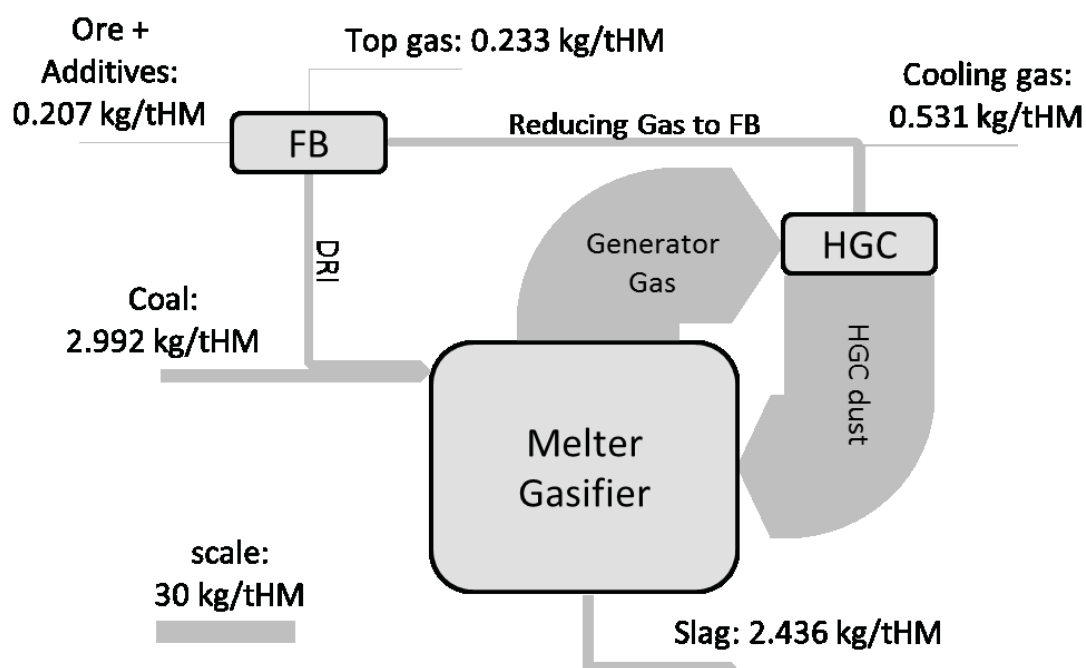
Figure 4.1: Sankey diagram for the mass flow of potassium

A similar diagram was developed for the mass flow of sodium, as shown in **Figure 4.2**. The data are given in **Table 4-2**. The total ratio of sodium in the iron ore is 0.015 %, that in the additives 0.007 %. This results in 0.242 kg Na per ton hot metal or 14.07 % of the total load in the fluidised bed reactor. The content of sodium oxide in the slag is 0.7 %, This are 1.69 kg Na per ton hot metal for a total slag amount of 326 kg per ton hot metal. Exactly as for potassium, the circulating sodium mass in the generator gas and HGC dust is more than ten times higher than the total input mass, as seen for the values of PtInp.

Table 4-3 and **Figure 4.3** show the data and Sankey diagram for the mass flow of zinc inside the FINEX® process. The data were provided from Primetals Technologies Austria GmbH. As there were no data available for zinc inside the input materials and hot metal, the diagram must be handled with caution. Furthermore, the dust concentration measurements varied largely (about 60 %).

Table 4-2: Data for Sankey diagram of sodium

Input FB	[kg/tHM]	[%]	Output FB	[kg/tHM]	[%]	PtInp [%]
Ore	0.232	13.5	DRI	1.546	90	69.20
Additives	0.010	0.57	Top Gas	0.172	10	7.70
Reducing Gas	1.476	85.93				
Sum	1.718	100	Sum	1.718	100	

Input MG	[kg/tHM]	[%]	Output MG	[kg/tHM]	[%]	
Coal	1.992	7.58	Slag	1.693	6.44	75.78
HGC dust	22.752	86.54	Generator Gas	24.597	93.56	1101.03
DRI	1.546	5.88				
Sum	26.290	100	Sum	26.290	100	

Input HGC	[kg/tHM]	[%]	Output HGC	[kg/tHM]	[%]	
Generator Gas	24.597	100	HGC dust	22.752	92.5	1018.44
Cooling Gas	0	0	Reducing Gas	1.476	6	66.07
			Cooling Gas	0.369	1.5	16.52
Sum	24.597	100	Sum	24.597	100	
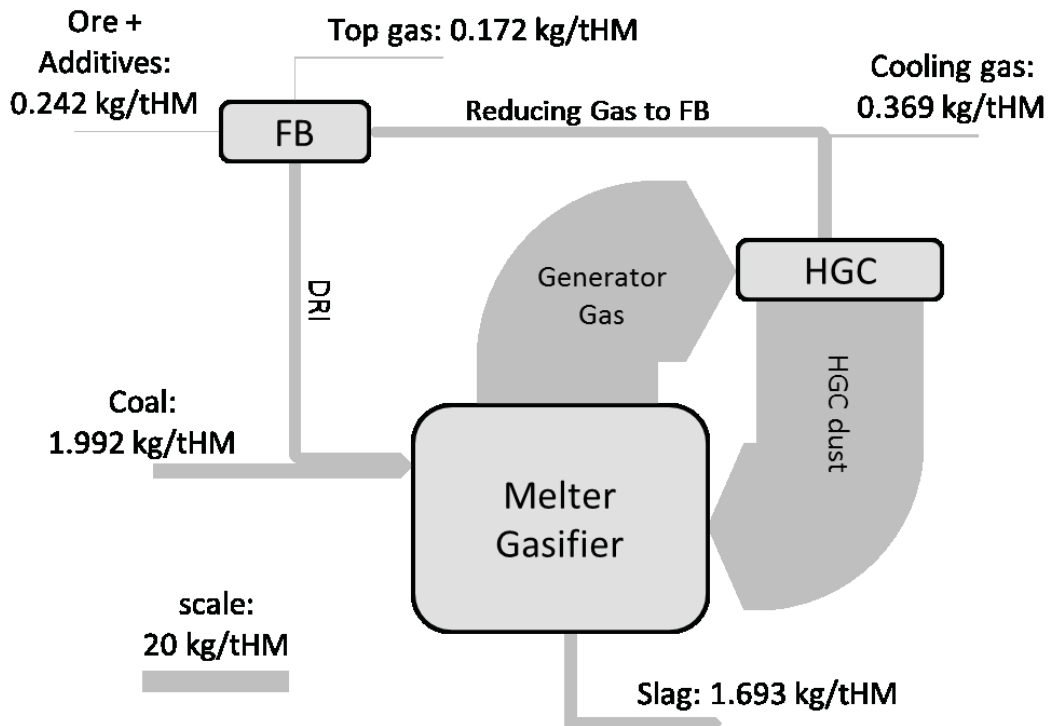
Figure 4.2: Sankey diagram for the mass flow of sodium

Table 4-3: Data for Sankey diagram of zinc

Input FB	[kg/tHM]	[%]	Output FB	[kg/tHM]	[%]
Ore	n.d.	--	DRI	0.078	94.27
Additives	n.d.	--	Top Gas	0.005	5.73
Reducing Gas	0.055	--			
Sum	0.055	0	Sum	0.083	100

Input MG	[kg/tHM]	[%]	Output MG	[kg/tHM]	[%]
Coal	n.d.	--	Slag	0.004	2.51
HGC dust	0.110	--	Generator Gas	0.155	97.49
DRI	0.078	--			
Sum	0.188	0	Sum	0.159	100

Input HGC	[kg/tHM]	[%]	Output HGC	[kg/tHM]	[%]
Generator Gas	0.155	100	HGC dust	0.110	70.96
Cooling Gas	0.000	0	Reducing Gas	0.055	23.23
			Cooling Gas	0.023	5.81
Sum	0.155	100	Sum	0.188	100
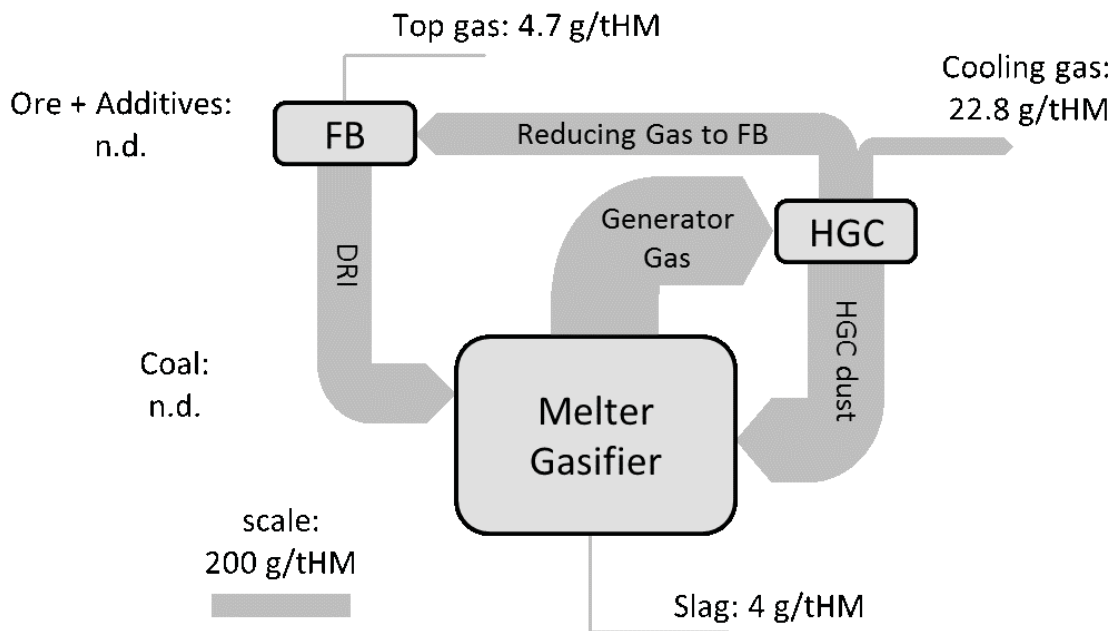
Figure 4.3: Sankey diagram for the mass flow of zinc

n.d.: no data available

4.2 Thermochemical model of the FINEX® process

For the thermochemical model and the calculation of the circuit flows, the FINEX® process is divided into different zones and stages. Each zone and stage has typical reaction conditions, which are given by the gas composition, gas amount, the total pressure and the temperature. The melter gasifier consists of six different zones and a slag zone. Two other zones are determined with the hot gas cyclone and the fluidized bed reactor. So, the whole process consists of totally nine different zones. Because the melter gasifier's zones are ordered in horizontal position across the height, each zone is split in a hot and a cold area with different temperatures. The hot zone is located at the outer range near the refractory lining and the cold zone in the middle of the reactor. The hot gas cyclone and the fluidised bed reactor are simulated just with one temperature.

The simulation runs by using two different software programs. Microsoft Office Excel© is used to define the process parameters and set the input amounts and analysis. The considering calculation is done with the programme FactSage™ 7.0 (Database: FactPS) including macro commands. An overview of the single process steps and their connections are given in **Figure 4.4**. The macro file links the Excel© file with the FactSage™ Equilib module to get the mass compositions and parameters (temperature and pressure) for the calculation. After the stable equilibrium phases are calculated, the results are sent back to the Excel file. This is executed for each zone.

The simulation is an iterative process. After a zone is calculated, the stable gaseous compounds and a given ratio of solid and liquid compounds (as dust) get into the upper zones, whereas the other part of solids and liquids descend into lower zones of the reactor. The cycle of the chemical species starts to build up. Depending on the process parameters, it takes about 100 to 300 iteration steps to get steady-state process conditions. **Chapter 4.2.2** describes this multi-stage reactor model more in detail.

The results can be seen in the Excel© sheet in different units and graphical illustrations. A Sankey diagram can be drawn automatically by using Visual Basic for Applications (VBA) in the Excel file.
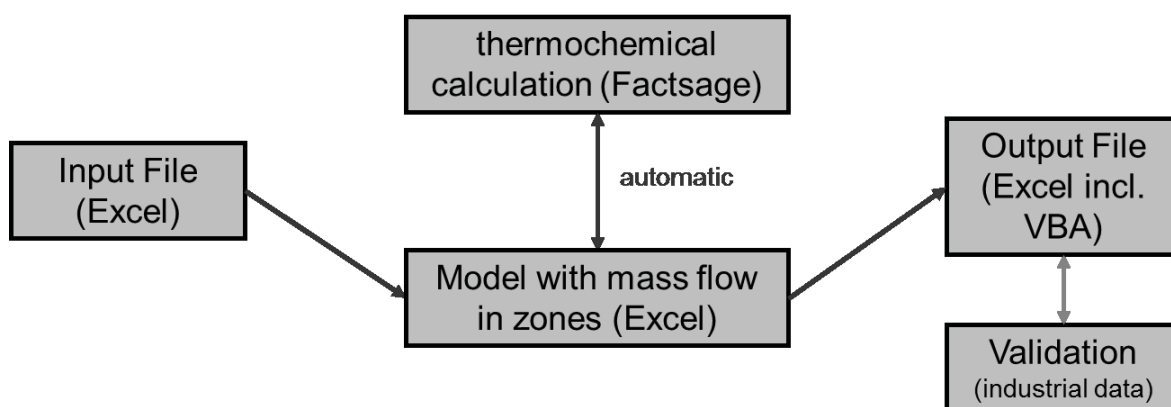
Figure 4.4: Connection between the single elements of the model

To perform a calculation, following steps must be executed:

- Open the Excel© file with macros
  (default: *CalcFINEX_cycle_Alkalis_Halides_Zn.xlsm*).

- Change different parameters (green cells) in the *Input Sheet* and *Profiles* sheet.

- Save the file as normal Excel© file (.xlsx). Therefore, the button inside the *Input Sheet* can be used.

- Open FactSage™ Equilib module and run the macro file
  (default: *FINEX_macro_calc.mac*) (In reactants window: *File → macro processing → Run macro… → Browse →* choose the macro file *→ Run macro*).

- After the calculation is finished, the results can be analysed in the stored .xlsx file.

Due to the time-consuming calculation, the update of the Equilib file for version 7.0 of February 2016 should be installed. Otherwise, an error will occur after a few iterations. Detailed information is shown on the webpage of FactSage™ (www.factsage.com).

For the calculated results, it is possible to create a Sankey diagram automatically following these steps (ensure that macros are enabled in Excel©):

- Open the Excel© file with macros
  (default: *CalcFINEX_cycle_Alkalis_Halides_Zn.xlsm*).

- Click the button *Draw Sankey diagram* inside the *Input Sheet*.

- Choose an element and a scaling factor and click on *Draw Sankey diagram*.

- Choose the Excel® file with calculated results (.xlsx).

The model calculates the cycle of five different elements: potassium (K), sodium (Na), chlorine (Cl), fluorine (F) and zinc (Zn), respectively. For each element, selected compounds are included in the calculation depending on the descriptions in **chapter 3**. These compounds are listed in **Table 4-4**.

Table 4-4: Selected compounds for the calculation model

Gaseous		Liquid		Solid	
K	NaF	K	Na_2CO_3	K	Na_2CO_3
KCN	NaOH	KCN	NaCl	KCN	NaCl
KCl	Zn	K_2CO_3	NaF	K_2CO_3	NaF
KF	$ZnCl_2$	KCl	Zn	KCl	Zn
KOH	ZnF_2	KF	ZnO	KF	ZnO
Na	HCl	Na	$ZnCl_2$	Na	ZnF_2
NaCN	HF	NaCN	ZnF_2	NaCN	
NaCl					

Due to the descriptions of the behaviour of these elements in **chapter 3**, they get into the process from various input materials in different compounds. Hereinafter the distribution basis for each element is described.

Potassium and sodium

Potassium and sodium is charged into the reactor in form of silicates (K_2SiO_3, Na_2SiO_3), chlorides (KCl, NaCl) and fluorides (KF, NaF). Due to thermochemical purposes, the alkali silicates are stable in the reduction steps of the process. They descend to the melter gasifier hearth and get dissolved in the slag. Due to the high carbon activity, they get partially reduced. Then the alkalis evaporate from the slag phase into the reactor as gaseous metals or cyanides. Pichler [38] developed a slag model by using different thermochemical data to simulate the ratio of evaporating alkalis. This slag model is described in **chapter 4.2.1**. The alkalis ascend in the reactor and get oxidised in upper zones by CO_2 and H_2O (also FeO). Furthermore, an adequate partial pressure of chlorine and fluorine can cause the creation of KCl, NaCl, KF and NaF. Lower temperatures lead to condensation and solidification of the alkali compounds.

Alkali chlorides and fluorides are mainly charged by coke and coal. The main part of these compounds is entering the process at the high temperature zone above the slag in vaporised

state. The other part is liquidised in the upper charbed of the melter gasifier and there it is inserted in the calculation process.

Chlorine and fluorine

The whole chlorine and fluorine is bounded to alkalis in the coal before charging in the reactor. As described above, these compounds either get vaporised in the slag-near zone or enters the simulation process in an upper charbed zone. In the Excel$^©$ input sheet, it can be chosen, which ratio of the chlorine and fluorine is bounded to potassium or sodium. Due to the higher stability of the fluorine compounds, it can be expected that they react in lower sections of the reactor. Of course, the chlorine and fluorine input from the pulverized coal injection (PCI) totally reacts in the zone, where the tuyères are located. Halides are discharged with the top gas and the slurry (after cleaning the cooling gas), so no halides can be found in the slag or the hot metal.

Zinc

The zinc is charged into the furnace mostly with the ore as oxide, ferrite, silicate and sulphide. The distribution of these compounds as well as the output masses of zinc for slag and hot metal can be set in the Excel$^©$ input sheet. Due to the different thermodynamic stability, the reaction takes place in different zones. The oxide and ferrite will be reduced in the pre-stage at the fluidised bed reactor. There the zinc amount from the ferrite vaporises due to the high temperatures. The zinc oxide is charged in solid state. The more stable zinc sulphide and silicate will descend in the melter gasifier and the reduced zinc gets vaporised in the slag-near zone. A part of the zinc is discharged by the slag and hot metal.

Further parameters which could be set individually in the process model are presented in **Table 4-5**. The listed values are for the standard model of the FINEX$^®$ process. The dust burner ratio gives the portion of the HGC dust, which reacts in zone 2 and ascends in the upper zone. The other part will completely descend with other solid and liquid material into the lower zone (Zone 3, compare **Figure 4.8**), because this material is partially liquidised and stick to the charged burden. For example, a dust burner ratio of 80 % means, that 80 % of the return material from the hot gas cyclone reacts in zone 2, whereas the other 20 % reacts in zone 3.

The gas separation rate of the fluidised bed reactor specifies the ratio of total hot gas cyclone gas, which is entering the fluidised bed reactor as reduction gas. The rest gets cleaned and returned to the hot gas cyclone as cooling gas. Beside the cooling gas, there is

also an excess gas stream, which is required to control the pressure in the melter gasifier. For the model, both the cooling gas and the excess gas are totally cleaned of all alkalis, halides and zinc compounds. Hence, there is no enrichment inside this cycle and the cooling gas only influences the gaseous atmosphere in respect of CO, CO_2, H_2, H_2O, N_2 and CH_4.

The slag basicity B_3 is calculated according to **equation (4-2)** and the slag composition for the standard model is listed in **Table 4-8**:

$$B_3 = \frac{\%CaO + \%MgO}{\%Al_2O_3} \qquad\qquad \textbf{(4-2)}$$

Table 4-5: Process parameters for a standard FINEX® process model

Generator gas conditions		Blast conditions		Hot gas cyclone conditions	
Temperature [°C]	1050	Temperature [°C]	25	Temperature [°C]	800
Top pressure abs. [bar]	4.5	Pressure abs. [bar]	5.5	Top pressure abs. [atm]	5.5
Gas volume [m³/tHM]	1500	Blast humidity [%]	0	Gas volume [m³/tHM]	1980
		Gas volume [m³/tHM]	400	Dust burner ratio [%]	100
		O_2-contant [%]	99.5	N_2 (dust burner) [m³/tHM]	45
		Flame temperature [°C]	2000		
		Coal (PCI) [kg/tHM]	150		
		N_2-rate (PCI) [m³/kg]	0.25		
Hot metal / Slag conditions		Cooling gas conditions		Fluidised bed reactor conditions	
Temperature [°C]	1500	Temperature	20	Temperature [°C]	750
Slag basicity (B_3)	1.43	Pressure abs. [bar]	5	Top pressure abs. [bar]	4
Productivity [tHM/h]	180	Gas vol. [m³/tHM]	480	Carrying gas N_2 [m³/tHM]	25
Slag amount [kg/tHM]	326			Total gas volume [m³/tHM]	1609
				Gas separation rate [%]	80

To set the gas profile for the melter gasifier in each zone, the conditions of the blast and the generator gas are used. By multiplying the oxygen content with the gas volume, the calculation of the total oxygen amount in the blast is possible. The complete reaction of the oxygen with carbon leads to the total CO amount in kmol/h. Together with nitrogen from the PCI, it results in the total gas volume and composition in the lowest zone (zone 6). On the other side, the specific gas streams in the generator gas are received by multiplying the vol-% of the gas with the total gas volume in kmol/h. The results give the gas flows in the highest reaction zone (zone 1). For the other zones the gas volume is a combination of the

described boundary areas (zone 6 and zone 1) with gas profiles from literature [39]. **Figure 4.5** shows the gas composition, pressure and temperature for the melter gasifier for each zone. Here, zone 7 is the slag and hot metal zone. **Table 4-6** presents the absolute values for the temperature, pressure and gas composition in each zone of the model.

The pressure is always defined as the total pressure (pressure absolute). The temperature stands for the gas temperature of the hot and cold area (± 100 °C). The model calculates the equilibrium according to this temperature. For the melter gasifier, the cold area is located in the middle of the reactor. This results from the central charging of cold coal briquettes from the top. The hot gas cyclone gas is composed of the generator gas after zone 1 (hot and cold area) and a cooling gas, which composition could also be defined individually.

As seen in **Table 4-5**, the slag basicity for the standard model is set to 1.43. Therefore, the slag composition is: 40 % CaO, 35 % SiO_2, 15 % Al_2O_3 and 10 % MgO. Other compounds, which could be set are K_2O, MnO, S, TiO_2, Fe_2O_3 and Na_2O). These values are directly linked to the slag model for calculating the activity of K_2O in the slag.

Table 4-6: Reaction zones of the standard melter gasifier

Stage	Melter Gasifier zone	Temperature [°C] (cold/hot area)	Pressure abs. [bar]	Gas composition [mol-%]					
				CO	CO_2	H_2	H_2O	N_2	CH_4
FB	Fluidised bed reactor	750	4.0	60	12	14	4	10	-
HGC	Hot gas cyclone	800	5.5	60	12	15	6	7	-
Zone 1	Dome/freeboard	950 / 1150	4.5	60	12	15	6	7	-
Zone 2	Dome/freeboard	900 / 1100	4.5	60	12	15	6	7	-
Zone 3	Upper charbed	650 / 850	4.55	68	12	12	5	3	-
Zone 4	Upper charbed	1180 / 1380	4.8	73	10	10	4	3	-
Zone 5	Lower charbed	1500 / 1700	5.0	80	6	7	3	4	-
Zone 6	Lower charbed	1900 / 2100	5.3	95	-	-	-	5	-
Slag zone	Hearth	1500	5.3	95	-	-	-	5	-

Finally, the separation rate of the hot gas cyclone and the fluidised bed reactor must be set. This is a factor, which represents the ratio of descending solid and liquid compounds, i.e. the particles, which are charged back into the melter gasifier. The value for the separated dust fraction, which is fed back from the hot gas cyclone into the reactor, is fixed with 90 %, that one for the fluidised bed reactor with 85 % for the standard model.
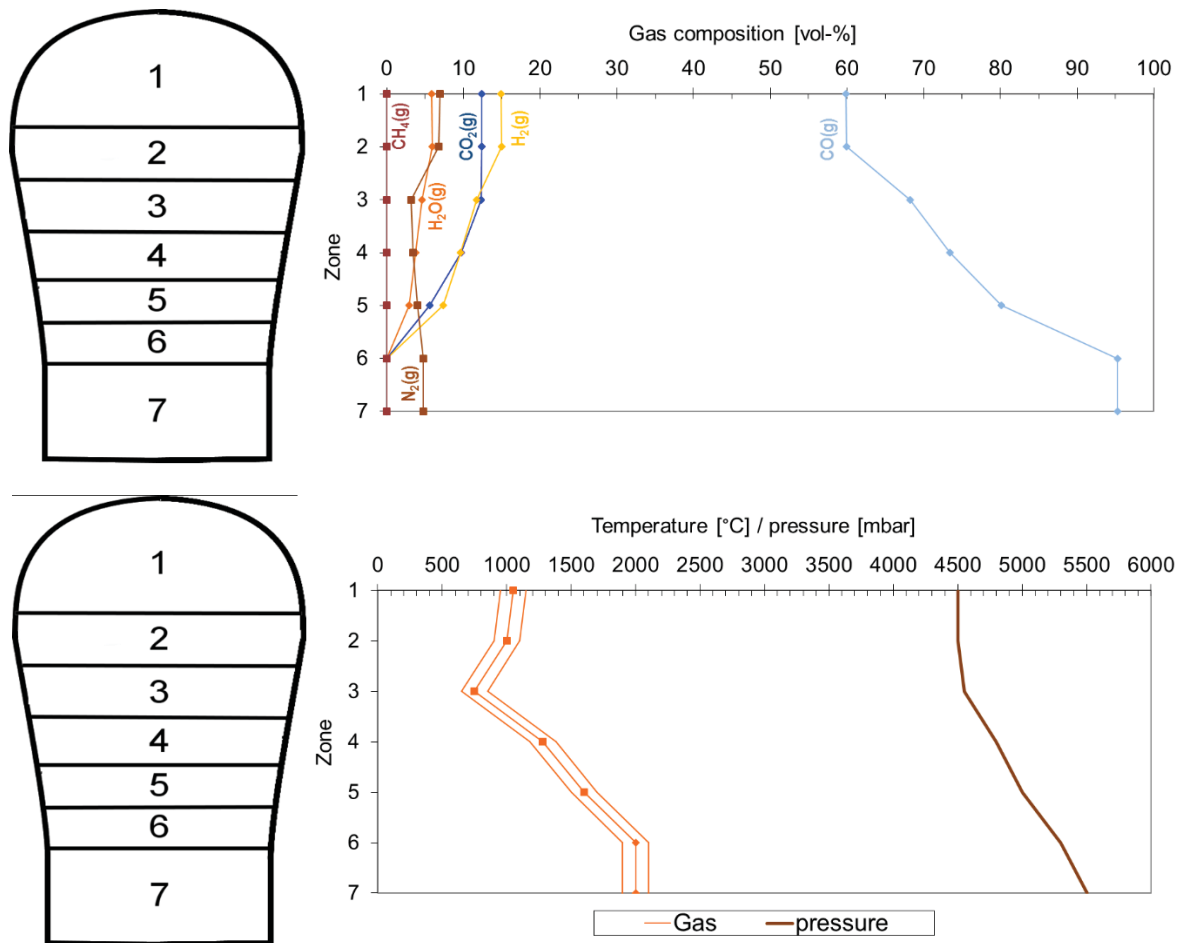
Figure 4.5: Gas profile for the melter gasifier,
top: gas composition, bottom: gas temperature and pressure

4.2.1 The slag model of alkalis

The slag model was developed by Pichler et al. [38,40,41]. It describes the evaporation rate of alkalis by the slag as a function of the basicity (actually, it is the optical basicity) and the slag temperature. Therefore, the alkali silicates (K_2SiO_3 and Na_2SiO_3) of the input material first get into the slag phase. There the silicate decomposes into K_2O/Na_2O and SiO_2. The silica and the alkalis dissolve in the slag and leave the reactor by the slag phase. Only a specific ratio of alkalis reacts with the dissolved carbon and nitrogen of the liquid phases (according to **equation (3-7)**, **(3-8)**, **(3-14)** and **(3-16)**, respectively). The main parameters are determined in **Figure 4.6**. To simplify the total reaction, a homogeneous liquid slag phase and gaseous phase are estimated.
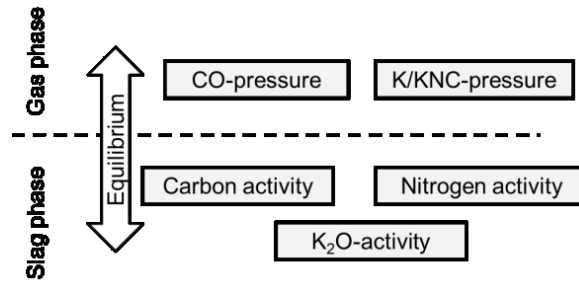
Figure 4.6: Simplified equilibrium conditions for the reduction and evaporation of alkalis

The equilibrium molar ratio of K and KCN according to **equation (3-7)** and **(3-14)** (similar for Na and NaCN) can be calculated with the following the **equations (4-3)** and **(4-4)**:

$$x_K = \sqrt{\frac{k \cdot a_{K_2O} \cdot a_C}{x_{CO} \cdot p_{ges}^3}} \qquad \text{(4-3)}$$

$$x_{KCN} = \sqrt{\frac{k \cdot a_{K_2O} \cdot a_C^3 \cdot a_N^2}{x_{CO} \cdot p_{ges}^3}} \qquad \text{(4-4)}$$

with x_K and x_{KCN} as the molar ratio of K and KCN, respectively, k as the equilibrium constant, a_i as the activity of species i, x_{CO} as the molar ratio of CO in the gas phase and p_{ges} as the total pressure above the slag phase in atm. Further calculations in the bottom zone lead to the amount of gaseous K and KCN per ton hot metal. The equilibrium constant k is calculated from the free reaction enthalpy ΔG of each reaction due to **equation (4-5)**:

$$k = e^{-\frac{\Delta G}{R \cdot T}} \;\; with \;\; \Delta G = \Delta H - \Delta S \cdot T \qquad \text{(4-5)}$$

where R is the universal gas constant, T the reaction temperature, ΔH the reaction enthalpy and ΔS the reaction entropy. Carbon monoxide is the product of the reduction of alkali silicate. Therefore, the partial pressure of CO above the slag phase influences the equilibrium. It is calculated by the molar ratio of CO in the gas phase above the slag and the total gas pressure in the hearth. Due to the high temperature and high carbon activity the hot blast oxygen will completely generate carbon monoxide.

The carbon activity in the liquid phase effects the reduction of the dissolved K_2O. An increasing carbon activity leads to higher amounts of K and KCN evaporation. Derived from the low oxygen potential in the hearth zone of the blast furnace (no FeO in the slag, carbon saturated hot metal), the carbon activity of the liquid phases can be determined as $a_C = 1$.

The nitrogen activity in the melt is calculated with **equation (4-6)**. It combines the interaction parameter, the equilibrium constant and the partial pressure of N_2 in the gaseous phase. The interaction parameter f_N combines the reactions of nitrogen with other elements like carbon, oxygen, etc. For defined conditions in the blast furnace hearth (1600 °C, carbon saturated in hot metal) it has the constant value of 3.606. The equilibrium constant k_N between dissolved nitrogen and gaseous N_2 depends on the slag temperature and follows an empirical function. **Equation (4-6)** combines the interaction parameter and the equilibrium constant with the partial pressure of N_2 in the gas (law of Sievert). The nitrogen activity influences directly the KCN-evaporation according to **equation (4-4)**.

$$a_N = f_N \cdot k_N \cdot \sqrt{p_{N_2}} \qquad \text{(4-6)}$$

with $\qquad f_N = 10^{(0,557)} = 3.606 \qquad$ for liquid phases (1600 °C) and

$$k_N = 10^{\left(\frac{-188}{T_{Slag}}+2.76\right)}$$

Pichler [38] combined empiric data with thermochemical equations and kinetics to find the activity of alkali oxides in the slag. Due to the high influence of the basicity, the optical basicity is included in the model. Each single slag compound (CaO, SiO_2, Al_2O_3, MgO, MnO, K_2O, etc.) is connected with a specific, theoretical optical basicity Λ_{th}. **Equation (4-7)** gives the total optical basicity of the mixture, where x_i is the molar ratio of compound i in the slag and n is the number of oxygen atoms of each compound (e.g. n = 2 for SiO_2, n = 3 for Al_2O_3).

$$\Lambda = \frac{\sum(x_i \cdot n_i \cdot \Lambda_{th\,i})}{\sum(x_i \cdot n_i)} \qquad \text{(4-7)}$$

Figure 4.7 shows the influence of the optical basicity on the evaporation rate of metallic potassium. The higher the optical basicity, the higher is the evaporation rate. Furthermore, the increase of the slag temperature leads to an increase of the evaporated alkali metal. The **equations (4-8)** and **(4-9)** represent the exponential regression of the evaporation rate of K_2O depending on the optical basicity and the slag temperature, respectively, with a_1, a_2, m and b as mathematical coefficients.

$$k_{K_2O} = \frac{a_1}{a_1 - a_2} \cdot (e^{(-a_2 \cdot \Lambda)} - e^{(-a_1 \cdot \Lambda)}) \qquad \text{(4-8)}$$

$$k_{K_2O} = m \cdot e^{(b \cdot T)} \qquad \text{(4-9)}$$
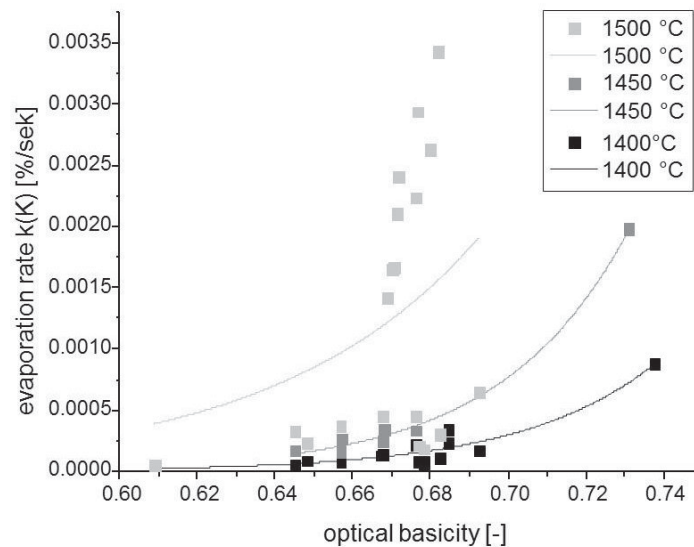
Figure 4.7: Evaporation rate k (empirical) in connection with the optical basicity of blast furnace near slag compositions and different temperatures [38]

Pichler [38] used an upscaling term to connect the evaporation rate with the activity of the alkali oxide in the slag at industrial near conditions in the blast furnace. Due to the similar process conditions in the melter gasifier, it can also be used in the FINEX® process model.

4.2.2 The multi-stage reactor model

As mentioned before, the model consists of totally nine different zones: One slag zone, six melter gasifier zones, a hot gas cyclone (HGC) zone and a fluidised bed reactor (FB) zone. A simplified overview of the model of the FINEX® process is shown in **Figure 4.8**. There the fluidised bed reactor, the melter gasifier and the hot gas cyclone are illustrated. The arrows show the mass flow for different elements for input and output streams: for instance, alkalis (yellow arrows), halides (green arrows), zinc compounds (dark blue arrows), gas and dust cycle compounds (grey arrows), cooling gas for hot gas cyclone (light blue arrow) and the output stream for slag, gas and dust (red arrows). The arrows from input materials mark the zone, in which they thermodynamically will react at the first time.

As the alkali silicates are very stable, they get into the model at the slag zone, as described in **chapter 4.2.1**. Zinc sulphide and zinc silicate are also very stable and will be reduced in lower sections of the melter gasifier by forming gaseous zinc. Zinc oxide and ferrite may be reduced even in the fluidized bed reactor. Most of the halides get into the process with coal and are present in different sections in the melter gasifier. The output

streams for the different compounds are coloured in red and they are represented by the top gas, the slag and the slurry after gas cleaning to provide a clean cooling gas.
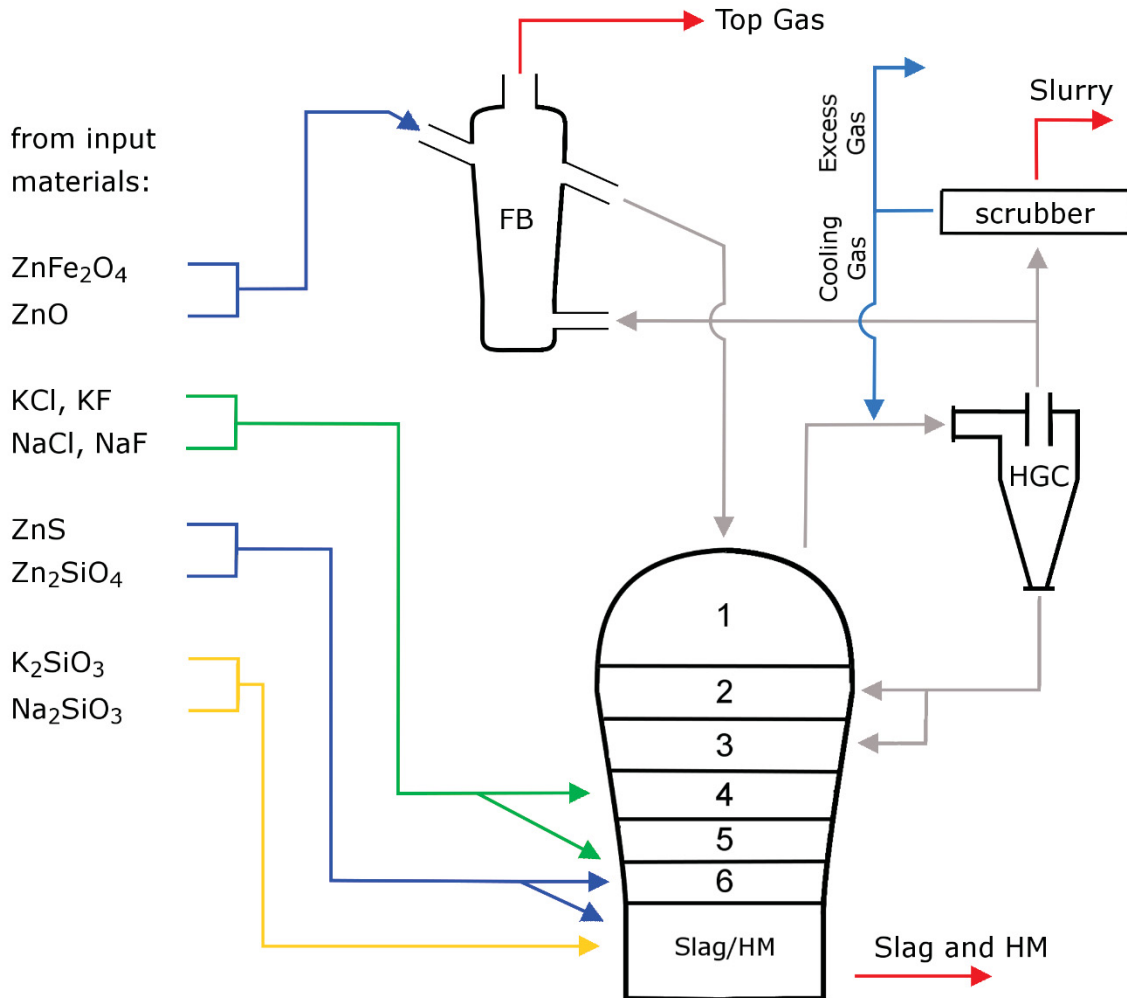
Figure 4.8: Simplified overview of the FINEX® process model

Each zone in the melter gasifier consists of a hot and a cold area. The gas flows from the hearth zone to the dome, so from zone 6 to zone 1. **Figure 4.9** shows the slag zone and zone 6, whereupon all other zones have an identical layout. The first alkalis enter the process by using the slag model described in **chapter 4.2.1**. There the evaporated species are separated in halves, whereupon 50 % get into the hot and 50 % into the cold area. After the calculation by FactSage™, the whole gaseous fraction rises in the upper zone (e.g. from zone 6 to zone 5). The solids and liquids are separated in descending and ascending particles. Based on industrial investigations the factor is between 30 – 40 % (35 % for the basic model) for ascending particles. This means, that 65 % of the stable solid and liquid compounds go down (mainly adhered to the burden material).
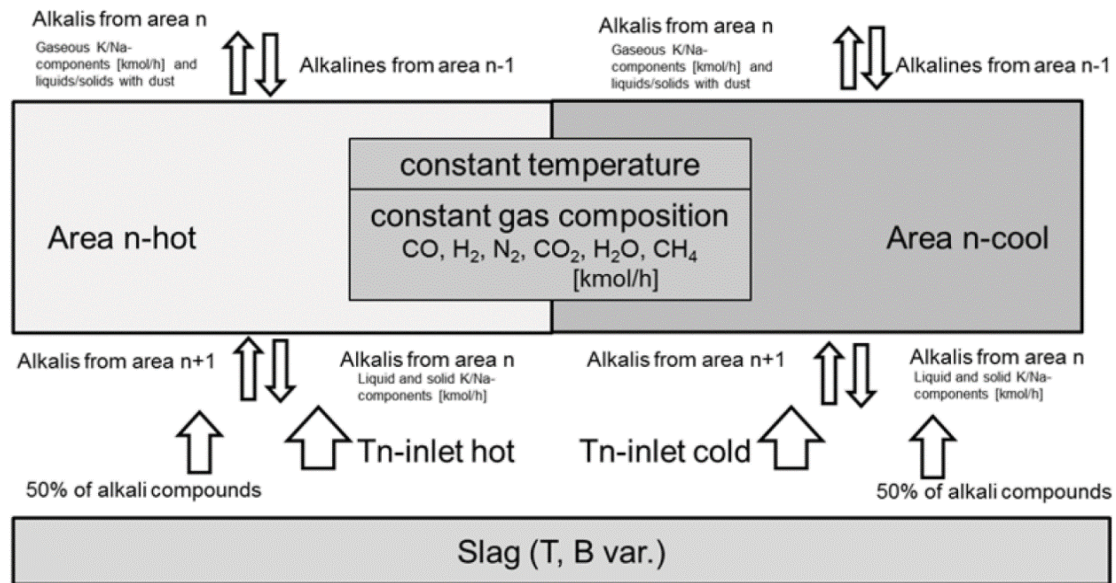
Figure 4.9: Connection between slag phase and the lowest reaction zone (zone 6)

Each reaction zone acts as ideal stirred reactor, where the different compounds have enough time to react with the process gas to their most stable composition. The main constituents of the gas mixture are CO, CO_2, N_2, CH_4, H_2 and H_2O in different ratios depending on the reaction area. Zone 1 represents the highest zone in the melter gasifier. Hence, the gaseous output is the generator gas, which enters the hot gas cyclone zone. After mixing with a defined cooling gas and temperature for the hot gas cyclone, 90 % of the stable solid and liquid products are separated from the gaseous compounds. They are charged back into the melter gasifier. The other 10 % are leaving this stage as dust with the gas. Then, this stream is divided into the reducing gas and the cooling gas (proportioning 4:1). The reducing gas enters the fluidised bed reactor, whereas the cooling gas gets cleaned. After the cleaning step, the gas is divided into a cooling gas stream, which is mixed with the generator gas to adjust the temperature at the hot gas cyclone inlet, and into an excess gas stream, which is required to control the pressure in the melter gasifier. As mentioned above, there is no enrichment inside the cooling gas cycle, because all alkalis, halides and zinc compounds are separated from the gas inside the scrubber. For the model, the cooling gas only influences the gas atmosphere in respect of CO, CO_2, H_2, H_2O, N_2 and CH_4. The pressure inside the hot gas cyclone is set as a constant process condition, independent of the excess gas.

The gas composition and amount for the fluidised bed reactor zone could be set individually. After the equilibrium calculation, 15 % of the stable solid and liquid species leave

the reactor with the top gas. Consequently, 85 % will be charged back into the melter gasifier.

After the first iteration from zone 6 to the fluidised bed reactor zone is done, the calculation starts from the beginning with the next iteration step. So, the stable compounds including K, Na, Cl, F and Zn are enriched in different zones of the model. The cycle of these elements will be built up.

4.2.3 Influence on the circuit flows by changing the process parameters

For the investigation of the influences on the FINEX® process four different parameters were chosen: the slag basicity and temperature, the hot gas cyclone temperature and the dust burner ratio. The parameters for the standard model (Stm) and the different calculations (Run01 to Run06) are listed in **Table 4-7**.

Table 4-7: Changed parameters to determine the influences on the process

	Stm	Run01	Run02	Run03	Run04	Run05	Run06
Slag basicity (B_3)	1.429	1.125	''	''	''	''	''
Slag temperature [°C]	1500	1400	''	''	''	''	''
HGC temperature [°C]	800	''	735	750	900	''	''
Dust burner ratio [%]	100	''	''	''	''	80	50

'': same value as standard model (Stm)

The different calculation results are illustrated in the distribution diagram for the different material streams and in the Sankey diagrams, both shown in the appendix. It must be considered that the values are the masses of the certain elements in the different compounds, not the mass of the compound. Therefore, the ratio of the different compounds depending on the total amount of the element can be determined.

The different material streams are shown in **Figure 4.10**. In each stream, the calculated species amounts could be solid, liquid or gaseous. The red arrows mark the output streams, i.e. slag, top gas (TG) and slurry from gas cleaning step. The circle streams are coloured in grey, e.g. the generator gas from melter gasifier to the hot gas cyclone (GG), the return material (dust) from the hot gas cyclone to the melter gasifer's zone 2 or 3 (RZ2 and RZ3, depending on the dust burner ratio), the reducing gas from the hot gas cyclone to the

fluidised bed reactor (RG), and the HCl from the fluidised bed reactor to the melter gasifier (RMG). The melter gasifier is separated in seven different zones (see **chapter 4.2**). The blue arrow just shows the stream for the cooling gas without interesting species amount due to total gas cleaning.
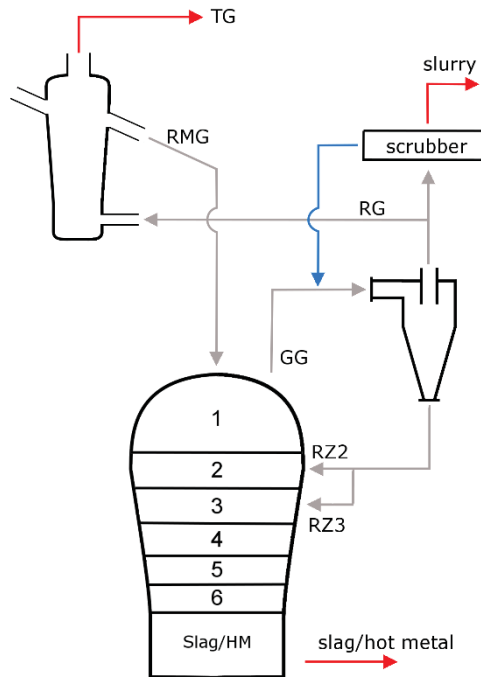
Figure 4.10: Process overview with different streams for result's description

Following a description of the results of the standard model is given. In **chapter 4.3** a comparison of the different calculations and industrial data is done.

All process parameters for the standard model can be seen in **Table 4-5**. The distribution diagrams and the Sankey diagrams are illustrated in appendix A.1 to A.10. In the case of potassium, it can be seen, that the generator gas (GG) is loaded with approximately 40 kg K/tHM. Most of the potassium (62 %) is bounded with chlorine as gaseous KCl and 22 % with fluorine as gaseous KF. The rest is gaseous K and KOH and only 3 % liquid KCl is stable due to the high temperatures in the dome (between 950 °C in the cold and 1150 °C in the hot area). After cooling in the hot gas cyclone and separation of the dust, 36 kg K/tHM are returned to zone 2 into the melter gasifier. The dust amount for zone 3 (RZ3) is not existing, because of a dust burner ratio of 100 %. In the hot gas cyclone, nearly all gaseous potassium converts into liquid KCl and solid K_2CO_3 (temperature 800 °C). Only a minor part stays as gaseous KCl, KF and KOH (totally 0.45 kg K/tHM in reducing gas and slurry). Overall, approximately 89 % of the total potassium input into the hot gas cyclone will be

separated and returned to the melter gasifier, about 2 % are dropped out during gas cleaning and the rest is conveyed with the reducing gas to the fluidised bed reactor (seen in the Sankey diagram for potassium in appendix A.2).

Inside the melter gasifier, the amounts of potassium rise above 110 kg K/tHM. Due to the low temperatures in zone 3 (650 °C in the cold and 850 °C in the hot area) and the input of the HGC dust, the enrichment takes place in this location. Nearly the whole potassium is bound to liquid or solid KCl and K_2CO_3. In the Sankey diagram, the widest streams are from zone 3 to zone 4 and backwards. In zone 3 the most compounds deposit, descend into zone 4 and vaporise due to higher temperatures. This generates the circle for potassium inside the melter gasifier. A second circle is provided by the hot gas cyclone.

The fluidised bed reactor represents a third cycle stream. The reducing gas is loaded with gaseous compounds (KCl, KF and KOH) and some dust particles (KCl and K_2CO_3). Due to the lower temperatures (750 °C) half of the gaseous agents deposit. 85 % of the solid and liquid compounds are returned with the HCl into the melter gasifier. The rest leaves the reactor with the top gas as dust (totally 685 g/tHM).

The slag contains 3.26 kg K/tHM. This value is calculated from the difference of the amount of total potassium input as silicates and the amount of vaporising potassium compounds from the slag calculated with the slag model. For a total slag amount of 326 kg/tHM, this makes up a content of 1.2 % K_2O in the slag.

The circulation of sodium is more distinctive than that from potassium. The distribution shows that the generation of NaF is more likely than NaCl. Due to the high stability of NaF and the high boiling point, it is difficult to bring sodium out of the melter gasifier. Nearly all the sodium converts into solid NaF inside the hot gas cyclone, except of 10 g Na/tHM which is bound in gaseous NaCl. Inside the melter gasifier, the sodium is present mainly as Na_2CO_3 and NaF in solid and liquid state. Furthermore, sodium reaches lower zones in comparison to potassium. There is an amount of 32 kg Na/tHM in zone 5, where it reacts, vaporises and ascends to upper zones. At the low temperatures in zone 3, the sodium compounds convert into liquids or solids and descend again. Therefore, a similar cycle like that one for potassium inside the melter gasifier is built up.

Most of the sodium leaves the process with the slag (approximately 73 % of total sodium input, see PtInp in appendix A.4). Only 110 g/tHM get out with the top gas as dust, because all gaseous sodium compounds react to solid NaF in the fluidised bed reactor. This emphasises the difficult removal of sodium once more.

For Run01, the slag basicity was changed in aspect to the CaO and SiO_2 content. Whereas the B_3-basicity for the standard model was set to 1.429, it was decreased to 1.125 for Run01. Additionally, the slag temperature was decreased to 1400 °C. The compositions and the temperatures of the slags are given in **Table 4-8**. The change of the slag basicity has only an influence on alkalis (K, Na) because of the slag model calculation described in **chapter 4.2.1**. The influence on chlorine and fluorine is declared due to the lower alkali masses vaporised by the slag. Thus, it leads to a shift of the chemical equilibrium.

Table 4-8: Slag composition for standard model and Run01

	Standard model	Run01
Slag basicity (B_3)	1.429	1.125
Slag temperature [°C]	1500	1400
CaO [%]	40	35
SiO_2 [%]	35	40
Al_2O_3 [%]	15	15
MgO [%]	10	10
MnO, S, TiO_2, Fe_2O_3 [%]	0	0

At the further calculations (Run02 to Run08) the hot gas cyclone temperature and the dust burner ratio were varied. Due to lower HGC temperatures it is expected, that more species deposit and are separated from the gas. Consequently, higher amounts are returned into the melter gasifier. The enrichment inside the furnace will increase.

The dust burner ratio specifies the portion of HGC dust, which reacts in zone 2, where the dust burner is usually installed. If the particles of the HGC dust are dragged by the descending solid and liquid material inside the gasifier, they will react in the lower located zone 3. So, a decreasing dust burner ratio effects, that more dust reacts in zone 3 instead of zone 2.

As seen in appendix A.9 and A.10 for the standard model, zinc is not changing its gaseous state, except in zone 3. All the zinc leaves the process with the top gas or the slurry after the cooling gas scrubber. This does not describe the behaviour like it is shown for industrial data in **chapter 4.1**. In the thermochemical model, forming of liquid or solid zinc compounds is not

present at temperatures above 700 °C. Consequently, a zinc cycle does not build up. Reasons for this fact are discussed in the conclusion.

4.3 Results

To compare the results from the different calculations and industrial data, various values are used. **Figure 4.11** shows the influence of the slag basicity and temperature on the output ratio of alkalis through the slag. Whereas the output ratio of potassium for the standard model (B_3 = 1.43, T_{Slag} = 1500 °C) reaches 63.2 % of total input load, it increases to 65.1 % in case of Run01 (B_3 = 1.125, T_{Slag} = 1400 °C). The same situation is found in case of sodium, where the output ratio changes from 72.8 % to 74.8 %. That is an additional mass of 100 g K and 60 g Na, respectively, which is discharged with the slag per ton of hot metal. This regards to the fact that the admittance of potassium and sodium in the slag increases with decreasing slag basicity and temperature. As seen in **Figure 4.12**, the change of basicity and temperature of the slag have low influence on the amount of HGC dust, since the mass of K, Na, Cl and F stay quiet constant.
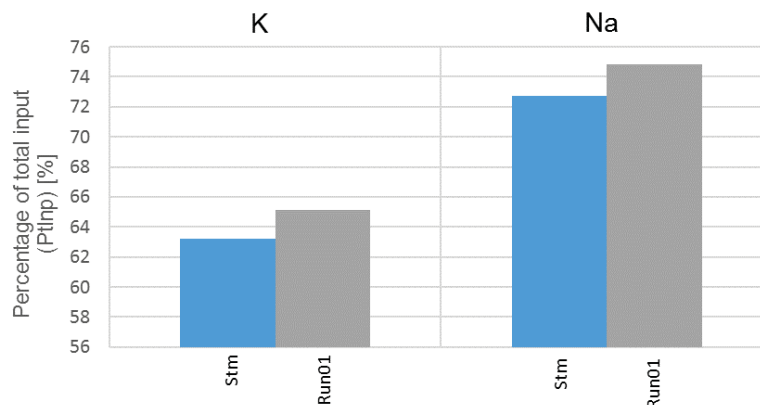
Figure 4.11: Influence of slag basicity and temperature on the output ratio through slag of K and Na
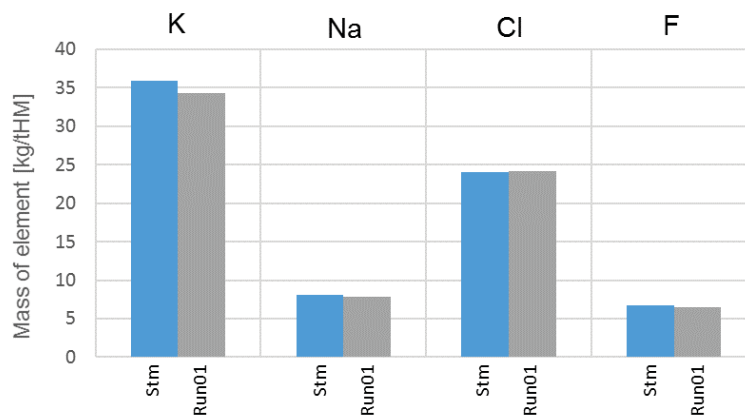
Figure 4.12: Influence of slag basicity and temperature on the mass of element in HGC dust

The influence of the HGC temperature is described by comparing the mass of each element in the HGC dust (**Figure 4.13**). There are also shown values for industrial data (ID) from the Sankey diagrams in **chapter 4.1.1**. The results strongly depend on the input amounts and analyses. These values are not exactly known for the industrial data, which are plotted in the diagrams. Therefore, a validation and comparison for the industrial data is not possible.

In case of potassium it can be seen, that a decrease of the HGC temperature leads to an increase of the solid and liquid compounds, which are separated by the hot gas cyclone. Chlorine follows this behaviour, because most of the chlorine is bound to potassium in form of KCl. By raising the temperature to 900 °C, the mass of HGC dust can be reduced significantly. Consequently, the amount of element in the top gas and slurry gets higher. This is illustrated in **Figure 4.14** for the mass ratio of total input, which leaves the furnace with the top gas or the slurry after the cooling gas scrubber. The effect on sodium is quite low, because it nearly totally reacts with fluorine to NaF. At these temperatures NaF is in solid state and minor amounts will be discharged with the top gas or slurry. The enrichment of chlorine inside the furnace during the iterations even effects a higher discharge than input amount. The output of fluorine increases by raising the HGC temperature due to the favourable formation of gaseous HF and KF at high temperatures (see distribution diagram for fluorine in appendix for Run04, appendix A.42). The amount of fluorine bound to HF increases from 38 g/tHM (Stm) to 72 g/tHM (Run04) in the slurry (+ 89 %) and the amount of fluorine bound to KF raises from 4 g/tHM up to 40 g/tHM (+ 900 %).
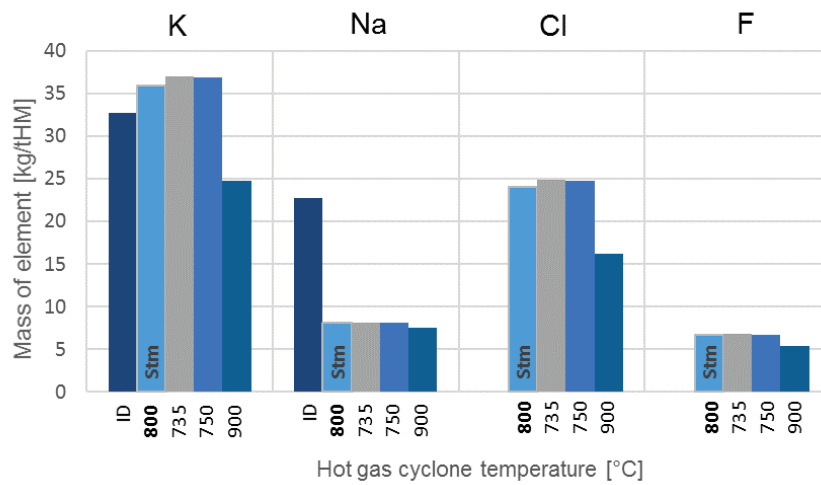
Figure 4.13: Influence of the HGC temperature on the mass of element in HGC dust
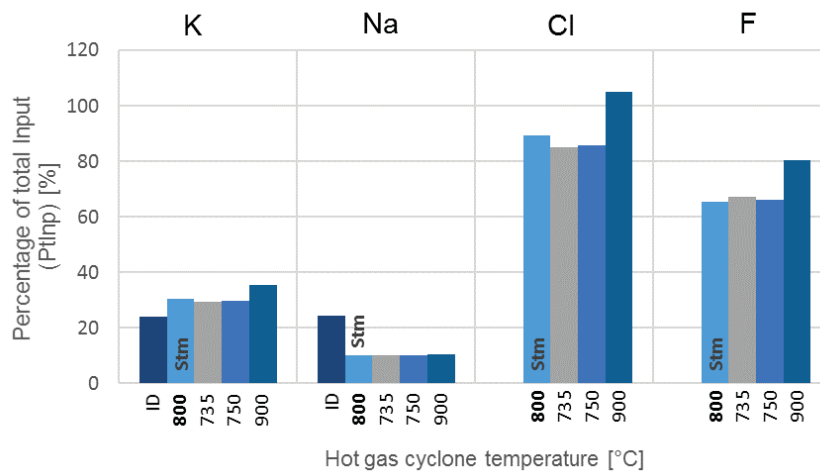
Figure 4.14: Influence of HGC temperature on percentage of output through top gas and slurry

The effect of different dust burner ratios (DBR) on the mass of element in the HGC dust is shown in **Figure 4.15**. There is a slight influence for potassium and chlorine, but overall the effect is minimal. However, the enrichment inside the melter gasifier is incredibly high. This is shown in **Figure 4.16**, where the mass of K, Na, Cl and F in zone 3 is plotted for different dust burner ratios. Zone 3 characterises the coldest zone inside the melter gasifier, where drying and pyrolysis take place. The amounts of all four elements increase by decreasing the dust burner ratio (also compare the different Sankey diagrams in the appendix for the standard model, Run05 and Run06).
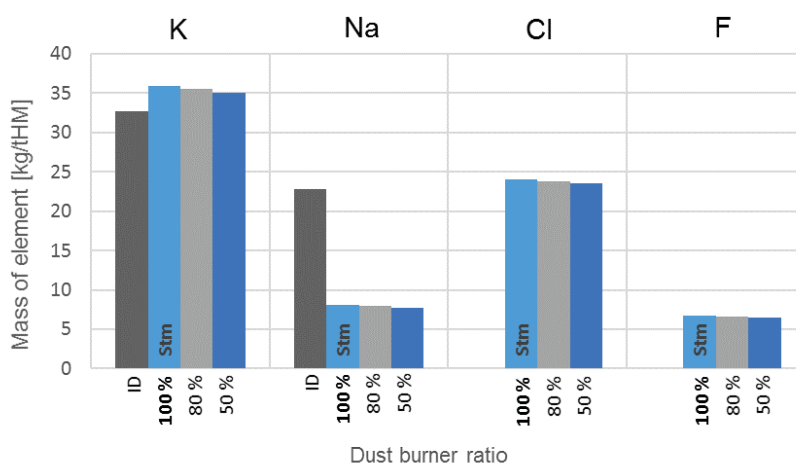
Figure 4.15: Influence of DBR on the mass of element in HGC dust
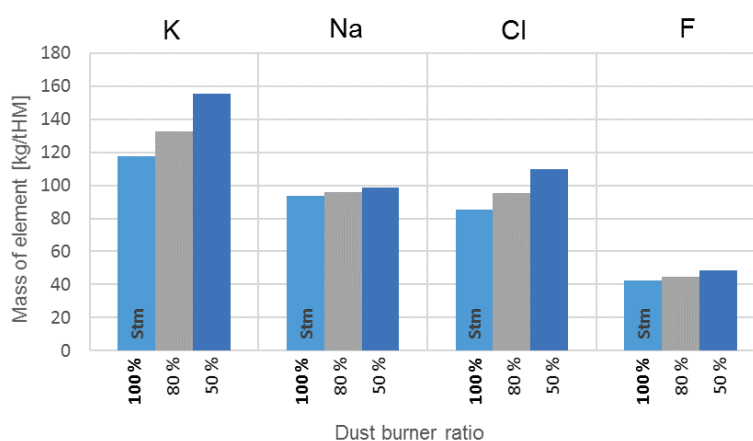
Figure 4.16: Influence of DBR on the mass of element in zone 3

4.4 Conclusion

A thermochemical model was developed to calculate the cycle of potassium, sodium, chlorine, fluorine and zinc inside the FINEX® process. The process is split up in nine different stages: seven zones inside the melter gasifier, the hot gas cyclone and the fluidised bed reactor. The calculations were done with the thermochemical software FactSage™ 7.0 and its database FactPS to get the equilibrium amounts for each element and compound inside the nine stages. A slag model calculates the amounts of potassium and sodium evaporated by the slag depending on the slag basicity and temperature. For a standard process

(standard model), different parameters were set with values from literature. Then, the slag basicity, temperature, hot gas cyclone temperature and a dust burner ratio were varied to point out the influences on the cycle of the elements. Distribution diagrams and Sankey diagrams show the results for the different cases.

Potassium:

The most stable compound of potassium is potassium chloride (KCl), of course at the presence of chlorine. At lower temperatures forming of potassium carbonate (K_2CO_3) is also possible. At the melter gasifier's high temperature zones, most of the potassium is bound to gaseous KCl and KF. The discharge happens mostly by the slag. This can even be raised by decreasing the slag basicity and temperature. An increase of the hot gas cyclone temperature enhances the output through the off-gas, of course, by forming more gaseous KCl due to a higher vapour pressure. Since the melting point of KCl (771 °C STP) is slightly higher than the boiling point of pure potassium (768 °C STP), a reduction of chlorine input and furthermore, a higher CO/CO_2 ratio will lead to a higher discharge for potassium, as seen in the stability diagram in **Figure 3.9**. Forming of liquid or solid KCl can harm the aggregate and reduce productivity. For the calculated results at the chosen conditions, pure metallic potassium is only stable above 1000 °C in gaseous state. Below this temperature it forms compounds such as KCl, KF or K_2CO_3. Liquid or solid potassium cyanide is not stable at any conditions due to the very low partial pressure of nitrogen. The amounts of potassium will enrich significantly if the returned dust from the melter gasifier reaches cold section inside the melter gasifier. The more liquid or solid compounds are present in lower sections, the higher is the enrichment inside the aggregate.

Sodium:

In contrast to potassium, sodium will be more stable in pure state in the gaseous phase at high temperatures, but also sodium chloride (NaCl) and sodium fluoride (NaF) makes up high portions. Liquid and solid NaF and Na_2CO_3 are stable even at higher temperatures (up to approximately 1400 °C) due to their high vapour pressures. Otherwise, the sodium will nearly totally react to solid NaF at region with temperatures below 900 °C. If the fluorine amount does not suffice, formation of liquid or solid Na_2CO_3 will take place. By raising the hot gas cyclone temperature above 800 °C, more gaseous compounds are present. Therefore, the output through the cooling gas scrubber (slurry) and the top gas is slightly higher. However, the major amounts of sodium are discharged through the slag (> 70 % of total input). This value can be increased by decreasing the slag basicity and temperature, like it is in the case

of potassium. Due to the addiction of sodium to form stable liquid or solid NaF, a great influence of hot gas cyclone temperature and dust burner ratio on the total output cannot be determined. The major effect on increased discharge is the slag basicity, temperature and amount.

Chlorine:

Below 1000 °C, KCl is the favourable compound, which is found inside the FINEX® process model. It is present in solid, liquid or gaseous state. At higher temperatures, the chlorine is also found as gaseous NaCl. High temperatures are preferred for a higher discharge with the top gas and the slurry after the cooling gas scrubber, because there is no output through the slag. Chlorine rather follows the behaviour of potassium if the process parameters are changed. In appearance of liquid and solid KCl, bulks can occur. Furthermore, a reaction with hydrogen leads to formation of hydrochloric acid and corrosion of the aggregate.

Fluorine:

At temperatures below 1000 °C nearly all fluorine is bound with sodium as NaF. At these temperatures NaF is in solid state. Above the melting point (995 °C STP) NaF is present as liquid compound, but also gaseous KF and NaF are stable in considerable portions. Therefore, the behaviour is strongly connected to that of sodium. By raising the hot gas cyclone temperature, the output of fluorine through the off-gas increases due to the higher formation of gaseous KF and HF (compare results for fluorine in appendix for standard model and Run04).

Zinc:

The behaviour of zinc and its compounds cannot be described with the developed thermochemical model. Zinc is present in gaseous state in all stages, except zone 3. Forming of liquid or solid zinc compounds cannot be determined, as they are not stable. To form such compounds the thermochemical equilibrium must be reached for the different reaction with the gaseous phase, e.g. CO_2 and H_2O (**equation (3-23)** and **(3-24)**). The partial pressure of zinc in each stage is very low (between $3.3 \cdot 10^{-4}$ and $1.5 \cdot 10^{-3}$). **Figure 4.17** shows the Gibbs free energy for the reaction of one mole gaseous zinc with CO_2 and H_2O for a partial pressure of zinc $p_{Zn} = 5 \cdot 10^{-4}$ atm. Additionally, the formation of ZnO by reducing FeO is plotted as a feasible reaction, according to **equation (4-10)**. It can be seen, that the

formation of ZnO is possible at temperatures below 740 °C due to negative values for the Gibbs free energy.

$$Zn(g) + FeO \rightarrow ZnO + Fe \qquad \text{(4-10)}$$
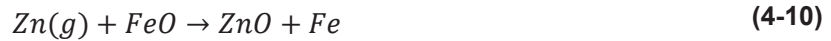
The oxidisation of zinc can also be favoured by higher partial pressures for zinc. In real aggregates the gaseous zinc is not totally distributed homogeneously inside the gas atmosphere. Consequently, it is possible that the partial pressure for zinc rises above the vapour pressure in single areas and ZnO is formed. The possibility of a formation of liquid or solid zinc sulphide (ZnS) was not proved, but there is a thermochemical stability of this phase during the presence of minor gaseous hydrogen sulphide (H_2S) inside the gas atmosphere. Additionally, the temperature varies within the aggregate. It is feasible, that the temperature reaches lower values in some regions than it is set for the model. Also kinetic aspects are of high importance for the precipitator efficiency, as the researches of Clark and Fray [34] and Cox and Fray [42] determine. The researchers concluded, that the adsorption of zinc is a rate-controlling step for zinc oxidation at temperatures below 800 °C.
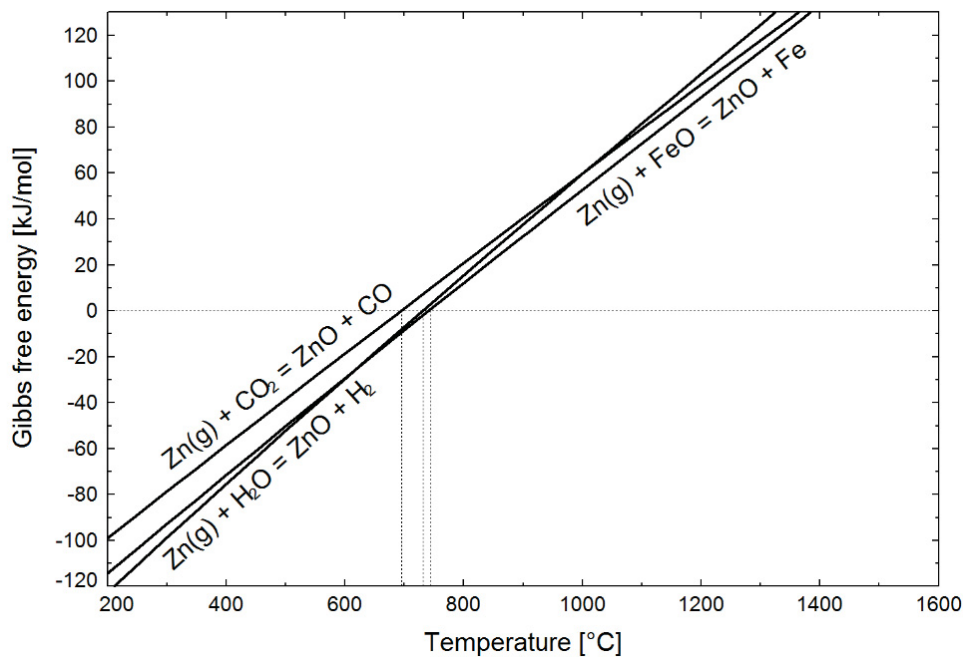
Figure 4.17: Gibbs free energy for 1 mol gaseous zinc as a function of temperature with a total pressure of 5.5 atm, p(Zn) = 0.0005 atm, CO/CO_2 = 60/12, H_2/H_2O = 15/5

List of references

[1]   World Steel Association, Statistics of crude steel, blast furnace iron and direct reduced iron production, https://www.worldsteel.org, Retrieved: Nov. 2016.

[2]   Chatterjee, A., Beyond the blast furnace, CRC Press, Boca Raton, Fla., 1994.

[3]   Remus, R., Best available techniques (BAT) reference document for iron and steel production: Industrial emissions directive 2010/75/EU (integrated pollution prevention and control), Publications Office of the European Union, Luxembourg, 2013.

[4]   Hasanbeigi, A., M. Arens und L. Price, Alternative emerging ironmaking technologies for energy-efficiency and carbon dioxide emissions reduction: A technical review, Renewable and Sustainable Energy Reviews 33 (2014), 645–658.

[5]   Almpanis-Lekkas, O., B. Weiss und W. Wukovits, Modelling of an ironmaking melter gasifier unit operation with multicomponent/multiphase equilibrium calculations, Journal of Cleaner Production 111 (2016), 161–171.

[6]   Lee, S.-C., M.-K. Shin, S. Joo und J.-K. Yoon, The Effects of Operational Parameters on the Transport Phenomena in COREX Melter-Gasifier, ISIJ International 40 (2000), 11, 1073–1079.

[7]   Costa, M.M., R. Schaeffer und E. Worrell, Exergy accounting of energy and materials flows in steel production systems, Energy 26 (2001), 4, 363–384.

[8]   HAN, L.-h., Z.-g. LUO, X.-l. ZHOU, H. ZHOU, Z.-s. ZOU und Y.-z. ZHANG, Influence of Burden Distribution on Temperature Distribution in COREX Melter Gasifier, Journal of Iron and Steel Research, International 20 (2013), 3, 30–35.

[9]   Skorianz, M., H. Mali, A. Pichler, F. Plaul, J. Schenk und B. Weiss, Reduction Behavior and Structural Evolution of Iron Ores in Fluidized Bed Technologies. Part 1: Method for the Determination, steel research int. (2015), n/a-n/a.

[10]   Primetals Technologies Ltd. and Posco Ltd., The Finex® Process: Economical and environmentally safe ironmaking, http://primetals.com/en/technologies/ironmaking/finex%C2%AE/Lists/FurtherInformation/The%20Finex%C2%AE%20process.pdf, Retrieved: 25.02.2016.

[11]   Chatterjee, A., Hot metal production by smelting reduction of iron oxide, PHI Learning, New Delhi, 2010.

[12]   LI, K.-j., J.-l. ZHANG, Z.-j. LIU, R. MAO und T.-j. YANG, Comprehensive Evaluation of OxyCup Process for Steelmaking Dust Treatment Based on Calculation of Mass Balance and Heat Balance, Journal of Iron and Steel Research, International 21 (2014), 6, 575–582.

[13]   Burke, P. und S. Gull, HIsmelt - The Alternative Ironmaking Technology, in: A.K. Jouhari, R.K. Galgali, V.N. Misra (Eds.), Smelting reduction for ironmaking: Proceedings of the National Conference, held at Bhubaneswar during 18-19 December, 2002, Allied Publishers, New Delhi, 2002, 61–71.

[14]   Birat, J.-P., Steel and CO2 - the ULCOS Program, CCS and Mineral Carbonation using Steelmaking Slag, ulcos.org/en/docs/Ref01__Birat_slag_finaal.pdf, Retrieved: Nov. 2016.

[15]   Meijer, K., C. Zeilstra, C. Teerhuis, M. Ouwehand und J. van der Stel, Developments in Alternative Ironmaking, Trans Indian Inst Met 66 (2013), 5-6, 475–481.

[16]   Pokhvisnev, Y., V. Romenets, V. Valavin, A. Zaytsev und S. Vandariev, Romelt Process - Promising Technology for Ironmaking, Metal 2002: 11th international metallurgical & materials conference, Červený zámek, Hradec nad Moravicí, Česká republika, (2002).

[17]   Pelton, A.D., Thermodynamics and Phase Diagrams of Materials, in: R.W. Cahn, P. Haasen, E.J. Kramer (Eds.), Materials Science and Technology, Wiley-VCH Verlag GmbH & Co. KGaA, Weinheim, Germany, 2006.

[18]   Hillert, M., Phase equilibria, phase diagrams and phase transformations: Their thermodynamic basis, 2nd ed., Cambridge University Press, Cambridge, 2008.

[19]   Bale, C.W., A.D. Pelton und W.T. Thompson, An Efficient Procedure for Computing Isothermal Predominance Diagrams, Canadian Metallurgical Quarterly 25 (2013), 2, 107–112.

[20]   Lin, R., Investigations of chlorine and alkali behaviour in the blast furnace and optimisation of blast furnace slag with respect to alkali retention capacity: Final report, Office for Official Publications of the European Communities, Luxembourg, 2003.

[21]   Abraham, K.P. und L.I. Staffansson, The Alkali Problem in the Blast Furnace, Scandinavian Journal of Metallurgy (1975), 4, 193–204.

[22]   Gudenau, H.W., H.P. Johann und S. Meimeth, Entfernung von Alkalien aus dem Hochofen, Stahl und Eisen 116 (1996), 9, 89–96.

[23]   Krol, L., J. Dankmeyer-Lanczny und J. Buzek, Angriff von Alkalien auf die Hochofenzustellungen aus Kohlenstoff und Graphit, Arch. Eisenhuettenwesen 52 (1981), 9, 341–344.

[24]   NARITA, K., T. ONOYE, Y. SATOH, M. MIYAMOTO, K. TANIGUCHI, S. KAMATANI, T. SATO und S. FUKIHARA, Effects of Alkalis and Zinc on the Wear of Blast Furnace Refractories and the Tuyere Displacement, ISIJ Int. 21 (1981), 12, 839–845.

[25]   Pilz, K., Verhalten von Kreislaufstoffen im Hochofenprozess, 1998.

[26]   Sulzbacher, Theoretische Überlegungen über das Verhalten von Alkalien im KR-Prozess, 1984.

[27]   KUWANO, Y. und M. TATE, Identification of Atomic Alkali Species in Experimental Blast Furnace by Spectroscopic Analysis, ISIJ Int. 22 (1982), 10, 790–793.

[28]   Gaskell, D.R., Introduction to metallurgical thermodynamics, 2. ed., Hemisphere Publishing Corp, Washington, 1981.

[29]   Bartusch, H., T. Hauck und H.-G. Grabietz, Balancing and behaviour of chlorine in the blast furnace process at Hüttenwerke Krupp Mannesmann, Stahl und Eisen 134 (2014), 1, 51–56.

[30]   Zabett, A. und W.-K. Lu, Thermodynamical computations for removal of alkali halides and lead compounds from electric arc furnace dust, Calphad 32 (2008), 3, 535–542.

[31]   Esezobor, D.E. und S.A. Balogun, Zinc accumulation during recycling of iron oxide wastes in the blast furnace, Ironmaking & Steelmaking 33 (2013), 5, 419–425.

[32]   Bronson, T.M., Oxidation and condensation of zinc fume in steelmaking off-gas systems, Dissertation, Utah, 2015.

[33]   Stansbury, K.L., An experimental study of the oxidation of zinc vapor, Master thesis, Golden, Colorado, 1987.

[34]   Clarke, J.A. und D.J. Fray, The rate of deposition and the morphology of zinc oxide deposited from Zn(v)/CO/CO2/Ar gas mixtures, J Mater Sci 13 (1978), 9, 1921–1925.

[35]   Micco, G. de, G.G. Fouga und A.E. Bohé, Chlorination of Zinc Oxide between 723 and 973 K, Metall and Materi Trans B 38 (2007), 6, 853–862.

[36]   Pickles, C.A., Thermodynamic analysis of the selective chlorination of electric arc furnace dust, Journal of hazardous materials 166 (2009), 2-3, 1030–1042.

[37]   VAI - Voest Alpine Industrieanlagenbau, Mass flow of potassium and sodium for COREX - Internal Data.

[38]   Pichler, A., J. Schenk, H. Stocker und C. Thaler, Thermochemical modelling of the alkali balance in blast furnaces, Proceedings Asia Steel 2015, Yokohama, 2015.

[39]   Geerdes, M., H. Toxopeus und C. van der Vliet, Modern blast furnace ironmaking: An introduction, IOS Press, Amsterdam, 2009.

[40]   Pichler, A., J. Schenk, F. Hauzenberger, H. Stocker und C. Thaler, Analysis of the alkali-distribution in ironmaking reactors by thermochemical modelling, ECIC 2016, Linz, Austria, 2016.

[41]   Pichler, A., J. Schenk, F. Hauzenberger, C. Thaler und H. Stocker, Influence of slag properties on the alkali-cycle of a blast furnace, Proceedings to AISTech 2016, Pittsburgh, 2016.

[42]   Cox, A. und D.J. Fray, Zinc reoxidation in the shaft of a zinc–lead Imperial Smelting Furnace - 1: Zinc–carbon–oxygen system with deposition initiated on a quartz substrate and subsequent propagation on zinc oxide, Mineral Processing and Extractive Metallurgy 109 (2013), 2, 97–104.

A Appendix - Results

Slag basicity B_3 = 1.125, slag temperature = 1400 °C

Hot gas cyclone temperature = 735 °C

Hot gas cyclone temperature = 750 °C

Hot gas cyclone temperature = 900 °C

Dust burner ratio = 80 %

Dust burner ratio = 50 %

A.1 Amount of potassium in kg/tHM in different compounds at each position – standard model
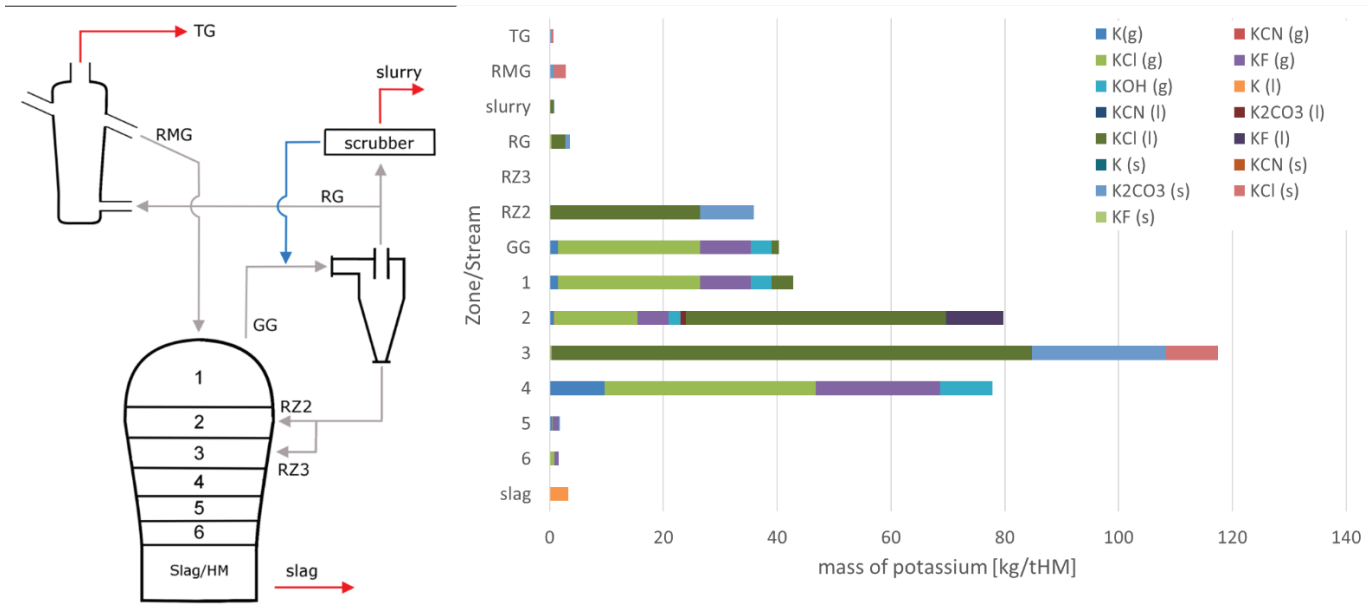
	slag	6	5	4	3	2	1	GG	RZ2	RZ3	RG	slurry	RMG	TG
K(g)	--	0.07	0.47	9.66	--	0.70	1.45	1.45	--	--	--	--	--	--
KCN (g)	--	0.01	--	0.02	--	0.01	0.02	0.02	--	--	--	--	--	--
KCl (g)	--	0.78	0.09	37.17	0.38	14.74	25.04	25.04	--	--	0.32	0.08	--	0.16
KF (g)	--	0.78	1.06	21.73	0.05	5.47	8.89	8.89	--	--	0.03	0.01	--	0.02
KOH (g)	--	--	0.18	9.24	0.01	2.03	3.61	3.61	--	--	0.01	--	--	--
K (l)	3.26	--	--	--	--	--	--	--	--	--	--	--	--	--
KCN (l)	--	--	--	--	--	--	--	--	--	--	--	--	--	--
K2CO3 (l)	--	--	--	--	--	1.00	--	--	--	--	--	--	--	--
KCl (l)	--	--	--	--	84.34	45.72	3.83	1.34	26.48	--	2.35	0.59	--	--
KF (l)	--	--	--	--	--	10.07	--	--	--	--	--	--	--	--
K (s)	--	--	--	--	--	--	--	--	--	--	--	--	--	--
KCN (s)	--	--	--	--	--	--	--	--	--	--	--	--	--	--
K2CO3 (s)	--	--	--	--	23.54	--	--	--	9.43	--	0.84	0.21	0.72	0.13
KCl (s)	--	--	--	--	9.16	--	--	--	--	--	--	--	2.15	0.38
KF (s)	--	--	--	--	--	--	--	--	--	--	--	--	--	--
Sum	3.26	1.65	1.81	77.82	117.49	79.75	42.83	40.35	35.90	--	3.55	0.89	2.87	0.68

A.2 Sankey diagram for potassium – standard model
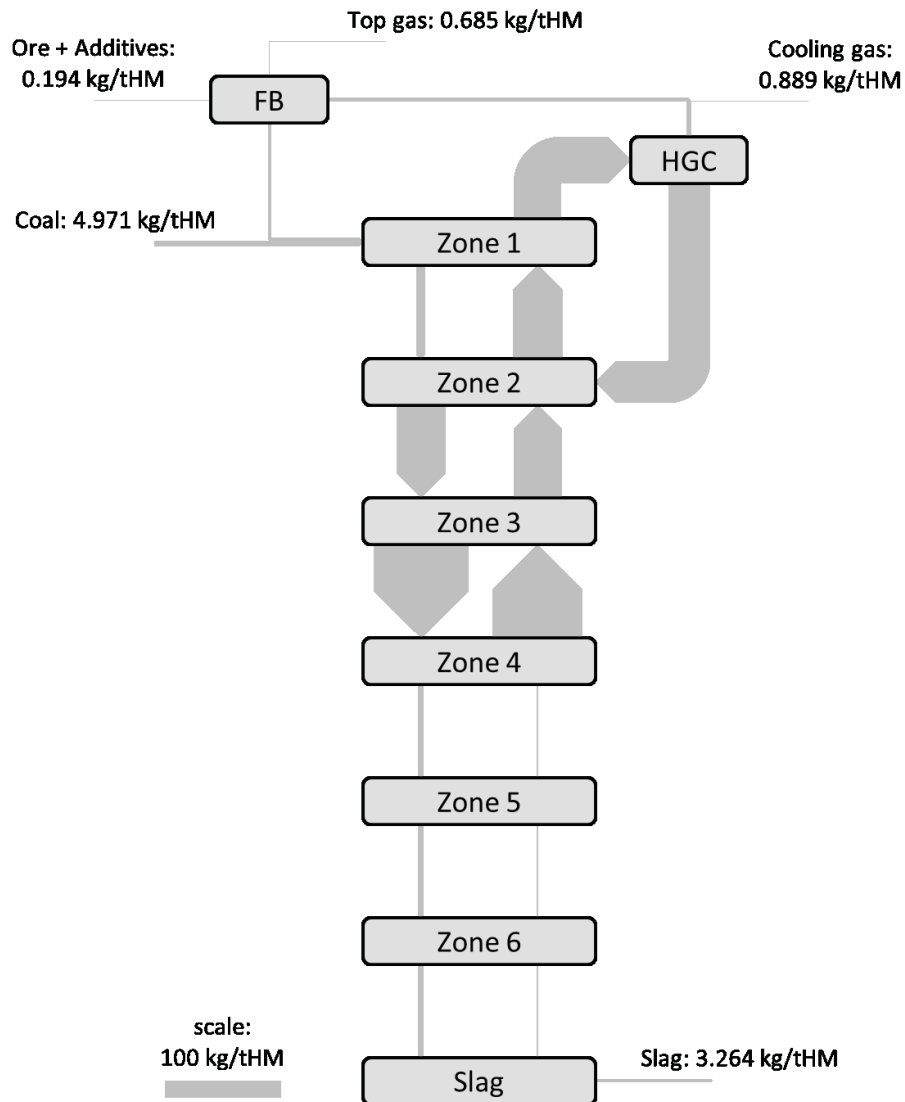
Input FB	[kg/tHM]	[%]	Output FB	[kg/tHM]	[%]	PtInp [%]
Ore	0.12	3.11	DRI	2.87	80.73	55.57
Additives	0.08	2.06	Top Gas	0.69	19.27	13.27
Reducing Gas	3.56	94.83				
Sum	3.75	100	Sum	3.56	100	

Discrepancy Input/Output: = 5.46 %

Input MG	[kg/tHM]	[%]	Output MG	[kg/tHM]	[%]	PtInp [%]
Coal	4.97	11.36	Slag	3.26	7.49	63.20
HGC dust	35.90	82.07	Generator Gas	40.35	92.51	781.11
DRI	2.87	6.56				
Sum	43.74	100	Sum	43.61	100	

Discrepancy Input/Output: = 0.3 %

Input HGC	[kg/tHM]	[%]	Output HGC	[kg/tHM]	[%]	PtInp [%]
Generator Gas	40.35	100.00	HGC dust	35.90	88.98	695.06
Cooling Gas	0.00	0.00	Reducing Gas	3.56	8.81	68.84
			Cooling Gas	0.89	2.20	17.21
Sum	40.35	100	Sum	40.35	100	

Discrepancy Input/Output: = 0.0 %

A.3 Amount of sodium in kg/tHM in different compounds at each position – standard model
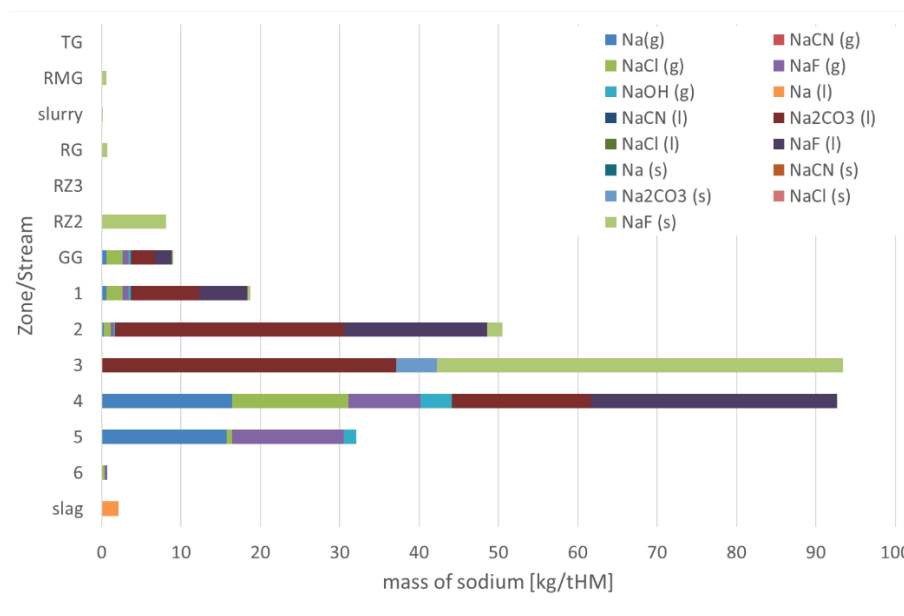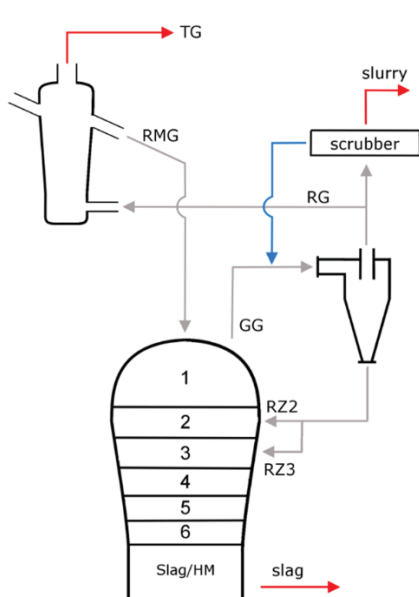
	slag	6	5	4	3	2	1	GG	RZ2	RZ3	RG	slurry	RMG	TG
Na(g)	--	0.08	15.77	16.41	--	0.24	0.60	0.60	--	--	--	--	--	--
NaCN (g)	--	0.02	0.01	0.03	--	0.00	0.01	0.01	--	--	--	--	--	--
NaCl (g)	--	0.29	0.69	14.67	0.01	0.93	2.03	2.03	--	--	0.01	--	--	--
NaF (g)	--	0.30	14.05	9.09	--	0.38	0.78	0.78	--	--	--	--	--	--
NaOH (g)	--	--	1.59	3.91	--	0.14	0.31	0.31	--	--	--	--	--	--
Na (l)	2.14	--	--	--	--	--	--	--	--	--	--	--	--	--
NaCN (l)	--	--	--	--	--	--	--	--	--	--	--	--	--	--
Na2CO3 (l)	--	--	--	17.58	37.12	28.85	8.59	3.01	--	--	--	--	--	--
NaCl (l)	--	--	--	--	--	--	--	--	--	--	--	--	--	--
NaF (l)	--	--	--	31.02	--	18.06	6.08	2.13	--	--	--	--	--	--
Na (s)	--	--	--	--	--	--	--	--	--	--	--	--	--	--
NaCN (s)	--	--	--	--	--	--	--	--	--	--	--	--	--	--
Na2CO3 (s)	--	--	--	--	5.11	--	--	--	--	--	--	--	--	--
NaCl (s)	--	--	--	--	--	--	--	--	--	--	--	--	--	--
NaF (s)	--	--	--	--	51.16	1.93	0.39	0.14	8.08	--	0.72	0.18	0.62	0.11
Sum	2.14	0.68	32.10	92.71	93.40	50.52	18.78	8.99	8.08	--	0.73	0.18	0.62	0.11

A.4 Sankey diagram for sodium – standard model
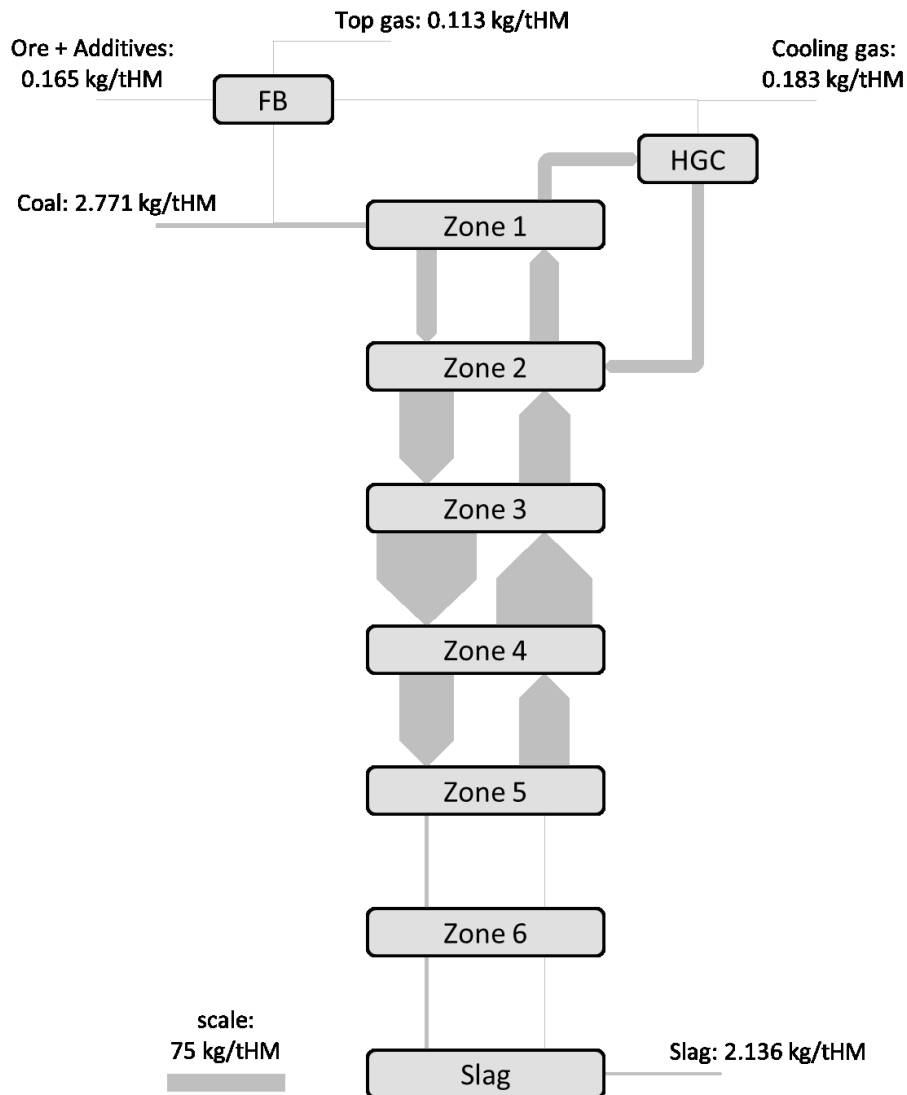
Input FB	[kg/tHM]	[%]	Output FB	[kg/tHM]	[%]	PtInp [%]
Ore	0.16	17.34	DRI	0.62	84.59	21.04
Additives	0.01	1.10	Top Gas	0.11	15.41	3.83
Reducing Gas	0.73	81.56				
Sum	0.90	100	Sum	0.73	100	

Discrepancy Input/Output: = 22.61 %

Input MG	[kg/tHM]	[%]	Output MG	[kg/tHM]	[%]	PtInp [%]
Coal	2.77	24.17	Slag	2.14	19.20	72.76
HGC dust	8.08	70.44	Generator Gas	8.99	80.80	306.18
DRI	0.62	5.39				
Sum	11.47	100	Sum	11.13	100	

Discrepancy Input/Output: = 3.05 %

Input HGC	[kg/tHM]	[%]	Output HGC	[kg/tHM]	[%]	PtInp [%]
Generator Gas	8.99	100.00	HGC dust	8.08	89.84	275.09
Cooling Gas	0.00	0.00	Reducing Gas	0.73	8.12	24.87
			Cooling Gas	0.18	2.03	6.22
Sum	8.99	100	Sum	8.99	100	

Discrepancy Input/Output: = 0.0 %

A.5 Amount of chlorine in kg/tHM in different compounds at each position – standard model
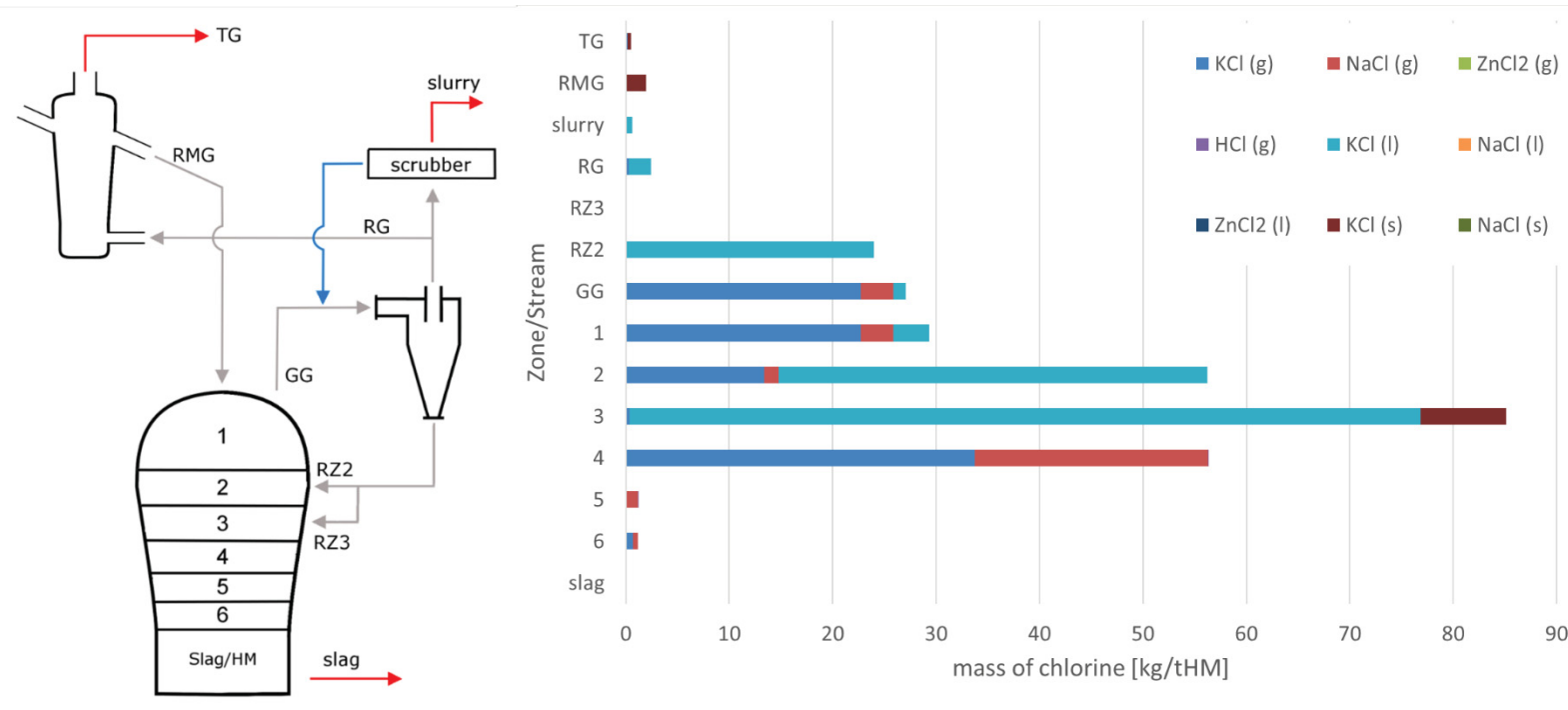
	slag	6	5	4	3	2	1	GG	RZ2	RZ3	RG	slurry	RMG	TG
KCl (g)	--	0.71	0.08	33.70	0.35	13.36	22.70	22.70	--	--	0.29	0.07	--	0.14
NaCl (g)	--	0.44	1.06	22.61	0.02	1.43	3.13	3.13	--	--	0.02	0.00	--	0.00
ZnCl2 (g)	--	--	--	--	--	--	--	--	--	--	--	--	--	--
HCl (g)	--	--	0.01	0.02	--	0.01	0.01	0.01	--	--	--	--	--	--
KCl (l)	--	--	--	--	76.47	41.45	3.47	1.21	24.00	--	2.13	0.53	--	--
NaCl (l)	--	--	--	--	--	--	--	--	--	--	--	--	--	--
ZnCl2 (l)	--	--	--	--	--	--	--	--	--	--	--	--	--	--
KCl (s)	--	--	--	--	8.30	--	--	--	--	--	--	--	1.95	0.34
NaCl (s)	--	--	--	--	--	--	--	--	--	--	--	--	--	--
Sum	--	1.15	1.15	56.33	85.13	56.25	29.31	27.06	24.00	--	2.44	0.61	1.95	0.49

A.6 Sankey diagram for chlorine – standard model

Top gas: 0.492 kg/tHM

Ore + Additives: 0.127 kg/tHM

Cooling gas: 0.610 kg/tHM

FB

HGC

Coal: 1.107 kg/tHM

Zone 1

Zone 2

Zone 3

Zone 4

Zone 5

Zone 6

scale: 75 kg/tHM

Slag
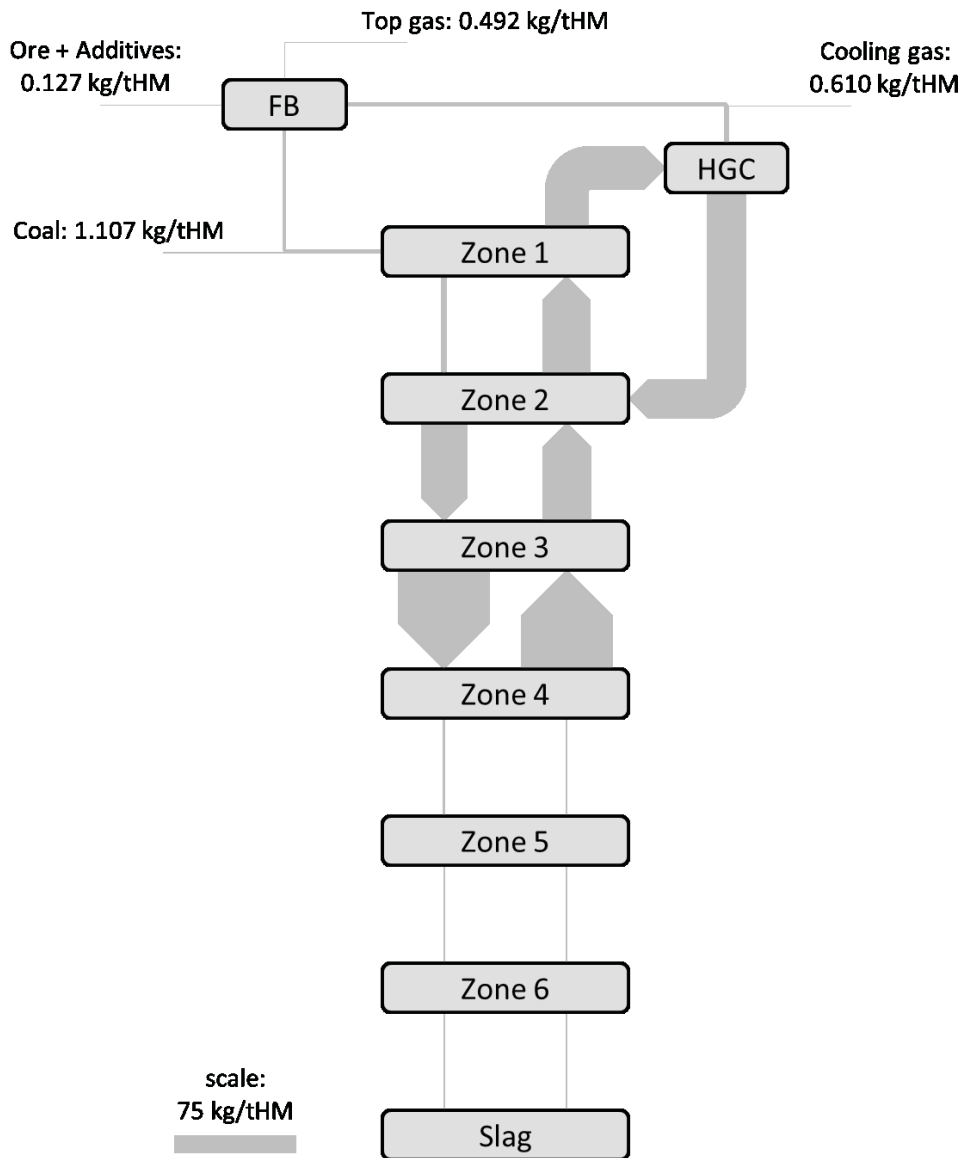
Input FB	[kg/tHM]	[%]	Output FB	[kg/tHM]	[%]	PtInp [%]
Ore	0.12	4.86	DRI	1.95	79.86	158.04
Additives	0.002	0.08	Top Gas	0.49	20.14	39.85
Reducing Gas	2.44	95.05				
Sum	2.57	100	Sum	2.44	100	

Discrepancy Input/Output: = 5.2 %

Input MG	[kg/tHM]	[%]	Output MG	[kg/tHM]	[%]	PtInp [%]
Coal	1.11	4.09	Slag	0.00	0.00	0.00
HGC dust	24.00	88.70	Generator Gas	27.06	100.00	2192.74
DRI	1.95	7.21				
Sum	27.06	100	Sum	27.06	100	

Discrepancy Input/Output: = 0.02 %

Input HGC	[kg/tHM]	[%]	Output HGC	[kg/tHM]	[%]	PtInp [%]
Generator Gas	27.06	100.00	HGC dust	24.00	88.72	1945.38
Cooling Gas	0.00	0.00	Reducing Gas	2.44	9.02	197.88
			Cooling Gas	0.61	2.26	49.47
Sum	27.06	100	Sum	27.06	100	

Discrepancy Input/Output: = 0.0 %

A.7 Amount of fluorine in kg/tHM in different compounds at each position – standard model
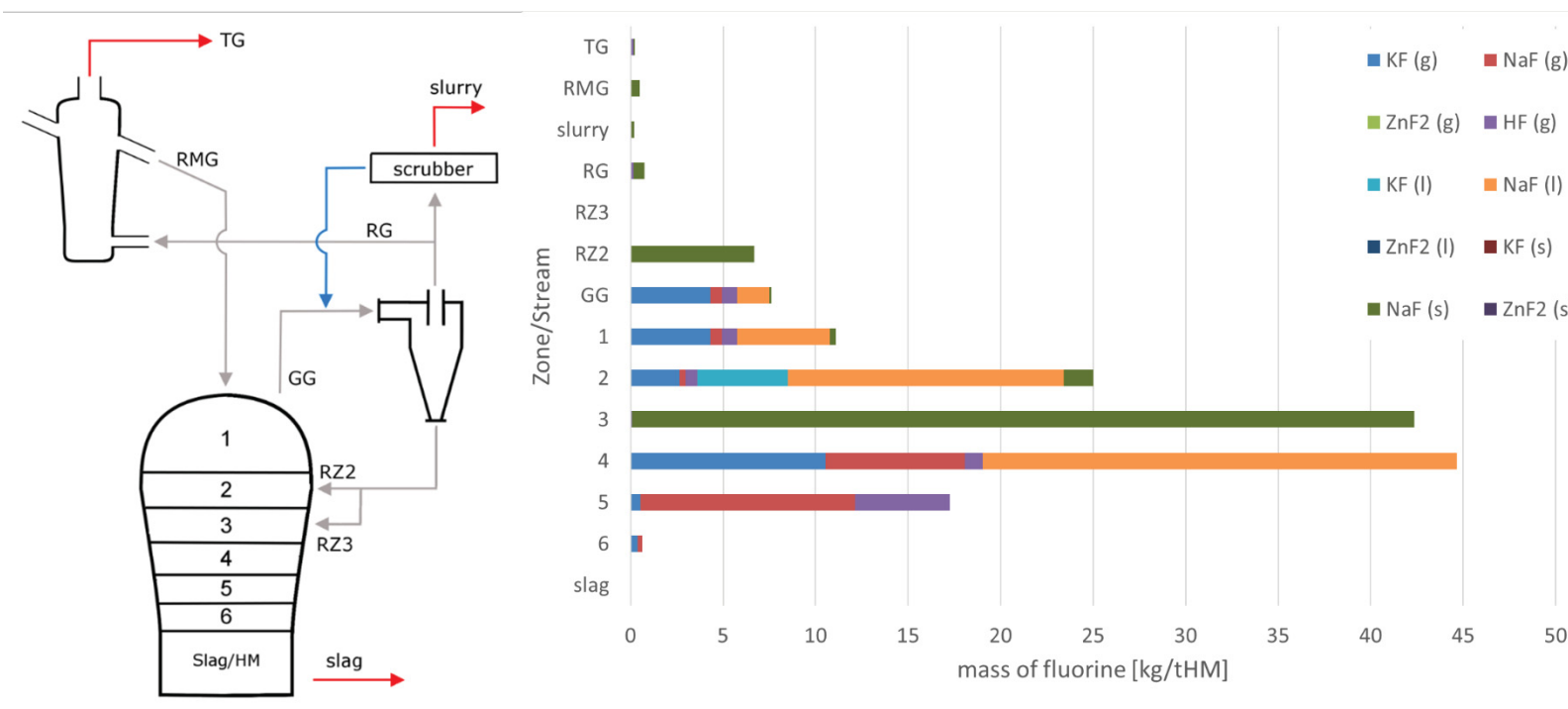
	slag	6	5	4	3	2	1	GG	RZ2	RZ3	RG	slurry	RMG	TG
KF (g)	--	0.38	0.52	10.56	0.03	2.66	4.32	4.32	--	--	0.02	0.00	--	0.01
NaF (g)	--	0.25	11.61	7.51	--	0.31	0.64	0.64	--	--	--	--	--	--
ZnF2 (g)	--	--	--	--	--	--	--	--	--	--	--	--	--	--
HF (g)	--	--	5.15	0.95	0.08	0.63	0.79	0.79	--	--	0.15	0.04	--	0.15
KF (l)	--	--	--	--	--	4.89	--	--	--	--	--	--	--	--
NaF (l)	--	--	--	25.62	--	14.92	5.02	1.76	--	--	--	--	--	--
ZnF2 (l)	--	--	--	--	--	--	--	--	--	--	--	--	--	--
KF (s)	--	--	--	--	--	--	--	--	--	--	--	--	--	--
NaF (s)	--	--	--	--	42.26	1.59	0.32	0.11	6.67	--	0.59	0.15	0.51	0.09
ZnF2 (s)	--	--	--	--	--	--	--	--	--	--	--	--	--	--
Sum	--	0.63	17.27	44.64	42.36	25.01	11.10	7.63	6.67	--	0.76	0.19	0.51	0.25

A.8 Sankey diagram for fluorine – standard model
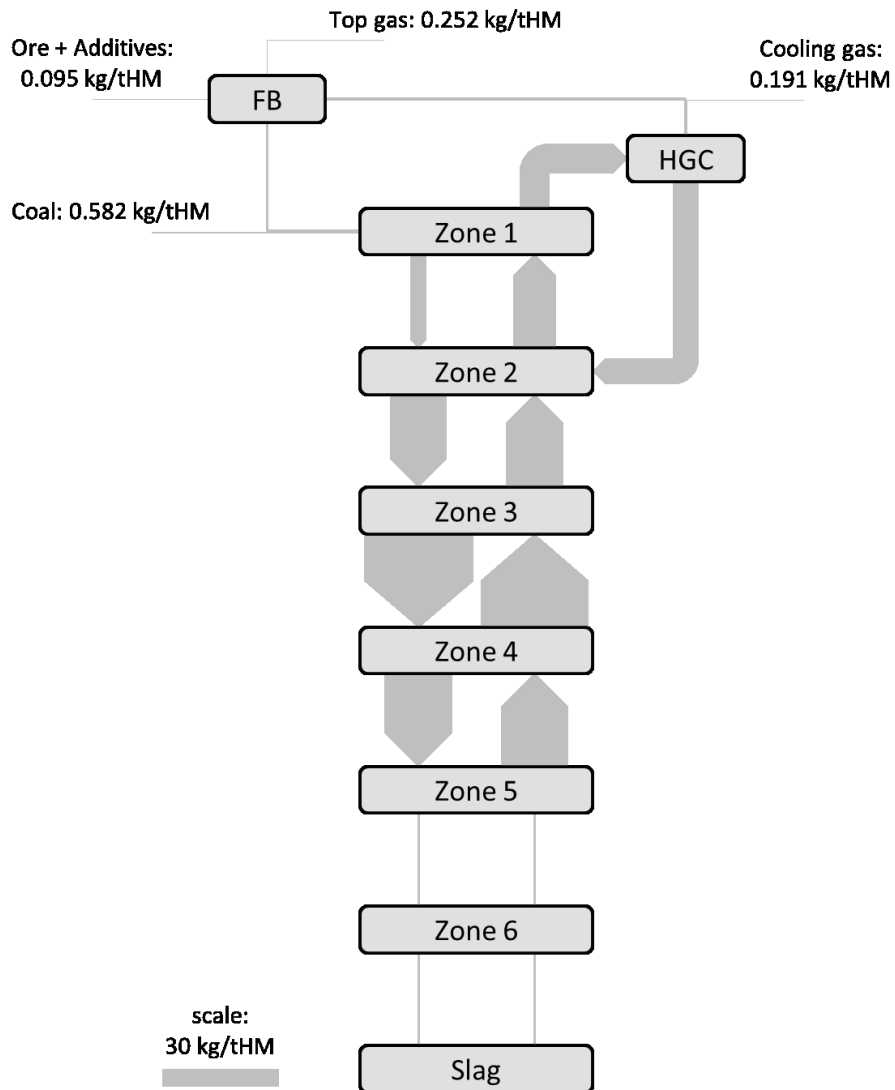
Input FB	[kg/tHM]	[%]	Output FB	[kg/tHM]	[%]	PtInp [%]
Ore	0.09	10.93	DRI	0.51	66.96	75.38
Additives	0.001	0.16	Top Gas	0.25	33.04	37.20
Reducing Gas	0.76	88.91				
Sum	0.86	100	Sum	0.76	100	

Discrepancy Input/Output: = 12.47 %

Input MG	[kg/tHM]	[%]	Output MG	[kg/tHM]	[%]	PtInp [%]
Coal	0.58	7.50	Slag	0.00	0.00	0.00
HGC dust	6.67	85.93	Generator Gas	7.63	100.00	1126.23
DRI	0.51	6.57				
Sum	7.76	100	Sum	7.63	100	

Discrepancy Input/Output: = 1.83 %

Input HGC	[kg/tHM]	[%]	Output HGC	[kg/tHM]	[%]	PtInp [%]
Generator Gas	7.63	100.00	HGC dust	6.67	87.50	985.50
Cooling Gas	0.00	0.00	Reducing Gas	0.76	10.00	112.58
			Cooling Gas	0.19	2.50	28.15
Sum	7.63	100	Sum	7.63	100	

Discrepancy Input/Output: = 0.0 %

A.9 Amount of zinc in kg/tHM in different compounds at each position – standard model
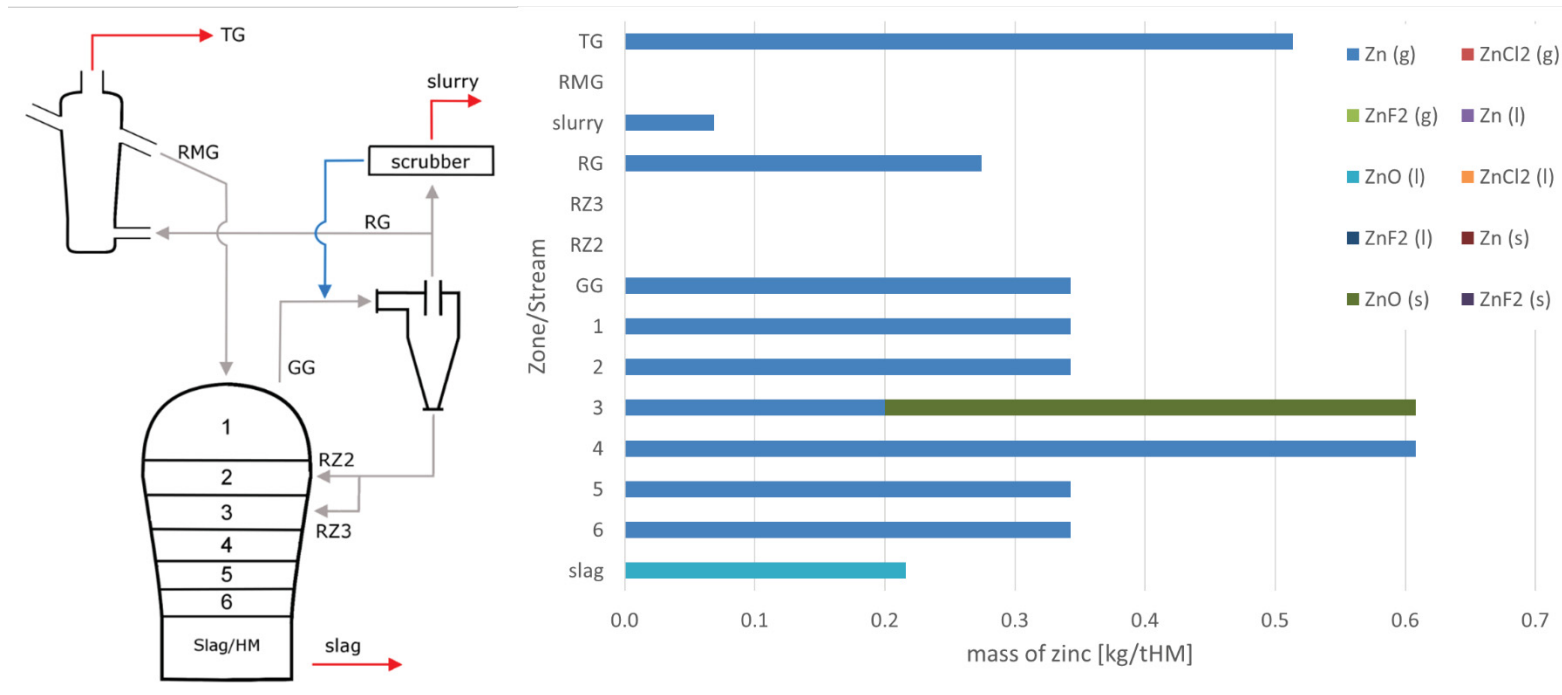
	slag	6	5	4	3	2	1	GG	RZ2	RZ3	RG	slurry	RMG	TG
Zn (g)	--	0.34	0.34	0.61	0.20	0.34	0.34	0.34	--	--	0.27	0.07	--	0.51
ZnCl2 (g)	--	--	--	--	--	--	--	--	--	--	--	--	--	--
ZnF2 (g)	--	--	--	--	--	--	--	--	--	--	--	--	--	--
Zn (l)	--	--	--	--	--	--	--	--	--	--	--	--	--	--
ZnO (l)	0.22	--	--	--	--	--	--	--	--	--	--	--	--	--
ZnCl2 (l)	--	--	--	--	--	--	--	--	--	--	--	--	--	--
ZnF2 (l)	--	--	--	--	--	--	--	--	--	--	--	--	--	--
Zn (s)	--	--	--	--	--	--	--	--	--	--	--	--	--	--
ZnO (s)	--	--	--	--	0.41	--	--	--	--	--	--	--	--	--
ZnF2 (s)	--	--	--	--	--	--	--	--	--	--	--	--	--	--
Sum	0.22	0.34	0.34	0.61	0.61	0.34	0.34	0.34	--	--	0.27	0.07	--	0.51

A.10 Sankey diagram for zinc – standard model

Top gas: 0.514 kg/tHM

Ore + Additives: 0.755 kg/tHM

Cooling gas: 0.069 kg/tHM

Coal: 0.034 kg/tHM

FB

HGC

Zone 1

Zone 2

Zone 3

Zone 4

Zone 5

Zone 6

scale: 1 kg/tHM

Slag/HM: 0.216 kg/tHM

Slag
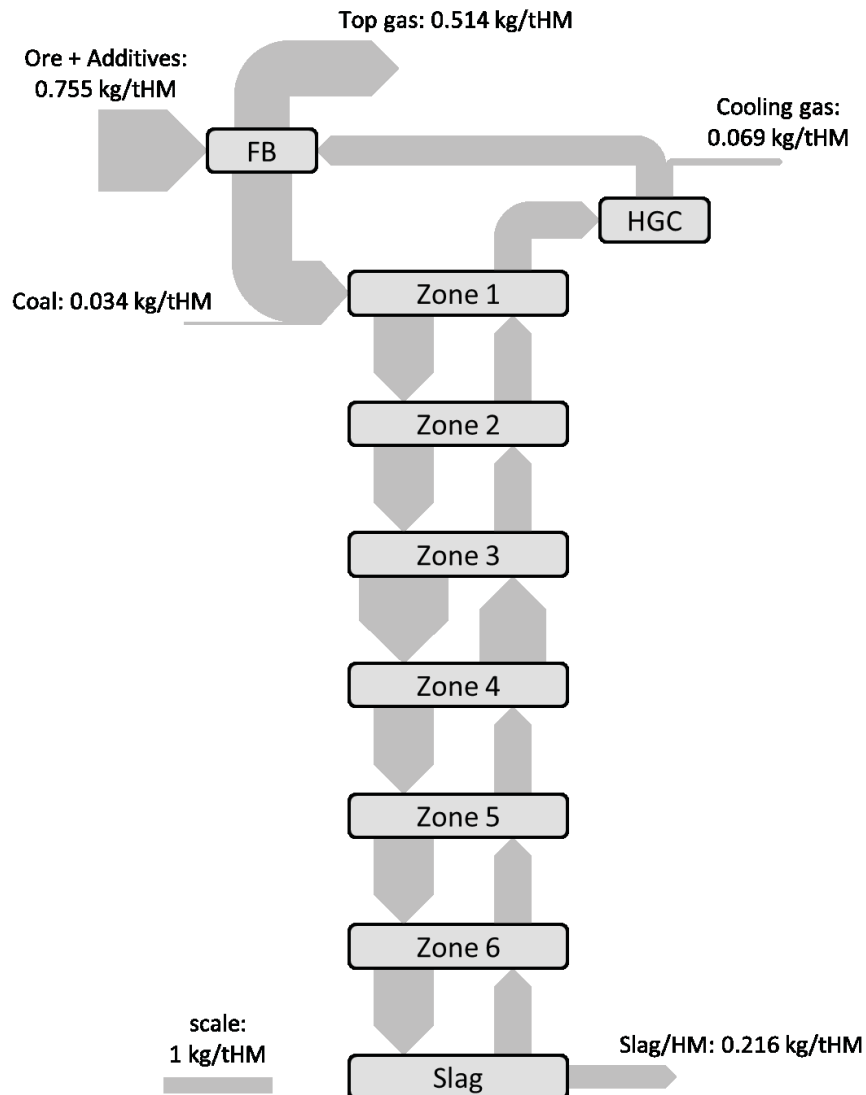
Input FB	[kg/tHM]	[%]	Output FB	[kg/tHM]	[%]	PtInp [%]
Ore	0.74	72.08	DRI	0.56	52.11	70.80
Additives	0.01	1.29	Top Gas	0.51	47.89	65.06
Reducing Gas	0.27	26.63				
Sum	1.03	100	Sum	1.07	100	

Discrepancy Input/Output: = 4.04 %

Input MG	[kg/tHM]	[%]	Output MG	[kg/tHM]	[%]	PtInp [%]
Coal	0.03	5.78	Slag	0.22	38.69	27.39
HGC dust	0.00	0.00	Generator Gas	0.34	61.31	43.40
DRI	0.56	94.22				
Sum	0.59	100	Sum	0.56	100	

Discrepancy Input/Output: = 6.14 %

Input HGC	[kg/tHM]	[%]	Output HGC	[kg/tHM]	[%]	PtInp [%]
Generator Gas	0.34	100.00	HGC dust	0.00	0.00	0.00
Cooling Gas	0.00	0.00	Reducing Gas	0.27	80.00	34.72
			Cooling Gas	0.07	20.00	8.68
Sum	0.34	100	Sum	0.34	100	

Discrepancy Input/Output: = 0.0 %

A.11 Amount of potassium in kg/tHM in different compounds at each position – Run01
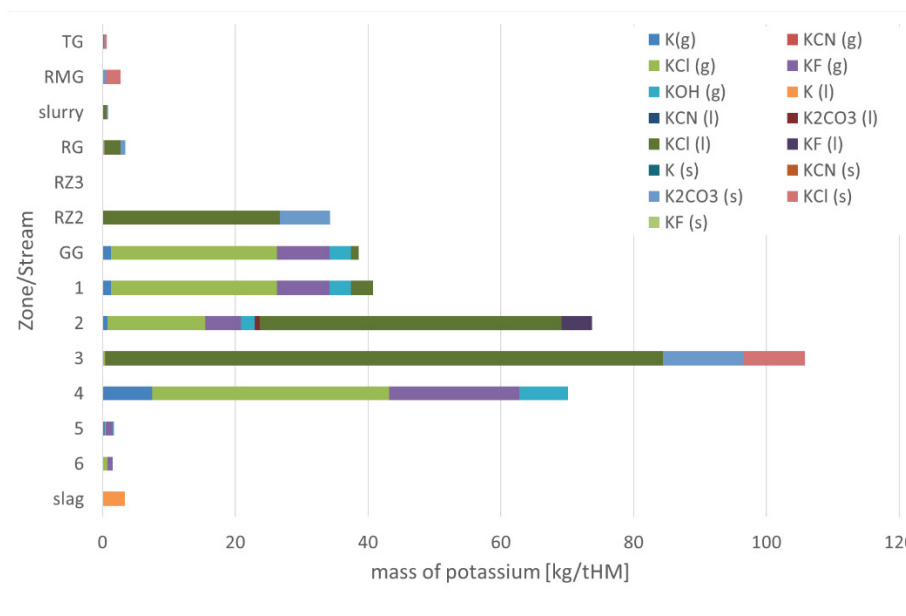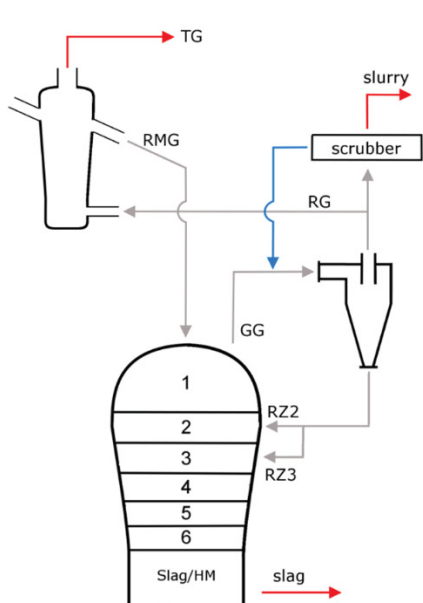
	slag	6	5	4	3	2	1	GG	RZ2	RZ3	RG	slurry	RMG	TG
K(g)	--	0.01	0.35	7.49	--	0.70	1.29	1.29	--	--	--	--	--	--
KCN (g)	--	--	--	0.02	--	0.01	0.02	0.02	--	--	--	--	--	--
KCl (g)	--	0.77	0.09	35.64	0.38	14.74	25.01	25.01	--	--	0.32	0.08	--	0.16
KF (g)	--	0.77	1.13	19.63	0.05	5.47	7.87	7.87	--	--	0.03	0.01	--	0.02
KOH (g)	--	--	0.13	7.38	0.01	2.03	3.20	3.20	--	--	0.01	--	--	--
K (l)	3.36	--	--	--	--	--	--	--	--	--	--	--	--	--
KCN (l)	--	--	--	--	--	--	--	--	--	--	--	--	--	--
K2CO3 (l)	--	--	--	--	--	0.66	--	--	--	--	--	--	--	--
KCl (l)	--	--	--	--	84.01	45.54	3.36	1.18	26.69	--	2.37	0.59	--	--
KF (l)	--	--	--	--	--	4.59	--	--	--	--	--	--	--	--
K (s)	--	--	--	--	--	--	--	--	--	--	--	--	--	--
KCN (s)	--	--	--	--	--	--	--	--	--	--	--	--	--	--
K2CO3 (s)	--	--	--	--	12.13	--	--	--	7.60	--	0.68	0.17	0.58	0.10
KCl (s)	--	--	--	--	9.23	--	--	--	--	--	--	--	2.17	0.38
KF (s)	--	--	--	--	--	--	--	--	--	--	--	--	--	--
Sum	3.36	1.55	1.71	70.16	105.82	73.75	40.74	38.55	34.29	--	3.41	0.85	2.75	0.66

A.12 Sankey diagram for potassium – Run01
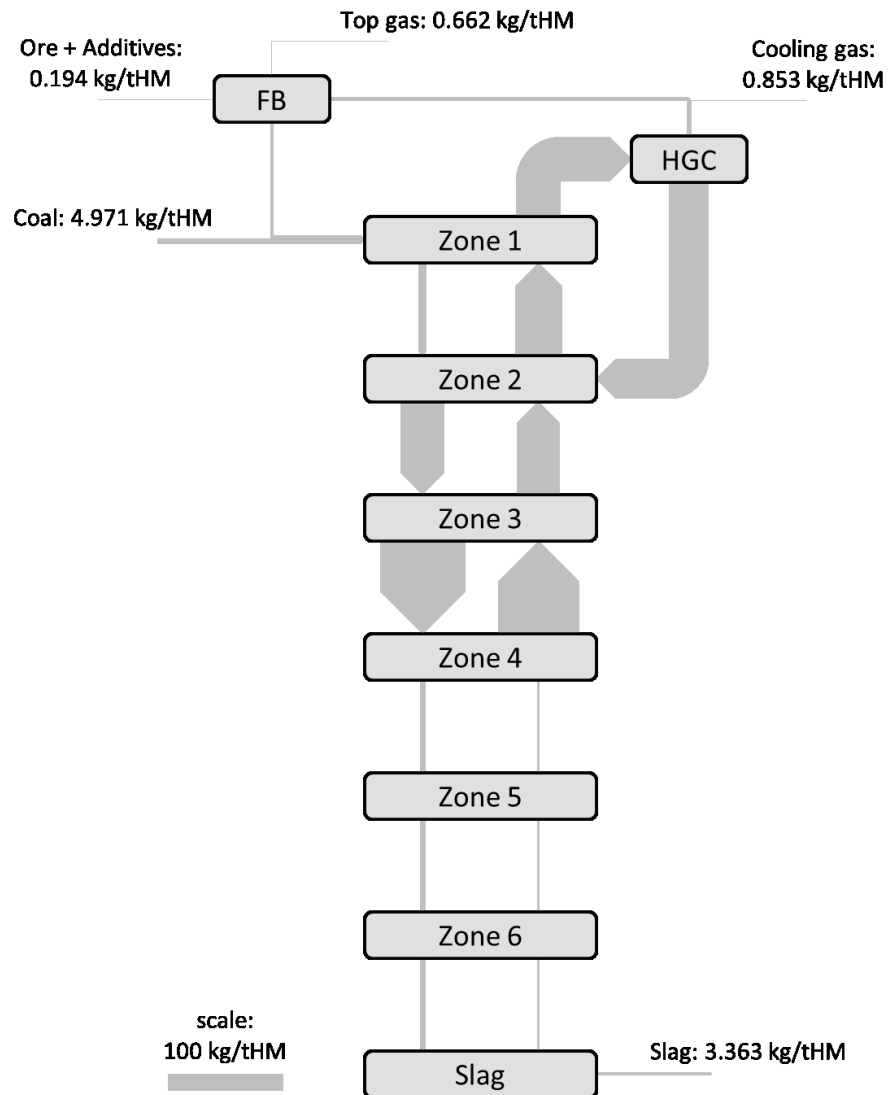
Input FB	[kg/tHM]	[%]	Output FB	[kg/tHM]	[%]	PtInp [%]
Ore	0.12	3.24	DRI	2.75	80.58	53.20
Additives	0.08	2.14	Top Gas	0.66	19.42	12.82
Reducing Gas	3.41	94.62				
Sum	3.60	100	Sum	3.41	100	

Discrepancy Input/Output: = 5.69 %

Input MG	[kg/tHM]	[%]	Output MG	[kg/tHM]	[%]	PtInp [%]
Coal	4.97	11.83	Slag	3.36	8.02	65.11
HGC dust	34.29	81.62	Generator Gas	38.55	91.98	746.38
DRI	2.75	6.54				
Sum	42.01	100	Sum	41.92	100	

Discrepancy Input/Output: = 0.22 %

Input HGC	[kg/tHM]	[%]	Output HGC	[kg/tHM]	[%]	PtInp [%]
Generator Gas	38.55	100.00	HGC dust	34.29	88.94	663.85
Cooling Gas	0.00	0.00	Reducing Gas	3.41	8.85	66.02
			Cooling Gas	0.85	2.21	16.51
Sum	38.55	100	Sum	38.55	100	

Discrepancy Input/Output: = 0.0 %

A.13 Amount of sodium in kg/tHM in different compounds at each position – Run01
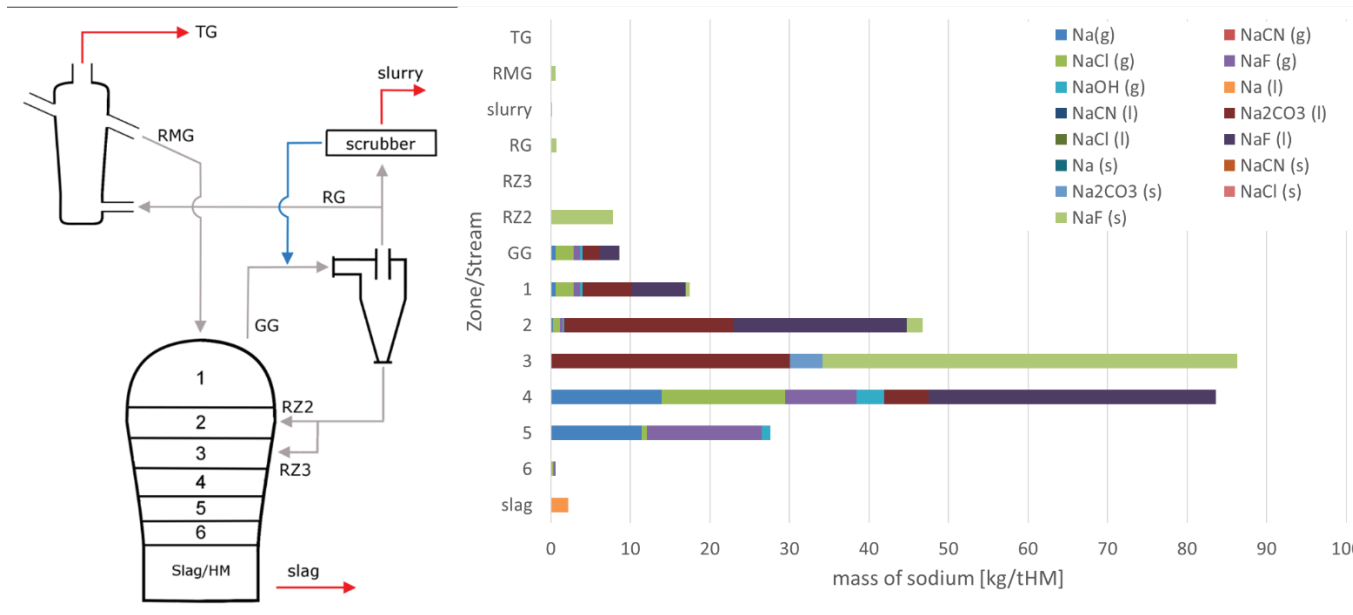
	slag	6	5	4	3	2	1	GG	RZ2	RZ3	RG	slurry	RMG	TG
Na(g)	--	0.01	11.39	13.95	--	0.24	0.60	0.60	--	--	--	--	--	--
NaCN (g)	--	0.01	0.01	0.02	--	0.00	0.01	0.01	--	--	--	--	--	--
NaCl (g)	--	0.29	0.68	15.47	0.01	0.93	2.29	2.29	--	--	0.01	--	--	--
NaF (g)	--	0.31	14.46	9.04	--	0.38	0.78	0.78	--	--	--	--	--	--
NaOH (g)	--	--	1.07	3.42	--	0.14	0.31	0.31	--	--	--	--	--	--
Na (l)	2.20	--	--	--	--	--	--	--	--	--	--	--	--	--
NaCN (l)	--	--	--	--	--	--	--	--	--	--	--	--	--	--
Na2CO3 (l)	--	--	--	5.64	30.05	21.25	6.20	2.17	--	--	--	--	--	--
NaCl (l)	--	--	--	--	--	--	--	--	--	--	--	--	--	--
NaF (l)	--	--	--	36.08	--	21.78	6.81	2.38	--	--	--	--	--	--
Na (s)	--	--	--	--	--	--	--	--	--	--	--	--	--	--
NaCN (s)	--	--	--	--	--	--	--	--	--	--	--	--	--	--
Na2CO3 (s)	--	--	--	--	4.09	--	--	--	--	--	--	--	--	--
NaCl (s)	--	--	--	--	--	--	--	--	--	--	--	--	--	--
NaF (s)	--	--	--	--	52.17	2.06	0.48	0.17	7.81	--	0.69	0.17	0.60	0.11
Sum	2.20	0.62	27.60	83.63	86.34	46.77	17.46	8.70	7.81	--	0.71	0.17	0.60	0.11

A.14 Sankey diagram for sodium – Run01
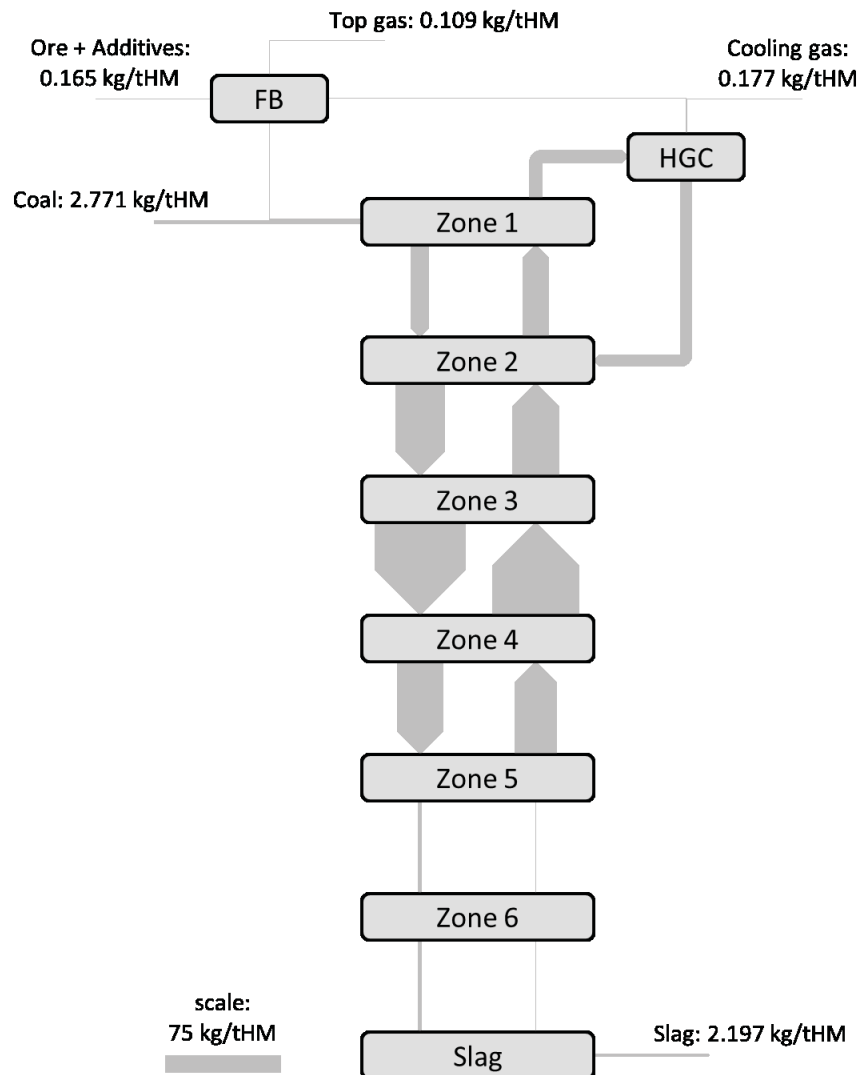
Input FB	[kg/tHM]	[%]	Output FB	[kg/tHM]	[%]	PtInp [%]
Ore	0.16	17.79	DRI	0.60	84.55	20.38
Additives	0.01	1.13	Top Gas	0.11	15.45	3.72
Reducing Gas	0.71	81.08				
Sum	0.87	100	Sum	0.71	100	

Discrepancy Input/Output: = 23.34 %

Input MG	[kg/tHM]	[%]	Output MG	[kg/tHM]	[%]	PtInp [%]
Coal	2.77	24.78	Slag	2.20	20.17	74.83
HGC dust	7.81	69.87	Generator Gas	8.70	79.83	296.19
DRI	0.60	5.35				
Sum	11.18	100	Sum	10.89	100	

Discrepancy Input/Output: = 2.64 %

Input HGC	[kg/tHM]	[%]	Output HGC	[kg/tHM]	[%]	PtInp [%]
Generator Gas	8.70	100.00	HGC dust	7.81	89.83	266.06
Cooling Gas	0.00	0.00	Reducing Gas	0.71	8.14	24.10
			Cooling Gas	0.18	2.03	6.02
Sum	8.70	100	Sum	8.70	100	

Discrepancy Input/Output: = 0.0 %

A.15 Amount of chlorine in kg/tHM in different compounds at each position – Run01
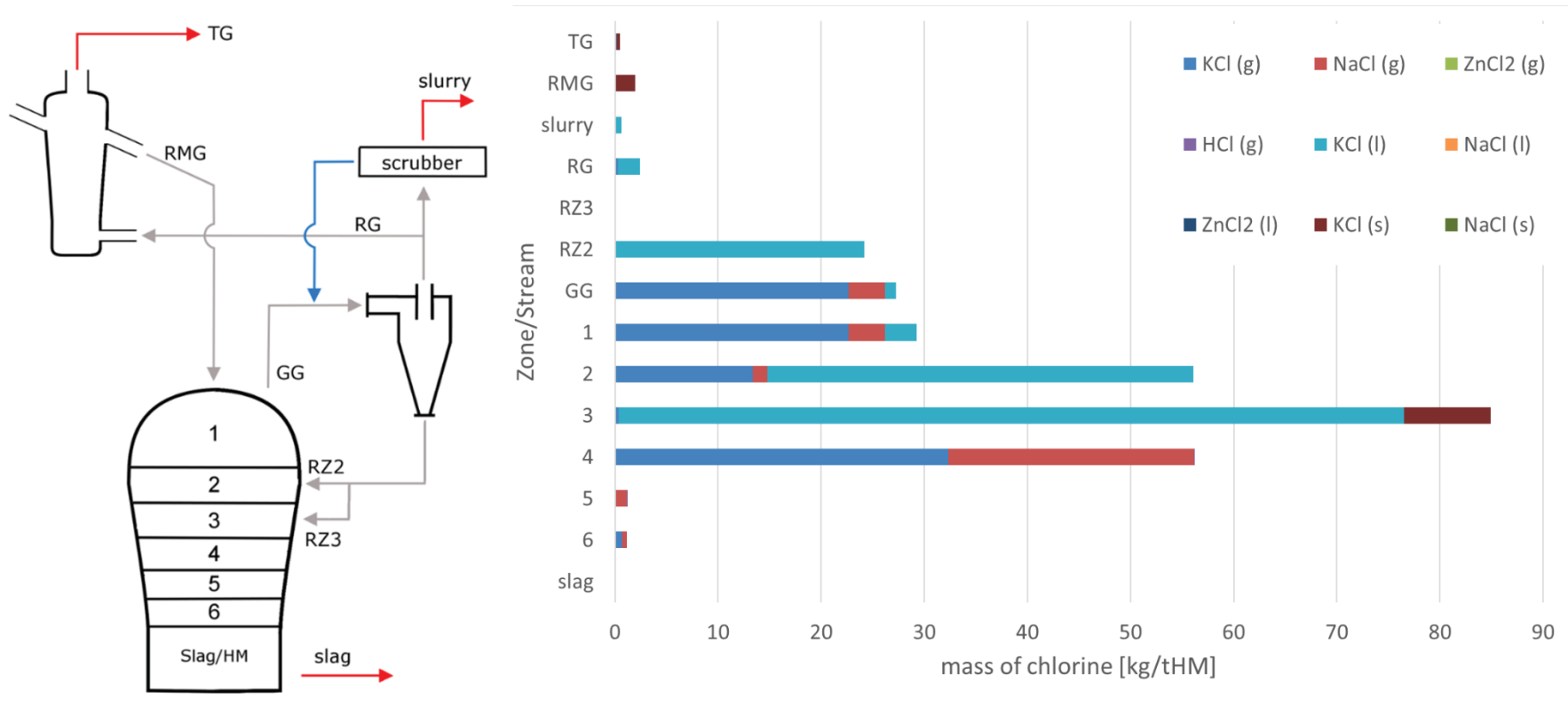
	slag	6	5	4	3	2	1	GG	RZ2	RZ3	RG	slurry	RMG	TG
KCl (g)	--	0.70	0.09	32.31	0.35	13.36	22.67	22.67	--	--	0.29	0.07	--	0.14
NaCl (g)	--	0.45	1.06	23.84	0.02	1.43	3.53	3.53	--	--	0.02	0.00	--	0.00
ZnCl2 (g)	--	--	--	--	--	--	--	--	--	--	--	--	--	--
HCl (g)	--	--	0.01	0.02	--	0.01	0.01	0.01	--	--	--	--	--	--
KCl (l)	--	--	--	--	76.16	41.29	3.05	1.07	24.20	--	2.15	0.54	--	--
NaCl (l)	--	--	--	--	--	--	--	--	--	--	--	--	--	--
ZnCl2 (l)	--	--	--	--	--	--	--	--	--	--	--	--	--	--
KCl (s)	--	--	--	--	8.36	--	--	--	--	--	--	--	1.97	0.35
NaCl (s)	--	--	--	--	--	--	--	--	--	--	--	--	--	--
Sum	--	1.15	1.15	56.18	84.90	56.09	29.26	27.28	24.20	--	2.46	0.61	1.97	0.49

A.16 Sankey diagram for chorine – Run01
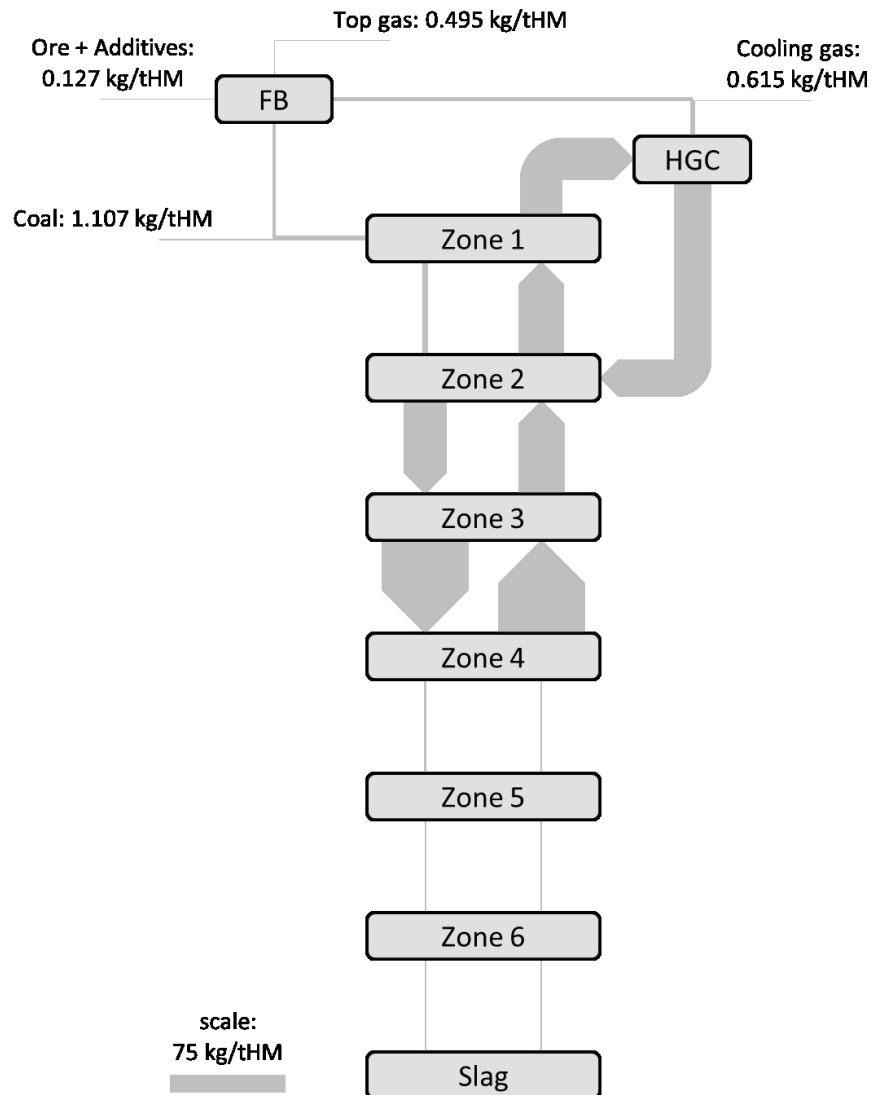
Input FB	[kg/tHM]	[%]	Output FB	[kg/tHM]	[%]	PtInp [%]
Ore	0.12	4.83	DRI	1.97	79.89	159.30
Additives	0.002	0.08	Top Gas	0.49	20.11	40.10
Reducing Gas	2.46	95.09				
Sum	2.59	100	Sum	2.46	100	

Discrepancy Input/Output: = 5.17 %

Input MG	[kg/tHM]	[%]	Output MG	[kg/tHM]	[%]	PtInp [%]
Coal	1.11	4.06	Slag	0.00	0.00	0.00
HGC dust	24.20	88.73	Generator Gas	27.28	100.00	2210.55
DRI	1.97	7.21				
Sum	27.27	100	Sum	27.28	100	

Discrepancy Input/Output: = 0.01 %

Input HGC	[kg/tHM]	[%]	Output HGC	[kg/tHM]	[%]	PtInp [%]
Generator Gas	27.28	100.00	HGC dust	24.20	88.72	1961.31
Cooling Gas	0.00	0.00	Reducing Gas	2.46	9.02	199.39
			Cooling Gas	0.62	2.26	49.85
Sum	27.28	100	Sum	27.28	100	

Discrepancy Input/Output: = 0.0 %

A.17 Amount of fluorine in kg/tHM in different compounds at each position – Run01
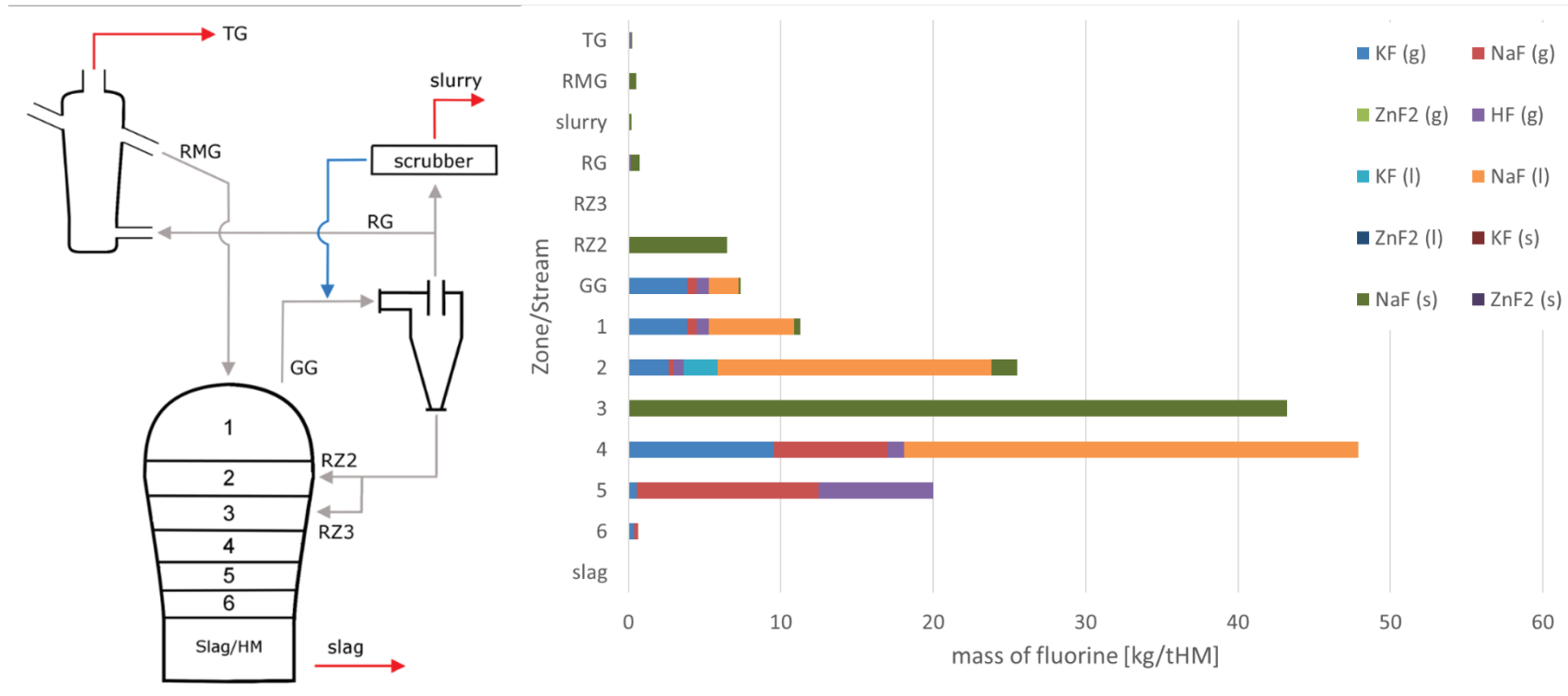
|	slag	6	5	4	3	2	1	GG	RZ2	RZ3	RG	slurry	RMG	TG
KF (g)	--	0.37	0.55	9.54	0.03	2.66	3.83	3.83	--	--	0.02	--	--	0.01
NaF (g)	--	0.25	11.94	7.47	--	0.31	0.64	0.64	--	--	--	--	--	--
ZnF2 (g)	--	--	--	--	--	--	--	--	--	--	--	--	--	--
HF (g)	--	--	7.48	1.08	0.08	0.63	0.79	0.79	--	--	0.14	0.04	--	0.14
KF (l)	--	--	--	--	--	2.23	--	--	--	--	--	--	--	--
NaF (l)	--	--	--	29.80	--	17.99	5.62	1.97	--	--	--	--	--	--
ZnF2 (l)	--	--	--	--	--	--	--	--	--	--	--	--	--	--
KF (s)	--	--	--	--	--	--	--	--	--	--	--	--	--	--
NaF (s)	--	--	--	--	43.10	1.70	0.39	0.14	6.45	--	0.57	0.14	0.49	0.09
ZnF2 (s)	--	--	--	--	--	--	--	--	--	--	--	--	--	--
Sum	--	0.63	19.97	47.89	43.21	25.53	11.28	7.37	6.45	--	0.73	0.18	0.49	0.24

A.18 Sankey diagram for fluorine – Run01
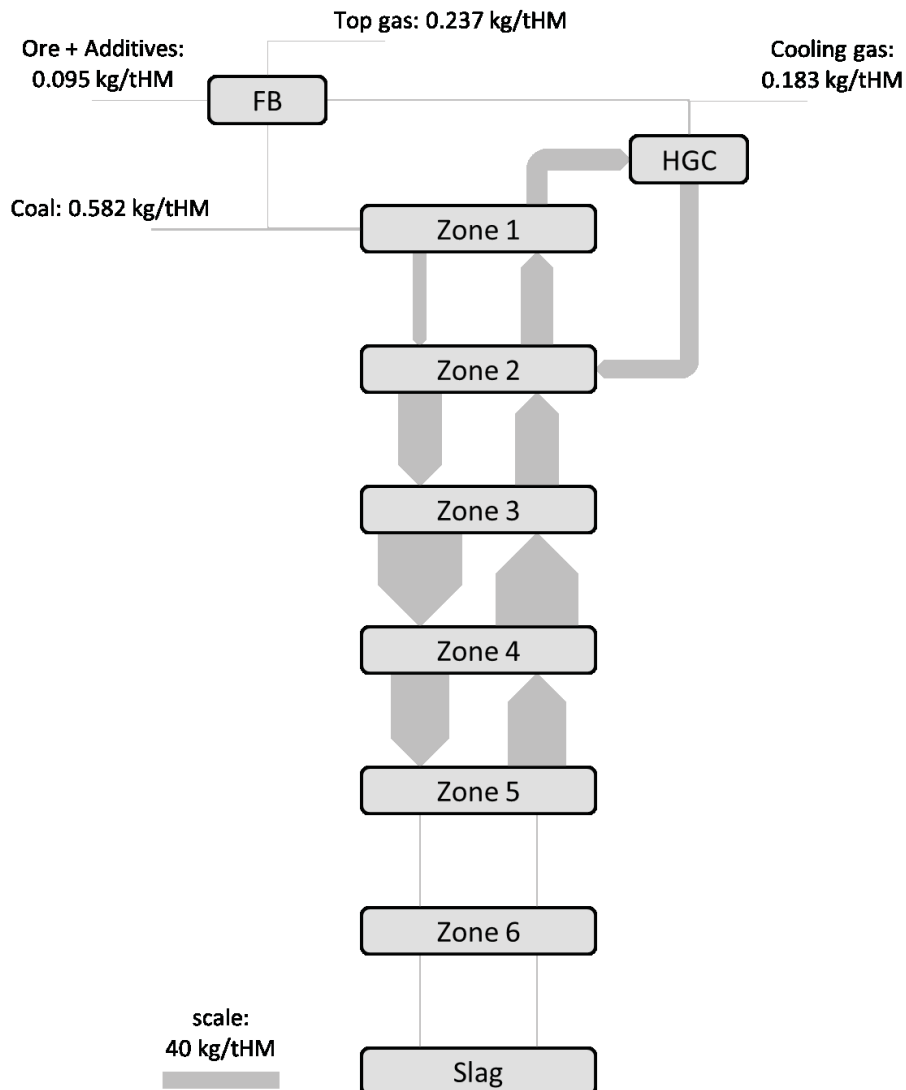
Input FB	[kg/tHM]	[%]	Output FB	[kg/tHM]	[%]	PtInp [%]
Ore	0.09	11.34	DRI	0.49	67.58	73.00
Additives	0.001	0.16	Top Gas	0.24	32.42	35.02
Reducing Gas	0.73	88.50				
Sum	0.83	100	Sum	0.73	100	
Discrepancy Input/Output: = 13.0 %						

Input MG	[kg/tHM]	[%]	Output MG	[kg/tHM]	[%]	PtInp [%]
Coal	0.58	7.73	Slag	0.00	0.00	0.00
HGC dust	6.45	85.70	Generator Gas	7.37	100.00	1087.90
DRI	0.49	6.57				
Sum	7.53	100	Sum	7.37	100	
Discrepancy Input/Output: = 2.2 %						

Input HGC	[kg/tHM]	[%]	Output HGC	[kg/tHM]	[%]	PtInp [%]
Generator Gas	7.37	100.00	HGC dust	6.45	87.59	952.88
Cooling Gas	0.00	0.00	Reducing Gas	0.73	9.93	108.02
			Cooling Gas	0.18	2.48	27.00
Sum	7.37	100	Sum	7.37	100	
Discrepancy Input/Output: = 0.0 %						

A.19 Amount of potassium in kg/tHM in different compounds at each position – Run02
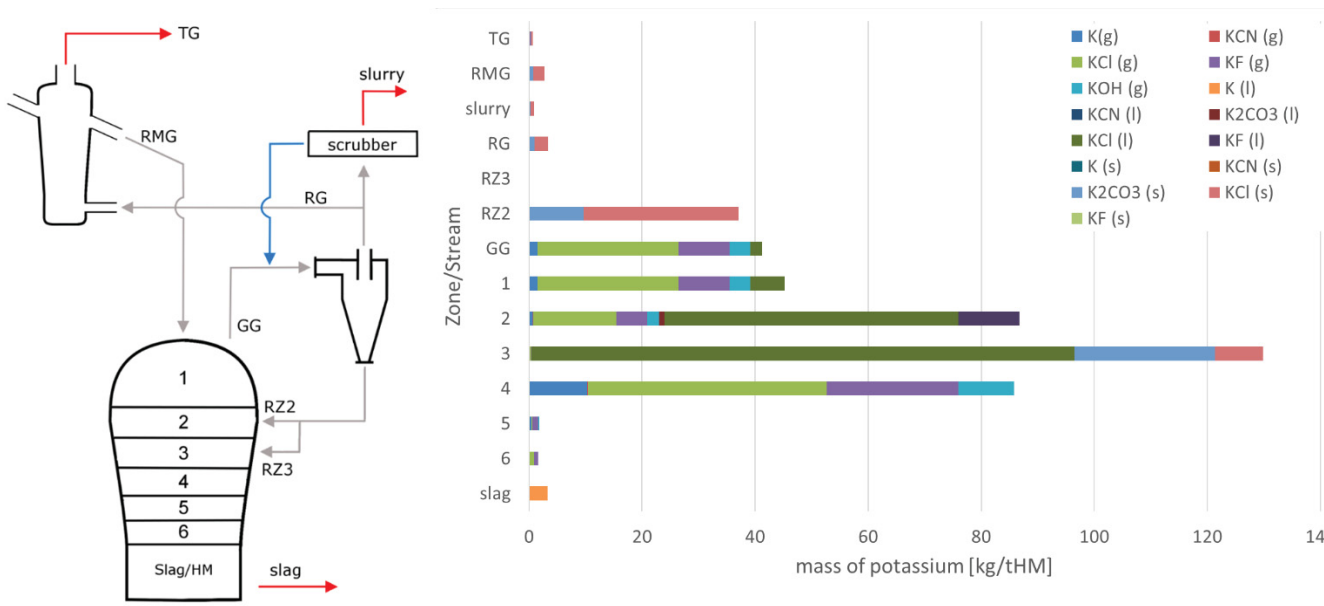
	slag	6	5	4	3	2	1	GG	RZ2	RZ3	RG	slurry	RMG	TG
K(g)	--	0.07	0.48	10.36	--	0.70	1.47	1.47	--	--	--	--	--	--
KCN (g)	--	0.01	--	0.02	--	0.01	0.02	0.02	--	--	--	--	--	--
KCl (g)	--	0.78	0.09	42.34	0.38	14.74	24.97	24.97	--	--	0.08	0.02	--	0.17
KF (g)	--	0.78	1.05	23.23	0.05	5.47	9.01	9.01	--	--	0.01	--	--	0.02
KOH (g)	--	--	0.18	9.87	0.01	2.03	3.66	3.66	--	--	--	--	--	--
K (l)	3.26	--	--	--	--	--	--	--	--	--	--	--	--	--
KCN (l)	--	--	--	--	--	--	--	--	--	--	--	--	--	--
K2CO3 (l)	--	--	--	--	--	1.01	--	--	--	--	--	--	--	--
KCl (l)	--	--	--	--	96.05	51.99	6.15	2.15	--	--	--	--	--	--
KF (l)	--	--	--	--	--	10.76	--	--	--	--	--	--	--	--
K (s)	--	--	--	--	--	--	--	--	--	--	--	--	--	--
KCN (s)	--	--	--	--	--	--	--	--	--	--	--	--	--	--
K2CO3 (s)	--	--	--	--	24.84	--	--	--	9.66	--	0.86	0.21	0.72	0.13
KCl (s)	--	--	--	--	8.49	--	--	--	27.38	--	2.43	0.61	1.99	0.35
KF (s)	--	--	--	--	--	--	--	--	--	--	--	--	--	--
Sum	3.26	1.65	1.81	85.82	129.84	86.71	45.27	41.27	37.04	--	3.38	0.84	2.71	0.67

A.20 Sankey diagram for potassium – Run02
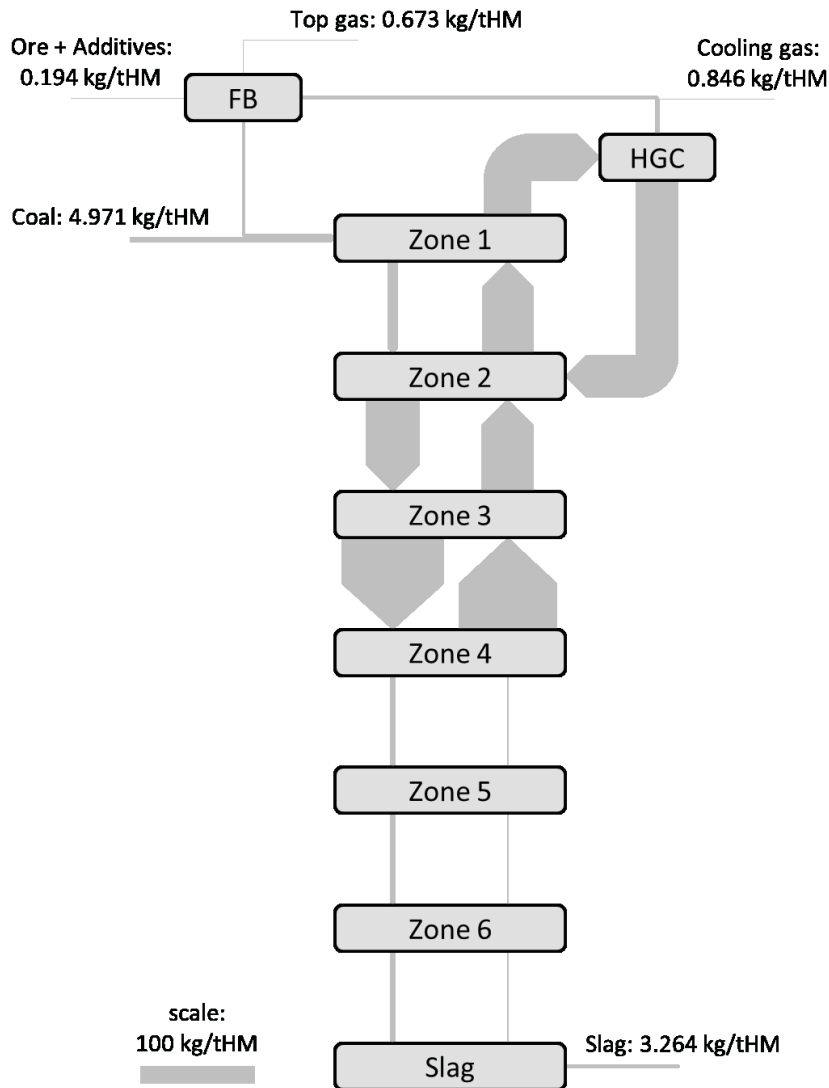
Input FB	[kg/tHM]	[%]	Output FB	[kg/tHM]	[%]	PtInp [%]
Ore	0.12	3.26	DRI	2.71	80.13	52.52
Additives	0.08	2.16	Top Gas	0.67	19.87	13.03
Reducing Gas	3.39	94.58				
Sum	3.58	100	Sum	3.39	100	

Discrepancy Input/Output: = 5.73 %

Input MG	[kg/tHM]	[%]	Output MG	[kg/tHM]	[%]	PtInp [%]
Coal	4.97	11.11	Slag	3.26	7.33	63.20
HGC dust	37.04	82.82	Generator Gas	41.27	92.67	799.09
DRI	2.71	6.07				
Sum	44.73	100	Sum	44.54	100	

Discrepancy Input/Output: = 0.42 %

| Input HGC	[kg/tHM]	[%]	Output HGC	[kg/tHM]	[%]	PtInp [%]
Generator Gas	41.27	100.00	HGC dust	37.04	89.75	717.15
Cooling Gas	0.00	0.00	Reducing Gas	3.39	8.20	65.55
			Cooling Gas	0.85	2.05	16.39
Sum	41.27	100	Sum	41.27	100	

Discrepancy Input/Output: = 0.0 %

A.21 Amount of sodium in kg/tHM in different compounds at each position – Run02
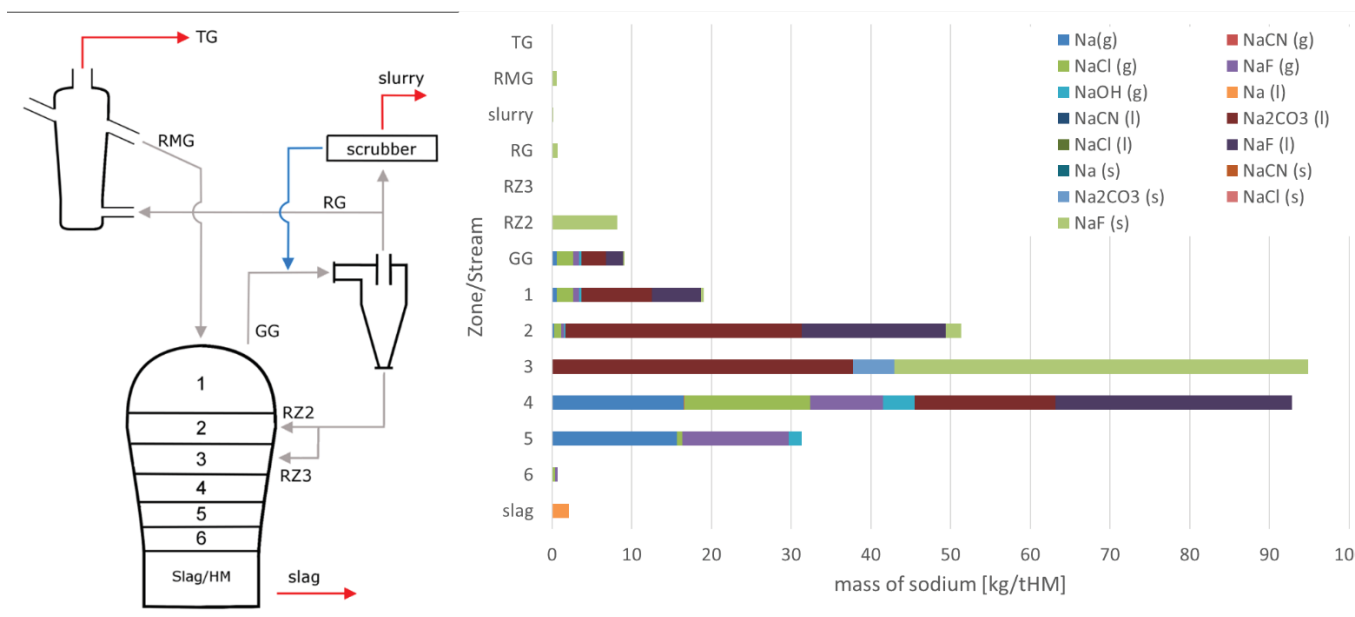
	slag	6	5	4	3	2	1	GG	RZ2	RZ3	RG	slurry	RMG	TG
Na(g)	--	0.08	15.65	16.52	--	0.24	0.60	0.60	--	--	--	--	--	--
NaCN (g)	--	0.02	0.01	0.03	--	0.00	0.01	0.01	--	--	--	--	--	--
NaCl (g)	--	0.29	0.69	15.83	0.01	0.93	2.00	2.00	--	--	--	--	--	--
NaF (g)	--	0.30	13.37	9.17	--	0.38	0.78	0.78	--	--	--	--	--	--
NaOH (g)	--	--	1.58	3.94	--	0.14	0.31	0.31	--	--	--	--	--	--
Na (l)	2.14	--	--	--	--	--	--	--	--	--	--	--	--	--
NaCN (l)	--	--	--	--	--	--	--	--	--	--	--	--	--	--
Na2CO3 (l)	--	--	--	17.72	37.75	29.67	8.84	3.09	--	--	--	--	--	--
NaCl (l)	--	--	--	--	--	--	--	--	--	--	--	--	--	--
NaF (l)	--	--	--	29.64	--	18.07	6.15	2.15	--	--	--	--	--	--
Na (s)	--	--	--	--	--	--	--	--	--	--	--	--	--	--
NaCN (s)	--	--	--	--	--	--	--	--	--	--	--	--	--	--
Na2CO3 (s)	--	--	--	--	5.21	--	--	--	--	--	--	--	--	--
NaCl (s)	--	--	--	--	--	--	--	--	--	--	--	--	--	--
NaF (s)	--	--	--	--	51.87	1.89	0.38	0.13	8.16	--	0.73	0.18	0.61	0.11
Sum	2.14	0.68	31.31	92.84	94.84	51.30	19.05	9.07	8.16	--	0.73	0.18	0.61	0.11

A.22 Sankey diagram for sodium – Run02
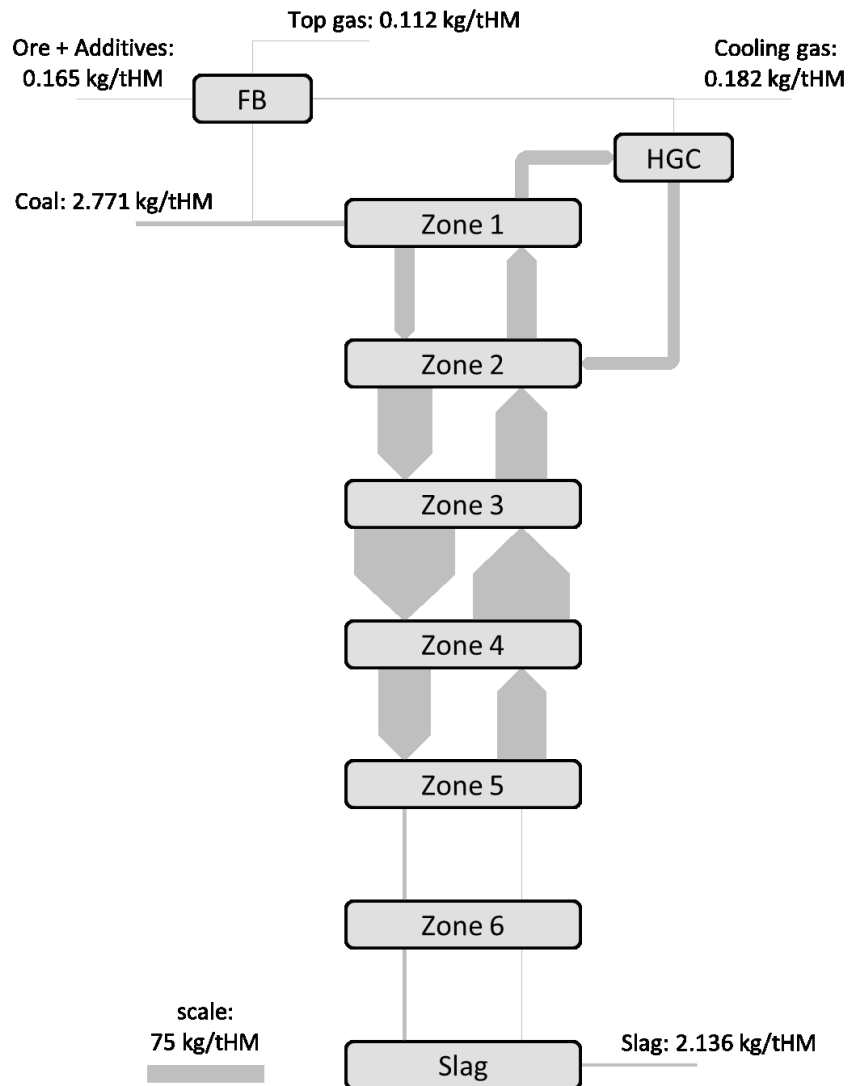
Input FB	[kg/tHM]	[%]	Output FB	[kg/tHM]	[%]	PtInp [%]
Ore	0.16	17.41	DRI	0.61	84.54	20.92
Additives	0.01	1.11	Top Gas	0.11	15.46	3.83
Reducing Gas	0.73	81.48				
Sum	0.89	100	Sum	0.73	100	

Discrepancy Input/Output: = 22.73 %

Input MG	[kg/tHM]	[%]	Output MG	[kg/tHM]	[%]	PtInp [%]
Coal	2.77	24.01	Slag	2.14	19.07	72.76
HGC dust	8.16	70.67	Generator Gas	9.07	80.93	308.76
DRI	0.61	5.32				
Sum	11.54	100	Sum	11.20	100	

Discrepancy Input/Output: = 3.04 %

Input HGC	[kg/tHM]	[%]	Output HGC	[kg/tHM]	[%]	PtInp [%]
Generator Gas	9.07	100.00	HGC dust	8.16	89.98	277.82
Cooling Gas	0.00	0.00	Reducing Gas	0.73	8.02	24.75
			Cooling Gas	0.18	2.00	6.19
Sum	9.07	100	Sum	9.07	100	

Discrepancy Input/Output: = 0.0 %

A.23 Amount of chlorine in kg/tHM in different compounds at each position – Run02
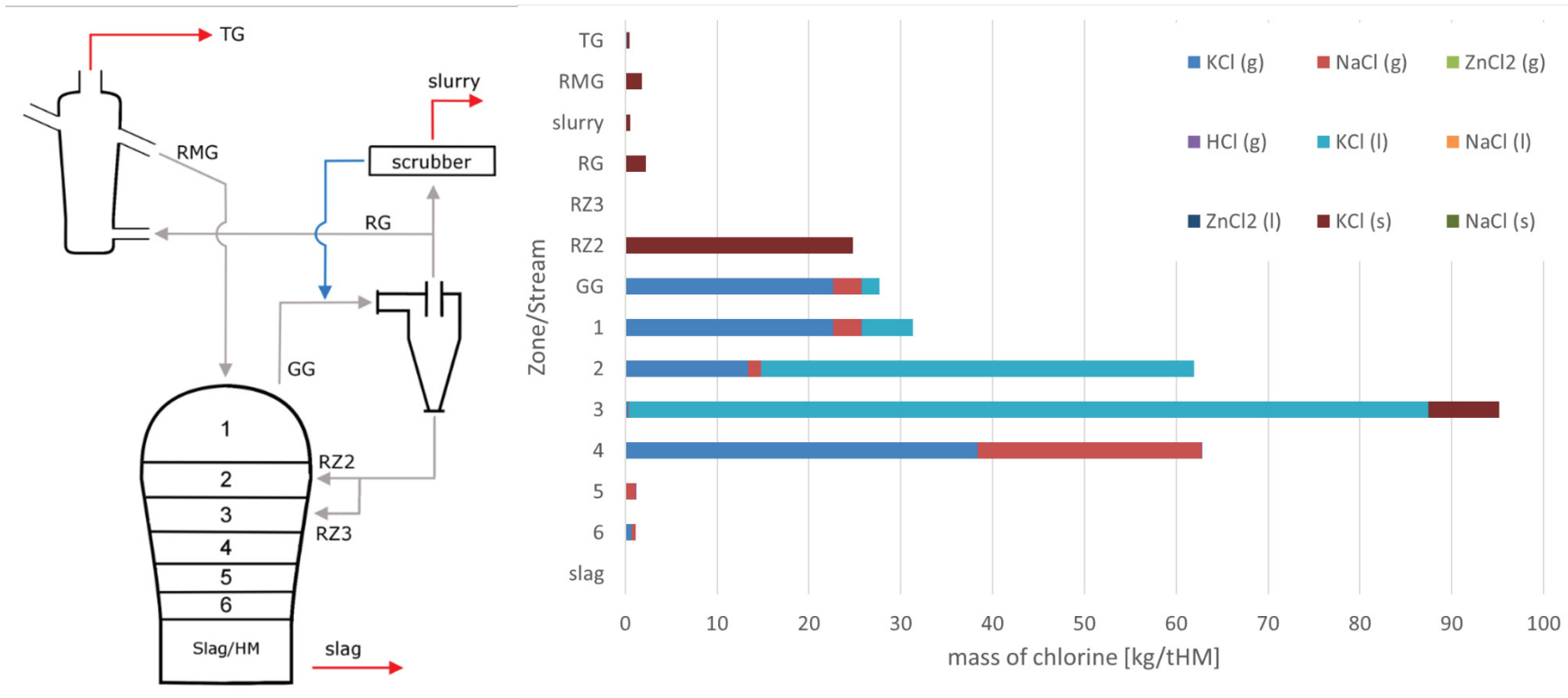
	slag	6	5	4	3	2	1	GG	RZ2	RZ3	RG	slurry	RMG	TG
KCl (g)	--	0.71	0.08	38.39	0.35	13.36	22.63	22.63	--	--	0.07	0.02	--	0.15
NaCl (g)	--	0.44	1.06	24.40	0.02	1.43	3.08	3.08	--	--	--	--	--	0.01
ZnCl2 (g)	--	--	--	--	--	--	--	--	--	--	--	--	--	--
HCl (g)	--	--	0.01	0.02	--	0.01	0.01	0.01	--	--	--	--	--	--
KCl (l)	--	--	--	--	87.09	47.14	5.57	1.95	--	--	--	--	--	--
NaCl (l)	--	--	--	--	--	--	--	--	--	--	--	--	--	--
ZnCl2 (l)	--	--	--	--	--	--	--	--	--	--	--	--	--	--
KCl (s)	--	--	--	--	7.70	--	--	--	24.82	--	2.21	0.55	1.80	0.32
NaCl (s)	--	--	--	--	--	--	--	--	--	--	--	--	--	--
Sum	--	1.15	1.15	62.81	95.15	61.94	31.30	27.68	24.82	--	2.28	0.57	1.80	0.48

A.24 Sankey diagram for chlorine – Run02
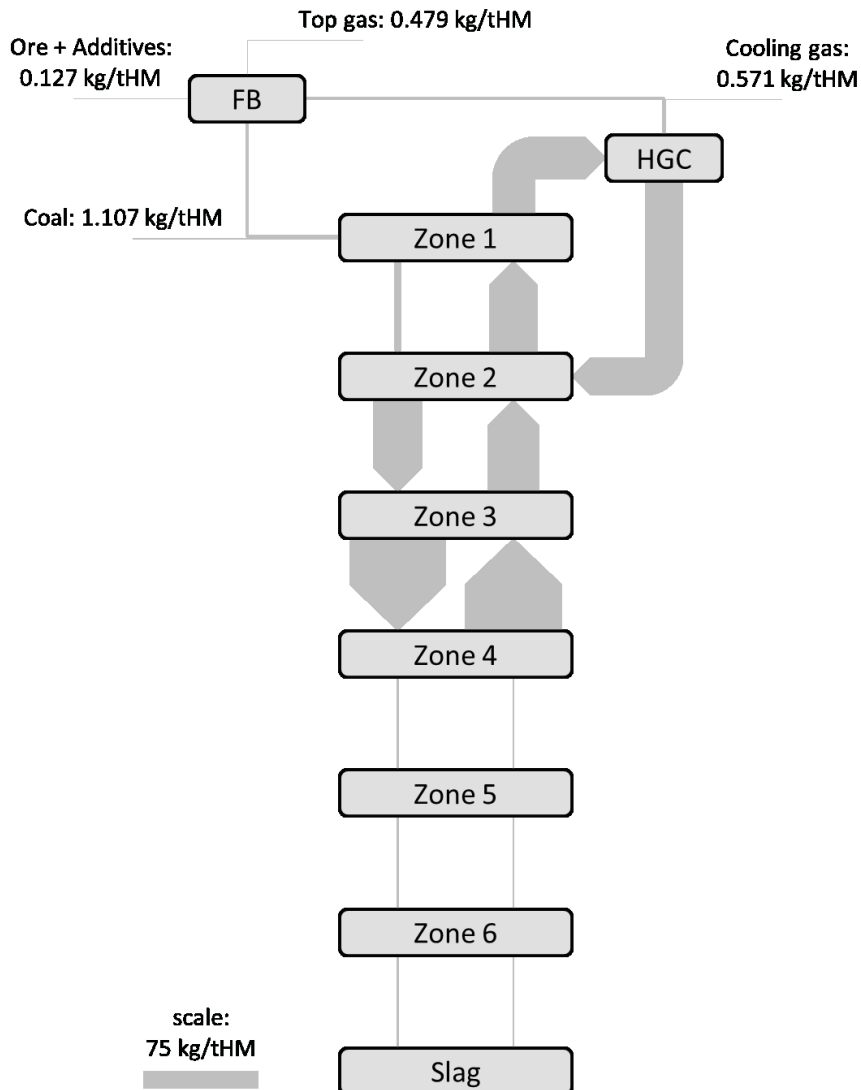
Input FB	[kg/tHM]	[%]	Output FB	[kg/tHM]	[%]	PtInp [%]
Ore	0.12	5.18	DRI	1.80	79.01	146.23
Additives	0.002	0.09	Top Gas	0.48	20.99	38.84
Reducing Gas	2.28	94.73				
Sum	2.41	100	Sum	2.28	100	

Discrepancy Input/Output: = 5.57 %

Input MG	[kg/tHM]	[%]	Output MG	[kg/tHM]	[%]	PtInp [%]
Coal	1.11	3.99	Slag	0.00	0.00	0.00
HGC dust	24.82	89.50	Generator Gas	27.68	100.00	2243.21
DRI	1.80	6.51				
Sum	27.74	100	Sum	27.68	100	

Discrepancy Input/Output: = 0.2 %

| Input HGC	[kg/tHM]	[%]	Output HGC	[kg/tHM]	[%]	PtInp [%]
Generator Gas	27.68	100.00	HGC dust	24.82	89.69	2011.88
Cooling Gas	0.00	0.00	Reducing Gas	2.28	8.25	185.07
			Cooling Gas	0.57	2.06	46.27
Sum	27.68	100	Sum	27.68	100	

Discrepancy Input/Output: = 0.0 %

A.25 Amount of fluorine in kg/tHM in different compounds at each position – Run02
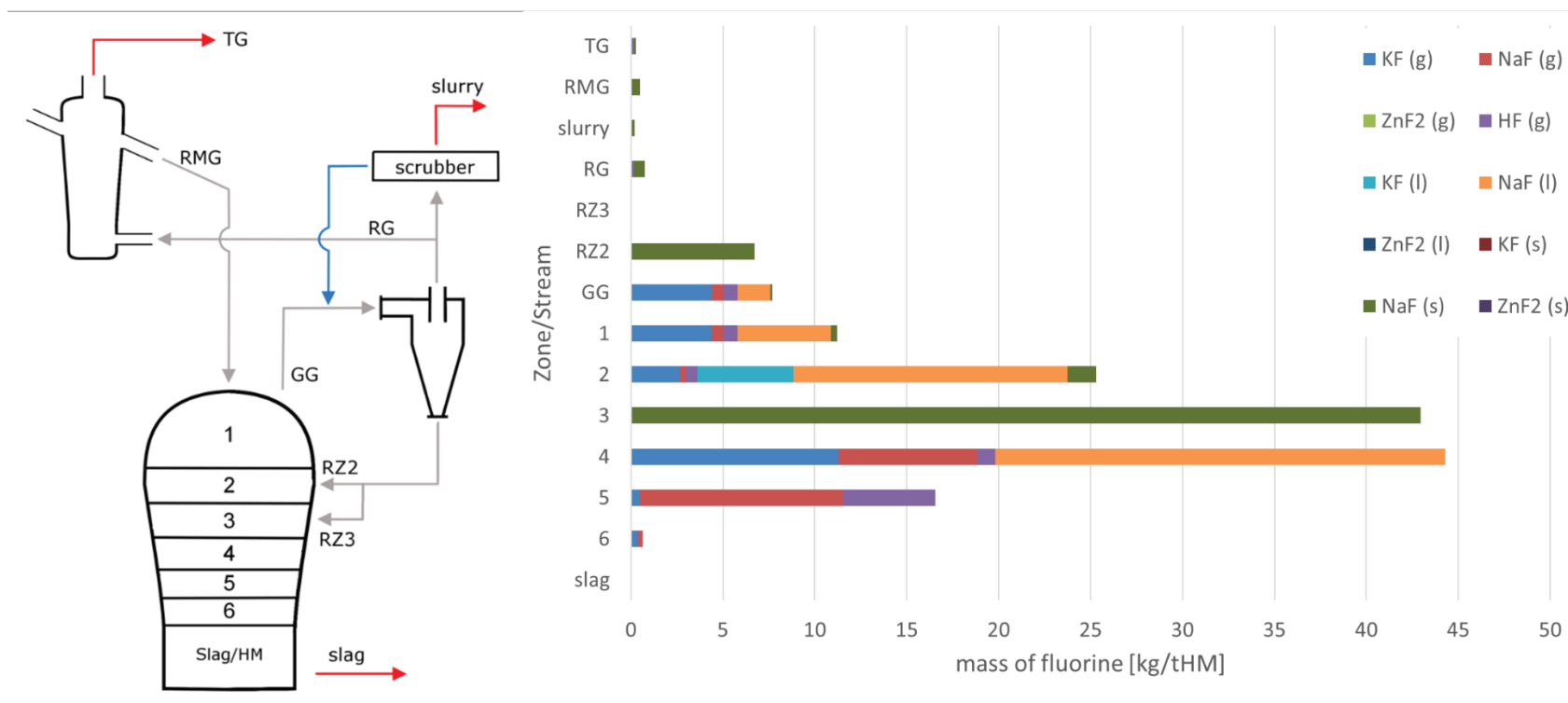
|	slag	6	5	4	3	2	1	GG	RZ2	RZ3	RG	slurry	RMG	TG
KF (g)	--	0.38	0.51	11.29	0.03	2.66	4.38	4.38	--	--	0.00	--	--	0.01
NaF (g)	--	0.25	11.05	7.58	--	0.31	0.64	0.64	--	--	--	--	--	--
ZnF2 (g)	--	--	--	--	--	--	--	--	--	--	--	--	--	--
HF (g)	--	--	4.98	0.95	0.08	0.63	0.79	0.79	--	--	0.17	0.04	--	0.16
KF (l)	--	--	--	--	--	5.23	--	--	--	--	--	--	--	--
NaF (l)	--	--	--	24.48	--	14.93	5.08	1.78	--	--	--	--	--	--
ZnF2 (l)	--	--	--	--	--	--	--	--	--	--	--	--	--	--
KF (s)	--	--	--	--	--	--	--	--	--	--	--	--	--	--
NaF (s)	--	--	--	--	42.85	1.56	0.31	0.11	6.74	--	0.60	0.15	0.51	0.09
ZnF2 (s)	--	--	--	--	--	--	--	--	--	--	--	--	--	--
Sum	--	0.63	16.54	44.30	42.95	25.32	11.20	7.70	6.74	--	0.77	0.19	0.51	0.26

A.26 Sankey diagram for fluorine – Run02
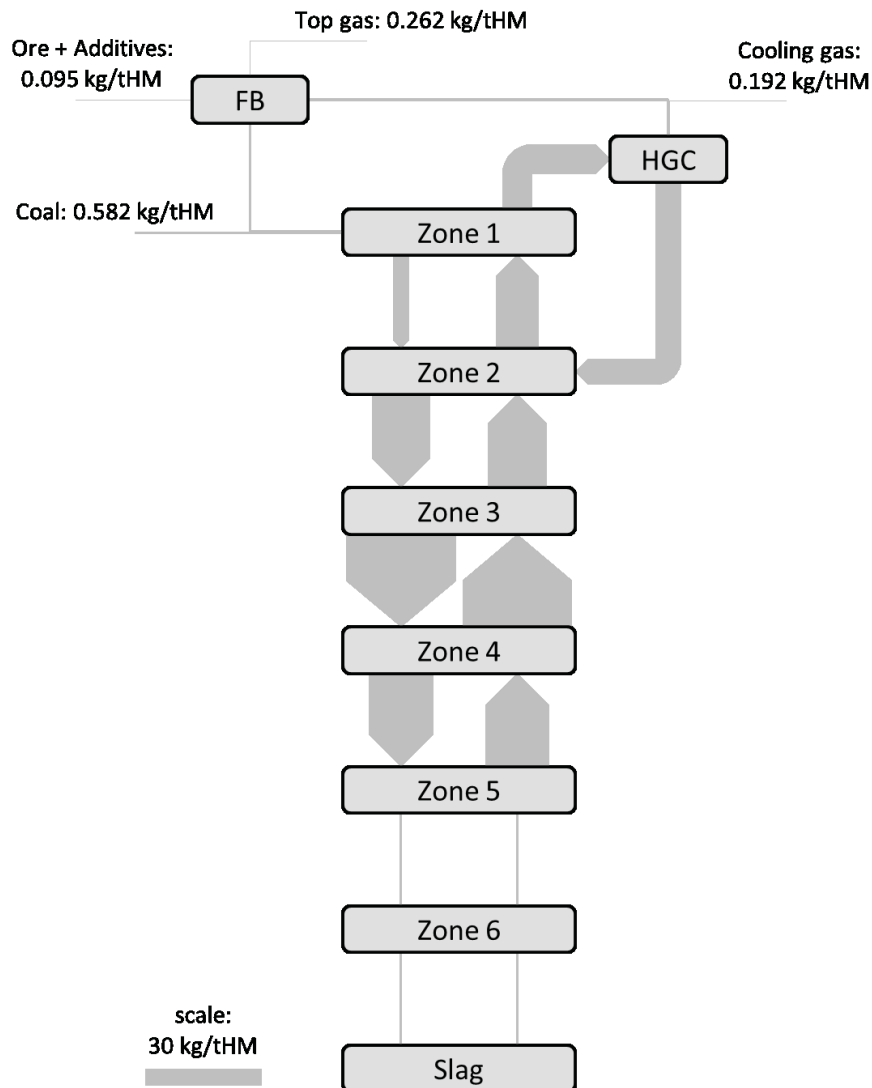
Input FB	[kg/tHM]	[%]	Output FB	[kg/tHM]	[%]	PtInp [%]
Ore	0.09	10.84	DRI	0.51	65.98	74.96
Additives	0.001	0.15	Top Gas	0.26	34.02	38.66
Reducing Gas	0.77	89.00				
Sum	0.86	100	Sum	0.77	100	

Discrepancy Input/Output: = 12.36 %

Input MG	[kg/tHM]	[%]	Output MG	[kg/tHM]	[%]	PtInp [%]
Coal	0.58	7.43	Slag	0.00	0.00	0.00
HGC dust	6.74	86.08	Generator Gas	7.70	100.00	1137.31
DRI	0.51	6.48				
Sum	7.83	100	Sum	7.70	100	

Discrepancy Input/Output: = 1.66 %

| Input HGC	[kg/tHM]	[%]	Output HGC	[kg/tHM]	[%]	PtInp [%]
Generator Gas	7.70	100.00	HGC dust	6.74	87.51	995.29
Cooling Gas	0.00	0.00	Reducing Gas	0.77	9.99	113.62
			Cooling Gas	0.19	2.50	28.41
Sum	7.70	100	Sum	7.70	100	

Discrepancy Input/Output: = 0.0 %

A.27 Amount of potassium in kg/tHM in different compounds at each position – Run03
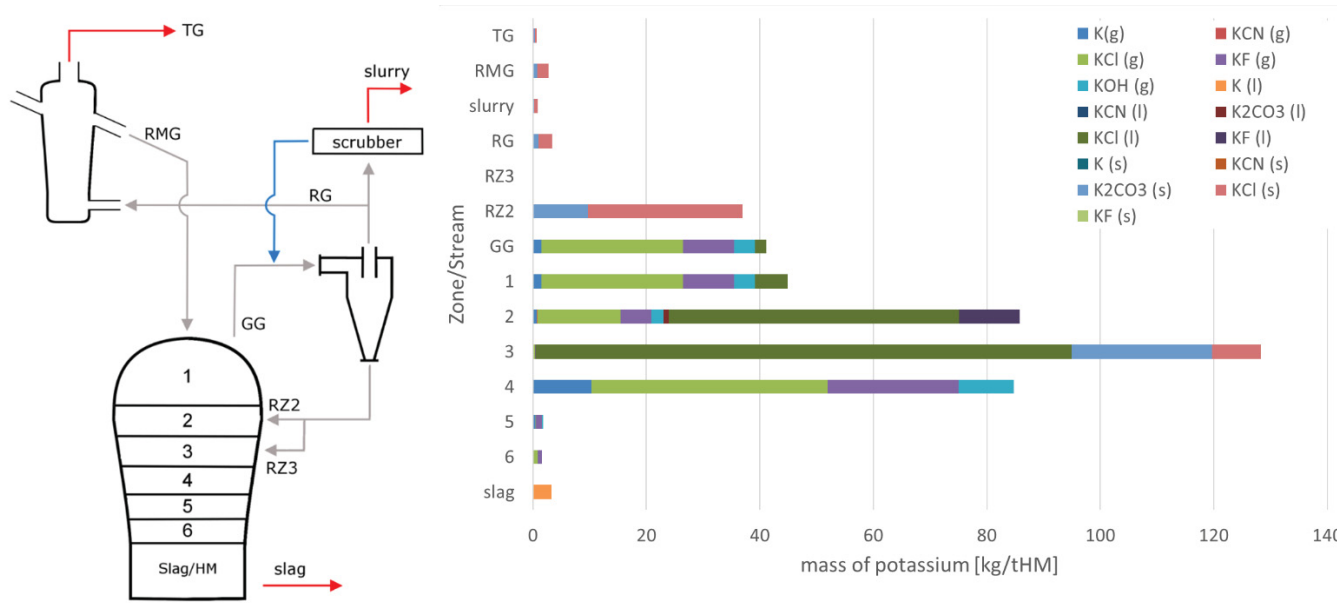
	slag	6	5	4	3	2	1	GG	RZ2	RZ3	RG	slurry	RMG	TG
K(g)	--	0.07	0.48	10.28	--	0.70	1.47	1.47	--	--	--	--	--	--
KCN (g)	--	0.01	--	0.02	--	0.01	0.02	0.02	--	--	--	--	--	--
KCl (g)	--	0.78	0.09	41.68	0.38	14.74	24.98	24.98	--	--	0.12	0.03	--	0.17
KF (g)	--	0.78	1.05	23.04	0.05	5.47	9.00	9.00	--	--	0.01	--	--	0.02
KOH (g)	--	--	0.18	9.79	0.01	2.03	3.65	3.65	--	--	--	--	--	--
K (l)	3.26	--	--	--	--	--	--	--	--	--	--	--	--	--
KCN (l)	--	--	--	--	--	--	--	--	--	--	--	--	--	--
K2CO3 (l)	--	--	--	--	--	1.01	--	--	--	--	--	--	--	--
KCl (l)	--	--	--	--	94.54	51.18	5.85	2.05	--	--	--	--	--	--
KF (l)	--	--	--	--	--	10.68	--	--	--	--	--	--	--	--
K (s)	--	--	--	--	--	--	--	--	--	--	--	--	--	--
KCN (s)	--	--	--	--	--	--	--	--	--	--	--	--	--	--
K2CO3 (s)	--	--	--	--	24.69	--	--	--	9.63	--	0.86	0.21	0.72	0.13
KCl (s)	--	--	--	--	8.60	--	--	--	27.26	--	2.42	0.61	2.02	0.36
KF (s)	--	--	--	--	--	--	--	--	--	--	--	--	--	--
Sum	3.26	1.65	1.81	84.80	128.27	85.82	44.96	41.16	36.89	--	3.41	0.85	2.74	0.67

A.28 Sankey diagram for potassium – Run03
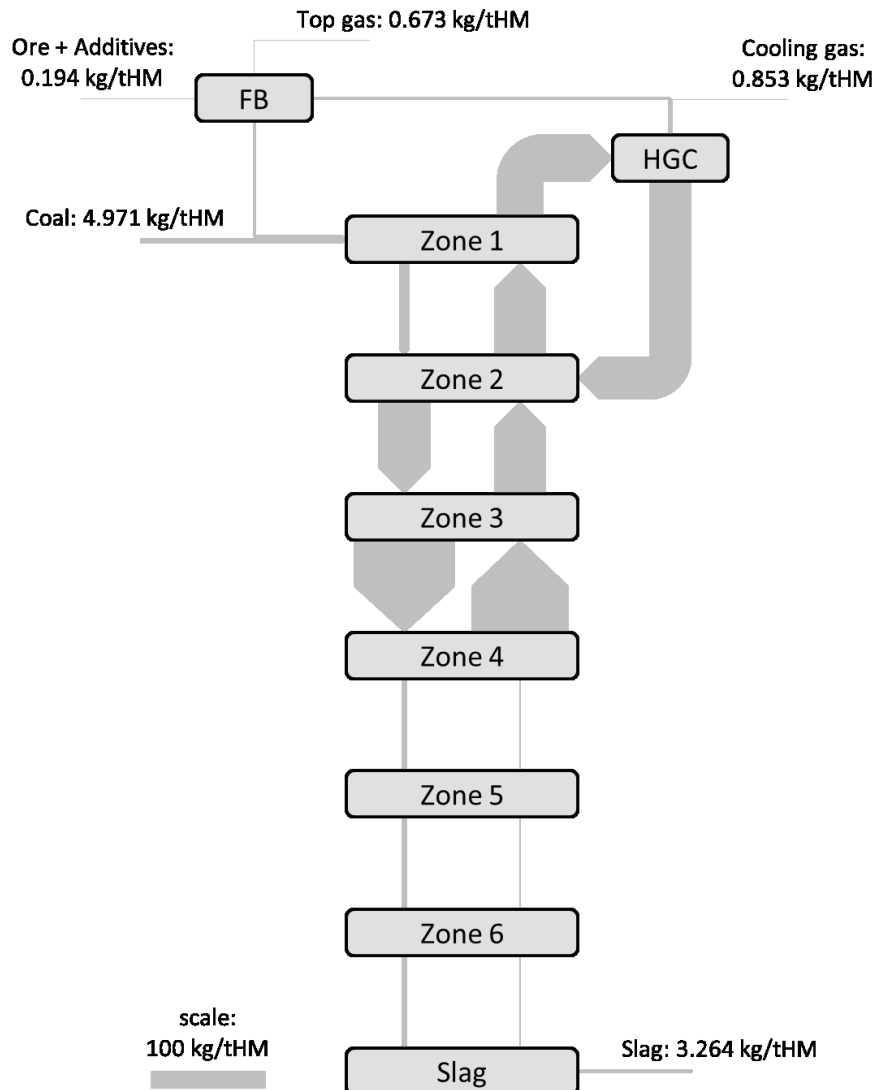
Input FB	[kg/tHM]	[%]	Output FB	[kg/tHM]	[%]	PtInp [%]
Ore	0.12	3.24	DRI	2.74	80.26	53.01
Additives	0.08	2.14	Top Gas	0.67	19.74	13.04
Reducing Gas	3.41	94.62				
Sum	3.61	100	Sum	3.41	100	

Discrepancy Input/Output: = 5.69 %

Input MG	[kg/tHM]	[%]	Output MG	[kg/tHM]	[%]	PtInp [%]
Coal	4.97	11.15	Slag	3.26	7.35	63.20
HGC dust	36.89	82.72	Generator Gas	41.16	92.65	796.83
DRI	2.74	6.14				
Sum	44.60	100	Sum	44.42	100	

Discrepancy Input/Output: = 0.41 %

| Input HGC	[kg/tHM]	[%]	Output HGC	[kg/tHM]	[%]	PtInp [%]
Generator Gas	41.16	100.00	HGC dust	36.89	89.64	714.27
Cooling Gas	0.00	0.00	Reducing Gas	3.41	8.29	66.04
			Cooling Gas	0.85	2.07	16.51
Sum	41.16	100	Sum	41.16	100	

Discrepancy Input/Output: = 0.0 %

A.29 Amount of sodium in kg/tHM in different compounds at each position – Run03
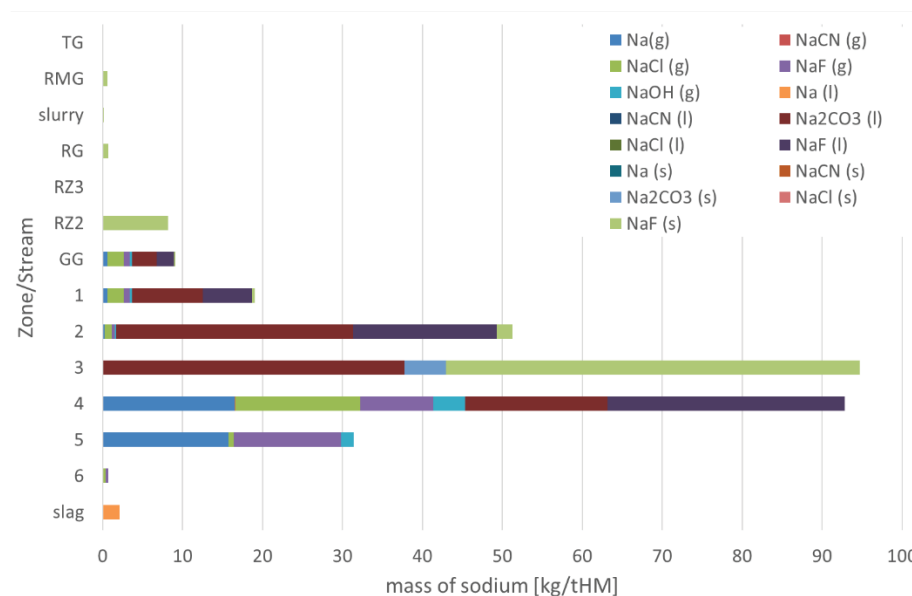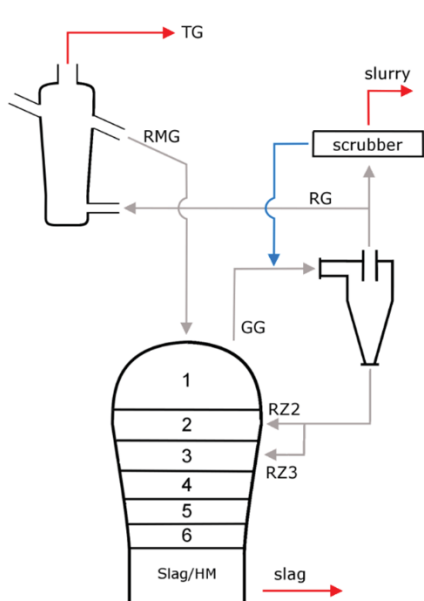
	slag	6	5	4	3	2	1	GG	RZ2	RZ3	RG	slurry	RMG	TG
Na(g)	--	0.08	15.72	16.52	--	0.24	0.60	0.60	--	--	--	--	--	--
NaCN (g)	--	0.02	0.01	0.03	--	0.00	0.01	0.01	--	--	--	--	--	--
NaCl (g)	--	0.29	0.69	15.69	0.01	0.93	2.00	2.00	--	--	--	--	--	--
NaF (g)	--	0.30	13.42	9.16	--	0.38	0.78	0.78	--	--	--	--	--	--
NaOH (g)	--	--	1.59	3.93	--	0.14	0.31	0.31	--	--	--	--	--	--
Na (l)	2.14	--	--	--	--	--	--	--	--	--	--	--	--	--
NaCN (l)	--	--	--	--	--	--	--	--	--	--	--	--	--	--
Na2CO3 (l)	--	--	--	17.86	37.79	29.62	8.82	3.09	--	--	--	--	--	--
NaCl (l)	--	--	--	--	--	--	--	--	--	--	--	--	--	--
NaF (l)	--	--	--	29.68	--	18.03	6.13	2.14	--	--	--	--	--	--
Na (s)	--	--	--	--	--	--	--	--	--	--	--	--	--	--
NaCN (s)	--	--	--	--	--	--	--	--	--	--	--	--	--	--
Na2CO3 (s)	--	--	--	--	5.17	--	--	--	--	--	--	--	--	--
NaCl (s)	--	--	--	--	--	--	--	--	--	--	--	--	--	--
NaF (s)	--	--	--	--	51.72	1.90	0.38	0.13	8.15	--	0.72	0.18	0.61	0.11
Sum	2.14	0.68	31.42	92.87	94.70	51.23	19.02	9.06	8.15	--	0.72	0.18	0.61	0.11

A.30 Sankey diagram for sodium – Run03

Top gas: 0.112 kg/tHM

Ore + Additives:
0.165 kg/tHM

Cooling gas:
0.182 kg/tHM

FB

HGC

Coal: 2.771 kg/tHM

Zone 1

Zone 2

Zone 3

Zone 4

Zone 5

Zone 6

scale:
75 kg/tHM

Slag

Slag: 2.136 kg/tHM
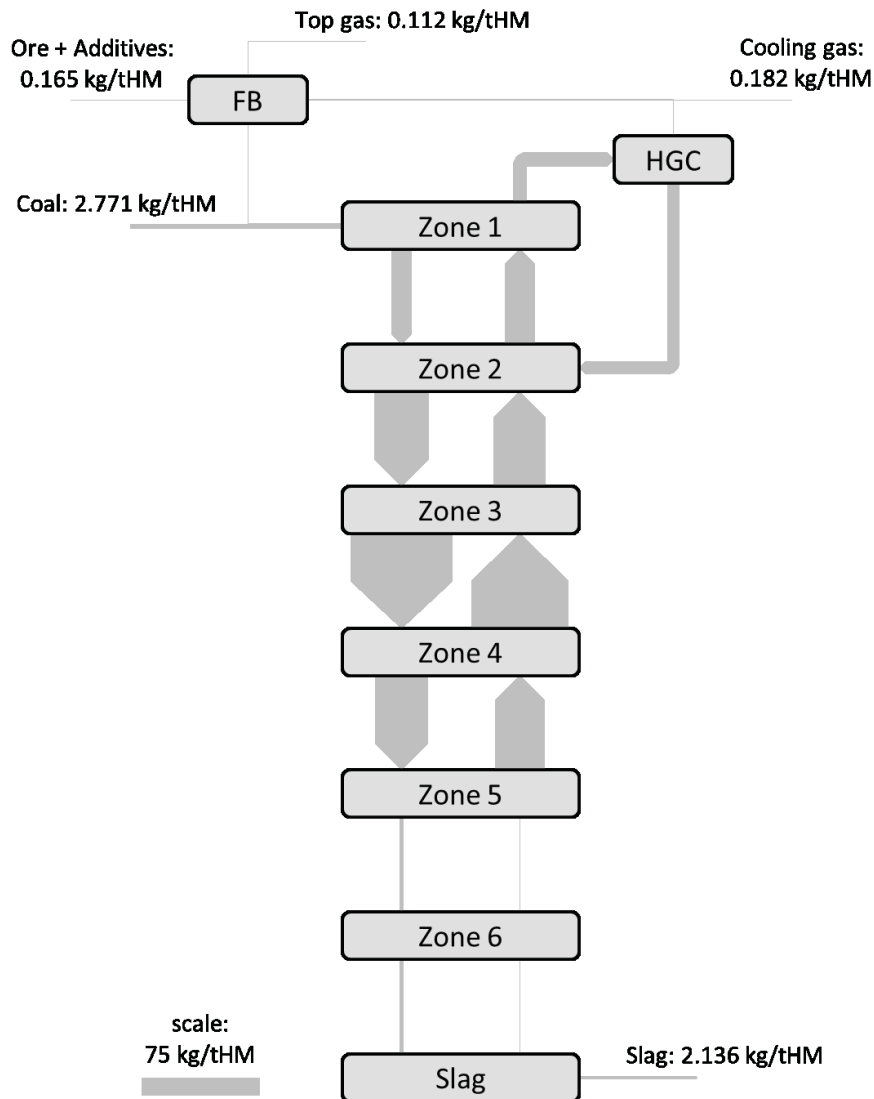
Input FB	[kg/tHM]	[%]	Output FB	[kg/tHM]	[%]	PtInp [%]
Ore	0.16	17.40	DRI	0.61	84.55	20.94
Additives	0.01	1.11	Top Gas	0.11	15.45	3.83
Reducing Gas	0.73	81.49				
Sum	0.89	100	Sum	0.73	100	

Discrepancy Input/Output: = 22.71 %

Input MG	[kg/tHM]	[%]	Output MG	[kg/tHM]	[%]	PtInp [%]
Coal	2.77	24.02	Slag	2.14	19.08	72.76
HGC dust	8.15	70.65	Generator Gas	9.06	80.92	308.52
DRI	0.61	5.33				
Sum	11.54	100	Sum	11.19	100	

Discrepancy Input/Output: = 3.04 %

| Input HGC	[kg/tHM]	[%]	Output HGC	[kg/tHM]	[%]	PtInp [%]
Generator Gas	9.06	100.00	HGC dust	8.15	89.97	277.56
Cooling Gas	0.00	0.00	Reducing Gas	0.73	8.03	24.77
			Cooling Gas	0.18	2.01	6.19
Sum	9.06	100	Sum	9.06	100	

Discrepancy Input/Output: = 0.0 %

A.31 Amount of chlorine in kg/tHM in different compounds at each position – Run03
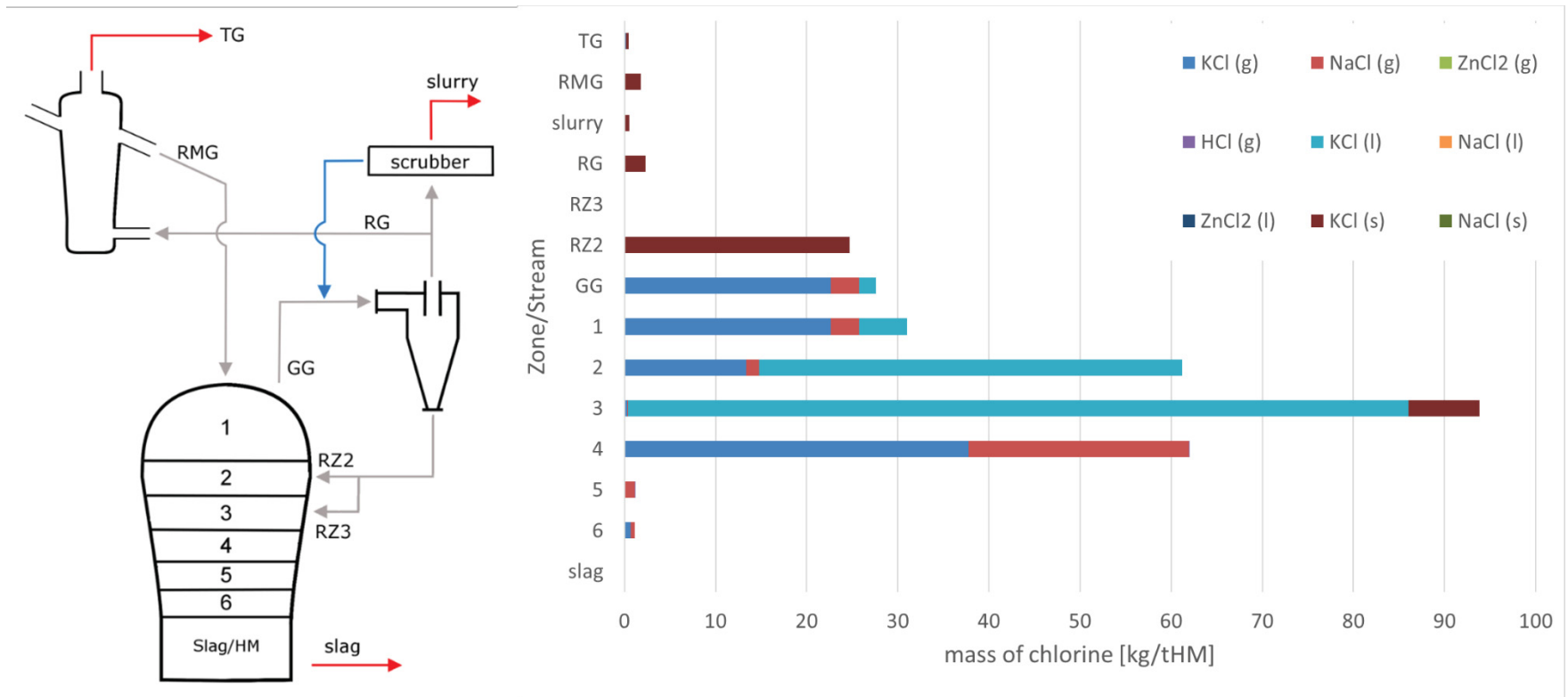
|	slag	6	5	4	3	2	1	GG	RZ2	RZ3	RG	slurry	RMG	TG
KCl (g)	--	0.71	0.08	37.78	0.35	13.36	22.65	22.65	--	--	0.11	0.03	--	0.15
NaCl (g)	--	0.44	1.06	24.18	0.02	1.43	3.09	3.09	--	--	--	--	--	0.01
ZnCl2 (g)	--	--	--	--	--	--	--	--	--	--	--	--	--	--
HCl (g)	--	--	0.01	0.02	--	0.01	0.01	0.01	--	--	--	--	--	--
KCl (l)	--	--	--	--	85.71	46.40	5.30	1.86	--	--	--	--	--	--
NaCl (l)	--	--	--	--	--	--	--	--	--	--	--	--	--	--
ZnCl2 (l)	--	--	--	--	--	--	--	--	--	--	--	--	--	--
KCl (s)	--	--	--	--	7.79	--	--	--	24.72	--	2.20	0.55	1.83	0.32
NaCl (s)	--	--	--	--	--	--	--	--	--	--	--	--	--	--
Sum	--	1.15	1.15	61.98	93.87	61.21	31.04	27.60	24.72	--	2.30	0.58	1.83	0.48

A.32 Sankey diagram for chorine – Run03
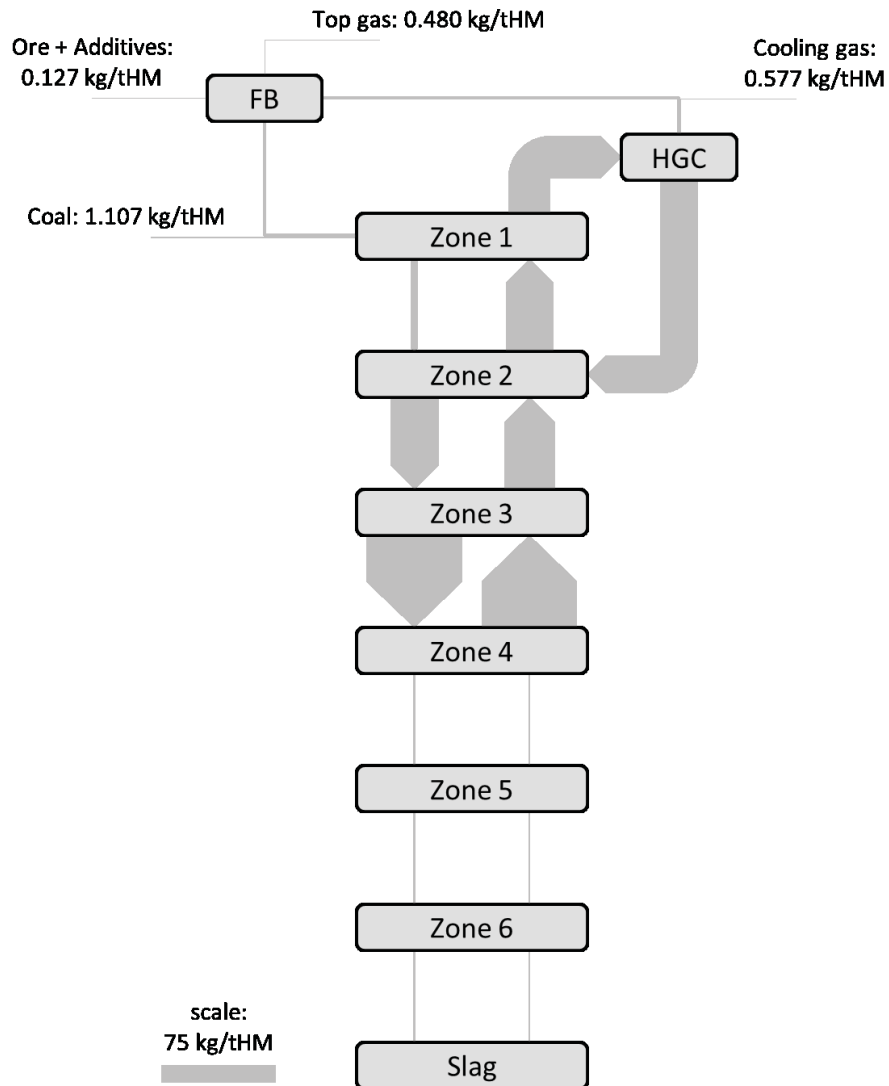
Input FB	[kg/tHM]	[%]	Output FB	[kg/tHM]	[%]	PtInp [%]
Ore	0.12	5.13	DRI	1.83	79.19	148.07
Additives	0.002	0.09	Top Gas	0.48	20.81	38.91
Reducing Gas	2.31	94.78				
Sum	2.43	100	Sum	2.31	100	

Discrepancy Input/Output: = 5.51 %

Input MG	[kg/tHM]	[%]	Output MG	[kg/tHM]	[%]	PtInp [%]
Coal	1.11	4.00	Slag	0.00	0.00	0.00
HGC dust	24.72	89.39	Generator Gas	27.60	100.00	2236.77
DRI	1.83	6.61				
Sum	27.65	100	Sum	27.60	100	

Discrepancy Input/Output: = 0.18 %

Input HGC	[kg/tHM]	[%]	Output HGC	[kg/tHM]	[%]	PtInp [%]
Generator Gas	27.60	100.00	HGC dust	24.72	89.55	2003.06
Cooling Gas	0.00	0.00	Reducing Gas	2.31	8.36	186.97
			Cooling Gas	0.58	2.09	46.74
Sum	27.60	100	Sum	27.60	100	

Discrepancy Input/Output: = 0.0 %

A.33 Amount of fluorine in kg/tHM in different compounds at each position – Run03
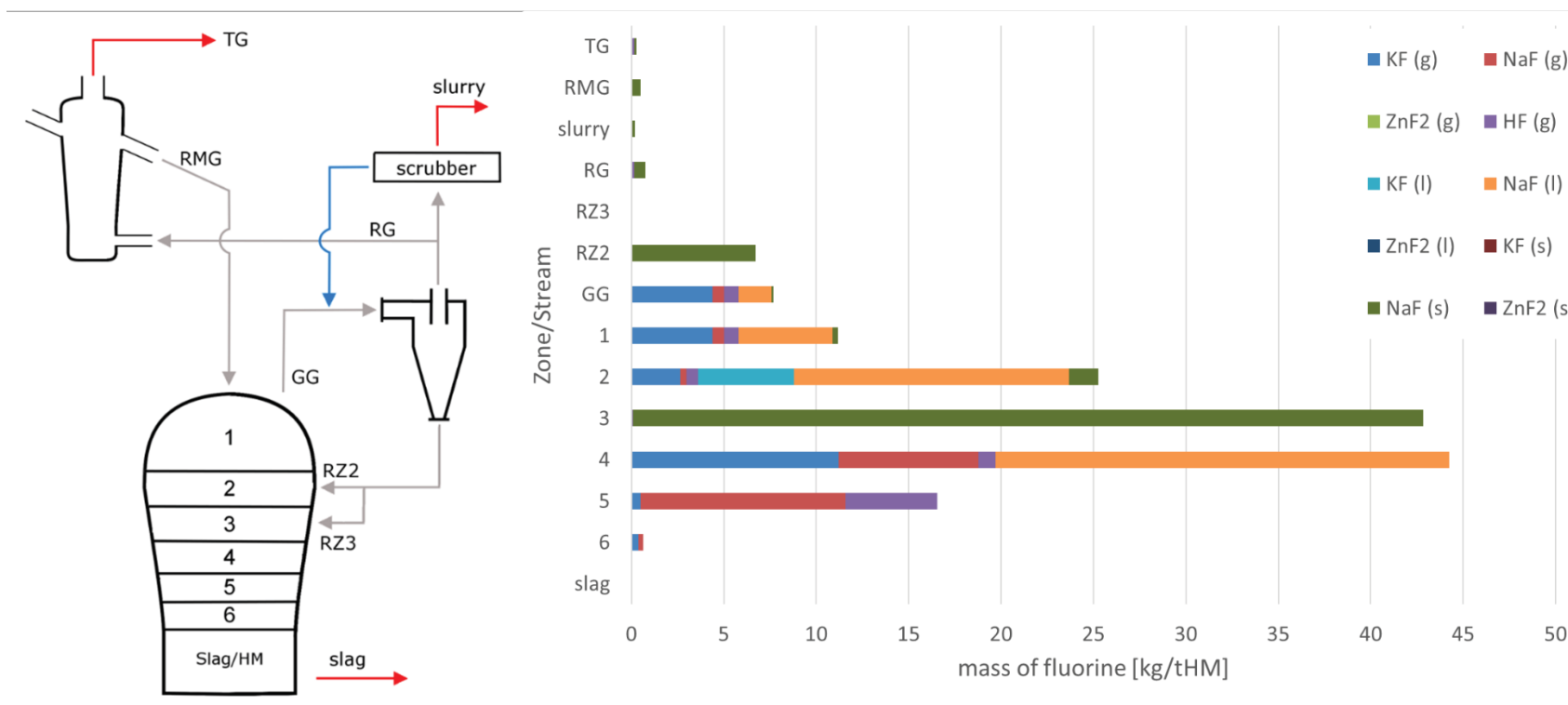
	slag	6	5	4	3	2	1	GG	RZ2	RZ3	RG	slurry	RMG	TG
KF (g)	--	0.38	0.51	11.19	0.03	2.66	4.37	4.37	--	--	0.01	--	--	0.01
NaF (g)	--	0.25	11.09	7.57	--	0.31	0.64	0.64	--	--	--	--	--	--
ZnF2 (g)	--	--	--	--	--	--	--	--	--	--	--	--	--	--
HF (g)	--	--	4.96	0.95	0.08	0.63	0.79	0.79	--	--	0.16	0.04	--	0.16
KF (l)	--	--	--	--	--	5.19	--	--	--	--	--	--	--	--
NaF (l)	--	--	--	24.52	--	14.89	5.06	1.77	--	--	--	--	--	--
ZnF2 (l)	--	--	--	--	--	--	--	--	--	--	--	--	--	--
KF (s)	--	--	--	--	--	--	--	--	--	--	--	--	--	--
NaF (s)	--	--	--	--	42.72	1.57	0.31	0.11	6.73	--	0.60	0.15	0.51	0.09
ZnF2 (s)	--	--	--	--	--	--	--	--	--	--	--	--	--	--
Sum	--	0.63	16.56	44.23	42.82	25.26	11.18	7.69	6.73	--	0.76	0.19	0.51	0.26

A.34 Sankey diagram for fluorine – Run03
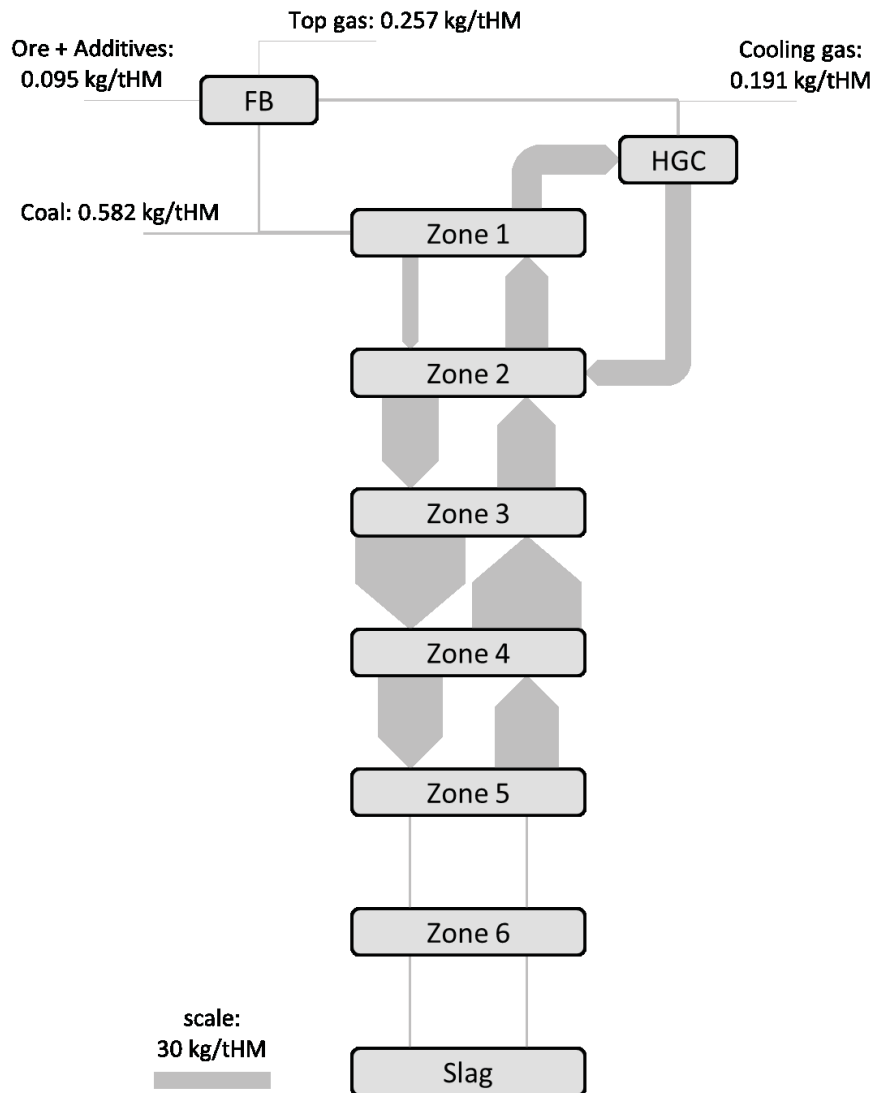
Input FB	[kg/tHM]	[%]	Output FB	[kg/tHM]	[%]	PtInp [%]
Ore	0.09	10.90	DRI	0.51	66.41	75.01
Additives	0.001	0.15	Top Gas	0.26	33.59	37.94
Reducing Gas	0.76	88.95				
Sum	0.86	100	Sum	0.76	100	

Discrepancy Input/Output: = 12.43 %

Input MG	[kg/tHM]	[%]	Output MG	[kg/tHM]	[%]	PtInp [%]
Coal	0.58	7.44	Slag	0.00	0.00	0.00
HGC dust	6.73	86.07	Generator Gas	7.69	100.00	1135.55
DRI	0.51	6.49				
Sum	7.82	100	Sum	7.69	100	

Discrepancy Input/Output: = 1.74 %

Input HGC	[kg/tHM]	[%]	Output HGC	[kg/tHM]	[%]	PtInp [%]
Generator Gas	7.69	100.00	HGC dust	6.73	87.57	994.35
Cooling Gas	0.00	0.00	Reducing Gas	0.76	9.95	112.95
			Cooling Gas	0.19	2.49	28.24
Sum	7.69	100	Sum	7.69	100	

Discrepancy Input/Output: = 0.0 %

A.35 Amount of potassium in kg/tHM in different compounds at each position – Run04
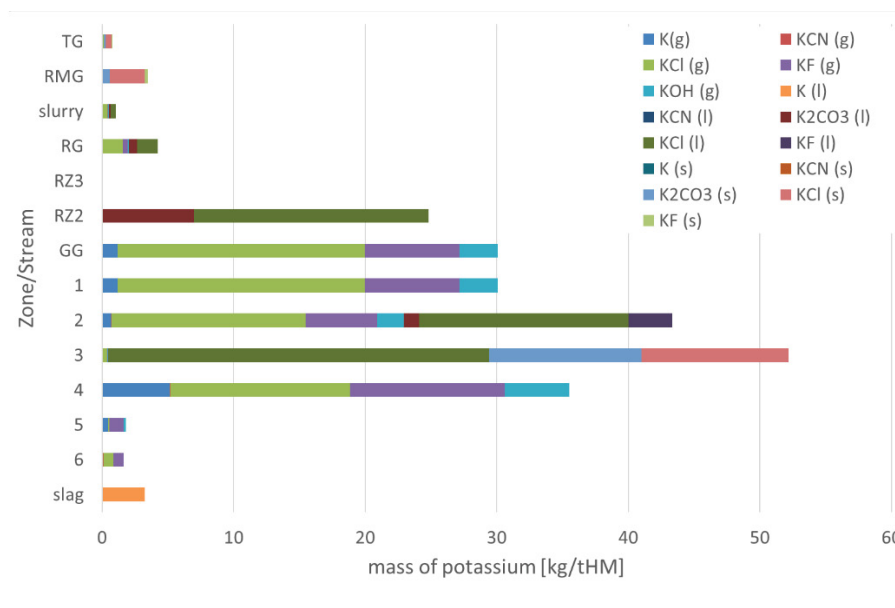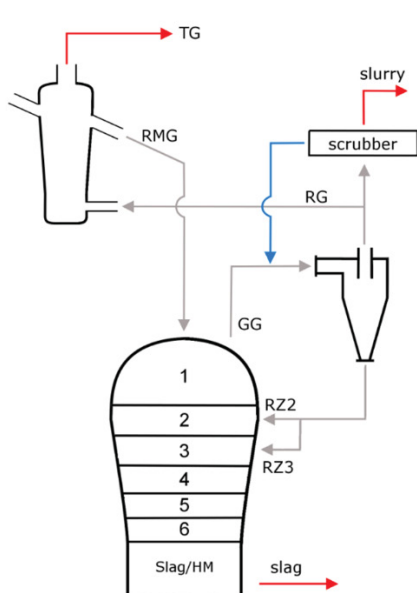
	slag	6	5	4	3	2	1	GG	RZ2	RZ3	RG	slurry	RMG	TG
K(g)	--	0.07	0.45	5.15	--	0.70	1.16	1.16	--	--	0.02	--	--	--
KCN (g)	--	0.01	--	0.02	--	0.01	0.02	0.02	--	--	0.00	--	--	--
KCl (g)	--	0.78	0.09	13.69	0.38	14.74	18.77	18.77	--	--	1.58	0.39	--	0.14
KF (g)	--	0.78	1.10	11.76	0.05	5.47	7.23	7.23	--	--	0.33	0.08	--	0.02
KOH (g)	--	--	0.17	4.91	0.01	2.03	2.92	2.92	--	--	0.10	0.02	--	--
K (l)	3.26	--	--	--	--	--	--	--	--	--	--	--	--	--
KCN (l)	--	--	--	--	--	--	--	--	--	--	--	--	--	--
K2CO3 (l)	--	--	--	--	--	1.13	--	--	6.98	--	0.62	0.16	--	--
KCl (l)	--	--	--	--	28.95	15.95	--	--	17.83	--	1.58	0.40	--	--
KF (l)	--	--	--	--	--	3.33	--	--	--	--	--	--	--	--
K (s)	--	--	--	--	--	--	--	--	--	--	--	--	--	--
KCN (s)	--	--	--	--	--	--	--	--	--	--	--	--	--	--
K2CO3 (s)	--	--	--	--	11.60	--	--	--	--	--	--	--	0.59	0.10
KCl (s)	--	--	--	--	11.21	--	--	--	--	--	--	--	2.65	0.47
KF (s)	--	--	--	--	--	--	--	--	--	--	--	--	0.21	0.04
Sum	3.26	1.65	1.81	35.53	52.21	43.36	30.10	30.10	24.81	--	4.23	1.05	3.46	0.77

A.36 Sankey diagram for potassium – Run04
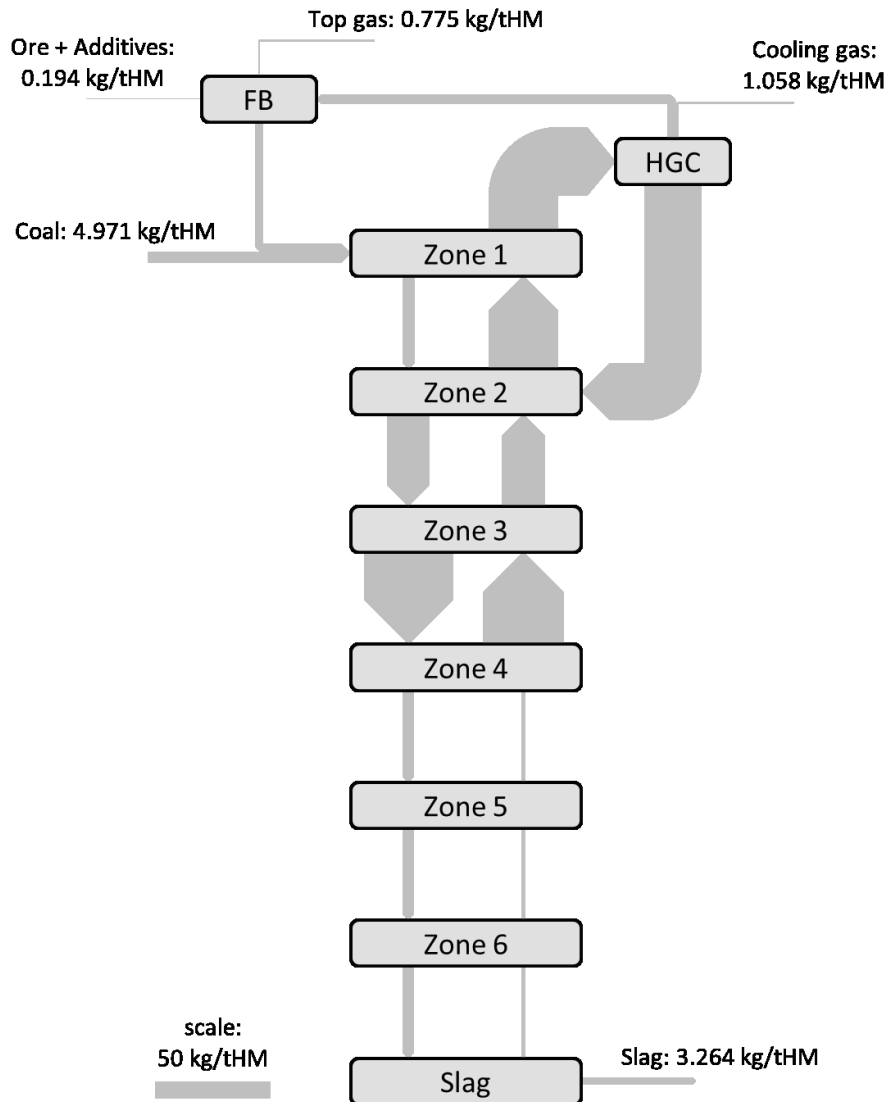
Input FB	[kg/tHM]	[%]	Output FB	[kg/tHM]	[%]	PtInp [%]
Ore	0.12	2.64	DRI	3.46	81.68	66.92
Additives	0.08	1.75	Top Gas	0.78	18.32	15.01
Reducing Gas	4.23	95.62				
Sum	4.43	100	Sum	4.23	100	

Discrepancy Input/Output: = 4.58 %

Input MG	[kg/tHM]	[%]	Output MG	[kg/tHM]	[%]	PtInp [%]
Coal	4.97	14.96	Slag	3.26	9.78	63.20
HGC dust	24.81	74.64	Generator Gas	30.10	90.22	582.70
DRI	3.46	10.40				
Sum	33.24	100	Sum	33.36	100	

Discrepancy Input/Output: = 0.38 %

Input HGC	[kg/tHM]	[%]	Output HGC	[kg/tHM]	[%]	PtInp [%]
Generator Gas	30.10	100.00	HGC dust	24.81	82.42	480.29
Cooling Gas	0.00	0.00	Reducing Gas	4.23	14.06	81.93
			Cooling Gas	1.06	3.52	20.48
Sum	30.10	100	Sum	30.10	100	

Discrepancy Input/Output: = 0.0 %

A.37 Amount of sodium in kg/tHM in different compounds at each position – Run04
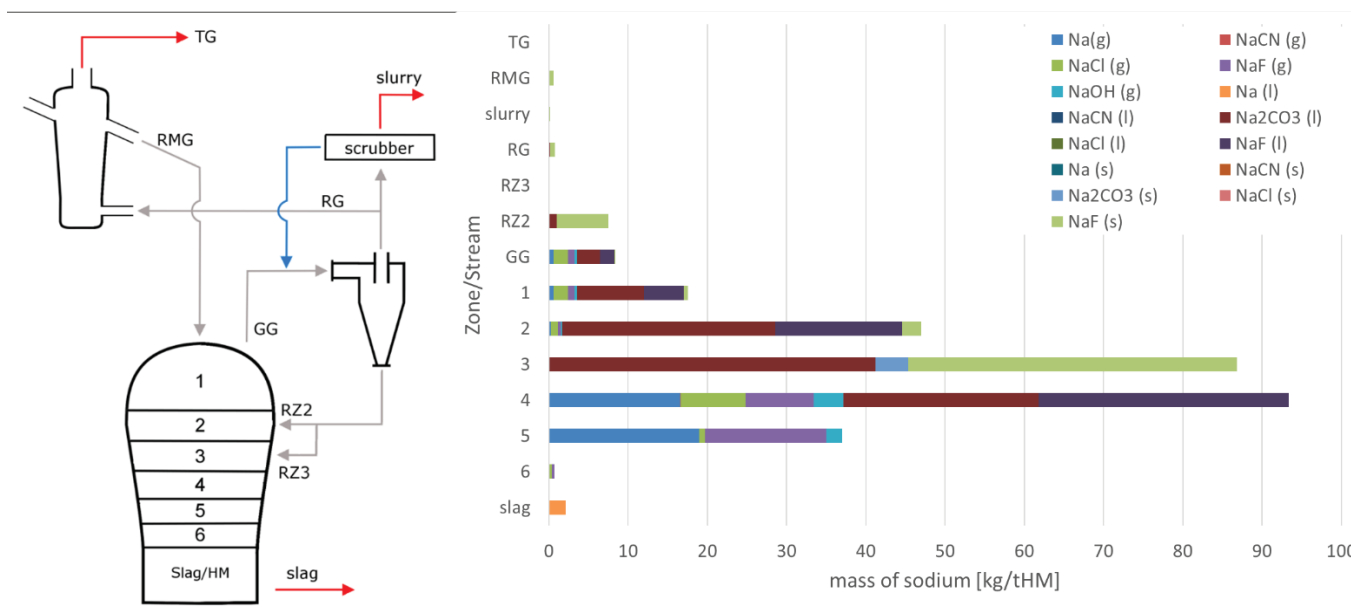
	slag	6	5	4	3	2	1	GG	RZ2	RZ3	RG	slurry	RMG	TG
Na(g)	--	0.08	18.99	16.59	--	0.24	0.59	0.59	--	--	--	--	--	--
NaCN (g)	--	0.02	0.01	0.03	--	0.00	0.01	0.01	--	--	--	--	--	--
NaCl (g)	--	0.29	0.69	8.16	0.01	0.93	1.84	1.84	--	--	0.06	0.02	--	--
NaF (g)	--	0.30	15.32	8.64	--	0.38	0.77	0.77	--	--	0.01	--	--	--
NaOH (g)	--	--	1.98	3.79	--	0.14	0.31	0.31	--	--	--	--	--	--
Na (l)	2.14	--	--	--	--	--	--	--	--	--	--	--	--	--
NaCN (l)	--	--	--	--	--	--	--	--	--	--	--	--	--	--
Na2CO3 (l)	--	--	--	24.63	41.20	26.92	8.52	2.98	1.00	--	0.09	0.02	--	--
NaCl (l)	--	--	--	--	--	--	--	--	--	--	--	--	--	--
NaF (l)	--	--	--	31.50	--	15.97	4.96	1.74	--	--	--	--	--	--
Na (s)	--	--	--	--	--	--	--	--	--	--	--	--	--	--
NaCN (s)	--	--	--	--	--	--	--	--	--	--	--	--	--	--
Na2CO3 (s)	--	--	--	--	4.14	--	--	--	--	--	--	--	--	--
NaCl (s)	--	--	--	--	--	--	--	--	--	--	--	--	--	--
NaF (s)	--	--	--	--	41.48	2.39	0.53	0.19	6.49	--	0.58	0.14	0.63	0.11
Sum	2.14	0.68	37.00	93.34	86.84	46.96	17.53	8.42	7.49	--	0.74	0.18	0.63	0.11

A.38 Sankey diagram for sodium – Run04
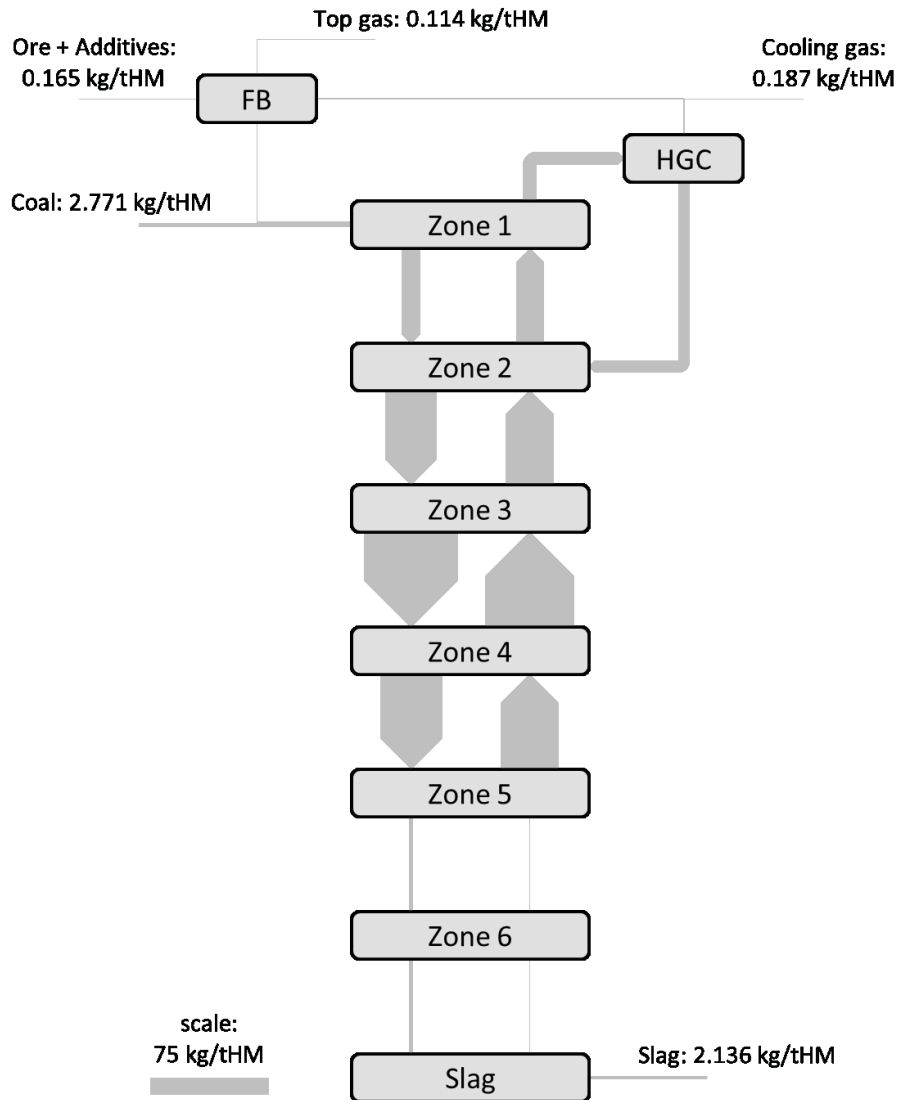
Input FB	[kg/tHM]	[%]	Output FB	[kg/tHM]	[%]	PtInp [%]
Ore	0.16	17.01	DRI	0.63	84.73	21.58
Additives	0.01	1.08	Top Gas	0.11	15.27	3.89
Reducing Gas	0.75	81.91				
Sum	0.91	100	Sum	0.75	100	

Discrepancy Input/Output: = 22.08 %

Input MG	[kg/tHM]	[%]	Output MG	[kg/tHM]	[%]	PtInp [%]
Coal	2.77	25.44	Slag	2.14	20.24	72.76
HGC dust	7.49	68.74	Generator Gas	8.42	79.76	286.78
DRI	0.63	5.82				
Sum	10.89	100	Sum	10.56	100	

Discrepancy Input/Output: = 3.16 %

| Input HGC	[kg/tHM]	[%]	Output HGC	[kg/tHM]	[%]	PtInp [%]
Generator Gas	8.42	100.00	HGC dust	7.49	88.90	254.95
Cooling Gas	0.00	0.00	Reducing Gas	0.75	8.88	25.47
			Cooling Gas	0.19	2.22	6.37
Sum	8.42	100	Sum	8.42	100	

Discrepancy Input/Output: = 0.0 %

A.39 Amount of chlorine in kg/tHM in different compounds at each position – Run04
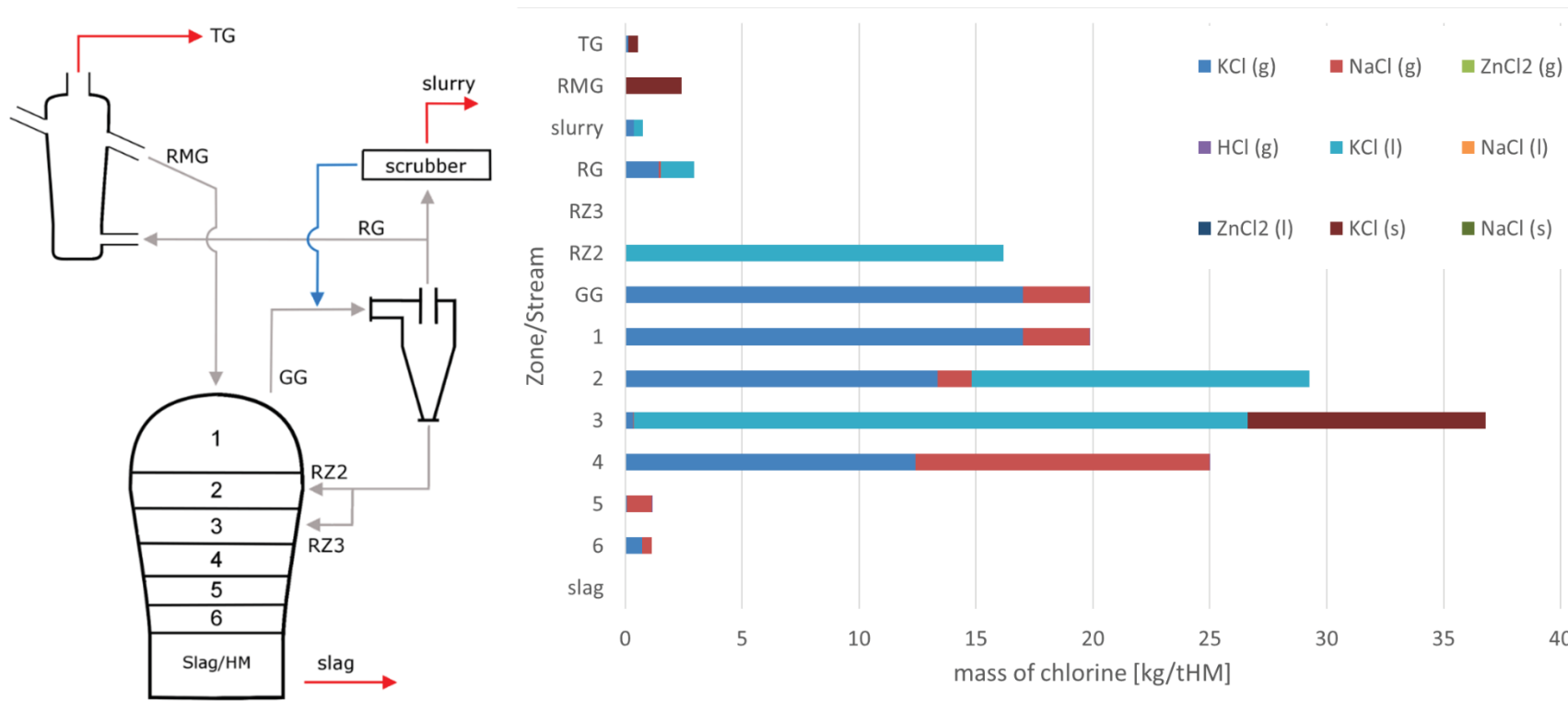
	slag	6	5	4	3	2	1	GG	RZ2	RZ3	RG	slurry	RMG	TG
KCl (g)	--	0.71	0.08	12.41	0.35	13.36	17.02	17.02	--	--	1.43	0.36	--	0.13
NaCl (g)	--	0.44	1.07	12.58	0.02	1.43	2.83	2.83	--	--	0.09	0.02	--	--
ZnCl2 (g)	--	--	--	--	--	--	--	--	--	--	--	--	--	--
HCl (g)	--	--	0.01	0.01	--	0.01	0.01	0.01	--	--	--	--	--	--
KCl (l)	--	--	--	--	26.25	14.46	--	--	16.16	--	1.44	0.36	--	--
NaCl (l)	--	--	--	--	--	--	--	--	--	--	--	--	--	--
ZnCl2 (l)	--	--	--	--	--	--	--	--	--	--	--	--	--	--
KCl (s)	--	--	--	--	10.17	--	--	--	--	--	--	--	2.41	0.42
NaCl (s)	--	--	--	--	--	--	--	--	--	--	--	--	--	--
Sum	--	1.15	1.15	25.00	36.78	29.26	19.87	19.87	16.16	--	2.96	0.74	2.41	0.55

A.40 Sankey diagram for chlorine – Run04
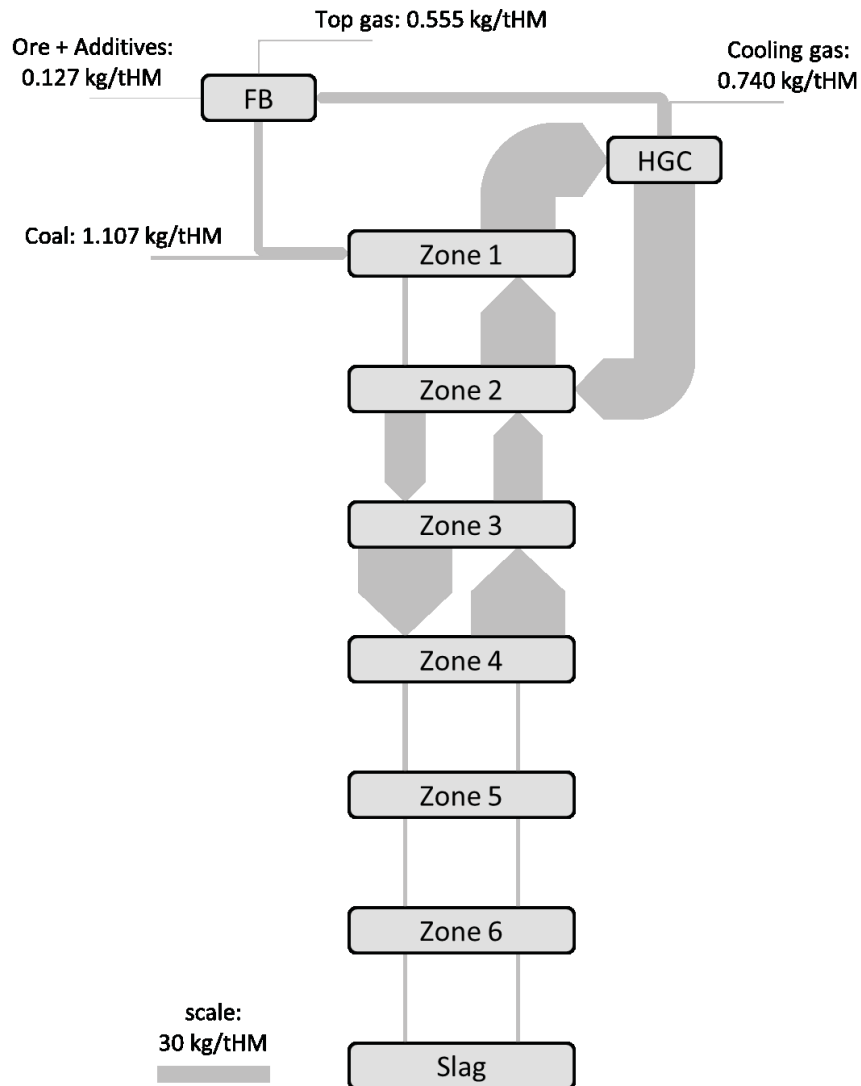
Input FB	[kg/tHM]	[%]	Output FB	[kg/tHM]	[%]	PtInp [%]
Ore	0.12	4.05	DRI	2.41	81.27	195.04
Additives	0.002	0.07	Top Gas	0.55	18.73	44.95
Reducing Gas	2.96	95.88				
Sum	3.09	100	Sum	2.96	100	

Discrepancy Input/Output: = 4.29 %

Input MG	[kg/tHM]	[%]	Output MG	[kg/tHM]	[%]	PtInp [%]
Coal	1.11	5.62	Slag	0.00	0.00	0.00
HGC dust	16.16	82.15	Generator Gas	19.87	100.00	1610.00
DRI	2.41	12.23				
Sum	19.68	100	Sum	19.87	100	

Discrepancy Input/Output: = 0.95 %

Input HGC	[kg/tHM]	[%]	Output HGC	[kg/tHM]	[%]	PtInp [%]
Generator Gas	19.87	100.00	HGC dust	16.16	81.37	1310.01
Cooling Gas	0.00	0.00	Reducing Gas	2.96	14.91	239.99
			Cooling Gas	0.74	3.73	60.00
Sum	19.87	100	Sum	19.87	100	

Discrepancy Input/Output: = 0.0 %

A.41 Amount of fluorine in kg/tHM in different compounds at each position – Run04
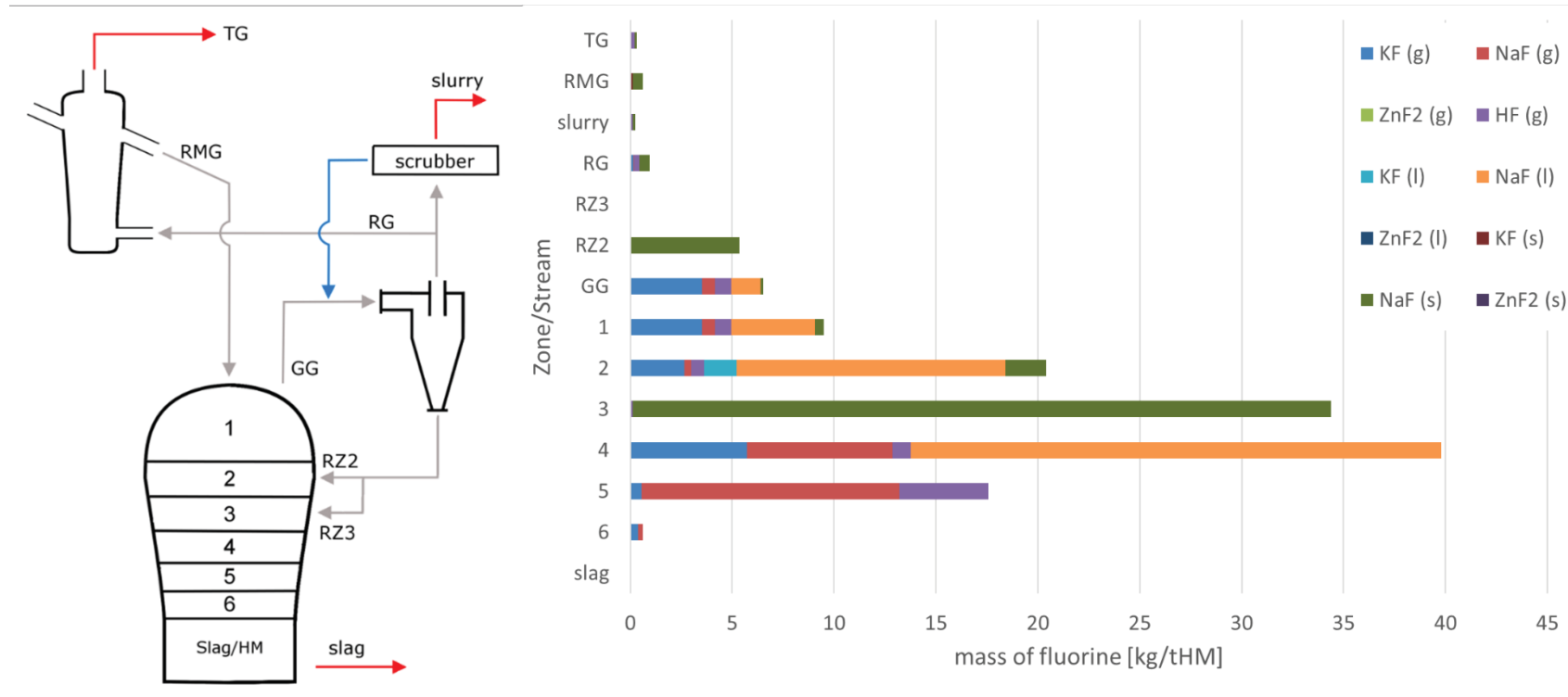
	slag	6	5	4	3	2	1	GG	RZ2	RZ3	RG	slurry	RMG	TG
KF (g)	--	0.38	0.53	5.72	0.03	2.66	3.51	3.51	--	--	0.16	0.04	--	0.01
NaF (g)	--	0.25	12.65	7.14	--	0.31	0.64	0.64	--	--	0.01	--	--	--
ZnF2 (g)	--	--	--	--	--	--	--	--	--	--	--	--	--	--
HF (g)	--	--	4.38	0.91	0.08	0.63	0.79	0.79	--	--	0.29	0.07	--	0.19
KF (l)	--	--	--	--	--	1.62	--	--	--	--	--	--	--	--
NaF (l)	--	--	--	26.02	--	13.19	4.10	1.43	--	--	--	--	--	--
ZnF2 (l)	--	--	--	--	--	--	--	--	--	--	--	--	--	--
KF (s)	--	--	--	--	--	--	--	--	--	--	--	--	0.10	0.02
NaF (s)	--	--	--	--	34.27	1.98	0.44	0.15	5.36	--	0.48	0.12	0.52	0.09
ZnF2 (s)	--	--	--	--	--	--	--	--	--	--	--	--	--	--
Sum	--	0.63	17.57	39.78	34.37	20.39	9.48	6.53	5.36	--	0.94	0.23	0.63	0.31

A.42 Sankey diagram for fluorine – Run04
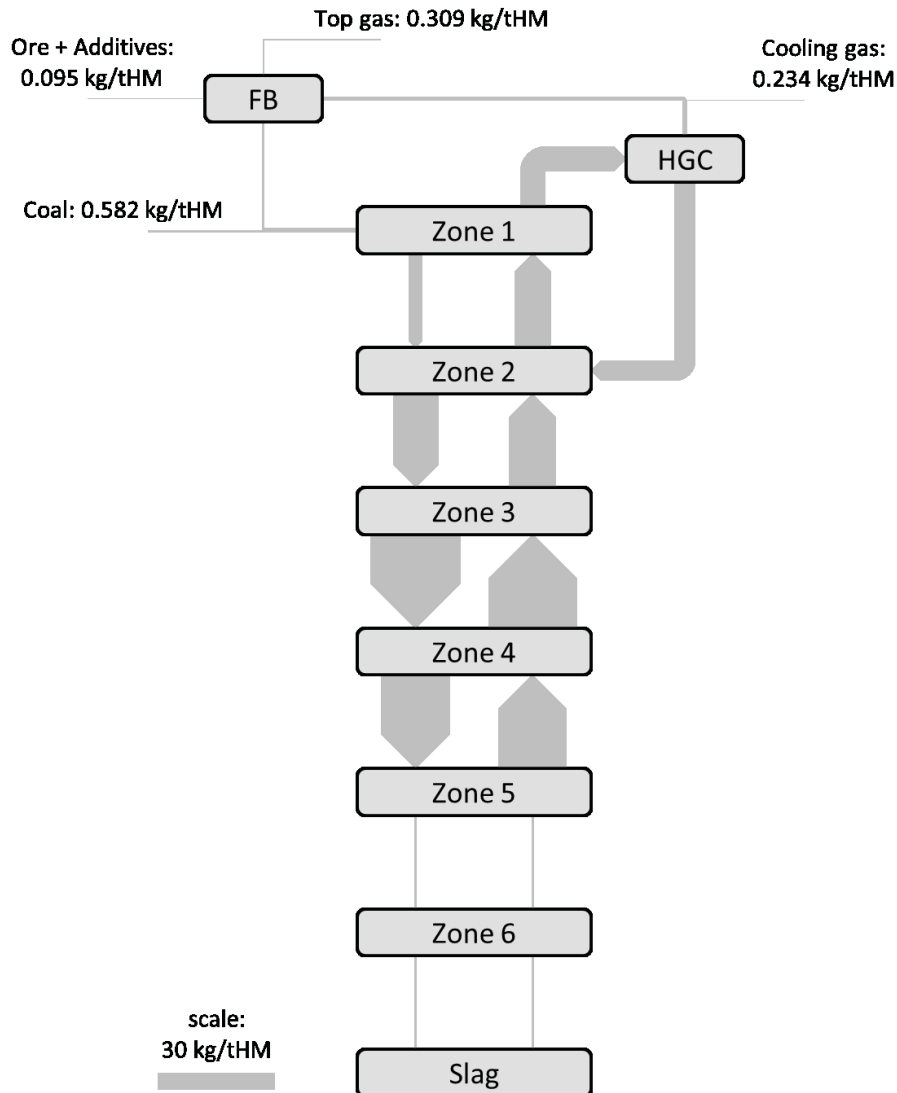
Input FB	[kg/tHM]	[%]	Output FB	[kg/tHM]	[%]	PtInp [%]
Ore	0.09	9.08	DRI	0.63	66.98	92.67
Additives	0.001	0.13	Top Gas	0.31	33.02	45.69
Reducing Gas	0.94	90.79				
Sum	1.03	100	Sum	0.94	100	

Discrepancy Input/Output: = 10.15 %

Input MG	[kg/tHM]	[%]	Output MG	[kg/tHM]	[%]	PtInp [%]
Coal	0.58	8.86	Slag	0.00	0.00	0.00
HGC dust	5.36	81.59	Generator Gas	6.53	100.00	964.43
DRI	0.63	9.55				
Sum	6.57	100	Sum	6.53	100	

Discrepancy Input/Output: = 0.59 %

Input HGC	[kg/tHM]	[%]	Output HGC	[kg/tHM]	[%]	PtInp [%]
Generator Gas	6.53	100.00	HGC dust	5.36	82.07	791.49
Cooling Gas	0.00	0.00	Reducing Gas	0.94	14.35	138.35
			Cooling Gas	0.23	3.59	34.59
Sum	6.53	100	Sum	6.53	100	

Discrepancy Input/Output: = 0.0 %

A.43 Amount of potassium in kg/tHM in different compounds at each position – Run05
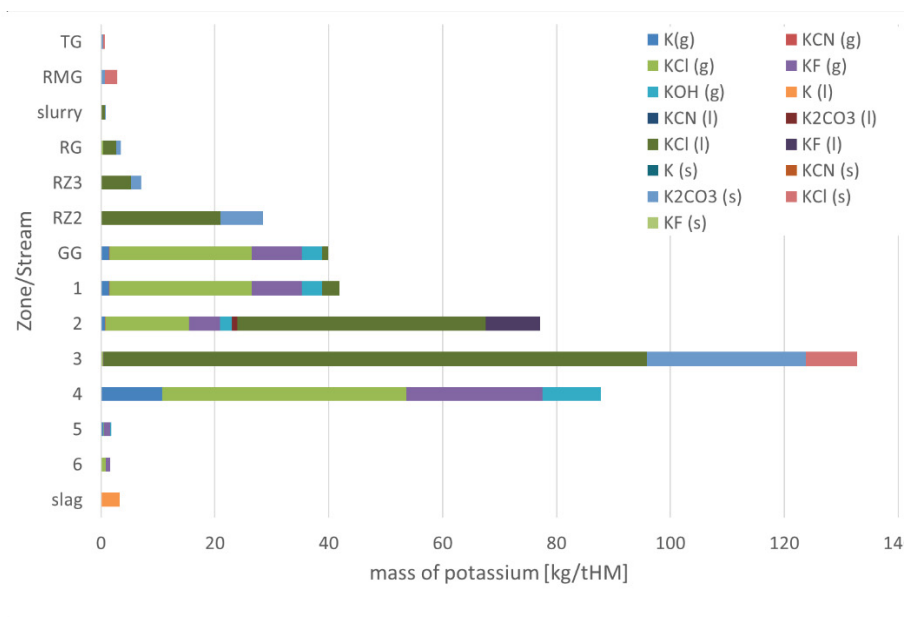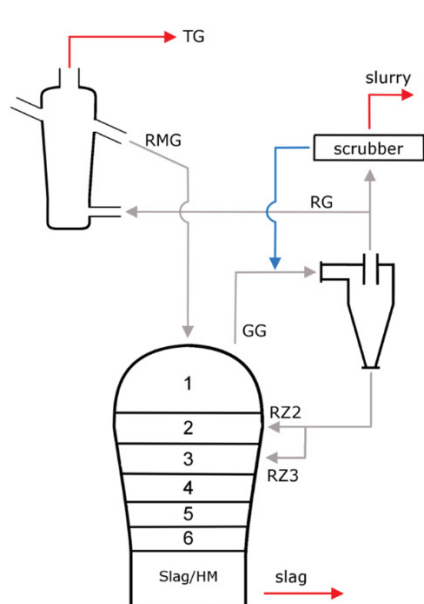
	slag	6	5	4	3	2	1	GG	RZ2	RZ3	RG	slurry	RMG	TG
K(g)	--	0.07	0.47	10.68	--	0.70	1.43	1.43	--	--	--	--	--	--
KCN (g)	--	0.01	--	0.02	--	0.01	0.02	0.02	--	--	--	--	--	--
KCl (g)	--	0.78	0.09	42.91	0.38	14.74	25.03	25.03	--	--	0.32	0.08	--	0.16
KF (g)	--	0.78	1.07	23.98	0.05	5.47	8.80	8.80	--	--	0.03	0.01	--	0.02
KOH (g)	--	--	0.18	10.20	0.01	2.03	3.57	3.57	--	--	0.01	--	--	--
K (l)	3.26	--	--	--	--	--	--	--	--	--	--	--	--	--
KCN (l)	--	--	--	--	--	--	--	--	--	--	--	--	--	--
K2CO3 (l)	--	--	--	--	--	0.98	--	--	--	--	--	--	--	--
KCl (l)	--	--	--	--	95.48	43.64	3.07	1.08	21.01	5.25	2.33	0.58	--	--
KF (l)	--	--	--	--	--	9.57	--	--	--	--	--	--	--	--
K (s)	--	--	--	--	--	--	--	--	--	--	--	--	--	--
KCN (s)	--	--	--	--	--	--	--	--	--	--	--	--	--	--
K2CO3 (s)	--	--	--	--	27.81	--	--	--	7.41	1.85	0.82	0.21	0.71	0.12
KCl (s)	--	--	--	--	9.09	--	--	--	--	--	--	--	2.13	0.38
KF (s)	--	--	--	--	--	--	--	--	--	--	--	--	--	--
Sum	3.26	1.65	1.81	87.78	132.82	77.15	41.92	39.92	28.42	7.10	3.52	0.88	2.84	0.68

A.44 Sankey diagram for potassium – Run05
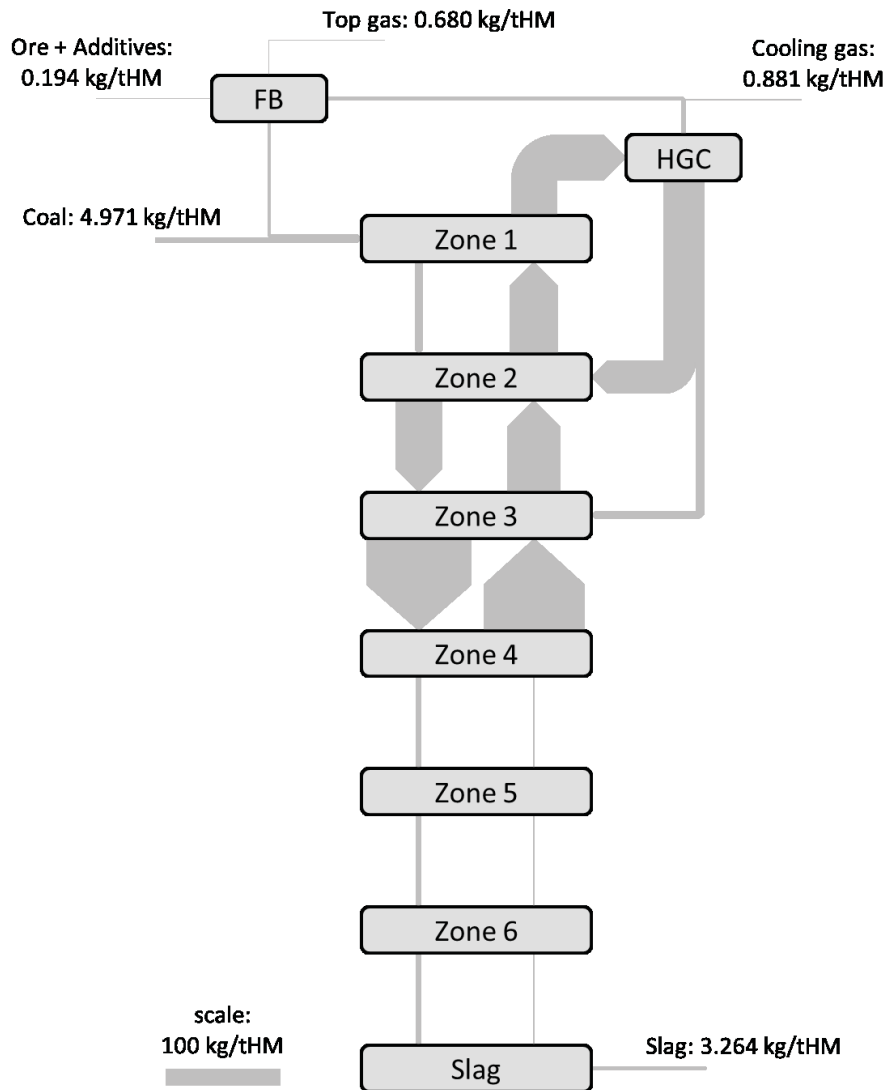
Input FB	[kg/tHM]	[%]	Output FB	[kg/tHM]	[%]	PtInp [%]
Ore	0.12	3.14	DRI	2.84	80.68	55.02
Additives	0.08	2.08	Top Gas	0.68	19.32	13.17
Reducing Gas	3.52	94.78				
Sum	3.72	100	Sum	3.52	100	

Discrepancy Input/Output: = 5.51 %

Input MG	[kg/tHM]	[%]	Output MG	[kg/tHM]	[%]	PtInp [%]
Coal	4.97	11.47	Slag	3.26	7.56	63.20
HGC dust	35.52	81.97	Generator Gas	39.92	92.44	772.96
DRI	2.84	6.56				
Sum	43.34	100	Sum	43.19	100	

Discrepancy Input/Output: = 0.34 %

Input HGC	[kg/tHM]	[%]	Output HGC	[kg/tHM]	[%]	PtInp [%]
Generator Gas	39.92	100.00	HGC dust	35.52	88.97	687.72
Cooling Gas	0.00	0.00	Reducing Gas	3.52	8.82	68.19
			Cooling Gas	0.88	2.21	17.05
Sum	39.92	100	Sum	39.92	100	

Discrepancy Input/Output: = 0.0 %

A.45 Amount of sodium in kg/tHM in different compounds at each position – Run05
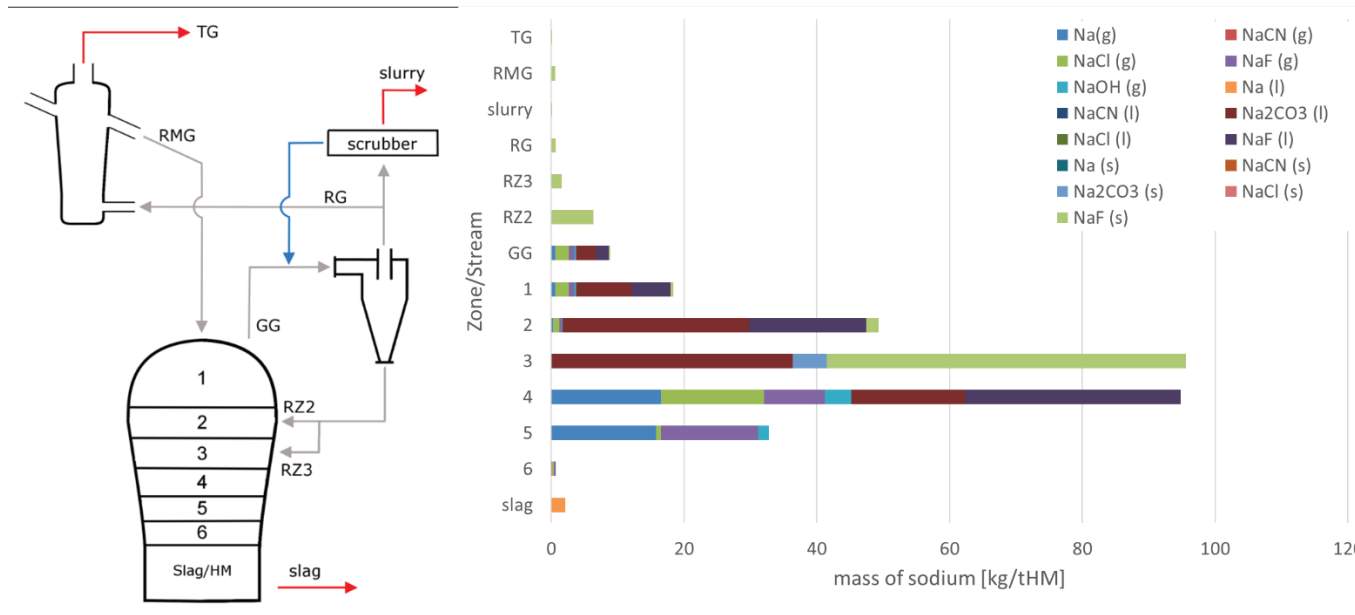
	slag	6	5	4	3	2	1	GG	RZ2	RZ3	RG	slurry	RMG	TG
Na(g)	--	0.08	15.78	16.50	--	0.24	0.60	0.60	--	--	--	--	--	--
NaCN (g)	--	0.02	0.01	0.03	--	0.00	0.01	0.01	--	--	--	--	--	--
NaCl (g)	--	0.29	0.69	15.52	0.01	0.93	2.05	2.05	--	--	0.01	--	--	--
NaF (g)	--	0.30	14.71	9.18	--	0.38	0.78	0.78	--	--	--	--	--	--
NaOH (g)	--	--	1.58	3.94	--	0.14	0.31	0.31	--	--	--	--	--	--
Na (l)	2.14	--	--	--	--	--	--	--	--	--	--	--	--	--
NaCN (l)	--	--	--	--	--	--	--	--	--	--	--	--	--	--
Na2CO3 (l)	--	--	--	17.18	36.37	28.15	8.37	2.93	--	--	--	--	--	--
NaCl (l)	--	--	--	--	--	--	--	--	--	--	--	--	--	--
NaF (l)	--	--	--	32.46	--	17.56	5.85	2.05	--	--	--	--	--	--
Na (s)	--	--	--	--	--	--	--	--	--	--	--	--	--	--
NaCN (s)	--	--	--	--	--	--	--	--	--	--	--	--	--	--
Na2CO3 (s)	--	--	--	--	5.09	--	--	--	--	--	--	--	--	--
NaCl (s)	--	--	--	--	--	--	--	--	--	--	--	--	--	--
NaF (s)	--	--	--	--	54.12	1.91	0.38	0.13	6.36	1.59	0.71	0.18	0.61	0.11
Sum	2.14	0.68	32.77	94.81	95.60	49.29	18.34	8.85	6.36	1.59	0.72	0.18	0.61	0.11

A.46 Sankey diagram for sodium – Run05
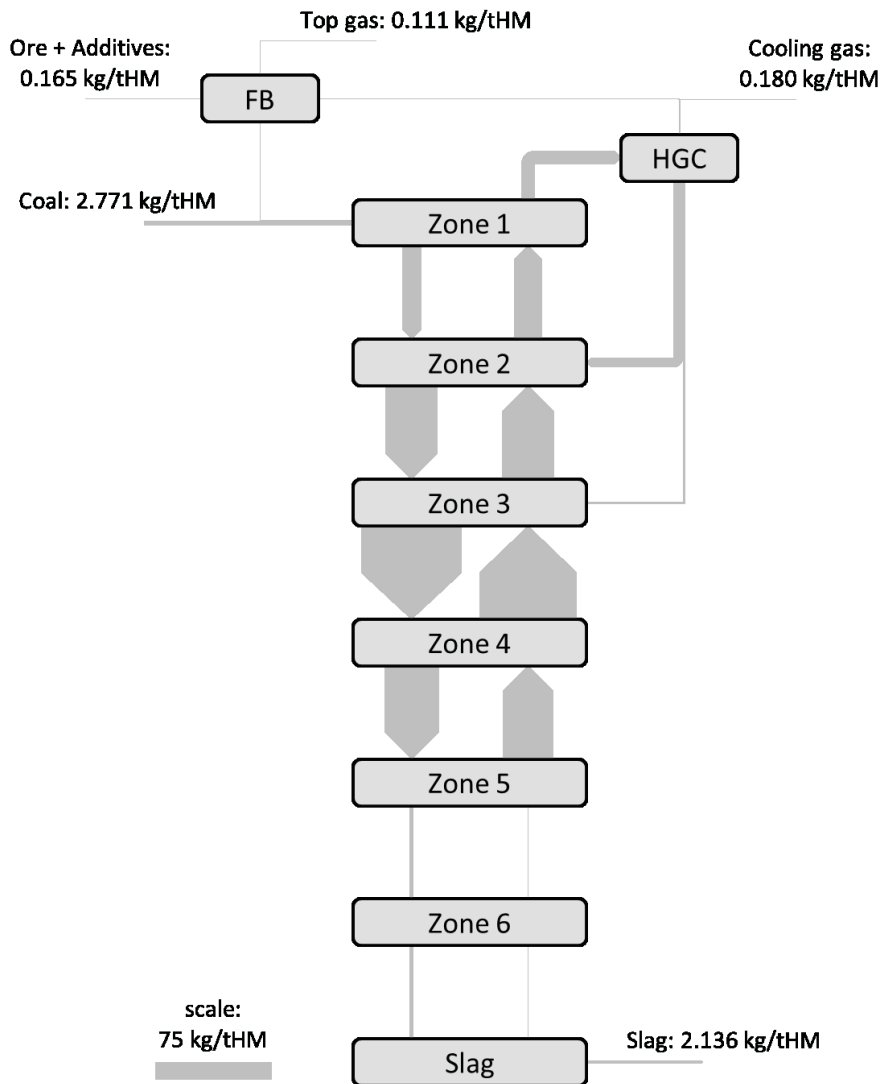
Input FB	[kg/tHM]	[%]	Output FB	[kg/tHM]	[%]	PtInp [%]
Ore	0.16	17.56	DRI	0.61	84.59	20.72
Additives	0.01	1.12	Top Gas	0.11	15.41	3.78
Reducing Gas	0.72	81.33				
Sum	0.88	100	Sum	0.72	100	

Discrepancy Input/Output: = 22.96 %

Input MG	[kg/tHM]	[%]	Output MG	[kg/tHM]	[%]	PtInp [%]
Coal	2.77	24.45	Slag	2.14	19.44	72.76
HGC dust	7.95	70.18	Generator Gas	8.85	80.56	301.49
DRI	0.61	5.37				
Sum	11.33	100	Sum	10.99	100	

Discrepancy Input/Output: = 3.13 %

Input HGC	[kg/tHM]	[%]	Output HGC	[kg/tHM]	[%]	PtInp [%]
Generator Gas	8.85	100.00	HGC dust	7.95	89.84	270.86
Cooling Gas	0.00	0.00	Reducing Gas	0.72	8.13	24.50
			Cooling Gas	0.18	2.03	6.12
Sum	8.85	100	Sum	8.85	100	

Discrepancy Input/Output: = 0.0 %

A.47 Amount of chlorine in kg/tHM in different compounds at each position – Run05
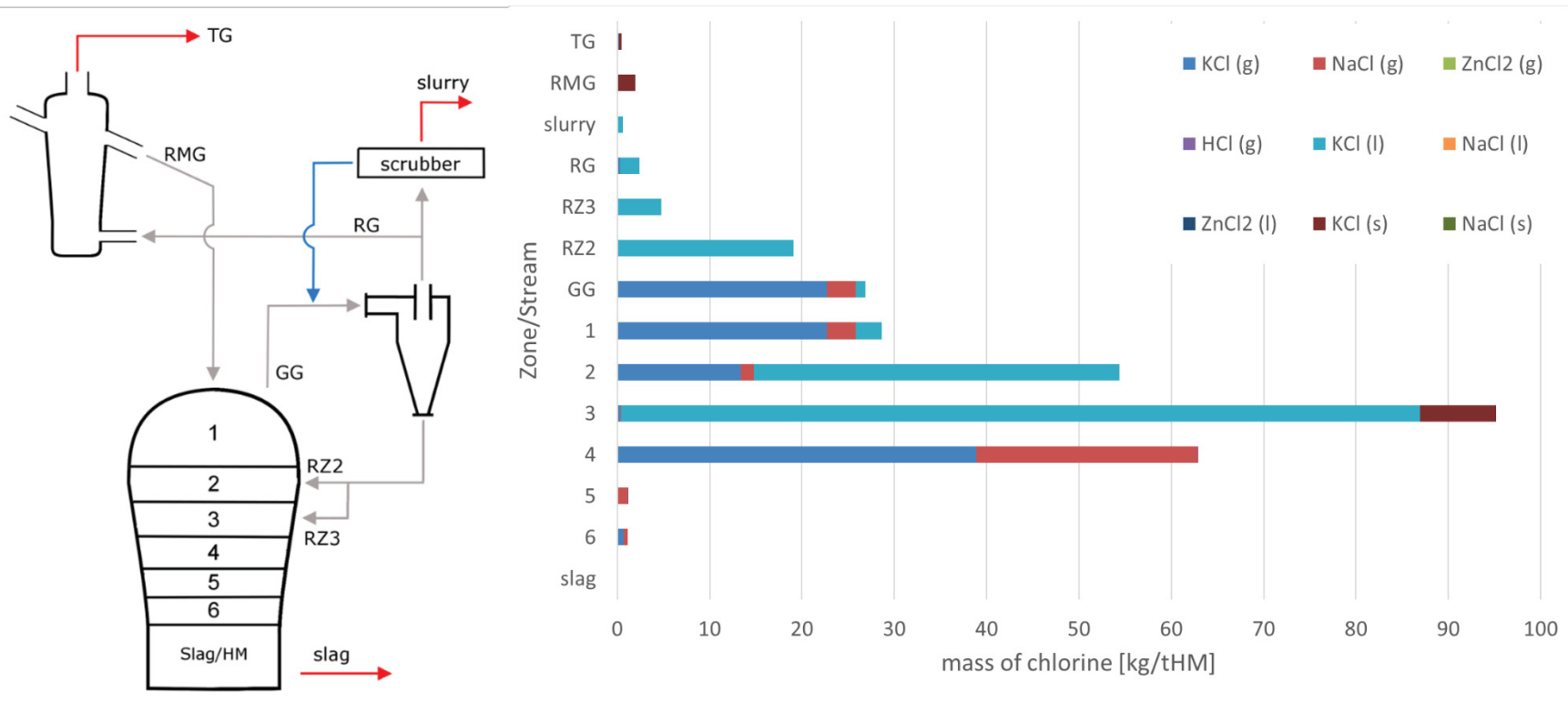
	slag	6	5	4	3	2	1	GG	RZ2	RZ3	RG	slurry	RMG	TG
KCl (g)	--	0.71	0.08	38.90	0.35	13.36	22.69	22.69	--	--	0.29	0.07	--	0.14
NaCl (g)	--	0.44	1.06	23.92	0.02	1.43	3.16	3.16	--	--	0.02	0.00	--	0.00
ZnCl2 (g)	--	--	--	--	--	--	--	--	--	--	--	--	--	--
HCl (g)	--	--	0.01	0.02	--	0.01	0.01	0.01	--	--	--	--	--	--
KCl (l)	--	--	--	--	86.56	39.56	2.79	0.98	19.05	4.76	2.12	0.53	--	--
NaCl (l)	--	--	--	--	--	--	--	--	--	--	--	--	--	--
ZnCl2 (l)	--	--	--	--	--	--	--	--	--	--	--	--	--	--
KCl (s)	--	--	--	--	8.24	--	--	--	--	--	--	--	1.94	0.34
NaCl (s)	--	--	--	--	--	--	--	--	--	--	--	--	--	--
Sum	--	1.15	1.15	62.84	95.17	54.37	28.65	26.84	19.05	4.76	2.42	0.61	1.94	0.49

A.48 Sankey diagram for chorine – Run05
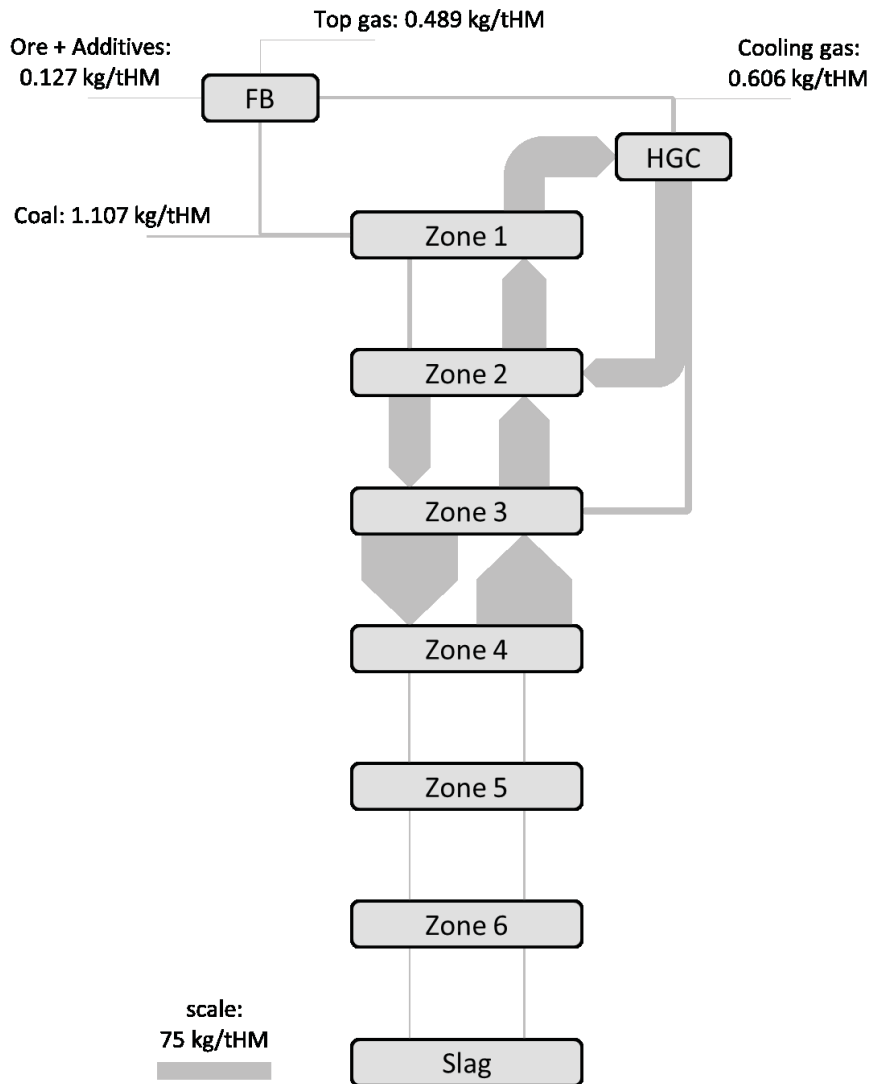
Input FB	[kg/tHM]	[%]	Output FB	[kg/tHM]	[%]	PtInp [%]
Ore	0.12	4.90	DRI	1.94	79.83	156.84
Additives	0.002	0.08	Top Gas	0.49	20.17	39.63
Reducing Gas	2.42	95.02				
Sum	2.55	100	Sum	2.42	100	

Discrepancy Input/Output: = 5.24 %

Input MG	[kg/tHM]	[%]	Output MG	[kg/tHM]	[%]	PtInp [%]
Coal	1.11	4.12	Slag	0.00	0.00	0.00
HGC dust	23.81	88.67	Generator Gas	26.84	100.00	2175.22
DRI	1.94	7.21				
Sum	26.85	100	Sum	26.84	100	

Discrepancy Input/Output: = 0.04 %

Input HGC	[kg/tHM]	[%]	Output HGC	[kg/tHM]	[%]	PtInp [%]
Generator Gas	26.84	100.00	HGC dust	23.81	88.71	1929.62
Cooling Gas	0.00	0.00	Reducing Gas	2.42	9.03	196.48
			Cooling Gas	0.61	2.26	49.12
Sum	26.84	100	Sum	26.84	100	

Discrepancy Input/Output: = 0.0 %

A.49 Amount of fluorine in kg/tHM in different compounds at each position – Run05
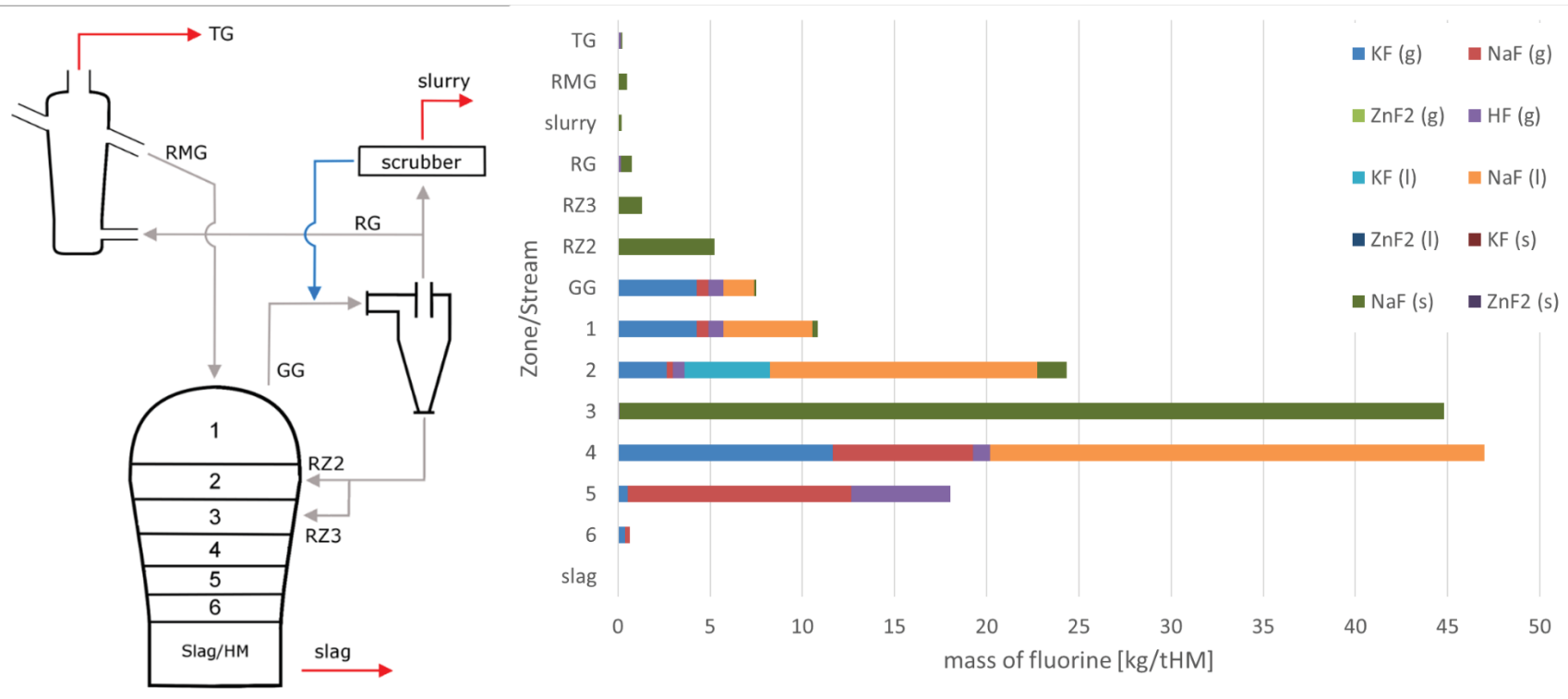
	slag	6	5	4	3	2	1	GG	RZ2	RZ3	RG	slurry	RMG	TG
KF (g)	--	0.38	0.52	11.65	0.03	2.66	4.28	4.28	--	--	0.02	0.00	--	0.01
NaF (g)	--	0.25	12.15	7.59	--	0.31	0.64	0.64	--	--	--	--	--	--
ZnF2 (g)	--	--	--	--	--	--	--	--	--	--	--	--	--	--
HF (g)	--	--	5.37	0.96	0.08	0.63	0.79	0.79	--	--	0.15	0.04	--	0.15
KF (l)	--	--	--	--	--	4.65	--	--	--	--	--	--	--	--
NaF (l)	--	--	--	26.81	--	14.50	4.83	1.69	--	--	--	--	--	--
ZnF2 (l)	--	--	--	--	--	--	--	--	--	--	--	--	--	--
KF (s)	--	--	--	--	--	--	--	--	--	--	--	--	--	--
NaF (s)	--	--	--	--	44.71	1.57	0.32	0.11	5.26	1.31	0.58	0.15	0.50	0.09
ZnF2 (s)	--	--	--	--	--	--	--	--	--	--	--	--	--	--
Sum	--	0.63	18.04	47.01	44.81	24.33	10.86	7.51	5.26	1.31	0.75	0.19	0.50	0.25

A.50 Sankey diagram for fluorine – Run05
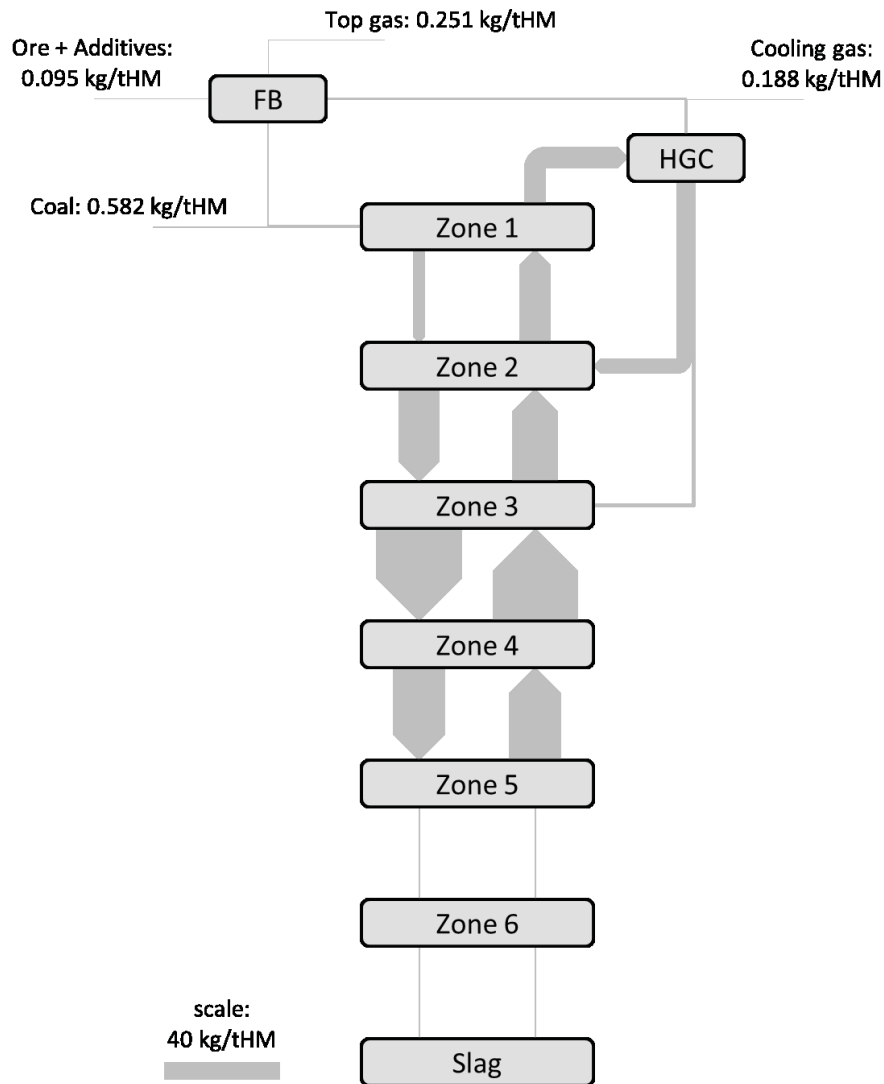
Input FB	[kg/tHM]	[%]	Output FB	[kg/tHM]	[%]	PtInp [%]
Ore	0.09	11.04	DRI	0.50	66.68	74.24
Additives	0.001	0.16	Top Gas	0.25	33.32	37.09
Reducing Gas	0.75	88.80				
Sum	0.85	100	Sum	0.75	100	
Discrepancy Input/Output: = 12.61 %						

Input MG	[kg/tHM]	[%]	Output MG	[kg/tHM]	[%]	PtInp [%]
Coal	0.58	7.60	Slag	0.00	0.00	0.00
HGC dust	6.57	85.83	Generator Gas	7.51	100.00	1109.52
DRI	0.50	6.57				
Sum	7.65	100	Sum	7.51	100	
Discrepancy Input/Output: = 1.9 %						

Input HGC	[kg/tHM]	[%]	Output HGC	[kg/tHM]	[%]	PtInp [%]
Generator Gas	7.51	100.00	HGC dust	6.57	87.46	970.36
Cooling Gas	0.00	0.00	Reducing Gas	0.75	10.03	111.33
			Cooling Gas	0.19	2.51	27.83
Sum	7.51	100	Sum	7.51	100	
Discrepancy Input/Output: = 0.0 %						

A.51 Amount of potassium in kg/tHM in different compounds at each position – Run06
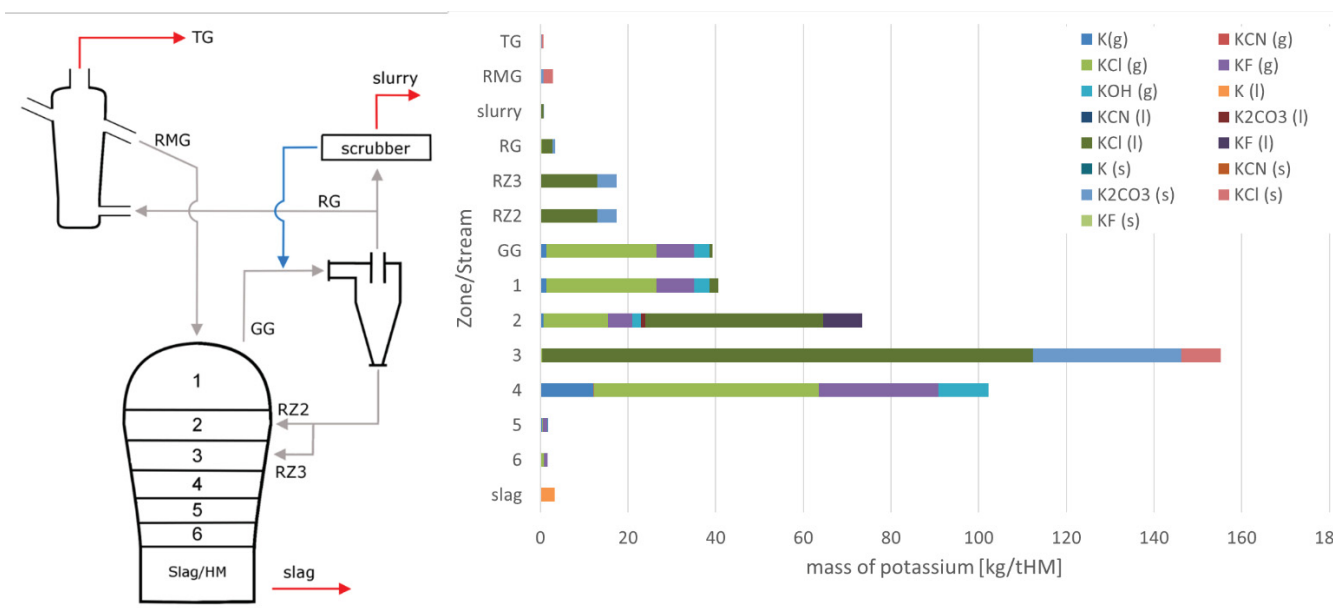
	slag	6	5	4	3	2	1	GG	RZ2	RZ3	RG	slurry	RMG	TG
K(g)	--	0.07	0.46	12.09	--	0.70	1.41	1.41	--	--	--	--	--	--
KCN (g)	--	0.01	--	0.02	--	0.01	0.02	0.02	--	--	--	--	--	--
KCl (g)	--	0.78	0.09	51.50	0.38	14.74	25.01	25.01	--	--	0.32	0.08	--	0.16
KF (g)	--	0.78	1.08	27.15	0.05	5.47	8.66	8.66	--	--	0.03	0.01	--	0.02
KOH (g)	--	--	0.18	11.54	0.01	2.03	3.51	3.51	--	--	0.01	--	--	--
K (l)	3.26	--	--	--	--	--	--	--	--	--	--	--	--	--
KCN (l)	--	--	--	--	--	--	--	--	--	--	--	--	--	--
K2CO3 (l)	--	--	--	--	--	0.96	--	--	--	--	--	--	--	--
KCl (l)	--	--	--	--	111.85	40.58	1.97	0.69	12.97	12.97	2.31	0.58	--	--
KF (l)	--	--	--	--	--	8.83	--	--	--	--	--	--	--	--
K (s)	--	--	--	--	--	--	--	--	--	--	--	--	--	--
KCN (s)	--	--	--	--	--	--	--	--	--	--	--	--	--	--
K2CO3 (s)	--	--	--	--	33.89	--	--	--	4.51	4.51	0.80	0.20	0.69	0.12
KCl (s)	--	--	--	--	8.99	--	--	--	--	--	--	--	2.11	0.37
KF (s)	--	--	--	--	--	--	--	--	--	--	--	--	--	--
Sum	3.26	1.65	1.81	102.30	155.18	73.33	40.59	39.31	17.48	17.48	3.47	0.87	2.80	0.67

A.52 Sankey diagram for potassium – Run06

Top gas: 0.673 kg/tHM

Ore + Additives: 0.194 kg/tHM

Cooling gas: 0.868 kg/tHM

FB

HGC

Coal: 4.971 kg/tHM

Zone 1

Zone 2

Zone 3

Zone 4

Zone 5

Zone 6

scale: 120 kg/tHM

Slag

Slag: 3.264 kg/tHM

Input FB	[kg/tHM]	[%]	Output FB	[kg/tHM]	[%]	PtInp [%]
Ore	0.12	3.18	DRI	2.80	80.62	54.21
Additives	0.08	2.11	Top Gas	0.67	19.38	13.03
Reducing Gas	3.47	94.71				
Sum	3.67	100	Sum	3.47	100	

Discrepancy Input/Output: = 5.59 %

Input MG	[kg/tHM]	[%]	Output MG	[kg/tHM]	[%]	PtInp [%]
Coal	4.97	11.63	Slag	3.26	7.67	63.20
HGC dust	34.97	81.82	Generator Gas	39.31	92.33	760.99
DRI	2.80	6.55				
Sum	42.74	100	Sum	42.57	100	

Discrepancy Input/Output: = 0.39 %

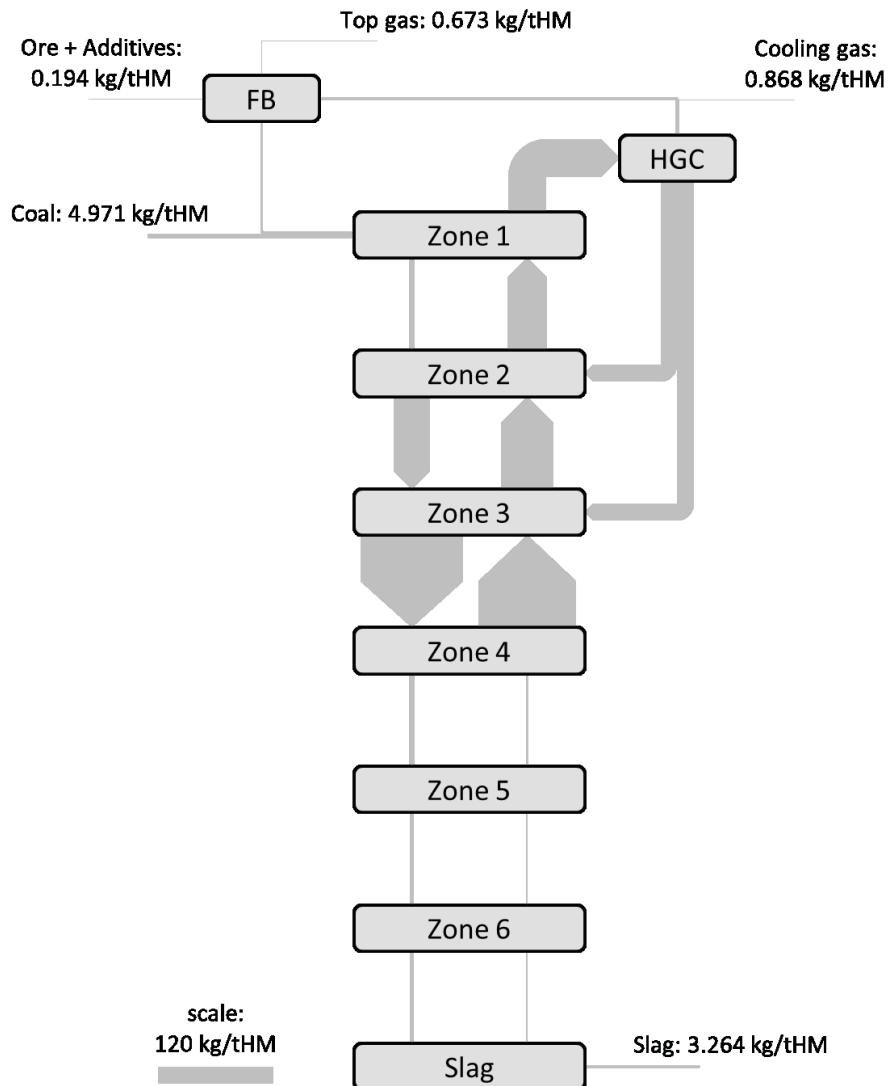| Input HGC	[kg/tHM]	[%]	Output HGC	[kg/tHM]	[%]	PtInp [%]
Generator Gas	39.31	100.00	HGC dust	34.97	88.96	676.95
Cooling Gas	0.00	0.00	Reducing Gas	3.47	8.84	67.23
			Cooling Gas	0.87	2.21	16.81
Sum	39.31	100	Sum	39.31	100	

Discrepancy Input/Output: = 0.0 %

A.53 Amount of sodium in kg/tHM in different compounds at each position – Run06
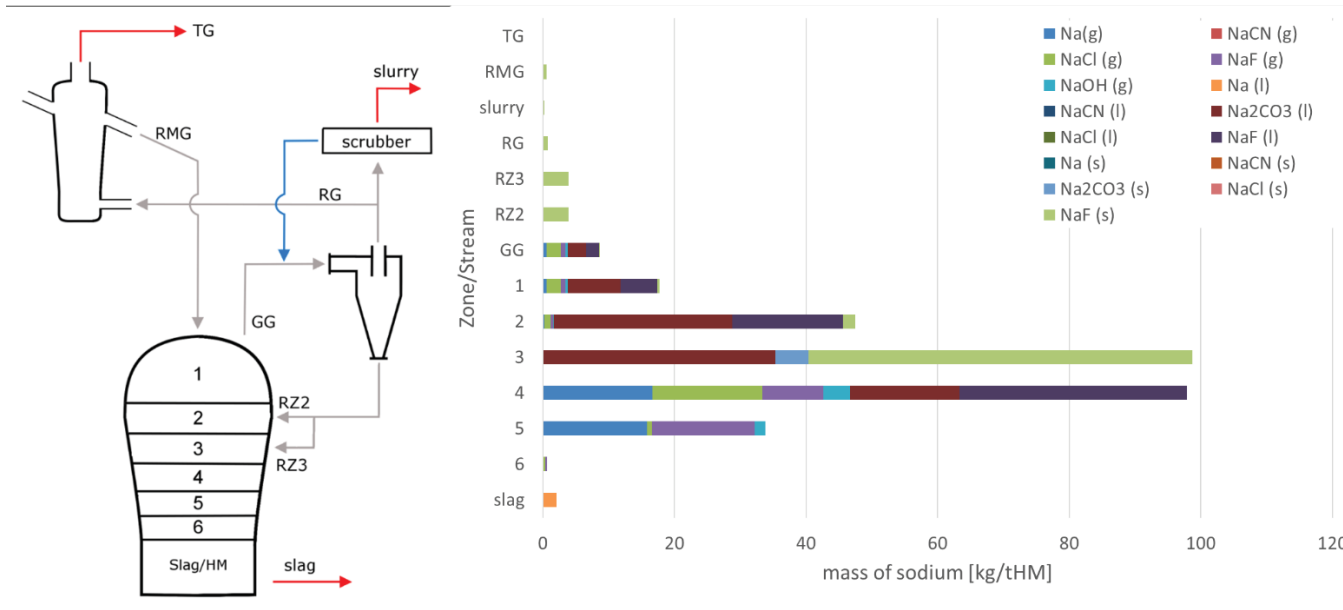
|	slag	6	5	4	3	2	1	GG	RZ2	RZ3	RG	slurry	RMG	TG
Na(g)	--	0.08	15.84	16.63	--	0.24	0.60	0.60	--	--	--	--	--	--
NaCN (g)	--	0.02	0.01	0.03	--	0.00	0.01	0.01	--	--	--	--	--	--
NaCl (g)	--	0.29	0.69	16.69	0.01	0.93	2.08	2.08	--	--	0.01	--	--	--
NaF (g)	--	0.30	15.70	9.32	--	0.38	0.78	0.78	--	--	--	--	--	--
NaOH (g)	--	--	1.58	3.99	--	0.14	0.31	0.31	--	--	--	--	--	--
Na (l)	2.14	--	--	--	--	--	--	--	--	--	--	--	--	--
NaCN (l)	--	--	--	--	--	--	--	--	--	--	--	--	--	--
Na2CO3 (l)	--	--	--	16.65	35.30	27.12	8.05	2.82	--	--	--	--	--	--
NaCl (l)	--	--	--	--	--	--	--	--	--	--	--	--	--	--
NaF (l)	--	--	--	34.59	--	16.82	5.51	1.93	--	--	--	--	--	--
Na (s)	--	--	--	--	--	--	--	--	--	--	--	--	--	--
NaCN (s)	--	--	--	--	--	--	--	--	--	--	--	--	--	--
Na2CO3 (s)	--	--	--	--	5.06	--	--	--	--	--	--	--	--	--
NaCl (s)	--	--	--	--	--	--	--	--	--	--	--	--	--	--
NaF (s)	--	--	--	--	58.37	1.87	0.37	0.13	3.89	3.89	0.69	0.17	0.59	0.10
Sum	2.14	0.68	33.81	97.89	98.75	47.49	17.71	8.65	3.89	3.89	0.70	0.17	0.59	0.10

A.54 Sankey diagram for sodium – Run06
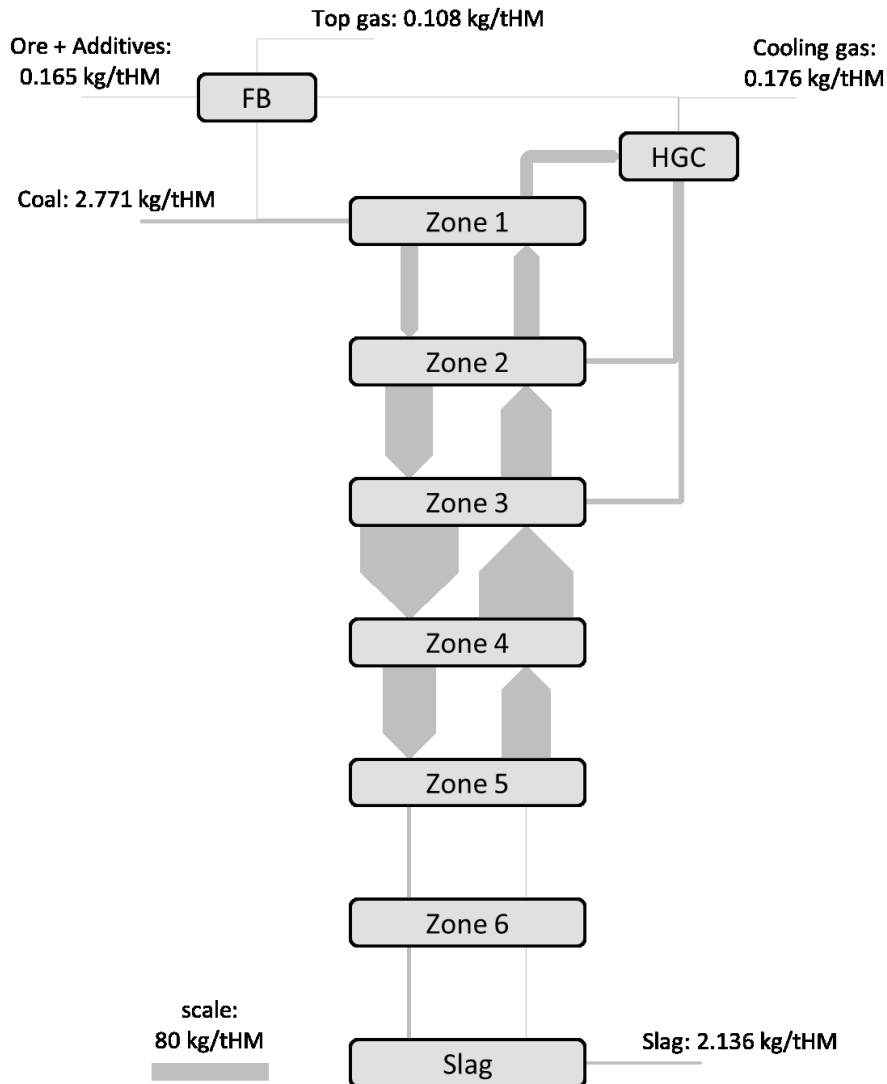
Input FB	[kg/tHM]	[%]	Output FB	[kg/tHM]	[%]	PtInp [%]
Ore	0.16	17.88	DRI	0.59	84.58	20.26
Additives	0.01	1.14	Top Gas	0.11	15.42	3.69
Reducing Gas	0.70	80.98				
Sum	0.87	100	Sum	0.70	100	

Discrepancy Input/Output: = 23.48 %

Input MG	[kg/tHM]	[%]	Output MG	[kg/tHM]	[%]	PtInp [%]
Coal	2.77	24.88	Slag	2.14	19.80	72.76
HGC dust	7.77	69.78	Generator Gas	8.65	80.20	294.68
DRI	0.59	5.34				
Sum	11.14	100	Sum	10.79	100	

Discrepancy Input/Output: = 3.25 %

Input HGC	[kg/tHM]	[%]	Output HGC	[kg/tHM]	[%]	PtInp [%]
Generator Gas	8.65	100.00	HGC dust	7.77	89.84	264.73
Cooling Gas	0.00	0.00	Reducing Gas	0.70	8.13	23.95
			Cooling Gas	0.18	2.03	5.99
Sum	8.65	100	Sum	8.65	100	

Discrepancy Input/Output: = 0.0 %

A.55 Amount of chlorine in kg/tHM in different compounds at each position – Run06
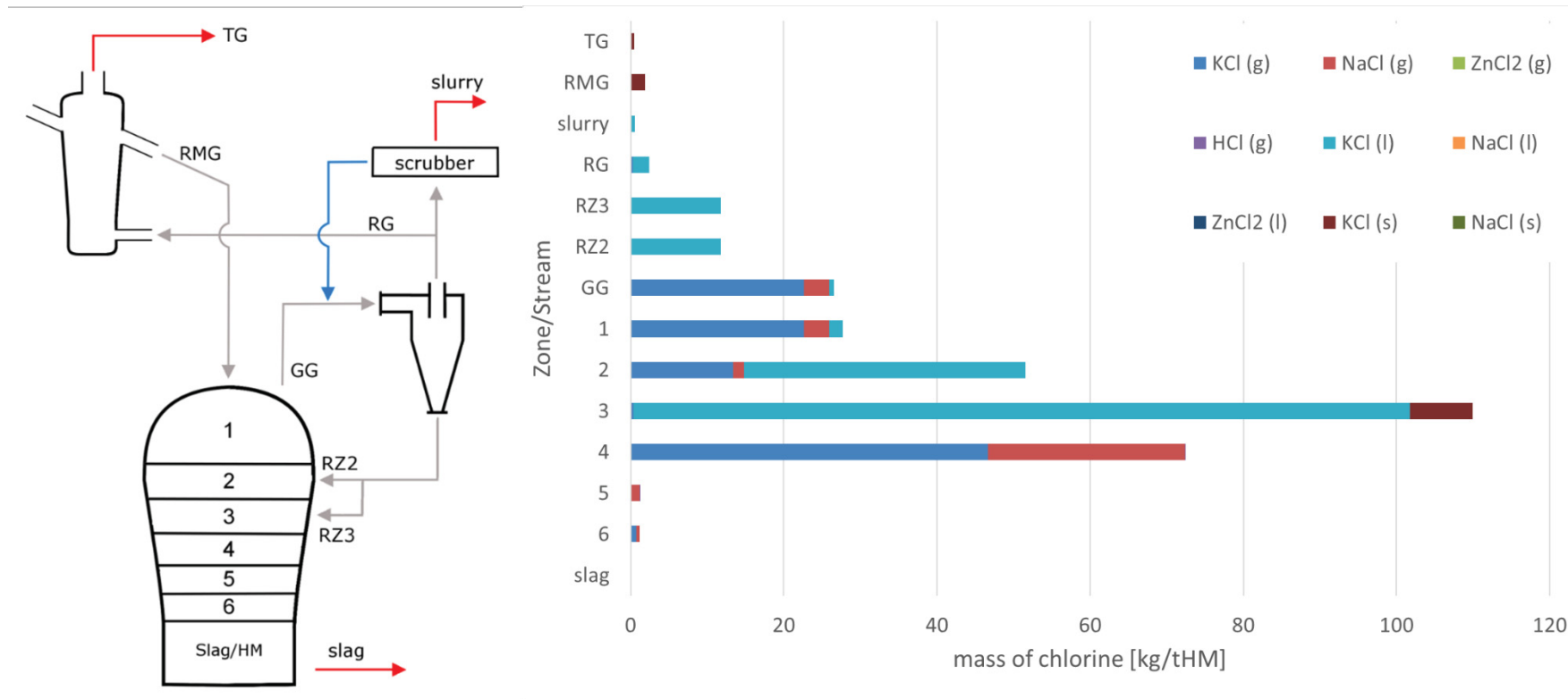
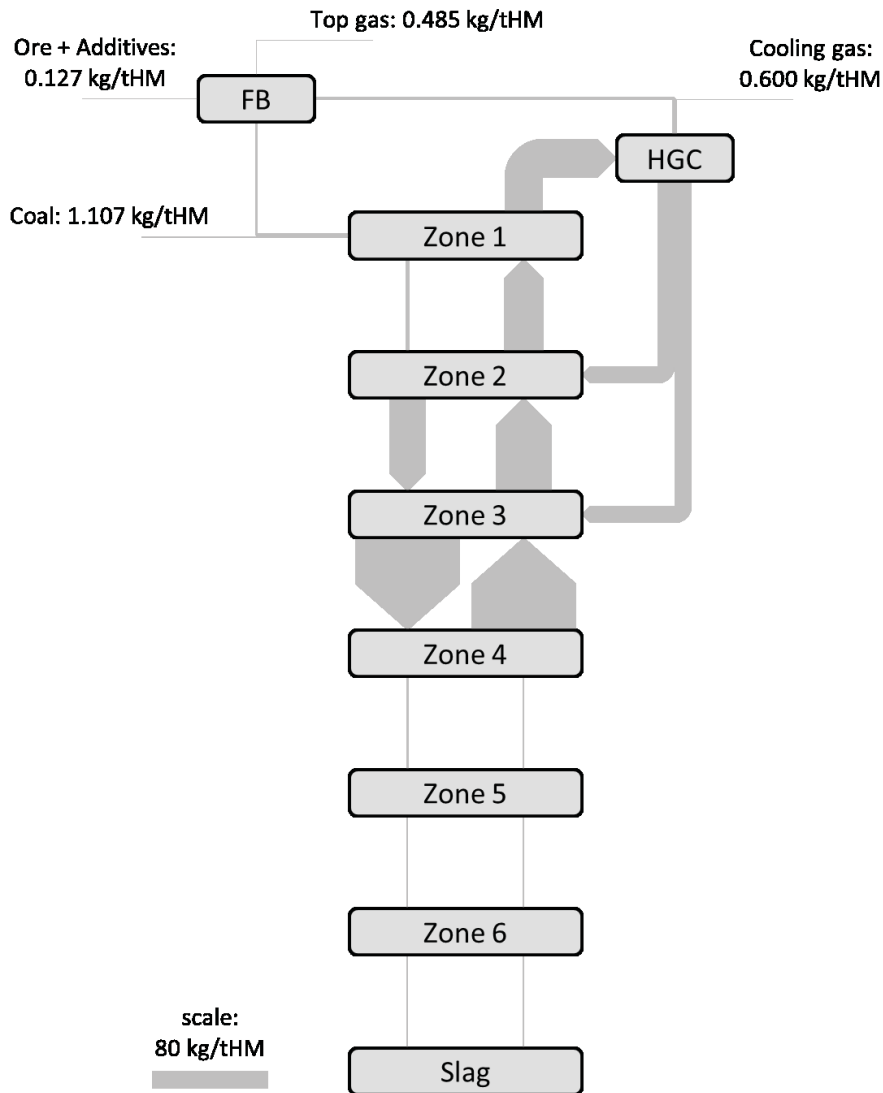|	slag	6	5	4	3	2	1	GG	RZ2	RZ3	RG	slurry	RMG	TG
KCl (g)	--	0.71	0.08	46.69	0.34	13.36	22.68	22.68	--	--	0.29	0.07	--	0.14
NaCl (g)	--	0.44	1.06	25.72	0.02	1.43	3.21	3.21	--	--	0.02	0.00	--	0.00
ZnCl2 (g)	--	--	--	--	--	--	--	--	--	--	--	--	--	--
HCl (g)	--	--	0.01	0.02	--	0.01	0.01	0.01	--	--	--	--	--	--
KCl (l)	--	--	--	--	101.41	36.79	1.78	0.62	11.76	11.76	2.09	0.52	--	--
NaCl (l)	--	--	--	--	--	--	--	--	--	--	--	--	--	--
ZnCl2 (l)	--	--	--	--	--	--	--	--	--	--	--	--	--	--
KCl (s)	--	--	--	--	8.15	--	--	--	--	--	--	--	1.91	0.34
NaCl (s)	--	--	--	--	--	--	--	--	--	--	--	--	--	--
Sum	--	1.15	1.15	72.43	109.93	51.60	27.68	26.52	11.76	11.76	2.40	0.60	1.91	0.48

A.56 Sankey diagram for chlorine – Run06

Input FB	[kg/tHM]	[%]	Output FB	[kg/tHM]	[%]	PtInp [%]
Ore	0.12	4.95	DRI	1.91	79.77	155.10
Additives	0.002	0.08	Top Gas	0.49	20.23	39.33
Reducing Gas	2.40	94.97				
Sum	2.53	100	Sum	2.40	100	

Discrepancy Input/Output: = 5.3 %

Input MG	[kg/tHM]	[%]	Output MG	[kg/tHM]	[%]	PtInp [%]
Coal	1.11	4.17	Slag	0.00	0.00	0.00
HGC dust	23.52	88.62	Generator Gas	26.52	100.00	2149.56
DRI	1.91	7.21				
Sum	26.54	100	Sum	26.52	100	

Discrepancy Input/Output: = 0.08 %

| Input HGC	[kg/tHM]	[%]	Output HGC	[kg/tHM]	[%]	PtInp [%]
Generator Gas	26.52	100.00	HGC dust	23.52	88.69	1906.52
Cooling Gas	0.00	0.00	Reducing Gas	2.40	9.04	194.43
			Cooling Gas	0.60	2.26	48.61
Sum	26.52	100	Sum	26.52	100	

Discrepancy Input/Output: = 0.0 %

A.57 Amount of fluorine in kg/tHM in different compounds at each position – Run06
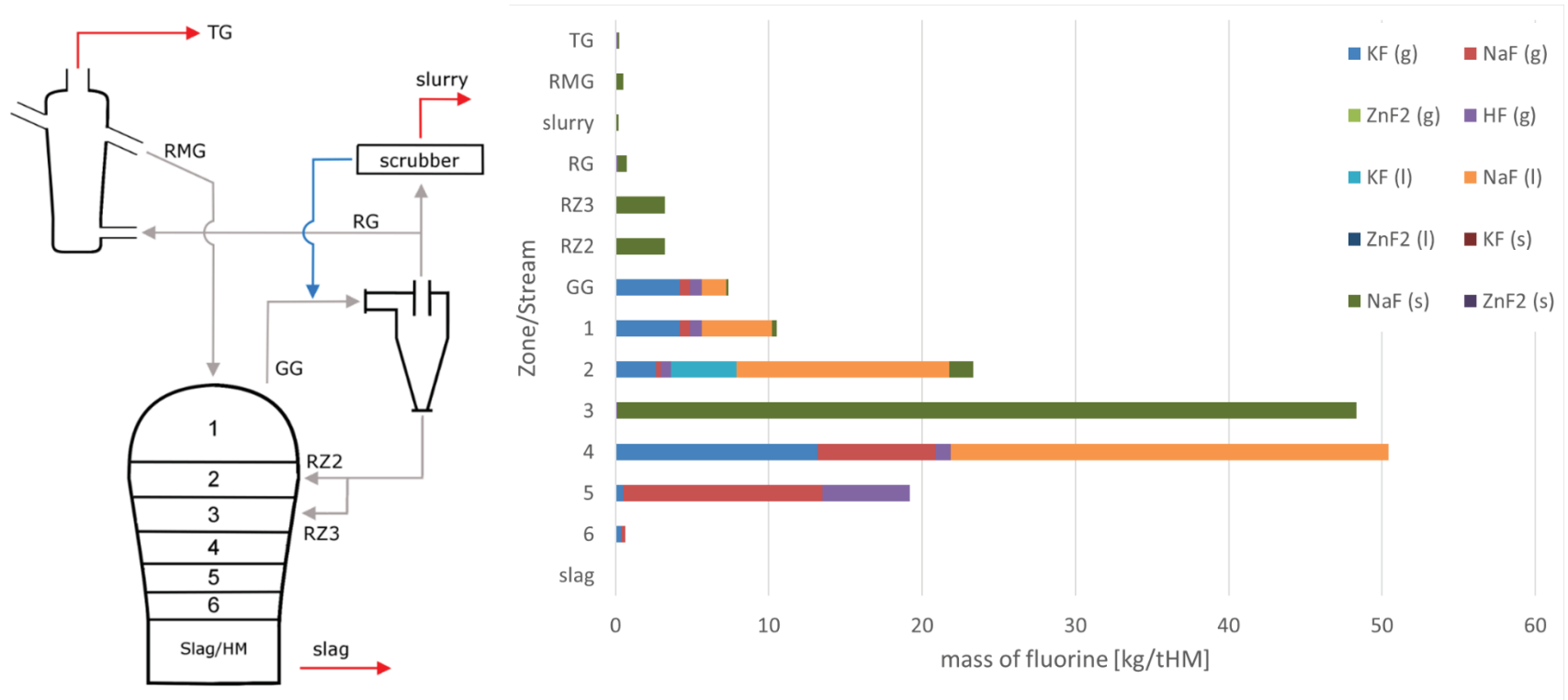
	slag	6	5	4	3	2	1	GG	RZ2	RZ3	RG	slurry	RMG	TG
KF (g)	--	0.38	0.52	13.19	0.03	2.66	4.21	4.21	--	--	0.02	0.00	--	0.01
NaF (g)	--	0.25	12.97	7.70	--	0.31	0.64	0.64	--	--	--	--	--	--
ZnF2 (g)	--	--	--	--	--	--	--	--	--	--	--	--	--	--
HF (g)	--	--	5.69	0.96	0.07	0.63	0.79	0.79	--	--	0.15	0.04	--	0.15
KF (l)	--	--	--	--	--	4.29	--	--	--	--	--	--	--	--
NaF (l)	--	--	--	28.58	--	13.89	4.56	1.59	--	--	--	--	--	--
ZnF2 (l)	--	--	--	--	--	--	--	--	--	--	--	--	--	--
KF (s)	--	--	--	--	--	--	--	--	--	--	--	--	--	--
NaF (s)	--	--	--	--	48.22	1.55	0.31	0.11	3.21	3.21	0.57	0.14	0.49	0.09
ZnF2 (s)	--	--	--	--	--	--	--	--	--	--	--	--	--	--
Sum	--	0.63	19.18	50.43	48.32	23.33	10.51	7.35	3.21	3.21	0.74	0.18	0.49	0.25

A.58 Sankey diagram for fluorine – Run06
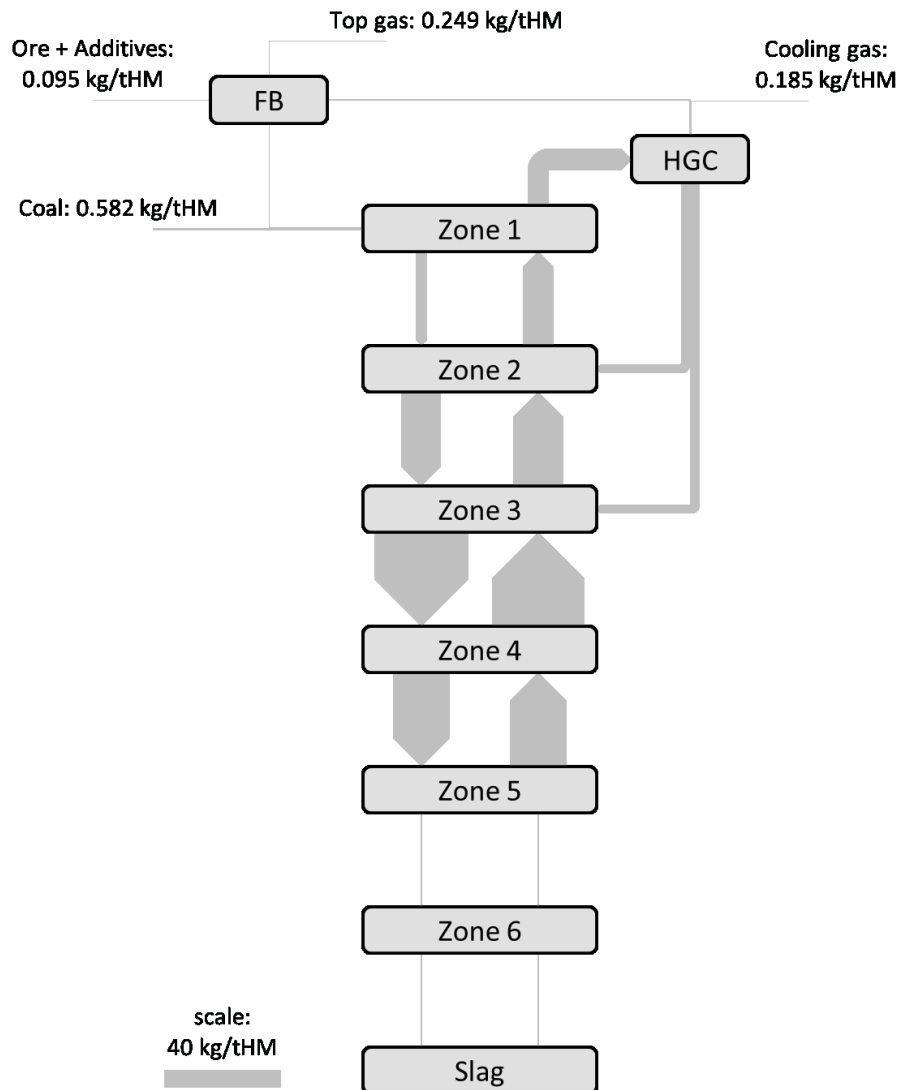
Input FB	[kg/tHM]	[%]	Output FB	[kg/tHM]	[%]	PtInp [%]
Ore	0.09	11.22	DRI	0.49	66.37	72.58
Additives	0.001	0.16	Top Gas	0.25	33.63	36.78
Reducing Gas	0.74	88.62				
Sum	0.84	100	Sum	0.74	100	

Discrepancy Input/Output: = 12.84 %

Input MG	[kg/tHM]	[%]	Output MG	[kg/tHM]	[%]	PtInp [%]
Coal	0.58	7.77	Slag	0.00	0.00	0.00
HGC dust	6.42	85.68	Generator Gas	7.35	100.00	1085.10
DRI	0.49	6.56				
Sum	7.49	100	Sum	7.35	100	

Discrepancy Input/Output: = 2.01 %

Input HGC	[kg/tHM]	[%]	Output HGC	[kg/tHM]	[%]	PtInp [%]
Generator Gas	7.35	100.00	HGC dust	6.42	87.40	948.40
Cooling Gas	0.00	0.00	Reducing Gas	0.74	10.08	109.36
			Cooling Gas	0.19	2.52	27.34
Sum	7.35	100	Sum	7.35	100	

Discrepancy Input/Output: = 0.0 %